Single-component multilayered self-assembling protein nanoparticles presenting glycan-trimmed uncleaved prefusion optimized envelope trimers as HIV-1 vaccine candidates

Yi-Nan Zhang[1#], Jennifer Paynter[1#], Aleksandar Antanasijevic[1,2#], Joe D. Allen[3#], Yi-Zong Lee[1], Mor Eldad[1], Jeffrey Copps[1,2], Maddy Newby[3], Linling He[1], Ian A. Wilson[1,2,4], Max Crispin[3], Andrew B. Ward[1,2], and Jiang Zhu[1,5]*

[1]Department of Integrative Structural and Computational Biology, The Scripps Research Institute, La Jolla, CA 92037, USA.

[2]IAVI Neutralizing Antibody Center, The Scripps Research Institute, La Jolla, CA 92037, USA.

[3]School of Biological Sciences, Highfield Campus, University of Southampton, Southampton, SO17 1BJ, UK.

[4]The Skaggs Institute for Chemical Biology, The Scripps Research Institute, La Jolla, CA 92037, USA.

[5]Department of Immunology and Microbiology, The Scripps Research Institute, La Jolla, CA 92037, USA.

[#] These authors contributed equally to this work

* Correspondence and requests for materials should be addressed to:

JZ: Phone: (858) 784-8157; Email: jiang@scripps.edu

ABSTRACT (150 words)

Uncleaved prefusion-optimized (UFO) design represents a general solution for stabilizing HIV-1 envelope glycoprotein (Env) trimers. Single-component, self-assembling protein nanoparticles (1c-SApNP) have been used to display optimized antigens as multivalent vaccine candidates. Here, we characterized the biophysical, structural, and antigenic properties of 1c-SApNPs that present the BG505 UFO trimer with wildtype and modified glycans. Glycan trimming improved HIV-1 Env recognition by broadly neutralizing antibodies (bNAbs) to the CD4 binding site and other major glycan-containing epitopes, increased the frequency of vaccine responders (FVR) when formulated with aluminum adjuvants, and steered antibody responses away from glycan-specific immunodominant epitopes. The mechanism of vaccine-induced immunity was examined in mice. Compared with the soluble trimer, two large 1c-SApNPs showed 420 times longer retention, 20-32 times greater presentation on follicular dendritic cell dendrites, and up-to-4 times stronger germinal center reactions in lymph node follicles. These findings can inform the next phase of HIV-1 vaccine development.

ONE-SENTENCE SUMMARY (125 characters)

Glycan trimming enables HIV-1 Env immunogens to elicit antibodies that overcome the glycan shield and improve the frequency of vaccine responders

42 **INTRODUCTION**

43 The HIV-1 envelope glycoprotein (Env) mediates cell entry and is the target of the host humoral
44 immune response. Functional Env is a trimer of noncovalent gp120-gp41 heterodimers, which are
45 generated from the proteolytic cleavage of a gp160 precursor (*1*). In addition to substantial genetic
46 diversity caused by an error-prone reverse transcriptase (*2*), HIV-1 exploits two Env-dependent
47 strategies to evade host immunity: (*i*) Env metastability causes Env misfolding, sheds gp120, and
48 leaves gp41 stumps on the virus (*3*), and (*ii*) host-produced glycans form a dense "glycan shield"
49 to mask the Env surface (*4*). Nonetheless, up to 30% of infected people eventually develop serum
50 neutralization against the majority of circulating HIV-1 strains. Hundreds of broadly neutralizing
51 antibodies (bNAbs) have been isolated from HIV-1-infected donors (*5*) and target seven different
52 epitope regions on Env: the CD4 binding site (CD4bs), three peptide-glycan epitopes (located at
53 the V2 apex, V3 base, and gp120-gp41 interface), silent face, fusion peptide (FP), and membrane-
54 proximal external region (MPER) (*6, 7*). These bNAbs and the characterization of their epitopes
55 have thus provided a number of templates for "antibody-guided" rational vaccine design (*8-11*).

56 The design and characterization of native-like Env trimers marked a milestone in modern
57 HIV-1 research (*12, 13*). While gp120-derived constructs are still promising CD4bs immunogens
58 (*14-18*), the ongoing HIV-1 vaccine efforts have largely shifted to Env trimers, as exemplified by
59 SOSIP (*19-22*), native flexibly linked (NFL) (*23-25*), and uncleaved prefusion optimized (UFO)
60 trimers (*26-28*). As the first rational trimer design, SOSIP transformed the HIV-1 vaccine field
61 and generated a wealth of information on Env structure and immunogenicity (*29*). Both SOSIP
62 and NFL are empirical designs that may require additional mutations to improve trimer stability
63 (e.g., SOSIP.v9 (*30*)). In contrast, UFO eliminates the root cause of Env metastability with only
64 two implementations, UFO and UFO-BG, which have been applied to diverse Envs (*26-28*). While

65 Env metastability can now be dealt with by these three trimer platforms, the glycan shield remains
66 a challenge due to its complex roles in Env-bNAb interactions (*31-36*). Liquid chromatography-
67 mass spectrometry (LC-MS) (*37-39*) and structural analysis by x-ray crystallography (*40-46*) and
68 cryo-electron microscopy (cryo-EM) (*47-49*) resulted in site-specific glycan profiles and atomic
69 details of bNAb-glycan interactions, respectively. These studies placed a premium on mimicking
70 the glycan shield of functional viral Env in vaccine design (*50*). Although "multistage" vaccine
71 strategies originated from the evolutionary analysis of bNAbs (*51*), glycans have become a major
72 consideration. Sequential Env immunogens with glycan deletion and reintroduction were designed
73 to guide B cell maturation toward bNAbs (*52-54*). Glycan-related immunodominance is another
74 compounding factor in bNAb elicitation using soluble trimers, as exemplified by glycan holes and
75 a neoepitope at the trimer base (*55, 56*). The former (small, exposed protein surfaces within the
76 glycan shield) are the primary target of autologous tier-2 NAbs in rabbits (*56-65*), whereas the
77 latter elicits non-neutralizing antibodies (nNAbs) in multiple species (*63, 66, 67*) and causes trimer
78 disassembly during immunization (*68*). In rodents, glycan epitopes at C3/V4 and C3/V5 accounted
79 for the autologous NAb response induced by BG505 Env (*69-71*). In nonhuman primates (NHPs),
80 the BG505 SOSIP trimer elicited an autologous NAb response to C3/465 (*60, 72*). Therefore, the
81 native-like trimer-induced autologous NAb response appears to be dominated by Env surfaces that
82 either lack or overexpress glycans, leading to contradictory views on the glycan shield in vaccine
83 design, i.e., glycan nativeness (*50*) *vs.* glycan removal or addition (*52-54, 73*). The manipulation
84 of individual glycans to minimize immunodominance or improve neutralization breadth proved to
85 be ineffective (*64*) and is unlikely to be a general solution for broadly protective vaccines.

86 Independent of Env design, the delivery of Env antigens in multimeric forms to mimic
87 virus-like particles (VLPs) has become a trend in recent vaccine research for HIV-1 (*74-77*) and

88 other viruses (*78-80*). With virus-like size and shape as well as a dense display of surface antigens,
89 VLPs can induce a more potent and long-lasting immune response than soluble antigens (*81-85*).
90 There are three major types of VLPs based on their chemical makeup: protein/lipid (e.g., enveloped
91 virus shells), protein-based (e.g., non-enveloped virus capsids and self-assembling proteins), and
92 lipid-based (e.g., liposomes). Protein nanoparticle (NP) engineering was the driving force in recent
93 technological advances in the vaccine field (*80*). Three technologies, SpyTag/SpyCatcher (termed
94 "SPY") (*86*), two-component NPs (2c-NP) (*87*), and single-component self-assembling protein
95 NPs (1c-SApNP) (*27, 88, 89*), have each been assessed for multiple viral targets. SPY utilizes an
96 isopeptide bond within a bacterial adhesin to covalently link antigens to VLPs or NPs (*90*). The
97 2c-NP and 1c-SA*p*NP platforms rely on in vitro (cell free) and in vivo (in producer cells) assembly,
98 respectively. In terms of vaccine production, SPY and 2c-NP achieve greater versatility at the price
99 of increased complexity and cost, as they both involve multiple plasmids, expression systems, and
100 purification methods. The 1c-SApNPs require a highly optimized antigen and NP carrier, which
101 are encoded within a single plasmid, to achieve manufacturability and quality (*91, 92*). VLPs and
102 NPs are more immunogenic because of their advantages in antigen trafficking to lymph nodes,
103 high-avidity follicular dendritic cell (FDC) interactions, antigen-presenting cell (APC) activation,
104 and germinal center (GC) reactions, which involve both innate and adaptive systems (*77, 93*). A
105 recent study of HIV-1 NP immunogens suggested that the density of the mannose patches is critical
106 for the FDC targeting of heavily glycosylated antigens (*94, 95*). Env trimers attached to iron oxide
107 NPs or aluminum salt have also been tested as multivalent HIV-1 vaccines (*96, 97*).

108 Here, we displayed the BG505 UFO trimer on multilayered 1c-SApNP platforms (*91, 92*)
109 as our second-generation vaccine candidates. A panel of Env-NP constructs was first designed for
110 biochemical, biophysical, and structural characterization to facilitate immunogen selection. Cryo-

111 EM yielded high-resolution structures for the multilayered E2p and I3-01v9 1c-SApNPs that each
112 present 20 BG505 UFO trimers, with localized reconstructions obtained for the trimer at 3.7 and
113 6.0 Å, respectively. Site-specific glycan analysis and antigenic profiling of the BG505 UFO trimer
114 and 1c-SApNPs bearing wildtype and modified glycans revealed distinct features. Unexpectedly,
115 endoglycosidase H (endo H) trimming of the glycan shield retained NP binding to NAbs/bNAbs
116 that require specific glycans for Env recognition and target the CD4bs. Negative-stain EM revealed
117 differential effects of glycan trimming on the angle of approach for bNAbs PGT128 and VRC01.
118 Next, we immunized mice and rabbits with UFO trimers and 1c-SApNPs bearing the wildtype and
119 trimmed glycans, which were formulated with conventional adjuvants. A prime-boost regimen that
120 administers glycan-trimmed and wildtype immunogens sequentially increased the frequency of
121 vaccine responders (FVR) in mice and diverged NAb responses away from glycan holes in rabbits,
122 providing a potential solution for mitigating glycan-related immunodominance. Lastly, we
123 analyzed vaccine delivery and immune responses at the intra-organ, intercellular, and intracellular
124 levels for the soluble trimer and 1c-SApNPs in mouse lymph nodes. E2p and I3-01v9 1c-SApNPs
125 showed 420 times longer follicular retention, 20-32 times greater presentation on FDC dendrites,
126 and up-to-4 times higher GC reactions than the trimer. Glycan trimming showed little effect on
127 1c-SA*p*NP trafficking to, and retention in, lymph nodes. Intact 1c-SApNPs and adjuvants in lymph
128 node tissues could be directly visualized by transmission electron microscopy (TEM). In summary,
129 our study presents a glycan trimming strategy to overcome the glycan shield challenges, in addition
130 to two BG505 UFO trimer-presenting 1c-SApNPs as HIV-1 vaccine candidates.

131 **RESULTS**

132 **Rational design and characterization of BG505 UFO trimer-presenting 1c-SApNPs**

133 In the UFO design paradigm, the N terminus of heptad repeat 1 ($HR1_N$, aa 547-569) is the trigger
134 of HIV-1 Env metastability and must be shortened and optimized (*26, 27*). Crystal structures were
135 determined for clade A, B, and C Envs bearing the $HR1_N$, UFO, and UFO-BG designs (*26, 27, 71,*
136 *98*). The $HR1_N$-redesigned BG505 trimer was displayed on ferritin (FR), E2p, and I3-01 NPs (*27,*
137 *88*). The reengineered I3-01, when formulated with a Toll-like receptor 3 (TLR3) agonist adjuvant,
138 elicited a potent tier 2 NAb response to HIV-1 in mice for the first time (*27, 71*). We have also
139 applied these NP platforms to design multivalent immunogens for other viruses (*89, 91, 92*).

140 Here we revisited the HIV-1 Env-NP vaccine design based on the high-resolution BG505
141 UFO trimer structure (*98*) and newly developed "multilayered" 1c-SA*p*NP platforms (*91, 92*). We
142 first modeled the BG505 UFO trimer (PDB ID: 6UTK) on wildtype FR, E2p, and I3-01, resulting
143 in particles with diameters of 30.2, 41.7, and 46.1 nm, respectively (**Fig. 1A**). The redesigned 8-
144 aa $HR1_N$ bend ("NPDWLPDM") forms a 24-Å triangle in the center of each UFO trimer (**Fig. 1A**,
145 middle). For FR and E2p, the superposition of BG505 gp140 C termini onto the N termini yielded
146 C_α root-mean-square deviations (RMSDs) of 1.0 and 11.4 Å, respectively. A 3-aa "ASG" linker,
147 with "AS" resulting from the restriction site between the Env and NP genes, enabled the proper
148 display of Env trimers on FR and E2p. For I3-01, a 10-aa $(G_4S)_2$ linker was added to overcome the
149 large spacing (50.5 Å) between the N termini of three subunits around each three-fold axis (*27, 89,*
150 *91, 92*). We then examined the multilayered 1c-SApNP design concept using a modeling approach
151 (**Fig. 1B**). Previously, we incorporated a locking domain (LD) and a pan-reactive $CD4^+$ T-cell
152 epitope (PADRE) into E2p and I3-01 60-mers through gene fusion (*91, 92*). We hypothesize that
153 antigens will fold properly on the NP surface upon self-assembly, while the LD and PADRE may
154 form an inner layer and a hydrophobic core to stabilize the NP shell and deliver a strong T-helper
155 signal, respectively (**Fig. 1B**, left). E2p-LD4-PADRE, which was used as a carrier for EBOV GP

156 (*92*), was modeled to visualize the multilayered structure (**Fig. 1B**, right). Briefly, E2p forms a
157 protein shell of 23.2 nm with a distance of 12.8 nm across the hollow interior measured at the
158 inward-facing tip (G382). LD4, a 58-aa dimeric protein domain (PDB ID: 2MG4), was fused to
159 the C terminus of E2p at the dimeric NP-forming interface with a 5-aa G_4S linker, resulting in a
160 smaller protein shell of 14.4 nm when icosahedral symmetry was applied. A 13-aa PADRE with
161 an extended backbone was fused to the C terminus of LD4 with a 2-aa GS linker, resulting in a
162 hydrophobic core with a diameter of ~5 nm. Based on structural modeling, a set of multilayered
163 BG505 UFO Env-NP constructs was designed and advanced to experimental validation (*92*).

164 Nineteen BG505 UFO Env-NP constructs were transiently expressed in 100-ml ExpiCHO
165 cells followed by PGT145 purification and size-exclusion chromatography (SEC) on a Superose
166 6 column (**Fig. 1C**). Overall, the BG505 UFO trimer can be displayed on wildtype FR, E2p, and
167 I3-01 NPs with high purity. Similar to our previous study (*92*), seven LDs (1-7) and five LDs (4-
168 5 and 7-9) were tested for E2p and I3-01, respectively. E2p-LD4 and I3-01-LD7 showed the
169 highest NP yield among various NP-LD combinations. Adding PADRE increased the NP yield by
170 5.2- to 8.6-fold relative to the wildtype NPs, measured by ultraviolet (UV) absorbance at 280 nm.
171 I3-01v9, a variant of I3-01 (*27*), further improved NP yield by 24% based on the UV value. Seven
172 SEC-purified NPs were analyzed by sodium dodecyl sulfate–polyacrylamide gel electrophoresis
173 (SDS-PAGE) under reducing conditions (**Fig. 1D**). E2p and I3-01 registered higher bands than FR
174 on the gel (~150 kDa). These seven NP samples were then analyzed by blue native polyacrylamide
175 gel electrophoresis (BN-PAGE) (**Fig. 1E**). While FR displayed a distinctive NP band, none of the
176 E2p and I3-01 NPs migrated down from the chambers due to their large size. The SEC-purified
177 FR, E2p-LD4-PADRE (E2p-L4P), and I3-01v9-LD7-PADRE (I3-01v9-L7P) were visualized by
178 negative stain EM, which showed an array of trimeric spikes on the surface of well-formed NPs

179 (**Fig. 1F**). Thermostability was assessed by differential scanning calorimetry (DSC) (**Fig. 1G**, **Fig.**
180 **S1A**). The melting temperature (T_m) of the three NPs was in the range of 66.9-68.3°C, comparable
181 to, but slightly lower than, the T_m of the BG505 UFO trimer (68.4°C) (*27*). The multilayered E2p
182 NP displayed a second peak in the thermogram (T_{m2} = 74.0°C), suggesting a stepwise unfolding
183 process upon heating. The particle size distribution was characterized by dynamic light scattering
184 (DLS) using a Zetasizer (**Fig. 1H**, **Fig. S1B**). Ferritin and I3-01v9 had an average particle size of
185 43.7 and 50.8 nm, respectively, whereas E2p displayed a wide distribution (50.8-68.7 nm).

186 The in vitro assessment of EBOV GP-NP (*92*) and HIV-1 Env-NP constructs demonstrated
187 advantages of multilayered protein NPs. In this study, FR, E2p-L4P, and I3-01v9-L7P were used
188 to present the BG505 UFO trimer as particulate HIV-1 immunogens (**Fig. S1C**). DSC and DLS
189 suggested that the multilayered E2p may adopt two distinct states in solution. Nonetheless, the two
190 multilayered SApNPs provide a general platform for designing VLP vaccines.

191 **Cryo-EM analysis of multilayered E2p and I3-01v9 NPs displaying the BG505 UFO trimer**

192 Cryo-EM played an essential role in the determination of high-resolution structures of native-like
193 Env trimers (*47-49*). Recently, cryo-EM was used to characterize 2c-NPs that display diverse Env
194 trimers (*99-102*). In most cases, nanometer resolution was obtained for the NP backbone, with 4-
195 7 Å resolution achieved for the displayed trimers after localized reconstruction (*100, 101*). Here,
196 we characterized the two multilayered BG505 UFO trimer-presenting 1c-SApNPs by cryo-EM.

197 Prior to cryo-EM, the PGT145/SEC-purified BG505 UFO trimer-presenting E2p-L4P and
198 I3-01v9-L7P NP samples were analyzed by negative stain EM to confirm their homogeneity (**Fig.**
199 **S2A**). In the micrographs, most NPs displayed appropriate size and morphology with only minimal
200 quantities of free trimers and partially assembled/disassembled particles. We then applied cryo-

201 EM to characterize the two NP immunogens (**Fig. 2**), with the data processing protocol described
202 in the Methods section (*100, 101*) and data acquisition parameters listed in **Table S1**. The BG505
203 UFO trimers are attached to the E2p and I3-01v9 scaffolds using peptide linkers (**Fig. S1C**). Due
204 to conformational flexibility, the antigen-corresponding signal (or density) was scattered in the 2D
205 classes and initial 3D maps (**Fig. 2A-B**, top left). Consequently, we were unable to reconstruct
206 high-resolution maps of full BG505 UFO trimer-presenting E2p-L4P and I3-01v9-L7P NPs. To
207 overcome this problem, we applied a previously developed data processing method, in which two
208 flexibly linked entities (i.e., the NP scaffold and Env trimer here) are analyzed independently
209 (*100*). The resulting maps are represented as a transparent gray mesh (**Fig. 2A-B**). The E2p-L4P
210 NP consists of the E2p shell (based on dihydrolipoyl transacetylase, PDB ID: 1B5S (*103*)), LD4
211 layer (PDB ID: 2MG4), and PADRE core (**Fig. 1B**). Focused refinement of the NP core converged
212 on the E2p shell, resulting in a 3.7 Å EM map; and the E2p model was then relaxed into the map
213 (**Fig. 2A**, right). The resulting structure displayed excellent agreement with the crystal structure of
214 this bacterial enzyme (*103*) with a C_α RMSD of 0.9 Å, suggesting a negligible effect of the surface-
215 displayed trimers and encapsulated LD4 layer and PADRE core on particle assembly. Although
216 additional density at the core of the NP and along the five-fold axes was observed in the EM map,
217 attempts to resolve their structures were unsuccessful (**Fig. S2B-C**). Therefore, although LD4 and
218 PADRE can significantly improve NP expression (**Fig. 1C**), they appear to have a highly flexible
219 structure. Based on the EM data, the LD4s may not assemble into a tightly knit shell as depicted
220 by computational modeling (**Fig. 1B**) and likely interact with each other in a less well-organized
221 fashion. The I3-01v9-L7P NP exhibited inherent flexibility due to the 10-aa GS linkers connecting
222 the surface trimers and NP backbone, resulting in relatively low-resolution EM maps. Nonetheless,

223 good fits were obtained by docking the structures of I3-01 (PDB ID: 5KP9 (*104*)) and BG505 UFO
224 trimer (PDB ID: 6UTK (*98*)) into the corresponding maps (**Fig. 2B**).

225 Altogether, cryo-EM confirmed the correct assembly of two multilayered 1c-SApNPs and
226 native-like structural features of surface-displayed BG505 UFO trimers. Given the wide particle
227 size distribution (**Fig. 1H**), we speculate that both our cryo-EM model and the previously reported
228 crystal structure (*103*) captured the ground state of E2p, in which the N-terminal loop (A184-S203)
229 is packed against the NP surface and E2p adopts the most compact NP conformation.

230 **Site-specific glycan analysis of BG505 UFO immunogens with wildtype and modified glycans**

231 The glycan shield is a defense mechanism used by HIV-1 to escape antibody neutralization (*4*).
232 However, the identification of glycan-reactive bNAbs (*6*) suggests that it can be exploited as a
233 vaccine target (*32, 33, 36*). The structure of the glycan shield has been extensively characterized
234 to facilitate rational vaccine design (*31*). Here, we determined the site-specific glycan profiles for
235 BG505 UFO trimers and NPs using LC-MS and a previously established protocol (*27, 71*).

236 Wildtype BG505 UFO Env glycosylation (**Fig. 3A**, **Fig. S3A**) is consistent with previous
237 reports on other BG505 Envs (*27, 38*). The trimer-associated mannose patches (TAMPs) at N156,
238 N160, N276, and N301 present primarily oligomannose-type glycans, suggesting correct folding
239 of the Env-NP fusion protein. This processing state is conserved across all samples, indicating that
240 particulate display does not disrupt glycan processing near the trimer apex. The intrinsic mannose
241 patch (IMP) around N332 consists of predominantly $Man_9GlcNAc_2$ glycans (*27, 38*). This pattern
242 was observed for all samples tested, demonstrating that the presentation of this glycan supersite is
243 unaffected by multivalent NP display. Complex-type glycans can be found at gp120 N88, N185e,
244 N301/N355 (although high mannose predominates), N398, N462, and across the N611, N618, and
245 N637 glycans on gp41 (**Fig. S3A**) (*27, 38*). Several potential *N*-linked glycosylation sites (PNGS)

246 lack an attached glycan at a proportion of the sites. For example, N133, N137, N185e, and N197
247 on gp120 are underoccupied, similar to the BG505 SOSIP trimer (*50*). Treatment with swainsonine
248 did not enrich hybrid-type glycans as expected from glycosidase inhibition, with a nearly identical
249 glycan profile to the wildtype trimer (**Fig. 3A**, **Fig. S3B**). Treatment with kifunensine produced
250 predominantly $Man_9GlcNAc_2$ glycans at most sites, with the exception of certain sites that were
251 still occupied by $Man_{5\text{-}8}GlcNAc_2$ due to mannosidase trimming (**Fig. 3A, Fig. S3C**).

252 BG505 UFO trimer-presenting SApNPs behaved similarly in terms of glycan processing
253 and occupancy (**Fig. 3A**, **Fig. S3D-F**). Moderate differences were noted for N133 and N137, where
254 FR is less occupied than E2p and I3-01v9, whereas the same FR sample is more occupied at N185h
255 compared to all other samples. However, soluble trimers and SApNPs showed markedly different
256 glycan profiles. Variations in glycan occupancy were noted for N133, N137, N185e, N185h and
257 N197 on gp120. Trimers were less occupied than SApNPs at all four glycan sites on gp41. This
258 pattern was most pronounced for N625, showing a ~50% increase in occupancy for three SApNPs.
259 Since glycan occupancy normally decreases toward the C terminus (*105*), a possible explanation
260 is that the NP subunit in effect shifts the relative position of gp41 and becomes the new C terminus
261 of the Env-NP fusion protein. Nevertheless, the increased glycan occupancy on gp41 will likely
262 be beneficial and diminish the elicitation or binding of nNAbs to the gp41 base and perhaps the
263 NP backbone. The processing of oligomannose-type glycans also differs between soluble trimers
264 and NPs, especially for sites outside the mannose patches. Two gp120 sites, N88 and N462, which
265 present complex-type glycans on soluble trimers, are less processed on NPs (e.g., N88 shifts from
266 25% to 90% oligomannose-type glycans). Restricted glycan processing was also observed for the
267 gp41 sites located proximal to the base of the NP-displayed Envs. The glycan presented at these
268 gp41 sites is $Man_5GlcNAc_2$, not unprocessed $Man_9GlcNAc_2$ or a complex-type glycan.

269 Endoglycosidase H (endo H) cleaves the chitobiose core of oligomannose- and hybrid-type
270 glycans and leaves a single GlcNAc residue attached to the asparagine. Endo H has been used in
271 the glycan analysis of diverse HIV-1 Envs (*39*). Here, the PGT145/SEC-purified E2p and I3-01v9
272 SApNPs were treated by endo Hf (a fusion of endo H and maltose-binding protein [MBP]) at 25°C
273 for 5 hours and purified again by SEC (**Fig. 3B**). Due to the significant difference in their molecular
274 weights, endo Hf appears as a well-separated peak in the SEC profile. Reducing SDS-PAGE
275 showed lower bands for the E2p and I3-01v9 SApNPs after endo H treatment (**Fig. 3C**), with the
276 structural integrity of glycan-trimmed SApNPs confirmed by negative stain EM (**Fig. 3D**).
277 Comparable T_m values from DSC suggest that glycan trimming has little to no effect on the
278 thermostability of SApNPs (**Fig. 3E**). Lastly, the glycan-trimmed and then SEC-purified SApNPs
279 were analyzed by LC-MS, showing the conversion of most oligomannose- and hybrid-type glycans
280 to a single GlcNAc residue (**Fig. 3F**, **Fig. S3G-H**). However, a rapid enzyme-linked
281 immunosorbent assay (ELISA) using an MBP-specific mouse antibody detected residual endo Hf
282 in SEC-purified SApNPs (**Fig. S3I**), which might still be able to trim glycans off the Env peptides
283 during LC-MS. To this end, reducing SDS-PAGE was used to analyze SApNPs treated with endo
284 H at 25°C *vs.* 37°C after 100°C denaturation (**Fig. 3G**). The denatured material showed the lowest
285 band on the gel, suggesting that some glycans are protected by the Env structure.

286 **Antigenicity of BG505 UFO immunogens with wildtype and modified glycans**

287 Native-like Env trimers of diverse origins that contain the modified $HR1_N$ bend or full UFO/UFO-
288 BG designs have been assessed against panels of bNAbs and nNAbs (*26-28*). Here, BG505 UFO
289 trimers and SApNPs with wildtype and modified glycans were tested for antibody binding using
290 bio-layer interferometry (BLI). The previously established 19-antibody panel (*27*) was extended

291 to include human bNAbs 438-B11 and VRC34, which target the N332 supersite (*98*) and FP (*106*),
292 respectively, and a potent mouse NAb, M4H2K1, which binds the C3/V4 region (*71*).

293 The peak antibody-binding signals were summarized according to immunogen valency
294 (trimer *vs.* NP) and glycan treatment (wildtype *vs*. kifunensine *vs.* endo H) (**Fig. 4A** and **Fig. S4**).
295 Analytical sensors were used for soluble trimers in the Octet experiments (**Fig. 4A**, top). Overall,
296 the wildtype BG505 UFO Env preferentially bound to (b)NAbs and not nNAbs, with the exception
297 of 19b and 446-52D, which target the immunodominant V3 tip (**Fig. S4A**). Kifunensine treatment
298 reduced Env binding to (b)NAbs that either interact with, or require the accommodation of, glycans
299 (**Fig. S4B**). PGT151, a bNAb that interacts with complex-type glycans at N611 and N637 (*47,*
300 *107-109*), showed undetectable binding to the BG505 UFO Env that displays unprocessed glycans
301 at these two sites. VRC01 binding was made more difficult by the modified glycan barrier around
302 the CD4bs due to the inhibition of ER α mannosidase I in CHO cells. Endo H treatment resulted
303 in an overall reduction of Env binding to glycan-reactive (b)NAbs (**Fig. S4C**). Compared with the
304 apex bNAbs, glycan trimming had a less severe but still noticeable impact on bNAbs to the glycan-
305 V3 supersite (e.g., PGT121 and PGT128), which interact with the GDIR motif and high-mannose
306 glycans at N332 and N301 (*44, 48, 110*). PGT151 barely recognized the glycan-trimmed BG505
307 UFO Env. Endo H treatment largely retained accessibility of the CD4bs to the VRC01 bNAb (*111,*
308 *112*) upon trimming of the glycan barrier surrounding this proteinaceous surface.

309 Antigenicity was then determined for three SApNPs displaying wildtype and modified Env
310 glycans, with respective trimers included as a control (**Fig. 4A**, bottom). The quantitation sensors
311 were utilized in these Octet assays to measure the avidity effect (*91, 92*). Wildtype SApNPs (**Fig.**
312 **S4D-G**) bound at elevated levels to (b)NAbs that target the V2 apex (×2.5-4.7), N332 supersite
313 (×2.0-3.9), and CD4bs (×1.4-1.6) and at reduced levels to (b)NAbs that recognize the FP (×0.4-

314 0.6) and gp120/gp41 interface (×0.2-0.7). When tested against nNAbs, enhanced binding was only
315 observed for the V3 tip (×2.6-4.0) but not the non-neutralizing CD4bs, CD4-induced (CD4i), and
316 gp41 epitopes. Thus, the multivalent display can exert a positive influence, as well as structural
317 constraints, on antibody recognition of an Env epitope depending on the location and accessibility
318 of this epitope on the NP surface (*27, 88, 100, 101*). Notably, the wildtype SApNPs only displayed
319 a moderate increase in VRC01 binding with a slow on-rate, suggesting the CD4bs is more occluded
320 compared to the V2 apex and glycan-V3 supersite on the NP surface. SApNPs bearing unprocessed
321 $Man_9GlcNAc_2$ glycans exhibited similar antigenic profiles (**Fig. S4H-K**) to wildtype SApNPs,
322 showing slightly lower binding signals across the antibody panel. Similar to the trimer presenting
323 unprocessed glycans, no PGT151 binding was observed, consistent with the specificity of PGT151
324 for complex-type glycans at N611 and N637. A similar but less severe effect was noted for VRC34,
325 which interacts with the N terminus of FP and the complex-type N88 glycan (*106*). Endo H-treated
326 SApNPs (**Fig. S4L-O**) demonstrated unique antigenic profiles, with markedly improved VRC01
327 binding (×2.0-2.3). Slightly lower binding signals were observed for most glycan-specific (b)NAbs
328 with the exception of two. PG16 binds to a high-mannose glycan at N160 and a hybrid-type glycan
329 at N173 (*41*). While the wildtype SApNPs bound to PG16 with signals 3.4-4.6-fold relative to the
330 trimer, glycan trimming showed a fold change of 19-25. PGT135 binding requires $ManGlcNAc_2$
331 at N386, $Man_6GlcNAc_2$ at N332, and $Man_8GlcNAc_2$ at N392 (*113*). The glycan-trimmed SApNPs
332 showed higher PGT135-binding signals than the wildtype SApNPs, 2.3-2.8 and 2.0-2.4-fold with
333 respect to their trimers. PGT151 binding was barely detectable for three SApNPs, but increased
334 binding was observed for another interface bNAb, 35O22 (*114*), and for the FP bNAb, VRC34
335 (*106*), due to the increased epitope accessibility after endo H treatment. Two nNAbs to the V3 tip,
336 19b and 446-52D, bound to glycan-trimmed SApNPs at comparable levels to wildtype SApNPs.

337 Negative stain EM was utilized to characterize bNAb interactions with the glycan-trimmed
338 BG505 UFO trimer (**Fig. 4B**, **Fig. S4P**). PGT128 binds the V3 base and high-mannose glycans at
339 N295 (absolutely required) and N301 or N332 (*44, 48, 115*). Previous structures suggest that the
340 mannose moieties of these glycans serve as anchors to orientate and stabilize the interaction with
341 PGT128 Fab, which binds the "GDIR" motif with the HCDR2 and HCDR3 tips (*44, 48*). The
342 removal of mannose groups at these three sites may destabilize PGT128 and affect its angle of
343 approach. Indeed, one endo H-treated BG505 UFO trimer could bind to one to three PGT128 Fabs,
344 with less resolved density for the bound Fabs in the 2D class averages (**Fig. 4B**). Comparison with
345 the cryo-EM model of the BG505 SOSIP/PGT128 complex (EMDB-3121 (*48*)) confirmed that
346 PGT128, albeit with greater flexibility, still bound to the same epitope. However, the angle of
347 approach could not be determined in this EM analysis. VRC01 targets a large proteinaceous area
348 of the CD4bs protected by a ring of glycans with the N276 glycan positioned as a critical barrier
349 to the development of VRC01-class bNAbs (*111, 112, 116, 117*). Trimming the glycan shield can
350 in principle improve the CD4bs recognition by VRC01-class bNAbs. Indeed, we obtained a 12.4
351 Å-resolution 3D model of the BG505 UFO/VRC01 complex, which superimposes well with the
352 previous EM models of BG505 SOSIP/VRC01 complexes (*118, 119*) (**Fig. 4C**).

353 BLI demonstrated a cross-panel improvement in bNAb binding to SApNPs compared with
354 soluble trimers, consistent with our previous studies (*27, 89, 91, 92*). Glycan trimming retained
355 bNAb binding to major glycan epitopes on the NP-displayed Env and improved recognition of the
356 CD4bs by VRC01-class bNAbs. Negative-stain EM confirmed that bNAbs PGT128 and VRC01
357 could still recognize their epitopes on the glycan-trimmed Env trimer. Altogether, glycan-trimmed
358 SApNPs may provide more effective immunogens due to more balanced epitope accessibility.

359 **Assessment of HIV-1 UFO Env immunogens with wildtype glycans in mice and rabbits**

360 While BG505 SOSIP and $HR1_N$-redesigned trimers were ineffective in NAb induction in mice (*27,*
361 *55*), a reengineered I3-01 NP displaying the $HR1_N$-redesigned trimer elicited potent tier 2 murine
362 NAbs to the C3/V4 epitope (*27, 71*). Recently, an autologous tier 2 NAb response was induced in
363 mice by iron oxide NP (IO-NP)-attached SOSIP trimers (*96*) and a DNA trimer vaccine (*70*), both
364 using long-boost intervals. In contrast to the challenges encountered in mice, native-like trimers
365 can readily elicit tier 2 NAbs in rabbits but mostly to specific holes in the glycan shield (*56*).

366 We first assessed wildtype BG505 UFO immunogens formulated with three commonly
367 used adjuvants in mice. We adopted an immunization protocol used in our previous vaccine studies
368 (*27, 89, 91, 92, 120*) (**Fig. 5A**). In brief, groups of eight mice were immunized four times at 3-
369 week intervals. SApNPs (30 μg/dose) were formulated with AddaVax (AV), aluminum phosphate
370 (AP), and aluminum hydroxide (AH). A non-adjuvanted group and a heterologous AV×2/AP×2
371 group were included as a negative control and for comparison, respectively. We performed TZM-
372 bl neutralization assays using purified mouse immunoglobulin G (IgG) from the last time point,
373 week 11 (**Fig. 5B**, **Fig. S5A**). Without adjuvant, both SApNPs failed to elicit tier 2 NAb responses
374 to BG505.T332N but I3-01v9 appeared to be more effective against a tier 1 clade B virus, SF162
375 (**Fig. S5A**, middle). E2p mixed with AV or AP and I3-01v9 mixed with AP or AH each showed
376 tier 2 NAb induction in one of the eight mice, with half maximal inhibitory concentration (IC_{50})
377 values of 200, 90, 21 and 36 μg/ml, respectively (**Fig. S5A**, top). However, switching the adjuvant
378 during the immunization proved ineffective. Adjuvanted SApNPs induced a robust tier 1 NAb
379 response (**Fig. 5A**, middle). When tested against a BG505 variant with a C3/V4 epitope knockout
380 mutation, I396R (**Fig. 5C, Fig. S5B**), reduced neutralization (by 45-82%) was noted for all four
381 mice that generated tier 2 NAb responses, suggesting that M4H2K1-like NAbs (*71*) may be present
382 in the serum. The remaining neutralizing activity may be attributed to C3/V5 (*70*) and other Env

383 epitopes. As a negative control, purified IgG from three tier 2 positive mice was tested against
384 pseudoparticles (pps) bearing the murine leukemia virus (MLV) Env, MLV-pps. Nonspecific
385 MLV-pp neutralization was not detected (**Fig. S5A**, bottom). Borderline neutralization of clade A
386 398F1 was observed in the TZM-bl assays against a 12-virus global panel (**Fig. S5C**).

387 We then tested an extended set of wildtype UFO immunogens in rabbits. Briefly, groups
388 of six rabbits were immunized three times at weeks 0, 8, and 24 with blood draws at 12 time points
389 throughout immunization (**Fig. 5D**). All antigens (100 μg per dose) were mixed with AV except
390 for I3-01v9 SApNPs, which were paired with AP. While the BG505 UFO trimer and its SApNPs
391 (FR, E2p, and I3-01v9) were the main focus of this rabbit study, a cocktail mixing equal amounts
392 (33 μg per dose) of SApNPs that present clade A BG505 UFO, clade B H078.14 UFO-BG, and
393 clade C CH505 UFO-BG trimers was created for each NP platform, resulting in seven groups in
394 total. Longitudinal NAb responses of rabbit sera to BG505.T332N, as measured by 50% inhibitory
395 dilution (ID_{50}) titers, were examined (**Fig. 5E**). While the overall kinetics were similar across all
396 groups, the cocktail groups exhibited an NP platform-dependent pattern in their NAb responses to
397 BG505.T332N. Reducing the BG505 dose to one-third for each cocktail formulation had negative
398 and negligible effects for FR and I3-01v9, respectively. The tier 2 NAb response became detectable
399 at week 10 (**Fig. 5E**, above dotted line). The ID50 titers reached the highest point at week 26, with
400 both I3-01v9 groups outperforming the BG505 UFO trimer, FR cocktail, and both E2p groups
401 (**Fig. 5E**, **Fig. S5D**). The advantage of particulate display was also evident when a tier 1 clade B
402 SF162 was tested, with a detectable response first observed at week 4 for the two I3-01v9 groups
403 (**Fig. S5E**). Rabbit samples at weeks 0, 2, 10, and 26 displayed no MLV-pp neutralization (**Fig.**
404 **S5F**). We then investigated the prevalence of glycan hole NAbs in the total polyclonal NAb
405 response. Plasma neutralization against four BG505.T332N mutants, Q130N, S241N, P291T, and

406 T465N as previously described (*71*), was tested for select samples (**Fig. 5F**). Filling glycan holes
407 could partially deplete neutralizing activity, consistent with our previous findings (*71*). The trimer
408 group exhibited a more visible reduction of percent neutralization against the 130/241/289 glycan
409 mutants, whereas particulate display expanded the autologous NAb response, with the glycan hole
410 at position 465 becoming a more prevalent target of the response. Finally, all SApNPs failed to
411 generate a strong cross-clade NAb response to other tier 2 isolates in a 12-virus global panel and,
412 in particular, no advantage in breadth was seen for the Env mixture vaccines (**Fig. S5G**).

413 **Assessment of BG505 UFO Env immunogens with trimmed glycans in mice and rabbits**

414 We investigated how glycan trimming affects Env-elicited NAb responses in mice and rabbits by
415 testing a homologous regimen ("regimen 1") with glycan-trimmed immunogens in all doses and a
416 heterologous prime-boost regimen ("regimen 2") with glycan-trimmed and wildtype immunogens
417 in doses 1-2 and 3-4, respectively (**Fig. 6A**). The ExpiCHO-produced BG505 UFO trimer was
418 treated with endo Hf and purified by SEC and an additional resin step (see Methods). Eight and
419 five CHO-K1 cell clones were developed to stably express BG505 UFO trimer-presenting E2p and
420 I3-01v9 SApNPs, respectively. The SApNPs produced by individual cell clones were structurally
421 evaluated by negative-stain EM (**Fig. S6A**) and then pooled for endo H treatment.

422 In the mouse study, groups of eight BALB/c mice were immunized four times, at three-
423 week intervals. The BG505 UFO trimer and SApNPs (30 μg per dose) were formulated with AV
424 or AP adjuvants, with the immunization experiment repeated for some formulation/regimen groups
425 to confirm their immunogenicity. The frequency of vaccine responders (FVR, the ratio of subjects
426 that generate an autologous tier 2 NAb response) was calculated for comparison. Overall, glycan
427 trimming (GT) by endo H substantially improved the FVR for the UFO trimer (FVR up to 86%;
428 **Fig. 6B**, left), E2p SApNP (up to 88%; **Fig. 6B**, middle), and I3-01v9 SApNP (up to 50%; **Fig.**

429 **6B**, right), in addition to the improved IC_{50} values and less within-group variation compared with
430 the equivalent formulations using wildtype immunogens (**Fig. S6B-D**). The AP adjuvant was
431 found to be associated with a higher FVR regardless of the Env immunogens tested, while regimen
432 2 (two GT primes + two WT boosts) appeared to have a slight advantage for the two SApNP/AP
433 formulations. To be consistent with wildtype Env immunization (**Fig. 5**), four SApNP groups that
434 tested the E2p/AV and I3-01v9/AP formulations in regimens 1 and 2 were selected for further
435 analysis. Two UFO trimer/AP groups and two E2p/AP groups (regimen 1 and 2 for both) were
436 included in some analyses for comparison. Similar to the improved neutralization against tier 2
437 clade A BG505.T332N, glycan trimming also increased the tier 1 NAb response against clade B
438 SF162 while showing no nonspecific MLV reactivity in TZM-bl assays (**Fig. S6B-D**). We then
439 tested a BG505.T332N variant with the C3/V4 epitope knockout mutation on the aforementioned
440 eight groups (**Fig. 6C, Fig. S6E**). Interestingly, most mice from the SApNP groups escaped this
441 immunodominant glycan epitope, in contrast to those in the trimer groups, which still targeted the
442 C3/V4 epitope. The vaccine responders from the E2p/AV and I3-01v9/AP groups, subject to IgG
443 sample availability, were further tested against a 12-virus global panel (**Fig. S6F**). The IC_{50} titers
444 showed borderline neutralization against 398 F1 (clade A) and CNE8 (CRF01 AE), while the less
445 stringent IC_{30} titers confirmed the advantages of the I3-01v9/AP over E2p/AV formulation.

446 A rapid screening study was performed in rabbits following the mouse protocol (**Fig. 6A**).
447 Four groups of six rabbits were immunized to compare the E2p/AV and I3-01v9/AP formulations
448 each combined with regimens 1 and 2. While purified IgG at week 0 exhibited a clean background
449 (**Fig. S6G**), purified IgG at week 11 neutralized autologous tier 2 BG505.T332N with patterns
450 largely resembling the mouse study. (**Fig. 6D, Fig. S6H**). Namely, BG505 I3-01v9 formulated
451 with AP outperformed E2p paired with AV, and, between the two I3-01v9 groups, regimen 2 was

452 slightly more effective than regimen 1 with a higher FVR (4 *vs.* 3 respectively; **Fig. 6E**). Similar
453 to the mouse study, purified IgG samples from weeks 0 and 11 were also tested in TZM-bl assays
454 against tier 1 clade B SF162 and the negative control, MLV (**Fig. S6G and H**). We then analyzed
455 the prevalence of glycan hole NAbs in select rabbit samples from each group (**Fig. 6F, Fig. S6I**).
456 Interestingly, purified IgG samples from the BG505 I3-01v9 regimen 2 group exhibited notably
457 more complete escape from the four glycan holes, supporting our notion that glycan trimming may
458 offer a general solution to overcome glycan holes in Env immunization. Lastly, select rabbit IgG
459 samples were tested against the 12-virus global panel (**Fig. S6J**), but the IC_{50}/IC_{30} titers showed
460 less pronounced cross-clade NAb responses compared with the mouse data (**Fig. S6F**).

461 Our results revealed the importance of glycan trimming in improving the immunogenicity
462 of HIV-1 Env vaccines in both trimer and NP forms. The 50-86% FVR noted for glycan-trimmed
463 trimer groups was rather surprising, given the past failures in tier 2 NAb elicitation by stabilized
464 BG505 trimers (*27, 55*) and difficulties in improving it (*70, 96*). Glycan trimming not only enabled
465 antibody access to a broad range of epitopes that would otherwise be occluded by the glycan shield
466 but also minimized glycan-related immunodominance (e.g., glycan holes and clusters). Boosting
467 with wildtype Env glycans may fine-tune NAb responses induced by the glycan-trimmed Env.

468 **Distribution, trafficking, and retention of HIV-1 Env trimers and SApNPs in lymph nodes**

469 Following a similar protocol (*120*), we studied the in vivo behavior of the wildtype BG505 UFO
470 trimer and SApNPs E2p and I3-01v9 to understand how they interact with immune cells and induce
471 immune responses. The endo H-treated I3-01v9 SApNP was included to probe the effect of glycan
472 trimming on the immunological characteristics of SApNPs. To induce a robust humoral response,
473 these vaccines must be transported to lymph nodes, accumulate in follicles, retain and present
474 native-like Env, and engage B cell receptors (BCRs) (*121-123*). Here, we first examined the

475 transport and distribution of BG505 UFO trimer-presenting SApNPs in lymph nodes via footpad
476 injections (4×10 μg/footpad). Mice were euthanized at 12 hours after a single-dose injection to
477 isolate brachial and popliteal sentinel lymph nodes for histological analysis. Immunostaining by
478 human bNAbs VRC01(*112*), PGT124 (*124*), and PGDM1400 (*125*) was used to detect the BG505
479 UFO Env presented on the SApNPs in lymph node tissue sections (**Fig. 7A**). Consistent with our
480 previous studies of SARS-CoV-2 spike SApNPs (*120*) and ovalbumin-conjugated gold NPs (*126*),
481 BG505 UFO trimer-presenting SApNPs accumulated in the centers of lymph node follicles at 12
482 hours after a single-dose injection (**Fig. 7A**, images on the left; **Fig. 7B**, schematics on the right).
483 Immunostaining images obtained from all three bNAbs demonstrate similar distributions in lymph
484 nodes (**Fig. 7A-B**, **Fig. S7A-B**). VRC01 (*112*) was selected to study the trafficking of four BG505
485 Env immunogens in lymph nodes because of its optimal signal-to-noise ratio.

486 We next determined the trafficking and retention patterns of the BG505 UFO trimer and
487 three SApNPs in lymph node follicles 30 minutes to 8 weeks after a single-dose injection (4×10
488 μg/footpad) (**Fig. 7C**). The injected dose was normalized to 40 μg of protein per mouse, or 10 μg
489 protein per footpad. Histological images indicated that both the BG505 UFO trimer and SApNPs
490 were transported into lymph nodes and accumulated in the subcapsular sinus within 30 minutes
491 (**Fig. 7C**). The BG505 UFO trimer was trafficked into lymph node follicles at 2 hours and cleared
492 within 12 hours. In contrast, the three SApNPs first appeared in lymph node follicles at 2 hours,
493 further accumulated at 12 hours, peaked at 48 hours, and remained detectable over a period of 5-8
494 weeks (**Fig. 7C**). The VRC01-stained area was quantified in a time-dependent manner, showing a
495 ~420-times longer retention for the three SApNPs *vs.* the soluble trimer (**Fig. 7C-D**). The area
496 under the curve (AUC) suggested that the exposure of SApNPs in lymph node follicles is 20-32
497 times higher than the soluble trimer (**Fig. 7E**). At 48 hours, a significantly greater accumulation,

498 46-66 times, was found when the BG505 UFO trimer was presented multivalently (**Fig. 7F**). These
499 findings are consistent with our previous studies (*120, 126*), in which small 5-15 nm particles are
500 cleared from the follicles within 48 hours but large 50-100 nm particles can persist for weeks. The
501 BG505 UFO trimer-presenting SApNPs displayed distinctively long retention compared with the
502 SARS-CoV-2 spike SApNPs (5-8 weeks *vs.* ~2 weeks), which correlates well with their antigen
503 thermostability (T_m), 68.4°C for the BG505 UFO Env *vs.* 47.6°C for the S2GΔHR2 spike (*27, 91*),
504 respectively. We also noted that trimming the glycan shield had very little impact on SApNP
505 distribution, trafficking, and retention in lymph nodes, in contrast to a recent report (*95*).

506 Antigen retention and presentation in lymph node follicles are critical for B cell stimulation
507 and affinity maturation through GC reactions (*121, 127*). FDCs form a network structure and play
508 roles in antigen collection and presentation in the center of lymph node follicles (*122, 123*). FDCs
509 retain soluble antigens, immune complexes, virus-like particles, viruses, and bacteria, and induce
510 GC initiation and maintenance (*122, 126, 128-130*). Based on our previous studies (*120, 126*), we
511 hypothesized that FDC networks are the major resident places for these BG505 Env immunogens.
512 To test this hypothesis, we injected mice with the UFO trimer and three SApNPs through footpads
513 (4×10 μg/footpad). Mice were sacrificed to collect sentinel lymph nodes at the peak of SApNP
514 accumulation (48 hours) and other timepoints (30 minutes to 8 weeks) after a single-dose injection
515 (**Fig. 7G**, **Fig. S7C-I**). Lymph node tissues were stained with bNAb VRC01 (*131*) for BG505 Env
516 (white), anti-CD21 antibodies for FDCs (green), and anti-CD169 antibodies for subcapsular sinus
517 macrophages (red). The signals of SApNPs colocalized with FDC ($CD21^+$) networks in lymph
518 node follicles at 48 hours (**Fig. 7G**), confirming the crucial role of FDC networks in mediating the
519 accumulation and retention of various Env immunogens in lymph node follicles.

520 **How HIV-1 Env SApNPs interact with FDCs and phagocytic cells in lymph nodes**

521 FDC networks create areas of high antigen density in lymph node follicles to facilitate effective
522 BCR crosslinking, B cell activation, and GC reactions (*77, 121, 122*). Our TEM analysis revealed
523 that FDCs can align ovalbumin-conjugated gold NPs (*126*) and SARS-CoV-2 spike-presenting
524 SApNPs (*120*) on their surfaces or dendrites through interactions between complement protein 3
525 (C3) and complement receptor 2 (CR2) (*126*). B cells are embraced by long FDC dendrites to
526 maximize interactions between multivalently displayed antigens and BCRs (*120, 126*). Here, we
527 studied the interface between FDC dendrites and B cells to better understand how FDCs process
528 HIV-1 SApNPs formulated with adjuvants to engage B cells. We injected mice with AV- or AP-
529 formulated SApNPs through their hind footpads (2×50 μg/footpad) (**Fig. 8A-F**, **Fig. S8A-V**). Fresh
530 popliteal sentinel lymph nodes were isolated at 2, 12 and 48 hours after a single-dose injection and
531 processed immediately for TEM analysis. The TEM images showed that FDC dendrites embrace
532 and interact with B cells in lymph node follicles (**Fig. 8A-C**, **Fig. S8A-M**). A large number of
533 intact E2p SApNPs (round-shaped granules, yellow arrows) and AV particles (oil-in-water nano-
534 emulsion of ~150 nm in size, green arrows) were aligned on FDC dendrites and B cell surfaces at
535 2, 12, and 48 hours (**Fig. 8A**, **Fig. S8A-C**). Notably, few E2p SApNPs were internalized in the
536 endolysosomes of B cells at 48 hours (**Fig. S8C**). I3-01v9 SApNPs (yellow arrows), wildtype and
537 glycan-trimmed alike, were similarly aligned on the FDC dendrites and B cell surfaces at 2, 12,
538 and 48 hours, without the colocalization of AP adjuvants (**Fig. 8B-C**, **Fig. S8D-I**).

539 Phagocytic cells, such as macrophages and dendritic cells in the subcapsular sinus and
540 medullary sinus of lymph nodes, capture large particles, immune complexes, viruses and bacteria
541 and transport them to migrating B cells and deposit them on the surface of FDCs via a complement
542 receptor-dependent mechanism (*122, 123, 132-134*). These immune cell populations also serve as
543 APCs that can further promote adaptive immunity. Here, we studied the association between

544 macrophages and adjuvanted SApNPs (**Fig. 8D-F**, **Fig. S8N-V**). E2p SApNPs and AV adjuvant
545 particles are colocalized and aligned on the surface or inside the endolysosomes of medullary sinus
546 macrophages at 2 hours (**Fig. 8D**, **Fig. S8N**). Wildtype and glycan-trimmed I3-01v9 SApNPs
547 behaved similarly to E2p SApNPs, with AP forming visible aggregates inside the endolysosomes
548 of macrophages and in the extracellular matrix (**Fig. 8E**, **Fig. S8O-U**).

549 Our results reveal how BG505 UFO trimer-presenting SApNPs associate with adjuvants in
550 the intercellular and intracellular compartments of lymph nodes. Three SApNPs showed similar
551 patterns of interaction with FDC networks, B cells, and phagocytic cells. Two common adjuvants
552 with different chemical properties, AV and AP, interact with cells in lymph nodes through different
553 immune pathways. FDC networks can retain SApNPs on long FDC dendrites and present them to
554 naïve B cells, which is an intrinsic feature independent of adjuvants (**Fig. S8J-K**).

555 **HIV-1 Env SApNPs induce more robust germinal center reactions than soluble trimers**

556 B cell somatic hypermutation, selection and affinity maturation occur in long-lived GCs and lead
557 to the formation of immune memory and development of (b)NAbs upon vaccination (*129, 135-*
558 *138*). Here, we studied whether the long-term retention of BG505 UFO trimer-presenting E2p and
559 I3-01v9 SApNPs can induce more robust and long-lived GCs in follicles than the soluble UFO
560 trimer. We first assessed GC reactions induced by wildtype I3-01v9 SApNP at 2 weeks after a
561 single-dose injection (4×10 μg/footpad). GC reactions, i.e., GC B cells ($GL7^+$) and T follicular
562 helper (T_{fh}) cells ($CD4^+Bcl6^+$), in sentinel lymph nodes were characterized by immunohistological
563 analysis. Robust GCs ($GL7^+$, red) were generated that were attached to FDC networks ($CD21^+$,
564 green) with clearly organized dark zone (DZ) and light zone (LZ) compartments in lymph node B
565 cell follicles ($B220^+$, blue) (**Fig. 9A**, left). T_{fh} cells ($CD4^+Bcl6^+$, co-labeled with cyan and red)
566 were mainly located in the LZ to support B cell affinity maturation and GC maintenance (**Fig. 9A**,

567 right). Next, we applied this analysis to the BG505 UFO-trimer and three SApNPs at 2, 5, and 8
568 weeks after a single-dose injection (**Fig. 9B**, **Fig. S9A-C**) and at 2 and 5 weeks after the boost
569 (**Fig. 9C**, **Fig. S9D, E**). Similarly, two metrics were defined to quantify GC reactions based on
570 immunohistological images: GC/FDC ratio (i.e., whether GC formation is associated with an FDC
571 network, %) and GC size (i.e., occupied area) (*120*). All four Env immunogens induced robust
572 GCs at 2 weeks after a single-dose injection (**Fig. 9B**, **Fig. S9A**). Surprisingly, the glycan-trimmed
573 I3-01v9 SApNP induced the largest GCs at 2 weeks (**Fig. 9B**). Following trimer immunization,
574 the GC/FDC ratio and GC size were low and decreased rapidly over time, whereas a single dose
575 of SApNPs generated long-lived GCs that persisted for 8 weeks (**Fig. 9B, D**, **Fig. S9C**). For the
576 soluble trimer, robust GCs can be restored after the boost (**Fig. 9C, E**, **Fig. S9D, E**). Overall, the
577 three SApNPs generated larger GCs than the soluble trimer, 2.3-4.2 times larger after one dose
578 (**Fig. 9B, D**) and 0.4-1.1 times larger after the boost (**Fig. 9C, E**), both measured at 8 weeks.

579 We next characterized GC reactions by flow cytometry. We collected sentinel lymph nodes
580 at 2, 5, and 8 weeks after a single-dose footpad injection (**Fig. 9F**, **Fig. S10A, B**) and at 2 and 5
581 weeks after the boost (**Fig. 9F**, **Fig. S10C**) (4×10 μg/injection). Fresh sentinel lymph nodes were
582 disaggregated into a single cell suspension and stained with an antibody cocktail. The GC reactions
583 were analyzed by flow cytometry. The percentage and number of GC B cells and T_{fh} cells were in
584 line with the immunohistological data (**Fig. 9A-E**). The three SApNPs outperformed the soluble
585 trimer at 2 weeks after a single-dose injection (**Fig. 9F**). Among the three SApNPs, the glycan-
586 trimmed I3-01v9 elicited the largest GC B cell and T_{fh} cell populations. For all tested immunogens,
587 GC reactions peaked at 2 weeks and declined over time. The populations of GC B cells and T_{fh}
588 cells induced by the soluble trimer were barely detectable at 8 weeks after a single-dose injection
589 (**Fig. 9F**). A boost effectively expanded the populations of GC B cells and T_{fh} cells but had little

590 effect on their percentages (**Fig. 9G**). In addition to size-dependent trafficking and retention in
591 lymph node follicles, GC reactions may also be influenced by adjuvants, considering that AV and
592 AP undergo different mechanisms of cellular interactions (**Fig. 8**). Overall, the three SApNPs
593 generated 3.4-6.6/0.7-1.8 times more GC B cells and 0.5-4.3/0.2-1.6 times more T_{fh} cells than the
594 soluble trimer at 8 weeks after the single-dose/boost injection, respectively (**Fig. 9F, G**). Together,
595 our analysis indicates that the much larger SApNPs can generate long-lived GCs in lymph nodes
596 more effectively than the soluble trimer, resulting in a strong Env-specific B cell response.

597 **DISCUSSION**

598 Over the last decade, HIV-1 vaccine research has been driven by advances in the identification of
599 bNAbs targeting diverse epitopes (*6, 7*) and development of native-like Env trimers (*12, 13*). Three
600 designs have been established as the leading Env trimer platforms, including SOSIP (*19, 29*), NFL
601 (*23, 25*), and UFO (*26, 27*). Multistage vaccine strategies that follow specific B cell maturation
602 events have been proposed and tested in knock-in mice carrying human bNAb (precursor) genes
603 (*51*). However, it is unclear whether such strategies will be relevant to human vaccination. Recent
604 HIV-1 vaccine research also received a boost from the engineering of protein particles to mimic
605 VLPs (*74-77, 80*). Various animal models have been used to assess HIV-1 Env vaccines. Although
606 rabbits can readily generate autologous tier 2 NAb responses, they mainly target strain-specific
607 holes in the glycan shield (*56*) or neoepitopes at the trimer base (*73*). The tier 2 NAb responses in
608 wildtype mice and NHPs are sporadic and often target glycan-rich regions on the Env that are
609 immunodominant in human infection (*67, 70, 71*). Although bNAb responses were occasionally
610 reported (*52, 58, 139-141*), it is unclear whether these are reproducible outcomes of a general
611 vaccine solution or coincidence. Therefore, despite all advances achieved to date, HIV-1 vaccine
612 development still faces critical challenges posed by the Env, an atypical viral antigen (*142*).

613 The glycan shield is at the heart of HIV-1 Env vaccine design (*31-36*). Ideally, an effective
614 vaccine strategy must overcome conflicting roles of Env glycans, namely, occluding NAb access
615 to conserved protein epitopes *vs.* participating in NAb-Env interactions. Here, we aimed to develop
616 such a strategy by combining our trimer stabilization (i.e., the UFO design (*26, 27*)) and particulate
617 display (i.e., the multilayered 1c-SAPNPs (*91, 92*)) platforms. The resulting BG505 UFO-E2p-
618 L4P and UFO-10GS-I3-01v9-L7P SApNPs were thoroughly evaluated both in vitro and in vivo.
619 Notably, a key element in our current vaccine strategy was glycan trimming. We hypothesized that
620 trimming structurally less essential glycans would improve epitope accessibility (e.g., CD4bs) and
621 minimize glycan-related immunodominance (e.g., strain-specific glycan holes or glycan patches),
622 while retaining Env binding to most glycan-reactive bNAbs. The success of this strategy may hinge
623 on glycan promiscuity (*115*), which allows various glycan sites and moieties to substitute for one
624 another in glycan-bNAb interactions. The avidity effect on the NP surface may further compensate
625 for weakened glycan-bNAb interactions on one trimmed Env trimer by enabling interactions with
626 surrounding Env trimers. As a result, we observed rather balanced interactions between glycan-
627 trimmed BG505 Env-SApNPs and bNAbs that target various protein and glycan epitopes (**Fig. 4**).
628 For in vivo evaluation, we used the mouse model as a primary indicator because it is inexpensive,
629 difficult, and known to generate tier 2 NAbs to epitopes that are found in human infection (*70, 71*).
630 Rabbits were tested to provide another immunogenicity readout and probe glycan holes. Most
631 common, but not the most potent (*143-145*), adjuvants were chosen because of their safety record
632 in humans. Instead of bNAb elicitation, we focused on increasing the frequency of vaccine
633 responders (FVR, defined as the ratio of tier 2 positive subjects in a group), because this is more
634 achievable and the low FVR has been a major challenge for trimer vaccines in mice, NHPs, and
635 also humans (*146*). Glycan-trimmed Env immunogens mixed with AP yielded a much higher FVR

636 in mice than the wildtype ones, 50-88% *vs.* 12.5%, with reduced glycan-related immunodominance
637 in mice and rabbits (**Fig. 6**). An in-depth mechanistic analysis provided much-needed insights into
638 the vaccine mode of action. The 5-to-8-week retention of E2p and I3-01v9 SApNPs in follicles
639 indicates sustained B cell maturation, suggesting that a longer interval between immunizations
640 should be used for these SApNPs. The identical trafficking, presentation and retention patterns for
641 I3-01v9 SApNPs with and without endo H treatment suggest that the density of mannose glycans
642 is not as critical for the follicular localization of HIV-1 NP immunogens as previously thought
643 (*95*). The stronger GC reactions and $CD4^+$ T_{fh} responses observed for the glycan-trimmed BG505
644 I3-01v9 SApNP were consistent with early studies where mannoses were immunosuppressive
645 (*147*), and the enzymatic removal of mannose moieties improved the gp120-induced IgG response
646 when formulated with alum, but not an oil-in-water adjuvant (*148*).

647 Future research may focus on several fronts. First, NAbs, as well as nNAbs, induced by
648 glycan-trimmed Env need to be mapped onto the wildtype Env surface (*63, 66*) to understand how
649 glycan trimming alters epitope targeting, as also investigated for influenza virus and SARS-CoV-
650 2 (*149, 150*). The epitope mapping of three stabilized trimers (i.e., SOSIP, NFL, and UFO) with
651 trimmed glycans may shed light on how to improve current HIV-1 trimer vaccine strategies (*146*).
652 Equally important is to investigate the degree of glycan trimming required to achieve optimal
653 immunogenicity, using high-resolution structural and/or glycan analyses. Second, the effect of Env
654 glycans on the immune system warrants a more in-depth investigation, e.g., the involvement of
655 mannose moieties in immunosuppression (*147*) *vs.* vaccine trafficking and immunogenicity (*94,*
656 *95*). Some of the critical questions (*95*) can now be answered using the tools in our mechanistic
657 analysis of SApNPs. Third, the immunization regimen requires extensive optimization. The 3-
658 week interval used in our rapid screening regimen is unsuitable for SApNPs with a retention time

659 of 5 weeks or longer. This explains why the two large SApNPs did not substantially outperform
660 the UFO trimer, as the 3-week interval would interrupt the process of generating memory B cells
661 and long-lived plasma cells and suppress the recall antibody response. A prolonged interval will
662 likely improve tier 2 NAb elicitation for the two large SApNPs. Various dose arrangements (e.g.,
663 fewer or more glycan-trimmed doses) need to be tested to optimize the prime-boost protocol. A
664 systematic comparison would be required to identify the most effective adjuvant for the two large
665 SApNPs, as shown in our SARS-CoV-2 vaccine study (*120*). The resulting vaccine formulation,
666 with an optimized regimen, could then be considered for evaluation in human trials.

667 **METHODS**

668 **Antibodies**

669 We utilized a panel of bNAbs and non-NAbs to characterize the antigenicity of various native-like
670 trimers and gp140 nanoparticles. Antibodies were requested from the NIH AIDS Reagent Program
671 (https://www.aidsreagent.org/) except for 438-B11(*98*), PGT151 (*107*), and M4H2K1 (*71*), which
672 were produced in-house together with the fragment antigen-binding (Fab) regions of PGT128 and
673 VRC01, using previously described protocols (*71*).

674 **Expression and purification of HIV-1 Env trimers and SApNPs**

675 The BG505 UFO trimer and SApNPs used for the in vitro characterization and in vivo assessment
676 of immunogens with wildtype glycans were transiently expressed in ExpiCHO cells (Thermo
677 Fisher) using a previously described protocol (*27*). Briefly, ExpiCHO™ cells were thawed and
678 incubated with ExpiCHO™ Expression Medium (Thermo Fisher) in a shaker incubator at 37°C,
679 135 rpm, and 8% CO_2. When the cells reached a density of 10×10^6/ml, ExpiCHO™ Expression
680 Medium was added to reduce the cell density to 6×10^6 ml^{-1} for transfection. ExpiFectamine™
681 CHO/plasmid DNA complexes were prepared for 100-ml transfection in ExpiCHO cells following

682 the manufacturer's instructions. Kifunensine (10 mg/L, Tocris Bioscience) and swainsonine (3.4
683 mg/L, Santa Cruz Biotechnology) were added at the time of ExpiCHO transfection to inhibit α-
684 mannosidase I and II to enrich oligomannose- and complex-type glycans, respectively. For Env
685 constructs tested in this study, 100 μg of antigen plasmid and 320 μl of ExpiFectamine^{TM} CHO
686 reagent were mixed in 7.7 ml of cold OptiPRO™ medium (Thermo Fisher). After the first feed on
687 day 1, ExpiCHO cells were cultured in a shaker incubator at 32°C, 120 rpm, and 8% CO_2 following
688 the Max Titer protocol with an additional feed on day 5 (Thermo Fisher). Culture supernatants
689 were harvested 13-14 days after transfection, clarified by centrifugation at 4000 rpm for 20 min,
690 and filtered using a 0.45 μm filter (Thermo Fisher). For the BG505 UFO trimer, Env protein was
691 extracted from the culture supernatants using a *Galanthus nivalis* lectin (GNL) column (Vector
692 Labs), whereas for all SApNPs, BG505 and non-BG505 (CH505 and H078.14) Env-fusion
693 proteins were purified using PGT145 and 2G12 columns, respectively. Trimer was purified on a
694 Superdex 200 Increase 10/300 GL column or a HiLoad 16/600 Superdex 200 PG column (GE
695 Healthcare), whereas SApNPs were characterized on a Superose 6 10/300 GL column. Protein
696 concentration was determined using UV_{280} absorbance with theoretical extinction coefficients.

697 **Generation of stable CHO cell lines expressing two BG505 UFO-Env NP vaccine candidates**
698 Stable CHO cell lines expressing BG505 UFO-E2p-L4P and UFO-10GS-I3-01v9-L7P NPs were
699 generated by the cationic lipid mediated transfection of a parental suspension culture adopted CHO
700 K1 host cell line (ATCC no. CCL-61) using bacterial artificial chromosomes (BACs) as gene
701 transfer vehicles (*151*). BAC vector modification and integration of the BG505 Env-NP expression
702 cassettes by recombineering were performed by Gen-H GmbH (Heidelberg, Germany). Parental
703 CHO K1 host cells were cultured in a 125 ml shake flask (Corning) in 20 ml CD CHO medium
704 (Gibco, Thermo Fisher) supplemented with 8 mM L-glutamine, 6.25 mg/ml phenol red and 1:100

705 Anti-Clumping Agent (Gibco, Thermo Fisher). Shaker flasks were cultivated in a humidified ISF1-
706 X incubator shaker (Kuhner) at 37°C, 125 rpm, and 5% CO_2, and multi-well plates were
707 maintained in a static incubator cabinet at 37°C and 5% CO_2. The passaging of cells for the purpose
708 of culture maintenance was performed every 3-4 days to starting cell densities of 0.3×10^6 cells/ml.
709 Per transfection, 1×10^6 cells were prepared in 1.8 ml CD DG44 medium (Gibco, Thermo Fisher),
710 5 µg BAC DNA, and 25 µg Lipofectin® (1 mg/ml; Thermo Fisher) diluted in 0.2 ml of CD DG44
711 medium, and transfection mixes were incubated for up to 48 hours in six-well plates (Greiner).
712 Following incubation, media of transfection pools were replaced with selection medium (CD CHO
713 medium + supplements and 0.5 mg/ml Geneticin sulphate (Sigma, catalog no. G418). Cultures
714 were transferred to 96-well plates (Thermo Fisher) and transfection cell pools were continuously
715 monitored for signs of cell growth and increasing viabilities, as well as BG505 Env-NP expression
716 by ELISA (NP capture: *Galanthus nivalis* lectin (GNL, Sigma) / NP detection: anti-HIV-1 gp120
717 mAb C2G12 (Polymun Scientific)). High NP expressing cell pools were expanded to 50 ml of
718 TubeSpin® Bioreactor tubes (TPP) and cell pools were evaluated for specific growth (µ) and
719 specific NP expression (qp). The top performing cell pools (2-4) were single-cell-cloned following
720 an in-house established limiting-dilution procedure in 384-well plates (Corning). Clonality was
721 confirmed using a Cell Metric plate imaging device (Solentim). Clonal cell populations were again
722 screened in 96-well plates (Thermo Fisher) by ELISA, and the 20 best performing clonal cell lines
723 were further evaluated in a small-scale screen (5 ml) in 50 ml TubeSpin® Bioreactor tubes (TPP)
724 with respect to cell growth and NP expression by ELISA in addition to non-reducing SDS-PAGE
725 and Western blot. Based on the evaluation results for the top 20 clones, the top eight cell clones
726 were selected for each BG505 Env-NP and challenged in small-scale fed-batch experiments with
727 the aim to identify clones that may have the potential to serve as prospective production clones

728 under good manufacturing practice (GMP) conditions. Fed batch experiments were performed in
729 125 ml shaker flasks with 45 ml culture volume using ActiPro medium (HyClone) and the
730 corresponding nutrient feeds Cell Boost 7a and 7b (both HyClone) in a shaking incubator. Small-
731 scale research cell banks (RCBs) were established and cryo-preserved to support future master cell
732 bank (MCB) establishment. Cell line development was performed at Polymun Scientific GmbH
733 (Klosterneuburg, Austria) through a contract from Uvax Bio.

734 **SDS-PAGE and BN-PAGE**

735 BG505 Env-NPs were analyzed by sodium dodecyl sulfate-polyacrylamide gel electrophoresis
736 (SDS-PAGE) and blue native-polyacrylamide gel electrophoresis (BN-PAGE). The proteins were
737 mixed with loading dye and added to either a 10% Tris-Glycine Gel (Bio-Rad) or a 4-12% Bis-
738 Tris NativePAGE^{TM} gel (Life Technologies). For SDS-PAGE under reducing conditions, the
739 proteins were first treated with dithiothreitol (DTT, 25 mM) and boiled for 5 min at 100 °C. SDS-
740 PAGE gels were run for 20 min at 250 V using SDS running buffer (Bio-Rad), and BN-PAGE
741 gels were run for 2-2.5 hours at 150 V using NativePAGE^{TM} running buffer (Life Technologies)
742 according to the manufacturer's instructions. The gels were stained using Coomassie Brilliant Blue
743 R-250 (Bio-Rad) and de-stained using a solution of 6% ethanol and 3% glacial acetic acid.

744 **Differential scanning calorimetry (DSC)**

745 Thermal melting curves of BG505 Env UFO-FR, UFO-E2p-L4P, and UFO-10GS-I3-01v9-L7P
746 SApNPs following PGT145 and SEC purification were obtained from a MicroCal PEAQ-DSC
747 Man instrument (Malvern). Samples of the E2p and I3-01v9 SApNPs after glycan trimming by
748 endo Hf and SEC purification were also analyzed. Briefly, the purified SApNP protein was buffer
749 exchanged into 1×PBS buffer and concentrated to 0.8 μM before analysis by the instrument.
750 Melting was probed at a scan rate of 60 $°C \cdot h^{-1}$ from 20°C to 100°C. Data processing, including

751 buffer correction, normalization, and baseline subtraction, was conducted using MicroCal PEAQ-
752 DSC software. Gaussian fitting was performed using Origin 9.0 software.

753 **Dynamic light scattering (DLS)**

754 Particle size distributions of BG505 Env-NPs based on three NP platforms (FR, E2p-L4P, and I3-
755 01v9-L7P) were obtained from a Zetasizer Ultra instrument (Malvern). PGT145/SEC-purified NPs
756 from ExpiCHO cells were diluted to 0.2 mg/ml using 1×PBS buffer, and 30 µl of the prepared NP
757 sample was added to a quartz batch cuvette (Malvern, catalog no. ZEN2112). Particle size was
758 measured at 25 °C in back scattering mode. Data processing was performed on the Zetasizer and
759 the particle size distribution was plotted using Origin 9.0 software.

760 **Endo H treatment and removal**

761 Glycan trimming of Env immunogens was performed using Endo-Hf, a fusion of endo H and MBP
762 (NEB, catalog no. P0703L), by mixing 20 µg of Env protein, 2 µl of 10×GlycoBuffer3, 5 µl of
763 endo H, and H_2O (if necessary) to make a 20 µl reaction. The mixture was kept at room temperature
764 (25°C) for 5 fours to facilitate enzymatic processing of the Env glycans. The reaction volume can
765 be scaled up proportionally to generate more glycan-trimmed material for immunization. After 5
766 hours of incubation, the mixture was passed through a Superose 6 column to remove the MBP-
767 tagged endo H. Both NP and endo Hf fractions were collected for quantitation of the residual endo
768 Hf using an anti-MBP mouse antibody (Sigma, catalog no. M6295-.2ML) in ELISA. While most
769 endo Hf can be readily removed from NP samples by SEC, a second purification step must be
770 included for the trimer because trimer and endo Hf have separate but close SEC peaks. Amylose
771 resin (NEB, catalog no. E8021S) was used to remove residual endo Hf from the SEC-purified
772 trimer fractions. The flow through was collected to quantify the residual endo Hf and then adjusted

773 to appropriate concentrations for in vitro and in vivo studies. To achieve the most complete glycan
774 trimming, 1-20 μg of the Env protein was mixed with 1 μl of Glycoprotein Denaturing Buffer
775 (NEB, 10×) and H_2O (if necessary) in a reaction volume of 10 μl. The reaction was then heated to
776 100°C for 10 min to denature the protein, prior to endo H treatment at 37°C for 1 hour. This
777 protocol was only used to test the maximum trimming of Env glycans by endo H in **Fig. 3G**. The
778 denatured, glycan-trimmed materials were not used in the animal studies.

779 **Enzyme-linked immunosorbent assay (ELISA)**

780 In this study, ELISA was performed to detect residual endo Hf in trimer and SApNP samples after
781 glycan trimming. Each well of a Costar™ 96-well assay plate (Corning) was first coated with 50
782 μl of PBS containing 0.2 μg of appropriate antigens. The plates were incubated overnight at 4 °C,
783 and then washed five times with wash buffer containing PBS and 0.05% (v/v) Tween 20. Each
784 well was then coated with 150 μl of a blocking buffer consisting of PBS and 40 mg ml^{-1} blotting-
785 grade blocker (Bio-Rad). The plates were incubated with the blocking buffer for 1 h at room
786 temperature, and then washed five times with wash buffer. The human bNAb VRC01 and MBP-
787 specific mouse antibody (Sigma, catalog no. M6295-.2ML) were diluted in blocking buffer to a
788 maximum concentration of 1 μg/ml and to reach ×466 dilution (as recommended by the
789 manufacturer), respectively, followed by a 10-fold dilution series. For each antibody dilution, a
790 total 50 μl volume was added to the appropriate wells. Each plate was incubated for 1 h at room
791 temperature, and then washed five times with PBS containing 0.05% Tween 20. A 1:5000 dilution
792 of goat anti-human IgG antibody (Jackson ImmunoResearch Laboratories) or 1:3000 dilution of
793 goat anti-mouse IgG antibody (Jackson ImmunoResearch Laboratories) was then made in wash
794 buffer (PBS containing 0.05% Tween 20), with 50 μl of this diluted secondary antibody added to
795 each well. The plates were incubated with the secondary antibody for 1 h at room temperature, and

796 then washed five times with PBS containing 0.05% Tween 20. Finally, the wells were developed
797 with 50 µl of TMB (Life Sciences) for 3-5 min before stopping the reaction with 50 µl of 2 N
798 sulfuric acid. The resulting plate readouts were measured at a wavelength of 450 nm. As a rapid
799 screening ELISA assay, only four antibody concentrations/dilutions were tested.

800 **Negative stain EM analysis**

801 The initial evaluation of various Env-NP samples was performed by the Core Microscopy Facility
802 at The Scripps Research Institute. All NP samples were prepared at the concentration of 0.01-0.05
803 mg/ml. Carbon-coated copper grids (400 mesh) were glow-discharged and 8 µl of each sample
804 was adsorbed for 2 min. Excess sample was wicked away and grids were negatively stained with
805 2% uranyl formate for 2 min. Excess stain was wicked away and the grids were allowed to dry.
806 Samples were analyzed at 80 kV with a Talos L120C transmission electron microscope (Thermo
807 Fisher) and images were acquired with a CETA 16M CMOS camera. The structural analysis of
808 glycan trimmed-treated BG505 UFO trimer bound to bNAbs PGT128 and VRC01 was performed
809 by the Core Microscopy Facility following the protocol described above. For each complex, a total
810 of 55 images were manually collected at a magnification of 73,000×. CryoSPARC 2 software (*152*)
811 on the Scripps Garibaldi cluster was used to analyze the EM images, including imaging processing,
812 particle picking, 2D classification, and 3D reconstruction (**Fig. S4P)**. The validation of BG505
813 UFO-E2p-L4P and UFO-10GS-I3-01v9-L7P NP samples prior to high-resolution cryo-EM was
814 performed in the Hazen EM facility at The Scripps Research Institute. The experiments were
815 performed as previously described (*100, 153*). The concentrated BG505 Env-NP samples were
816 diluted to 50 µg/ml in TBS buffer (Alfa Aesar) and loaded onto the carbon-coated 400-mesh Cu
817 grid. Prior to sample application the grids were glow-discharged at 15 mA for 30 s. The samples
818 were blotted off the grids after 10 s and negatively stained with 2 % (w/v) uranyl-formate for 60

819 s. A Tecnai Spirit electron microscope (120 keV) featuring a Tietz 4k × 4k TemCam-F416 CMOS
820 camera was used for data acquisition. Nominal magnification was 52,000 ×. The resulting pixel
821 size at the specimen plane was 2.05 Å, and the defocus was set to -1.50 µm. Total electron dose
822 per image was adjusted to 25 e-/Å2. Images were recorded using the Leginon software suite (*154*).
823 Data were visualized in the Appion data processing suite (*155*).

824 **Cryo-EM analysis of two BG505 UFO trimer-presenting SApNPs**

825 The cryo-EM grid preparation was performed as the following. BG505 UFO-E2p-L4P and UFO-
826 10GS-I3-01v9-L7P samples were concentrated to 1.5 and 2.5 mg/ml, respectively. Immediately
827 prior to grid application, lauryl maltose neopentyl glycol (LMNG) was added to each sample at a
828 final concentration of 0.005 mM. Quantifoil R 2/1 holey carbon copper grids (Cu 400 mesh) were
829 the main type of grids used. The grids were pretreated with Ar/O2 plasma (Gatan Solarus 950
830 plasma system) for 10 s before sample loading. Vitrobot mark IV (Thermo Fisher Scientific) was
831 used for the sample application, blotting, and vitrification steps. The temperature was set to 10°C,
832 humidity was 100 %, blotting force was set to 0, wait time was 10 s, and blotting time varied in
833 the range of 3.5-5.5 s. For grid preparation, 3 µl of the NP sample (with LMNG) was loaded onto
834 plasma-activated grids. Following the blot step the grids were plunge-frozen into liquid ethane
835 cooled with liquid nitrogen. The cryo-EM data were collected from two microscopes. Specifically,
836 the I3-01v9-L7P NP data were collected on the Talos Arctica TEM (Thermo Fisher Scientific)
837 operating at 200 kV. The E2p-L4P NP data were acquired on an FEI Titan Krios TEM at 300 kV
838 (Thermo Fisher Scientific). Both microscopes were equipped with the Gatan K2 Summit direct
839 electron detector camera and sample autoloader. The Leginon software suite (*154*) was used for
840 automated data acquisition. Data collection parameters are shown in **Table S1**. Cryo-EM data were
841 processed as described previously (*100*). MotionCor2 (*156*) was used for frame alignment and

842 dose-weighting and GCTF was applied for the estimation of CTF parameters. The early processing
843 steps were performed in CryoSPARC 2 (*152*). Particles were picked using template picker,
844 extracted and subjected to two rounds of 2D classification to eliminate bad picks and
845 heterogeneously looking particles. After the 2D cleaning step, 17097 and 4806 particles were
846 retained for BG505 UFO-E2p-L4P and UFO-I3-01v9-L7P NPs for further processing steps. These
847 particle subsets were transferred to Relion/3.0 (*157*). Ab-initio reconstruction in cryoSPARC was
848 used to generate the starting reference models for the 3D steps in Relion. Two iterative rounds of
849 3D classification and refinement with imposed icosahedral symmetry restraints were applied to
850 produce the final 3D maps of the E2p-L4P and I3-01v9-L7P NP scaffolds. A soft solvent mask
851 around the corresponding NP scaffold was introduced for 3D classification, 3D refinement, and
852 postprocessing steps to exclude signal contributions from flexibly linked BG505 trimers and
853 additional stabilizing domains (e.g., LD4 in E2p-L4P). For the E2p-L4P NP, the final subset had
854 7,672 particles and yielded a map resolution of 3.7 Å. For the I3-01v9-L7P NP, the final subset
855 consisted of 4,806 particle projection images and was reconstructed to 6.0 Å resolution.

856 For the analysis of NP-attached BG505 UFO trimers, we used the localized reconstruction
857 method (*158*). Localized reconstruction v1.2.0 was applied to extract subparticles corresponding
858 to the trimer antigens from pre-aligned E2p-LD4 and I3-01v9 particle datasets. Each NP presents
859 20 trimers on the surface. The starting trimer datasets consisted of 153,400 (20 × 7,672) and 96,120
860 (20 × 4,806) subparticles for BG505 UFO-E2p-L4P and UFO-10GS-I3-01v9-L7P, respectively.
861 Subparticle datasets were subjected to two rounds of 2D classification and two rounds of 3D
862 classification in Relion/3.0 (*157*) to eliminate cropped, overlapping, and heterogeneously looking
863 particles. For the 3D steps, we applied an HIV-1 Env trimer model from negative stain EM, low-
864 pass filtered to 40 Å resolution. The final subset consisted of 6,726 and 3,723 particles for E2p-

865 L4P and I3-01v9-L7P-displayed BG505 UFO trimers. These subsets were subjected to 3D
866 refinement. In the case of E2p-L4P-displayed trimers, a soft solvent mask around the trimer was
867 used for the 3D refinement and postprocessing steps. C3 symmetry restraints were imposed during
868 refinement. Maps at 7.4 and 10.4 Å resolution were obtained for E2p-L4P and I3-01v9-L7P-bound
869 BG505 UFO trimers, respectively. The resulting maps after 3D refinement and postprocessing,
870 and corresponding half-maps and solvent masks were submitted to the Electron Microscopy Data
871 Bank (EMDB). Model refinement was performed only for the E2p-L4P NP scaffold, using the B-
872 factor-sharpened map after postprocessing. The structure of dihydrolipoyl transacetylase from
873 PDB entry 1B5S (*103*) was used as a starting model. Iterative rounds of manual model building in
874 Coot (*159*) and Rosetta relaxed refinement (*160*) were applied to generate the final structures.
875 Model evaluation was performed using the EMRinger (*161*) and MolProbity (*162*) packages, with
876 statistics reported in **Table S2**. The model was submitted to the Protein Data Bank (PDB).

877 **Site-specific glycan analysis of BG505 trimer and SApNP immunogens**

878 Three 50 µg aliquots of each sample were denatured for 1 h in 50 mM Tris/HCl, pH 8.0, containing
879 6 M urea and 5 mM DTT. Next, Env proteins were reduced and alkylated by adding 20 mM
880 iodoacetamide (IAA) and incubated for 1 h in the dark, followed by 1 h of incubation with 20 mM
881 DTT to eliminate residual IAA. The alkylated Env proteins were buffer-exchanged into 50 mM
882 Tris/HCl, pH 8.0 using Vivaspin columns (3 kDa) and digested separately overnight using trypsin,
883 chymotrypsin or elastase (Mass Spectrometry Grade, Promega) at a ratio of 1:30 (w/w). The next
884 day, the peptides were dried and extracted using C18 Zip-tip (MerckMilipore). The peptides were
885 dried again, resuspended in 0.1% formic acid, and analyzed by nanoLC-ESI MS with an Easy-
886 nLC 1200 (Thermo Fisher Scientific) system coupled to a Fusion mass spectrometer (Thermo
887 Fisher Scientific) using higher energy collision-induced dissociation (HCD) fragmentation.

888 Peptides were separated using an EasySpray PepMap RSLC C18 column (75 µm × 75 cm). A
889 trapping column (PepMap 100 C18 3 µM 75 µM × 2cm) was used in line with the LC prior to
890 separation with the analytical column. The LC conditions were the following: 275 min linear
891 gradient consisting of 0-32% acetonitrile in 0.1% formic acid over 240 min followed by 35 min of
892 80% acetonitrile in 0.1% formic acid. The flow rate was set to 200 nl/min. The spray voltage was
893 set to 2.7 kV and the temperature of the heated capillary was set to 40 °C. The ion transfer tube
894 temperature was set to 275 °C. The scan range was 400-1600 *m/z*. The HCD collision energy was
895 set to 50%, appropriate for the fragmentation of glycopeptide ions. Precursor and fragment
896 detection were performed using an Orbitrap at a resolution MS1 = 100,000 MS2 = 30,000. The
897 AGC target for MS1 = 4e5 and MS2 = 5e4 and injection time: MS1 = 50ms MS2 = 54ms.

898 Glycopeptide fragmentation data were extracted from the raw file using Byonic™ (Version
899 3.5) and Byologic™ software (Version 3.5; Protein Metrics). The glycopeptide fragmentation data
900 were evaluated manually for each glycopeptide; the peptide was scored as true-positive when the
901 correct b and y fragment ions were observed along with oxonium ions corresponding to the glycan
902 identified. The MS data were searched using the Protein Metrics 305 N-glycan library. The relative
903 amounts of each glycan at each site, as well as the unoccupied proportion, were determined by
904 comparing the extracted chromatographic areas for different glycotypes with an identical peptide
905 sequence. All charge states for a single glycopeptide were summed. The precursor mass tolerance
906 was set to 4 part per million (ppm) and 10 ppm for fragments. A 1% false discovery rate (FDR)
907 was applied. Glycans were categorized according to the composition detected.
908 HexNAc(2)Hex(9−5) was classified as M9 to M5, HexNAc(3)Hex(5−6)X as Hybrid with
909 HexNAc(3)Fuc(1)X classified as Fhybrid. Complex-type glycans were classified according to the
910 number of HexNAc residues, which are attributed to the number of processed antenna/bisecting

911 GlcNAc (B), and fucosylation (F). For example, HexNAc(3)Hex(3-4)X was assigned to A1,
912 HexNAc(4)X to A2/A1B, HexNAc(5)X to A3/A2B, and HexNAc(6)X to A4/A3B. If all of these
913 compositions had a fucose, then they were assigned to the corresponding FA category. Note that
914 this analytical approach does not distinguish between isomers, which could influence formal
915 assignment of the number of antennae in some cases.

916 **Bio-layer interferometry (BLI)**

917 The antigenic profiles of BG505 Env immunogens, the UFO trimers and SApNPs with wildtype
918 and modified glycan shields, were measured using an Octet RED96 instrument (FortéBio, Pall
919 Life Sciences) against a large panel of HIV-1 NAbs, bNAbs, and nNAbs in the IgG form. All
920 assays were performed with agitation set to 1000 rpm in FortéBio 1× kinetic buffer. The final
921 volume for all solutions was 200 µl per well. Assays were performed at 30 °C in solid black 96-
922 well plates (Geiger Bio-One). For UFO trimers, 5 µg/ml antibody in 1× kinetic buffer was loaded
923 onto the surface of anti-human Fc Capture Biosensors (AHC) for 300 s. For UFO trimer-presenting
924 SApNPs, anti-human Fc Quantitation Biosensors (AHQ) were used because they have been shown
925 to be more suitable for measuring the avidity effect for particulate immunogens (*27, 89, 91, 92*).
926 Notably, the respective trimer was also measured using AHQ biosensors to facilitate comparisons
927 of antibody binding with trimer-presenting SApNPs. A 60 s biosensor baseline step was applied
928 prior to the analysis of the association of the antibody on the biosensor to the antigen in solution
929 for 200 s. A two-fold concentration gradient of antigen, starting at 266.7 nM for the UFO trimer,
930 14.9 nM for the FR SApNP, and 5.5 nM for the E2p and I3-01v9 SApNPs, was used in a titration
931 series of six. The dissociation of the interaction was followed for 300 s. The correction of baseline
932 drift was performed by subtracting the mean value of shifts recorded for a sensor loaded with
933 antibody but not incubated with antigen, and for a sensor without antibody but incubated with

934 antigen. Octet data were processed by FortéBio's data acquisition software v.8.1. Peak signals at
935 the highest antigen concentration were summarized in a matrix and color-coded accordingly to
936 facilitate comparisons between different vaccine platforms and glycan treatments.

937 **Mouse immunization and sample collection**

938 Similar immunization protocols have been used in our previous vaccine studies (*27, 89, 91, 92,*
939 *120*). Briefly, Institutional Animal Care and Use Committee (IACUC) guidelines were followed
940 with animal subjects tested in the immunization study. Eight-week-old BALB/c mice were
941 purchased from The Jackson Laboratory and housed in ventilated cages in environmentally
942 controlled rooms at The Scripps Research Institute, in compliance with an approved IACUC
943 protocol and Association for Assessment and Accreditation of Laboratory Animal Care
944 (AAALAC) international guidelines. Mice were immunized at weeks 0, 3, 6, and 9 with 200 µl of
945 antigen/adjuvant mix containing 30 µg of vaccine antigen and 100 µl of adjuvant, AddaVax, Adju-
946 Phos, or Alhydrogel (InvivoGen), via the intraperitoneal (i.p.) route. Blood was collected 2 weeks
947 after each injection. All bleeds were performed through the retro-orbital sinus using heparinized
948 capillary tubes into EDTA-coated tubes. Samples were spun at 1200 rpm for 10 min to separate
949 plasma (top layer) and the rest of the whole blood layer. Upon heat inactivation at 56 °C for 30
950 min, plasma was spun at 2000 rpm for 10 min to remove precipitates. The rest of the whole blood
951 layer was diluted with an equal volume of PBS and then overlaid on 4.5 ml of Ficoll in a 15 ml
952 SepMate^{TM} tube (STEMCELL Technologies) and spun at 1200 rpm for 10 min at 20 °C to separate
953 peripheral blood mononuclear cells (PBMCs). Cells were washed once in PBS and then
954 resuspended in 1 ml of ACK Red Blood Cell lysis buffer (Lonza). After washing with PBS,
955 PBMCs were resuspended in 2 ml of Bambanker Freezing Media (Lymphotec). Spleens were
956 harvested at week 11 and ground against a 70-µm cell strainer (BD Falcon) to release splenocytes

957 into a cell suspension. Splenocytes were centrifuged, washed in PBS, treated with 5 ml of ACK
958 lysing buffer (Lonza), and frozen with 3 ml of Bambanker freezing media. Total plasma from week
959 11 was purified using CaptureSelect™ IgG-Fc (Multispecies) Affinity Matrix (Thermo Scientific)
960 following the manufacturer's instructions. Purified IgG samples from individual mice were
961 analyzed in TZM-bl assays to determine the vaccine-induced neutralizing response.

962 **Rabbit immunization and sample collection**

963 The Institutional Animal Care and Use Committee (IACUC) guidelines were followed for the
964 animal subjects tested in the immunization studies. For the evaluation of wildtype Env and Env-
965 NP immunogens using a long regimen, rabbit immunization and blood sampling were performed
966 under a subcontract at Covance (Denver, PA). Seven groups of female New Zealand White rabbits,
967 six rabbits per group, were immunized intramuscularly (i.m.) with 100 μg of HIV-1 Env antigen
968 formulated in 250 μl of adjuvant, AddaVax or Adju-Phos (InvivoGen), with a total volume of 500
969 μl, at weeks 0, 8, and 24. Blood samples (15 ml each) were collected at day 0 and weeks 1, 2, 4,
970 6, 8, 10, 12, 16, 20, 24, 26, and 28. Plasma was separated from blood and heat inactivated for the
971 TZM-bl neutralization assays. For the assessment of glycan-trimmed Env-NP immunogens using
972 a short regimen, rabbit immunization and blood sampling were performed under a subcontract at
973 ProSci (San Diego, CA). Four groups of female New Zealand White rabbits, six rabbits per group,
974 were intramuscularly (i.m.) immunized with 30 μg of vaccine antigen formulated in 250 μl of
975 adjuvant, AddaVax or Adju-Phos (InvivoGen), with a total volume of 500 μl, at weeks 0, 3, 6, 9,
976 and 12. Blood samples, 20 ml each time, were collected from the auricular artery at day 0 (Pre)
977 and weeks 2, 5, 8, 11, 14, and 16. More than 100 ml of blood was taken at week 16, via cardiac
978 puncture, for PBMC isolation. Plasma samples were heat inactivated for further characterization,
979 and purified rabbit IgGs were assessed in TZM-bl neutralization assays.

980 **Pseudovirus production and neutralization assays**

981 Pseudoviruses were generated by the transfection of HEK293T cells with an HIV-1 Env expressing
982 plasmid and an Env-deficient genomic backbone plasmid (pSG3ΔEnv), as previously described
983 (*163*). HIV-1 Env expressing vectors for BG505 (catalog no. 11518), SF162 (catalog no. 10463),
984 and the 12-virus global panel (*164*) (catalog no. 12670) were obtained through the NIH AIDS
985 Reagent Program (https://www.aidsreagent.org/). A T332N mutation was introduced into BG505
986 Env to produce the BG505.T332N clone. Other BG505.T332N mutants were created by
987 introducing mutations as previously described (*56, 60, 69*). Pseudoviruses were harvested 72 h
988 post-transfection for use in the neutralization assays. The neutralizing activity of each mouse or
989 rabbit sample was assessed using a single round of replication pseudovirus assay and TZM-bl
990 target cells, similar to that described previously (*163*). Briefly, pseudovirus was incubated with
991 serial dilutions of antibodies or heat inactivated rabbit plasma in a 96-well flat bottom plate for 1
992 h at 37 °C before TZM-bl cells were seeded in the plate. For purified mouse and rabbit IgGs, a
993 starting concentration of 300 μg/ml was used, or an initial dilution of either 40-times or 100-times
994 for rabbit plasma, and then subjected to 3-times serial dilutions in the TZM-bl assays. Samples
995 were tested in duplicate with a full series of dilutions unless otherwise specified in the Results,
996 with such exceptions including tests against the 12-virus global panel performed in singlet to
997 conserve purified IgG samples. Luciferase reporter gene expression was quantified 60-72 h after
998 infection upon lysis and the addition of Bright-Glo™ Luciferase substrate (Promega). Data were
999 retrieved from a BioTek microplate reader with Gen 5 software. Values from experimental wells
1000 were compared against a well containing virus only, with background luminescence from a series
1001 of uninfected wells subtracted from both. Dose-response neutralization curves were then fit by
1002 nonlinear regression in GraphPad Prism 9.3.1, with IC_{30}, IC_{50}, and ID_{50} calculated with constraints

1003 set between 0 to 100. As a negative control, pseudoparticles displaying the envelope glycoproteins
1004 of MLV (MLV-pps) were tested in the TZM-bl assays following the same protocol.

1005 **Histology, immunostaining, and imaging**

1006 For the mechanistic study of HIV-1 Env vaccine distribution, trafficking, cellular interaction, and
1007 induced GCs in lymph nodes, vaccines were intradermally injected into mouse footpads using a
1008 29-gauge insulin needle under 3% isoflurane anesthesia with oxygen. Similar immunization and
1009 tissue analysis protocols were used in our previous study (*120*). The administered dose was 80 µl
1010 of antigen/adjuvant mix containing 40 µg of vaccine antigen per mouse or 10 µg per footpad. Mice
1011 were euthanized 30 min to 8 weeks after a single-dose injection. The axillary and popliteal sentinel
1012 lymph nodes were collected for histological analysis. Fresh lymph nodes were merged into frozen
1013 section compound (VWR International, catalog no. 95057-838) in a plastic cryomold (Tissue-Tek
1014 at VWR, catalog no. 4565). Sample molds were merged into liquid nitrogen and then stored at -
1015 80°C before shipping to The Centre for Phenogenomics in Canada for sample processing,
1016 immunostaining, and imaging. Tissue sections were sliced 8 µm thick on a cryostat (Cryostar
1017 NX70) and collected on charged slides. Samples were then fixed in 10% neutral buffered formalin
1018 and further permeabilized in PBS that contained 0.5% Triton X-100 before staining. The slides
1019 were blocked with protein Block (Agilent) to prevent nonspecific antibody binding. Primary
1020 antibody was then applied on the sections and incubated overnight at 4°C. After washing with
1021 TBST, secondary antibodies that were conjugated with either biotin or a fluorophore were used,
1022 and the samples were incubated for 1 h at 25 °C. Lymph node sections were stained with bNAbs
1023 VRC01 (*112*), PGT124 (*124*), and PGDM1400 (*125*) (1:50), and biotinylated goat anti-human
1024 secondary antibody (Abcam, catalog no. ab7152, 1:300), followed by streptavidin-horseradish

1025 peroxidase (HRP) reagent (Vectastain Elite ABC-HRP Kit, Vector, catalog no. PK-6100) and
1026 diaminobenzidine (DAB) (ImmPACT DAB, Vector, catalog no. SK-4105).

1027 To visualize interactions between HIV-1 Env vaccines and cells in mouse lymph nodes,
1028 FDCs were labeled using anti-CD21 primary antibody (Abcam, catalog no. ab75985, 1:1800),
1029 followed by anti-rabbit secondary antibody conjugated with Alexa Fluor 555 (Thermo Fisher,
1030 catalog no. A21428, 1:200). B cells were labeled using anti-B220 antibody (eBioscience, catalog
1031 no. 14-0452-82, 1:100) followed by anti-rat secondary antibody conjugated with Alexa Fluor 647
1032 (Thermo Fisher, catalog no. A21247, 1:200). Subcapsular sinus macrophages were labeled using
1033 anti-sialoadhesin (CD169) antibody (Abcam, catalog no. ab53443, 1:600) followed by anti-rat
1034 secondary antibody conjugated with Alexa Fluor 488 (Abcam, catalog no. ab150165, 1:200). HIV-
1035 1 vaccine-induced GCs were studied using immunostaining, GC B cells stained using rat anti-GL7
1036 antibody (FITC; BioLegend, catalog no. 144604, 1:250), T_{fh} cells stained using anti-CD4 antibody
1037 (BioLegend, catalog no. 100402, 1:100) followed by anti-rat secondary antibody conjugated with
1038 Alexa Fluor 488 (Abcam, catalog no. ab150165, 1:1000), GC cells stained using Bcl6 antibody
1039 (Abcam, catalog no. ab220092, 1:300) followed by anti-rabbit secondary antibody conjugated with
1040 Alexa Fluor 555 (Thermo Fisher, catalog no. A21428, 1:1000). Nuclei were labeled using 4′,6-
1041 diamidino-2-phenylindole (DAPI) (Sigma-Aldrich, catalog no. D9542, 100 ng/ml).

1042 The stained lymph node sections were scanned using an Olympus VS-120 slide scanner
1043 with a Hamamatsu ORCA-R2 C10600 digital camera for bright-field and fluorescent images. The
1044 transport of HIV-1 BG505 Env immunogens and their induced GCs in mouse lymph nodes were
1045 quantified through bright-field and fluorescent images using ImageJ software (*165*).

1046 **Electron microscopy analysis of protein nanoparticles and lymph node tissues**

1047 TEM analysis was conducted by the Core Microscopy Facility at The Scripps Research Institute.
1048 To visualize interactions of BG505 UFO Env-SApNPs with FDCs and phagocytic cells in lymph
1049 nodes using TEM, mice were injected with 140 µl of antigen/adjuvant mix containing 100 µg of
1050 vaccine antigen (40 µl of adjuvant) into the two hind footpads or 50 µg per footpad. Popliteal
1051 sentinel lymph nodes were isolated 2, 12, and 48 hours after administration, bisected and immersed
1052 in oxygenated 2.5% glutaraldehyde and 4% paraformaldehyde in 0.1 M sodium cacodylate buffer
1053 (pH 7.4) fixative overnight at 4ºC. The lymph node tissues were washed using 0.1 M sodium
1054 cacodylate buffer and post-fixed in buffered 1% osmium tetroxide and 1.5% potassium
1055 ferrocyanide for 1-1.25 hours at 4°C. The samples were rinsed in Corning Cell Culture Grade
1056 Water and stained *en bloc* with 0.5% uranyl acetate overnight at 4°C. The tissues were rinsed with
1057 double-distilled H_2O and dehydrated through a graded series of ethanol followed by acetone,
1058 infiltrated with LX-112 (Ladd) epoxy resin, and polymerized at 60°C. Ultrathin tissue sections (70
1059 nm) were prepared on copper grids for TEM imaging. Tissue samples were imaged at 80 kV with
1060 a Talos L120C transmission electron microscope (Thermo Fisher), and images were acquired with
1061 a CETA 16M CMOS camera.

1062 **Lymph node disaggregation, cell staining, and flow cytometry**

1063 GC B cells ($GL7^+B220^+$) and T_{fh} cells ($CD3^+CD4^+CXCR5^+PD\text{-}1^+$) were characterized using flow
1064 cytometry (**Fig. S10A**). Mice were euthanized 2, 5, and 8 weeks after a single-dose injection and
1065 2 and 5 weeks after the boost injection (4×10 µg/footpad each time). Fresh axillary, brachial, and
1066 popliteal sentinel lymph nodes were isolated. After mechanically disaggregating the lymph node
1067 tissues, samples were merged in enzyme digestion solution in an Eppendorf tube containing 958
1068 µl of Hanks' balanced salt solution (HBSS) buffer (Thermo Fisher Scientific, catalog no.
1069 14185052), 40 µl of 10 mg/ml collagenase IV (Sigma-Aldrich, catalog no. C5138), and 2 µl of 10

1070 mg/ml DNase (Roche, catalog no. 10104159001). Lymph node tissues were incubated at 37°C for
1071 30 min and filtered through a 70 μm cell strainer. Samples were spun down at 400 × *g* for 10 min
1072 to isolate cell pellets, which were resuspended in HBSS blocking buffer with 0.5% (w/v) bovine
1073 serum albumin and 2 mM EDTA. Anti-CD16/32 antibody (BioLegend, catalog no. 101302) was
1074 added to block the nonspecific binding of Fc receptors, while the sample solution was kept on ice
1075 for 30 min. Samples were then transferred to 96-well microplates with pre-prepared cocktail
1076 antibodies, which included the Zombie NIR live/dead stain (BioLegend, catalog no. 423106),
1077 Brilliant Violet 510 anti-mouse/human CD45R/B220 antibody (BioLegend, catalog no. 103247),
1078 FITC anti-mouse CD3 antibody (BioLegend, catalog no. 100204), Alexa Fluor 700 anti-mouse
1079 CD4 antibody (BioLegend, catalog no. 100536), PE anti-mouse/human GL7 antibody (BioLegend,
1080 catalog no. 144608), Brilliant Violet 605 anti-mouse CD95 (Fas) antibody (BioLegend, catalog
1081 no. 152612), Brilliant Violet 421 anti-mouse CD185 (CXCR5) antibody (BioLegend, catalog no.
1082 145511), and PE/Cyanine7 anti-mouse CD279 (PD-1) antibody (BioLegend, catalog no. 135216).
1083 The cell samples mixed with antibody cocktail were placed on ice for 30 min and centrifuged to
1084 remove excess antibody. After washing with the HBSS blocking solution, cells were fixed with
1085 1.6% paraformaldehyde (Thermo Fisher Scientific, catalog no. 28906) in HBSS on ice for 30 min.
1086 The samples were then placed in HBSS blocking solution at 4°C. Sample events were acquired by
1087 a 5-laser AZE5 flow cytometer (Yeti, Bio-Rad) with Everest software at the Core Facility of The
1088 Scripps Research Institute. The data were analyzed using FlowJo 10 software.

1089 **Statistical analysis**

1090 Data were collected from 8 mice per group in the immunization study and 3-10 mice per group in
1091 the mechanistic analysis. All of the statistical analyses were performed and graphs were generated
1092 using GraphPad Prism 9.3.1 software. For the vaccine transport and GC study in lymph nodes,

1093 different vaccine groups were compared using one-way ANOVA, followed by Tukey's multiple
1094 comparison *post hoc* test. Statistical significance is indicated as the following in the figures: ns
1095 (not significant), $*p < 0.05$, $**p < 0.01$, $***p < 0.001$, $****p < 0.0001$. To assess the highest level
1096 of improvement in FVR, one comparison was made for each vaccine platform (trimer or SApNP)
1097 between the wildtype group (or a representative wildtype group, when multiple existed) and the
1098 glycan-trimmed group that had the highest FVR (or the highest average, when multiple repeats
1099 existed). This statistical comparison was performed using a two-tailed Fisher exact test.

1100 **SUPPLEMENTARY MATERIALS**

1101 Supplementary material for this article is available at XXX.

1102 Tables S1 and S2.

1103 Figures S1-S9.

1104 **ACKNOWLEDGEMENTS**

1105 Y.-N.Z. acknowledges support from the Natural Sciences and Engineering Research Council of
1106 Canada (NSERC) for the postdoctoral fellowship. We thank M. Ganguly, K. Duffin, and G.
1107 Ossetchkine at The Centre for Phenogenomics for their technical support in immunohistology. We
1108 thank K. Vanderpool, T. Fassel, and S. Henderson of the Core Microscopy Facility at The Scripps
1109 Research Institute for their expert assistance in the TEM analysis. We thank A. Saluk, B. Seegers,
1110 and B. Monteverde of the Flow Cytometry Core Facility at The Scripps Research Institute for their
1111 technical support in flow cytometry. We thank P. Berman and D. Burton for helpful discussions
1112 and M. Arends for proofreading the manuscript. **Funding:** This work was supported by the
1113 International AIDS Vaccine Initiative (IAVI) through grant INV-008352/OPP1153692 (M.C.) and
1114 the IAVI Neutralizing Antibody Center through the Collaboration for AIDS Vaccine Discovery
1115 grant (INV-034657) (I.A.W., A.B.W.), and INV-008352/OPP1153692 (M.C.) funded by the Bill

and Melinda Gates Foundation; Scripps Consortium for HIV/AIDS Vaccine Development (CHAVD 1UM1 AI144462) (M.C., A.B.W. and I.A.W.); HIV Vaccine Research and Design (HIVRAD) program (P01 AI124337) (J.Z.); NIH grants R01 AI129698 (J.Z.) and R01 AI140844 (J.Z., I.A.W.); Ufovax/SFP-2018-0416 (J.Z.) and Ufovax/SFP-2018-1013 (J.Z.). **Author contributions:** Project design by Y.-N.Z., J.P., L.H., I.A.W., and J.Z.; immunogen expression and purification by M.E. and L.H.; negative stain EM and cryo-EM by A.A., Y.-Z.L., J.C., and A.B.W.; glycan analysis by J.D.A., M.N., and M.C.; mouse and rabbit sample preparation, and plasma and IgG neutralization by J.P. and L.H.; mouse immunization, lymph node isolation, immunohistology, TEM, and flow cytometry by Y.-N.Z.; manuscript written by Y.-N.Z., A.A., J.P., J.D.A., I.A.W., M. C., A.B.W. and J.Z. All authors were asked to comment on the manuscript. The Scripps Research Institute manuscript number is 30193. **Competing interests:** The authors declare that they have no competing interests. **Data and material availability:** All data and codes to understand and assess the conclusions of this research are available in the main text, Supplementary Materials, PDB (accession code XXX) and EMDB (accession code EMD-YYY). Additional data related to this paper may be requested from the authors.

References

1. R. Wyatt, J. Sodroski, The HIV-1 envelope glycoproteins: fusogens, antigens, and immunogens. *Science* **280**, 1884-1888 (1998).
2. R. P. Smyth, M. P. Davenport, J. Mak, The origin of genetic diversity in HIV-1. *Virus Res.* **169**, 415-429 (2012).
3. P. L. Moore *et al.*, Nature of nonfunctional envelope proteins on the surface of human immunodeficiency virus type 1. *J. Virol.* **80**, 2515-2528 (2006).
4. X. P. Wei *et al.*, Antibody neutralization and escape by HIV-1. *Nature* **422**, 307-312 (2003).
5. D. R. Burton, J. R. Mascola, Antibody responses to envelope glycoproteins in HIV-1 infection. *Nat. Immunol.* **16**, 571-576 (2015).
6. D. Sok, D. R. Burton, Recent progress in broadly neutralizing antibodies to HIV. *Nat. Immunol.* **19**, 1179-1188 (2018).
7. L. E. McCoy, D. R. Burton, Identification and specificity of broadly neutralizing antibodies against HIV. *Immunol. Rev.* **275**, 11-20 (2017).

1147 8. D. R. Burton *et al.*, A blueprint for HIV vaccine discovery. *Cell Host Microbe* **12**, 396-
1148 407 (2012).
1149 9. L. M. Walker, D. R. Burton, Rational antibody-based HIV-1 vaccine design: current
1150 approaches and future directions. *Curr. Opin. Immunol.* **22**, 358-366 (2010).
1151 10. B. F. Haynes, G. Kelsoe, S. C. Harrison, T. B. Kepler, B-cell-lineage immunogen design
1152 in vaccine development with HIV-1 as a case study. *Nat. Biotechnol.* **30**, 423-433 (2012).
1153 11. F. Klein *et al.*, Antibodies in HIV-1 vaccine development and therapy. *Science* **341**,
1154 1199-1204 (2013).
1155 12. R. W. Sanders, J. P. Moore, Native-like Env trimers as a platform for HIV-1 vaccine
1156 design. *Immunol. Rev.* **275**, 161-182 (2017).
1157 13. A. B. Ward, I. A. Wilson, The HIV-1 envelope glycoprotein structure: nailing down a
1158 moving target. *Immunol. Rev.* **275**, 21-32 (2017).
1159 14. D. Sok *et al.*, Priming HIV-1 broadly neutralizing antibody precursors in human Ig loci
1160 transgenic mice. *Science* **353**, 1557-1560 (2016).
1161 15. J. G. Jardine *et al.*, Priming a broadly neutralizing antibody response to HIV-1 using a
1162 germline-targeting immunogen. *Science* **349**, 156-161 (2015).
1163 16. J. Jardine *et al.*, Rational HIV immunogen design to target specific germline B cell
1164 receptors. *Science* **340**, 711-716 (2013).
1165 17. L. Scharf *et al.*, Structural basis for germline antibody recognition of HIV-1
1166 immunogens. *eLife* **5**, e13783 (2016).
1167 18. A. J. Borst *et al.*, Germline VRC01 antibody recognition of a modified clade C HIV-1
1168 envelope trimer and a glycosylated HIV-1 gp120 core. *eLife* **7**, e37688 (2018).
1169 19. R. W. Sanders *et al.*, A next-generation cleaved, soluble HIV-1 Env trimer, BG505
1170 SOSIP.664 gp140, expresses multiple epitopes for broadly neutralizing but not non-
1171 neutralizing antibodies. *PLoS Pathog.* **9**, e1003618 (2013).
1172 20. P. Pugach *et al.*, A native-like SOSIP.664 trimer based on an HIV-1 subtype B Env gene.
1173 *J. Virol.* **89**, 3380-3395 (2015).
1174 21. J.-P. Julien *et al.*, Design and structure of two HIV-1 clade C SOSIP.664 trimers that
1175 increase the arsenal of native-like Env immunogens. *Proc. Natl. Acad. Sci. U. S. A.* **112**,
1176 11947-11952 (2015).
1177 22. K. Sliepen *et al.*, Structure and immunogenicity of a stabilized HIV-1 envelope trimer
1178 based on a group-M consensus sequence. *Nat. Commun.* **10**, 2355 (2019).
1179 23. S. K. Sharma *et al.*, Cleavage-independent HIV-1 Env trimers engineered as soluble
1180 native spike mimetics for vaccine design. *Cell Rep.* **11**, 539-550 (2015).
1181 24. J. Guenaga *et al.*, Glycine substitution at helix-to-coil transitions facilitates the structural
1182 determination of a stabilized subtype C HIV envelope glycoprotein. *Immunity* **46**, 792-
1183 803 (2017).
1184 25. J. Guenaga *et al.*, Structure-guided redesign increases the propensity of HIV Env to
1185 generate highly stable soluble trimers. *J. Virol.* **90**, 2806-2817 (2015).
1186 26. L. Kong *et al.*, Uncleaved prefusion-optimized gp140 trimers derived from analysis of
1187 HIV-1 envelope metastability. *Nat. Commun.* **7**, 12040 (2016).
1188 27. L. He *et al.*, HIV-1 vaccine design through minimizing envelope metastability. *Sci. Adv.*
1189 **4**, eaau6769 (2018).
1190 28. Q. Wang *et al.*, Stabilized diverse HIV-1 envelope trimers for vaccine design. *Emerg.*
1191 *Microbes & Infect.* **9**, 775-786 (2020).

1192 29. R. Derking, R. W. Sanders, Structure-guided envelope trimer design in HIV-1 vaccine
1193 development: a narrative review. *J. Int. AIDS Soc.* **24**, e25797 (2021).
1194 30. I. del Moral-Sanchez *et al.*, High thermostability improves neutralizing antibody
1195 responses induced by native-like HIV-1 envelope trimers. *Npj Vaccines* **7**, 27 (2022).
1196 31. M. Crispin, A. B. Ward, I. A. Wilson, Structure and immune recognition of the HIV
1197 glycan shield. *Annu. Rev. Biophys.* **47**, 499-523 (2018).
1198 32. K. J. Doores, The HIV glycan shield as a target for broadly neutralizing antibodies. *FEBS*
1199 *J.* **282**, 4679-4691 (2015).
1200 33. K. Wagh, B. H. Hahn, B. Korber, Hitting the sweet spot: exploiting HIV-1 glycan shield
1201 for induction of broadly neutralizing antibodies. *Curr. Opin. HIV AIDS* **15**, 267-274
1202 (2020).
1203 34. V. Hariharan, R. S. Kane, Glycosylation as a tool for rational vaccine design. *Biotechnol.*
1204 *Bioeng.* **117**, 2556-2570 (2020).
1205 35. C. N. Scanlan, J. Offer, N. Zitzmann, R. A. Dwek, Exploiting the defensive sugars of
1206 HIV-1 for drug and vaccine design. *Nature* **446**, 1038-1045 (2007).
1207 36. G. E. Seabright, K. J. Doores, D. R. Burton, M. Crispin, Protein and glycan mimicry in
1208 HIV vaccine design. *J. Mol. Biol.* **431**, 2223-2247 (2019).
1209 37. A. J. Behrens *et al.*, Molecular architecture of the cleavage-dependent mannose patch on
1210 a soluble HIV-1 envelope glycoprotein trimer. *J. Virol.* **91**, e01894-01816 (2017).
1211 38. A. J. Behrens *et al.*, Composition and antigenic effects of individual glycan sites of a
1212 trimeric HIV-1 envelope glycoprotein. *Cell Rep.* **14**, 2695-2706 (2016).
1213 39. L. W. Cao *et al.*, Global site-specific N-glycosylation analysis of HIV envelope
1214 glycoprotein. *Nat. Commun.* **8**, 13 (2017).
1215 40. F. Garces *et al.*, Affinity maturation of a potent family of HIV antibodies is primarily
1216 focused on accommodating or avoiding glycans. *Immunity* **43**, 1053-1063 (2015).
1217 41. M. Pancera *et al.*, Structural basis for diverse N-glycan recognition by HIV-1-
1218 neutralizing V1-V2-directed antibody PG16. *Nat. Struct. Mol. Biol.* **20**, 804-813 (2013).
1219 42. J. S. McLellan *et al.*, Structure of HIV-1 gp120 V1/V2 domain with broadly neutralizing
1220 antibody PG9. *Nature* **480**, 336-343 (2011).
1221 43. H. B. Gristick *et al.*, Natively glycosylated HIV-1 Env structure reveals new mode for
1222 antibody recognition of the CD4-binding site. *Nat. Struct. Mol. Biol.* **23**, 906-915 (2016).
1223 44. R. Pejchal *et al.*, A potent and broad neutralizing antibody recognizes and penetrates the
1224 HIV glycan shield. *Science* **334**, 1097-1103 (2011).
1225 45. E. M. Cale *et al.*, Virus-like particles identify an HIV V1V2 apex-binding neutralizing
1226 antibody that lacks a protruding loop. *Immunity* **46**, 777-791.e710 (2017).
1227 46. M. Pancera *et al.*, Structure and immune recognition of trimeric pre-fusion HIV-1 Env.
1228 *Nature* **514**, 455-461 (2014).
1229 47. J. H. Lee, G. Ozorowski, A. B. Ward, Cryo-EM structure of a native, fully glycosylated,
1230 cleaved HIV-1 envelope trimer. *Science* **351**, 1043-1048 (2016).
1231 48. J. H. Lee, N. de Val, D. Lyumkis, A. B. Ward, Model building and refinement of a
1232 natively glycosylated HIV-1 Env protein by high-resolution cryoelectron microscopy.
1233 *Structure* **23**, 1943-1951 (2015).
1234 49. D. Lyumkis *et al.*, Cryo-EM structure of a fully glycosylated soluble cleaved HIV-1
1235 envelope trimer. *Science* **342**, 1484-1490 (2013).
1236 50. R. Derking *et al.*, Enhancing glycan occupancy of soluble HIV-1 envelope trimers to
1237 mimic the native viral spike. *Cell Rep.* **35**, 108933 (2021).

1238 51. R. Andrabi, J. N. Bhiman, D. R. Burton, Strategies for a multi-stage neutralizing
1239 antibody-based HIV vaccine. *Curr. Opin. Immunol.* **53**, 143-151 (2018).
1240 52. V. Dubrovskaya *et al.*, Vaccination with glycan-modified HIV NFL envelope trimer-
1241 liposomes elicits broadly neutralizing antibodies to multiple sites of vulnerability.
1242 *Immunity* **51**, 915-929.e917 (2019).
1243 53. V. Dubrovskaya *et al.*, Targeted N-glycan deletion at the receptor-binding site retains
1244 HIV Env NFL trimer integrity and accelerates the elicited antibody response. *PLoS*
1245 *Pathog.* **13**, e1006614 (2017).
1246 54. B. Briney *et al.*, Tailored immunogens direct affinity maturation toward HIV neutralizing
1247 antibodies. *Cell* **166**, 1459-1470.e1411 (2016).
1248 55. J. K. Hu *et al.*, Murine antibody responses to cleaved soluble HIV-1 envelope trimers are
1249 highly restricted in specificity. *J. Virol.* **89**, 10383-10398 (2015).
1250 56. L. E. McCoy *et al.*, Holes in the glycan shield of the native HIV envelope are a target of
1251 trimer-elicited neutralizing antibodies. *Cell Rep.* **16**, 2327-2338 (2016).
1252 57. E. T. Crooks *et al.*, Vaccine-elicited tier 2 HIV-1 neutralizing antibodies bind to
1253 quaternary epitopes involving glycan-deficient patches proximal to the CD4 binding site.
1254 *PLoS Pathog.* **11**, e1004932 (2015).
1255 58. J. E. Voss *et al.*, Elicitation of neutralizing antibodies targeting the V2 apex of the HIV
1256 envelope trimer in a wild-type animal model. *Cell Rep.* **21**, 222-235 (2017).
1257 59. R. P. Ringe *et al.*, Closing and opening holes in the glycan shield of HIV-1 envelope
1258 glycoprotein SOSIP trimers can redirect the neutralizing antibody response to the newly
1259 unmasked epitopes. *J. Virol.* **93**, e01656-01618 (2019).
1260 60. P. J. Klasse *et al.*, Epitopes for neutralizing antibodies induced by HIV-1 envelope
1261 glycoprotein BG505 SOSIP trimers in rabbits and macaques. *PLoS Pathog.* **14**, e1006913
1262 (2018).
1263 61. P. J. Klasse *et al.*, Sequential and simultaneous immunization of rabbits with HIV-1
1264 envelope glycoprotein SOSIP.664 trimers from clades A, B and C. *PLoS Pathog.* **12**,
1265 e1005864 (2016).
1266 62. S. Bale *et al.*, Cleavage-independent HIV-1 trimers from CHO cell lines elicit robust
1267 autologous tier 2 neutralizing antibodies. *Front. Immunol.* **9**, 1116 (2018).
1268 63. M. Bianchi *et al.*, Electron-microscopy-based epitope mapping defines specificities of
1269 polyclonal antibodies elicited during HIV-1 BG505 envelope trimer immunization.
1270 *Immunity* **49**, 288-300.e288 (2018).
1271 64. Y. H. R. Yang *et al.*, Autologous antibody responses to an HIV envelope glycan hole are
1272 not easily broadened in rabbits. *J. Virol.* **94**, e01861-01819 (2020).
1273 65. A. Schorcht *et al.*, The glycan hole area of HIV-1 envelope trimers contributes
1274 prominently to the induction of autologous neutralization. *J. Virol.* **96**, e0155221 (2022).
1275 66. A. Antanasijevic *et al.*, Polyclonal antibody responses to HIV Env immunogens resolved
1276 using cryoEM. *Nat. Commun.* **12**, 4817 (2021).
1277 67. F. Z. Zhao *et al.*, Mapping neutralizing antibody epitope specificities to an HIV Env
1278 trimer in immunized and in infected rhesus macaques. *Cell Rep.* **32**, 108122 (2020).
1279 68. H. L. Turner *et al.*, Disassembly of HIV envelope glycoprotein trimer immunogens is
1280 driven by antibodies elicited via immunization. *Sci. Adv.* **7**, eabh2791 (2021).
1281 69. L. Lei *et al.*, The HIV-1 envelope glycoprotein C3/V4 region defines a prevalent
1282 neutralization epitope following immunization. *Cell Rep.* **27**, 586-598.e586 (2019).

1283 70. Z. Y. Xu *et al.*, Induction of tier-2 neutralizing antibodies in mice with a DNA-encoded
1284 HIV envelope native like trimer. *Nat. Commun.* **13**, 695 (2022).
1285 71. S. Kumar *et al.*, Neutralizing antibodies induced by first-generation gp41-stabilized HIV-
1286 1 envelope trimers and nanoparticles. *mBio* **12**, e00429-00421 (2021).
1287 72. T. P. Charles *et al.*, The C3/465 glycan hole cluster in BG505 HIV-1 envelope is the
1288 major neutralizing target involved in preventing mucosal SHIV infection. *PLoS Pathog.*
1289 **17**, e1009257 (2021).
1290 73. D. W. Kulp *et al.*, Structure-based design of native-like HIV-1 envelope trimers to
1291 silence non-neutralizing epitopes and eliminate CD4 binding. *Nat. Commun.* **8**, 1655
1292 (2017).
1293 74. P. J. M. Brouwer, R. W. Sanders, Presentation of HIV-1 envelope glycoprotein trimers on
1294 diverse nanoparticle platforms. *Curr. Opin. HIV AIDS* **14**, 302-308 (2019).
1295 75. B. Asbach, R. Wagner, Particle-based delivery of the HIV envelope protein. *Curr. Opin.*
1296 *HIV AIDS* **12**, 265-271 (2017).
1297 76. M. Brinkkemper, K. Sliepen, Nanoparticle vaccines for inducing HIV-1 neutralizing
1298 antibodies. *Vaccines* **7**, 76 (2019).
1299 77. S. Thalhauser, D. Peterhoff, R. Wagner, M. Breunig, Critical design criteria for
1300 engineering a nanoparticulate HIV-1 vaccine. *J. Control. Release* **317**, 322-335 (2020).
1301 78. Z. Y. Xu, D. W. Kulp, Protein engineering and particulate display of B-cell epitopes to
1302 facilitate development of novel vaccines. *Curr. Opin. Immunol.* **59**, 49-56 (2019).
1303 79. D. J. Irvine, B. J. Read, Shaping humoral immunity to vaccines through antigen-
1304 displaying nanoparticles. *Curr. Opin. Immunol.* **65**, 1-6 (2020).
1305 80. B. Nguyen, N. H. Tolia, Protein-based antigen presentation platforms for nanoparticle
1306 vaccines. *Npj Vaccines* **6**, (2021).
1307 81. Q. Zhao, S. Li, H. Yu, N. Xia, Y. Modis, Virus-like particle-based human vaccines:
1308 quality assessment based on structural and functional properties. *Trends Biotechnol.* **31**,
1309 654-663 (2013).
1310 82. W. A. Rodriguez-Limas, K. Sekar, K. E. J. Tyo, Virus-like particles: the future of
1311 microbial factories and cell-free systems as platforms for vaccine development. *Curr.*
1312 *Opin. Biotechnol.* **24**, 1089-1093 (2013).
1313 83. G. T. Jennings, M. F. Bachmann, Coming of age of virus-like particle vaccines. *Biol.*
1314 *Chem.* **389**, 521-536 (2008).
1315 84. C. Ludwig, R. Wagner, Virus-like particles - universal molecular toolboxes. *Curr. Opin.*
1316 *Biotechnol.* **18**, 537-545 (2007).
1317 85. E. V. L. Grgacic, D. A. Anderson, Virus-like particles: Passport to immune recognition.
1318 *Methods* **40**, 60-65 (2006).
1319 86. B. Zakeri *et al.*, Peptide tag forming a rapid covalent bond to a protein, through
1320 engineering a bacterial adhesin. *Proc. Natl. Acad. Sci. U. S. A.* **109**, E690-E697 (2012).
1321 87. J. B. Bale *et al.*, Accurate design of megadalton-scale two-component icosahedral protein
1322 complexes. *Science* **353**, 389-394 (2016).
1323 88. L. He *et al.*, Presenting native-like trimeric HIV-1 antigens with self-assembling
1324 nanoparticles. *Nat. Commun.* **7**, 12041 (2016).
1325 89. L. He *et al.*, Proof of concept for rational design of hepatitis C virus E2 core nanoparticle
1326 vaccines. *Sci. Adv.* **6**, eaaz6225 (2020).
1327 90. T. U. J. Bruun, A. M. C. Andersson, S. J. Draper, M. Howarth, Engineering a rugged
1328 nanoscaffold to enhance plug-and-display vaccination. *ACS Nano* **12**, 8855-8866 (2018).

1329 91. L. He *et al.*, Single-component, self-assembling, protein nanoparticles presenting the
1330 receptor binding domain and stabilized spike as SARS-CoV-2 vaccine candidates. *Sci.*
1331 *Adv.* **7**, eabf1591 (2021).
1332 92. L. He *et al.*, Single-component multilayered self-assembling nanoparticles presenting
1333 rationally designed glycoprotein trimers as Ebola virus vaccines. *Nat. Commun.* **12**, 2633
1334 (2021).
1335 93. M. F. Bachmann, G. T. Jennings, Vaccine delivery: a matter of size, geometry, kinetics
1336 and molecular patterns. *Nat. Rev. Immunol.* **10**, 787-796 (2010).
1337 94. T. Tokatlian *et al.*, Innate immune recognition of glycans targets HIV nanoparticle
1338 immunogens to germinal centers. *Science* **363**, 649-654 (2019).
1339 95. B. J. Read *et al.*, Mannose-binding lectin and complement mediate follicular localization
1340 and enhanced immunogenicity of diverse protein nanoparticle immunogens. *Cell Rep.* **38**,
1341 110217 (2022).
1342 96. R. P. Ringe *et al.*, Neutralizing antibody induction by HIV-1 envelope glycoprotein
1343 SOSIP trimers on iron oxide nanoparticles may be impaired by mannose binding lectin. *J.*
1344 *Virol.* **94**, e01883-01819 (2020).
1345 97. T. J. Moyer *et al.*, Engineered immunogen binding to alum adjuvant enhances humoral
1346 immunity. *Nat. Med.* **26**, 430–440 (2020).
1347 98. S. Kumar *et al.*, A VH1-69 antibody lineage from an infected Chinese donor potently
1348 neutralizes HIV-1 by targeting the V3 glycan supersite. *Sci. Adv.* **6**, eabb1328 (2020).
1349 99. P. J. M. Brouwer *et al.*, Immunofocusing and enhancing autologous Tier-2 HIV-1
1350 neutralization by displaying Env trimers on two-component protein nanoparticles. *Npj*
1351 *Vaccines* **6**, 24 (2021).
1352 100. A. Antanasijevic *et al.*, Structural and functional evaluation of de novo-designed, two-
1353 component nanoparticle carriers for HIV Env trimer immunogens. *PLoS Pathog.* **16**,
1354 e1008665 (2020).
1355 101. P. J. M. Brouwer *et al.*, Enhancing and shaping the immunogenicity of native-like HIV-1
1356 envelope trimers with a two-component protein nanoparticle. *Nat. Commun.* **10**, 4272
1357 (2019).
1358 102. G. Ueda *et al.*, Tailored design of protein nanoparticle scaffolds for multivalent
1359 presentation of viral glycoprotein antigens. *eLife* **9**, e57659 (2020).
1360 103. T. Izard *et al.*, Principles of quasi-equivalence and Euclidean geometry govern the
1361 assembly of cubic and dodecahedral cores of pyruvate dehydrogenase complexes. *Proc.*
1362 *Natl. Acad. Sci. U. S. A.* **96**, 1240-1245 (1999).
1363 104. Y. Hsia *et al.*, Design of a hyperstable 60-subunit protein icosahedron. *Nature* **535**, 136-
1364 139 (2016).
1365 105. A. J. Behrens, M. Crispin, Structural principles controlling HIV envelope glycosylation.
1366 *Curr. Opin. Struct. Biol.* **44**, 125-133 (2017).
1367 106. R. Kong *et al.*, Fusion peptide of HIV-1 as a site of vulnerability to neutralizing antibody.
1368 *Science* **352**, 828-833 (2016).
1369 107. E. Falkowska *et al.*, Broadly neutralizing HIV antibodies define a glycan-dependent
1370 epitope on the prefusion conformation of gp41 on cleaved envelope trimers. *Immunity* **40**,
1371 657-668 (2014).
1372 108. C. Blattner *et al.*, Structural delineation of a quaternary, cleavage-dependent epitope at
1373 the gp41-gp120 interface on intact HIV-1 Env trimers. *Immunity* **40**, 669-680 (2014).

1374 109. L. W. Cao *et al.*, Differential processing of HIV envelope glycans on the virus and
1375 soluble recombinant trimer. *Nat. Commun.* **9**, 3693 (2018).
1376 110. L. Kong *et al.*, Complete epitopes for vaccine design derived from a crystal structure of
1377 the broadly neutralizing antibodies PGT128 and 8ANC195 in complex with an HIV-1
1378 Env trimer. *Acta Crystallogr. D Biol. Crystallogr.* **71**, 2099-2108 (2015).
1379 111. T. Zhou *et al.*, Structural basis for broad and potent neutralization of HIV-1 by antibody
1380 VRC01. *Science* **329**, 811-817 (2010).
1381 112. X. Wu *et al.*, Rational design of envelope identifies broadly neutralizing human
1382 monoclonal antibodies to HIV-1. *Science* **329**, 856-861 (2010).
1383 113. L. Kong *et al.*, Supersite of immune vulnerability on the glycosylated face of HIV-1
1384 envelope glycoprotein gp120. *Nat. Struct. Mol. Biol.* **20**, 796-803 (2013).
1385 114. J. Huang *et al.*, Broad and potent HIV-1 neutralization by a human antibody that binds
1386 the gp41–gp120 interface. *Nature* **515**, 138-142 (2014).
1387 115. D. Sok *et al.*, Promiscuous glycan site recognition by antibodies to the high-mannose
1388 patch of gp120 broadens neutralization of HIV. *Sci. Transl. Med.* **6**, 236ra263 (2014).
1389 116. L. Kong *et al.*, Key gp120 glycans pose roadblocks to the rapid development of VRC01-
1390 class antibodies in an HIV-1-infected Chinese donor. *Immunity* **44**, 939-950 (2016).
1391 117. T. Zhou *et al.*, Multidonor analysis reveals structural elements, genetic determinants, and
1392 maturation pathway for HIV-1 neutralization by VRC01-class antibodies. *Immunity* **39**,
1393 245-258 (2013).
1394 118. R. Derking *et al.*, Comprehensive antigenic map of a cleaved soluble HIV-1 envelope
1395 trimer. *PLoS Pathog.* **11**, e1004767 (2015).
1396 119. R. Henderson *et al.*, Disruption of the HIV-1 envelope allosteric network blocks CD4-
1397 induced rearrangements. *Nat. Commun.* **11**, 520 (2020).
1398 120. Y. N. Zhang *et al.*, Mechanism of a COVID-19 nanoparticle vaccine candidate that elicits
1399 a broadly neutralizing antibody response to SARS-CoV-2 variants. *Sci. Adv.* **7**, eabj3107
1400 (2021).
1401 121. R. Rappuoli, Glycoconjugate vaccines: principles and mechanisms. *Sci. Transl. Med.* **10**,
1402 eaat4615 (2018).
1403 122. J. G. Cyster, B cell follicles and antigen encounters of the third kind. *Nat. Immunol.* **11**,
1404 989-996 (2010).
1405 123. B. A. Heesters, R. C. Myers, M. C. Carroll, Follicular dendritic cells: dynamic antigen
1406 libraries. *Nat. Rev. Immunol.* **14**, 495-504 (2014).
1407 124. L. M. Walker *et al.*, A limited number of antibody specificities mediate broad and potent
1408 serum neutralization in selected HIV-1 infected individuals. *PLoS Pathog.* **6**, e1001028
1409 (2010).
1410 125. D. Sok *et al.*, Recombinant HIV envelope trimer selects for quaternary-dependent
1411 antibodies targeting the trimer apex. *Proc. Natl. Acad. Sci. U. S. A.* **111**, 17624-17629
1412 (2014).
1413 126. Y. N. Zhang *et al.*, Nanoparticle size influences antigen retention and presentation in
1414 lymph node follicles for humoral immunity. *Nano Lett* **19**, 7226-7235 (2019).
1415 127. A. Singh, Eliciting B cell immunity against infectious diseases using nanovaccines. *Nat.*
1416 *Nanotechnol.* **16**, 16-24 (2021).
1417 128. R. Rappuoli, D. Serruto, Self-assembling nanoparticles usher in a new era of vaccine
1418 design. *Cell* **176**, 1245-1247 (2019).

1419 129. G. D. Victora, M. C. Nussenzweig, Germinal centers. *Annu. Rev. Immunol.* **30**, 429-457
1420 (2012).
1421 130. J. López-Sagaseta, E. Malito, R. Rappuoli, M. J. Bottomley, Self-assembling protein
1422 nanoparticles in the design of vaccines. *Comput Struct Biotechnol J* **14**, 58-68 (2016).
1423 131. Y. Li *et al.*, Mechanism of neutralization by the broadly neutralizing HIV-1 monoclonal
1424 antibody VRC01. *J. Virol.* **85**, 8954-8967 (2011).
1425 132. T. G. Phan, I. Grigorova, T. Okada, J. G. Cyster, Subcapsular encounter and
1426 complement-dependent transport of immune complexes by lymph node B cells. *Nat.*
1427 *Immunol.* **8**, 992-1000 (2007).
1428 133. T. G. Phan, J. A. Green, E. E. Gray, Y. Xu, J. G. Cyster, Immune complex relay by
1429 subcapsular sinus macrophages and noncognate B cells drives antibody affinity
1430 maturation. *Nat. Immunol.* **10**, 786-793 (2009).
1431 134. S. F. Gonzalez *et al.*, Capture of influenza by medullary dendritic cells via SIGN-R1 is
1432 essential for humoral immunity in draining lymph nodes. *Nat. Immunol.* **11**, 427-434
1433 (2010).
1434 135. C. D. Allen, T. Okada, J. G. Cyster, Germinal-center organization and cellular dynamics.
1435 *Immunity* **27**, 190-202 (2007).
1436 136. L. Mesin, J. Ersching, G. D. Victora, Germinal center B cell dynamics. *Immunity* **45**,
1437 471-482 (2016).
1438 137. S. Crotty, T follicular helper cell differentiation, function, and roles in disease. *Immunity*
1439 **41**, 529-542 (2014).
1440 138. C. Viant *et al.*, Antibody affinity shapes the choice between memory and germinal center
1441 B cell fates. *Cell* **183**, 1298-1311.e1211 (2020).
1442 139. E. T. Crooks *et al.*, Engineering well-expressed, V2-immunofocusing HIV-1 envelope
1443 glycoprotein membrane trimers for use in heterologous prime-boost vaccine regimens.
1444 *PLoS Pathog.* **17**, e1009807 (2021).
1445 140. P. Martinez-Murillo *et al.*, Particulate array of well-ordered HIV clade C Env trimers
1446 elicits neutralizing antibodies that display a unique V2 cap approach. *Immunity* **46**, 804-
1447 817 (2017).
1448 141. K. Xu *et al.*, Epitope-based vaccine design yields fusion peptide-directed antibodies that
1449 neutralize diverse strains of HIV-1. *Nat. Med.* **24**, 857–867 (2018).
1450 142. P. J. Klasse, G. Ozorowski, R. W. Sanders, J. P. Moore, Env exceptionalism: why are
1451 HIV-1 Env glycoproteins atypical immunogens? *Cell Host Microbe* **27**, 507-518 (2020).
1452 143. R. W. Sanders *et al.*, HIV-1 neutralizing antibodies induced by native-like envelope
1453 trimers. *Science* **349**, aac4223 (2015).
1454 144. M. Pauthner *et al.*, Elicitation of robust tier 2 neutralizing antibody responses in
1455 nonhuman primates by HIV envelope trimer immunization using optimized approaches.
1456 *Immunity* **46**, 1073-1088 (2017).
1457 145. T. Q. Zhou *et al.*, Quantification of the impact of the HIV-1-glycan shield on antibody
1458 elicitation. *Cell Rep.* **19**, 719-732 (2017).
1459 146. K. V. Houser *et al.*, Safety and immunogenicity of an HIV-1 prefusion-stabilized
1460 envelope trimer (Trimer 4571) vaccine in healthy adults: A first-in-human open-label,
1461 randomized, dose-escalation, phase 1 clinical trial. *eClinicalMedicine* **Published Online**,
1462 (2022).
1463 147. M. M. Shan *et al.*, HIV-1 gp120 mannoses induce immunosuppressive responses from
1464 dendritic cells. *PLoS Pathog.* **3**, 1637-1650 (2007).

1465 148. K. Banerjee *et al.*, Enzymatic removal of mannose moieties can increase the immune
1466 response to HIV-1 gp120 in vivo. *Virology* **389**, 108-121 (2009).
1467 149. H.-Y. Huang *et al.*, Vaccination with SARS-CoV-2 spike protein lacking glycan shields
1468 elicits enhanced protective responses in animal models. *Sci. Transl. Med.* **14**, eabm0899
1469 (2022).
1470 150. J. R. Chen *et al.*, Vaccination of monoglycosylated hemagglutinin induces cross-strain
1471 protection against influenza virus infections. *Proc. Natl. Acad. Sci. U. S. A.* **111**, 2476-
1472 2481 (2014).
1473 151. K. Zboray *et al.*, Heterologous protein production using euchromatin-containing
1474 expression vectors in mammalian cells. *Nucleic Acids Res.* **43**, e102 (2015).
1475 152. A. Punjani, J. L. Rubinstein, D. J. Fleet, M. A. Brubaker, cryoSPARC: algorithms for
1476 rapid unsupervised cryo-EM structure determination. *Nat. Methods* **14**, 290–296 (2017).
1477 153. G. Ozorowski *et al.*, Effects of adjuvants on HIV-1 envelope glycoprotein SOSIP trimers
1478 in vitro. *J. Virol.* **92**, e00381-00318 (2018).
1479 154. C. Suloway *et al.*, Automated molecular microscopy: The new Leginon system. *J. Struct.*
1480 *Biol.* **151**, 41-60 (2005).
1481 155. G. C. Lander *et al.*, Appion: An integrated, database-driven pipeline to facilitate EM
1482 image processing. *J. Struct. Biol.* **166**, 95-102 (2009).
1483 156. S. Q. Zheng *et al.*, MotionCor2: anisotropic correction of beam-induced motion for
1484 improved cryo-electron microscopy. *Nat. Methods* **14**, 331-332 (2017).
1485 157. J. Zivanov *et al.*, New tools for automated high-resolution cryo-EM structure
1486 determination in RELION-3. *eLife* **7**, e42166 (2018).
1487 158. S. L. Ilca *et al.*, Localized reconstruction of subunits from electron cryomicroscopy
1488 images of macromolecular complexes. *Nat. Commun.* **6**, 8843 (2015).
1489 159. P. Emsley, M. Crispin, Structural analysis of glycoproteins: building N-linked glycans
1490 with Coot. *Acta Crystallogr. D Biol. Crystallogr.* **74**, 256-263 (2018).
1491 160. R. Y. R. Wang *et al.*, Automated structure refinement of macromolecular assemblies
1492 from cryo-EM maps using Rosetta. *Elife* **5**, e17219 (2016).
1493 161. B. A. Barad *et al.*, EMRinger: side chain directed model and map validation for 3D cryo-
1494 electron microscopy. *Nat. Methods* **12**, 943-946 (2015).
1495 162. C. J. Williams *et al.*, MolProbity: More and better reference data for improved all-atom
1496 structure validation. *Protein Sci.* **27**, 293-315 (2018).
1497 163. M. Sarzotti-Kelsoe *et al.*, Optimization and validation of the TZM-bl assay for
1498 standardized assessments of neutralizing antibodies against HIV-1. *J. Immunol. Methods*
1499 **409**, 131-146 (2014).
1500 164. A. deCamp *et al.*, Global panel of HIV-1 Env reference strains for standardized
1501 assessments of vaccine-elicited neutralizing antibodies. *J. Virol.* **88**, 2489-2507 (2014).
1502 165. C. A. Schneider, W. S. Rasband, K. W. Eliceiri, NIH Image to ImageJ: 25 years of image
1503 analysis. *Nat Methods* **9**, 671-675 (2012).
1504
1505

1506 **Figure Legends**

1507 **Fig. 1. Rational design and characterization of BG505 UFO trimer-presenting nanoparticles.**

1508 (**A**) BG505 UFO Env (middle) and three UFO trimer-presenting SApNPs (FR: left; E2p and I3-

1509 01: right). In the inset (center), ribbon representation of BG505 UFO gp140 protomer (PDB ID:
1510 6UTK) is shown in transparent molecular surface with gp120 in cornflower blue, gp41 in magenta,
1511 and the redesigned $HR1_N$ loop in yellow (as both ribbon and molecular surface models). Surface
1512 representations are shown for FR 24-mer and E2p/I3-01 60-mers presenting 8 and 20 BG505 UFO
1513 trimers, respectively. The NP carrier is colored in gray and the three protomers of each BG505
1514 UFO trimer are colored differently. The NP size is indicated by diameter (in nm). (**B**) Schematic
1515 representation of a multilayered NP (left), which contains an inner layer of locking domains (LD)
1516 and a cluster of T-help epitopes (PADRE), and molecular surface model of E2p (brown, PDB ID:
1517 1B5S) with stepwise incorporation of LD4 (cyan, PDB ID: 2MG4) and PADRE (purple). (**C**) SEC
1518 profiles of BG505 UFO trimer-presenting FR (panel 1), E2p (panel 2), E2p-LD1-7 (panel 3), E2p-
1519 LD4-PADRE (or E2p-L4P, panel 4), I3-01 (panel 5), I3-01-LD4-5/7-9 (panel 6), and I3-01/v9-
1520 LD7-PADRE (or I3-01/v9-L7P, panel 7) after PGT145 purification. (**D**) and (**E**) Reducing SDS-
1521 PAGE and BN-PAGE of BG505 UFO-FR, E2p, and I3-01/v9 SApNPs after PGT145 purification,
1522 with LD and PADRE variants included for E2p and I3-01. (**F**) Negative stain EM images of
1523 PGT145-purified BG505 UFO-FR, E2p-L4P, and I3-01v9-L7P SApNPs. (**G**) Thermostability of
1524 BG505 UFO-FR, E2p-L4P, and I3-01v9-L7P SApNPs, with T_m, $\Delta T_{1/2}$, and T_{on} measured by DSC.
1525 (**H**) Particle size distribution of BG505 UFO-FR, E2p-L4P, and I3-01v9-L7P SApNPs measured
1526 by DLS. Multiple measurements were obtained for each SApNP, with the average particle size
1527 labeled on the distribution plot.

1528 **Fig. 2. Cryo-EM analysis of the multilayered BG505 UFO trimer-presenting nanoparticles.**
1529 Two PGT145/SEC-purified SApNPs, BG505 UFO-E2p-L4P (**A**) and UFO-10GS-I3-01v9-L7P
1530 (**B**), were analyzed. Representative raw cryo-EM micrographs, 2D classes and 3D maps featuring
1531 full NPs (with trimer antigens) are displayed in the top left part of the corresponding panels.

1532 Focused classification and refinement were applied to reconstruct a 3D map of the SApNP core
1533 (top and bottom right), while the localized reconstruction approach was used for extraction and
1534 analysis of trimer subparticles (bottom left). The maps are represented as transparent gray mesh
1535 and the corresponding models are shown as ribbons (NPs - orange; trimer antigens - blue). The
1536 refined model is presented for the E2p NP backbone, while the I3-01v9 and trimer maps are fitted
1537 with previously reported models (PDB ID: 5KP9 and 6UTK).

1538 **Fig. 3. Glycan analysis of BG505 Env immunogens with wildtype and modified glycans.** (**A**)
1539 Comparison of site-specific occupancy and oligomannose-type glycan content for the BG505 UFO
1540 trimer (wildtype, swainsonine, and kifunensine) and three SApNPs (wildtype). The plotted data
1541 represent the mean of three analytical repeats, with trimers shown as circles and NPs as squares.
1542 The oligomannose content was determined by adding all glycan compositions containing
1543 HexNAc(2). (**B**) SEC profiles of BG505 UFO-E2p-L4P and UFO-10GS-I3-01v9-L7P SApNPs
1544 upon endo H treatment. (**C**) Reducing SDS-PAGE of BG505 UFO-E2p-L4P and UFO-10GS-I3-
1545 01v9-L7P SApNPs before and after glycan trimming by endo H. (**D**) EM images of glycan-
1546 trimmed BG505 UFO-E2p-L4P and UFO-10GS-I3-01v9-L7P SApNPs. (**E**) Thermostability of
1547 glycan-trimmed BG505 UFO-E2p-L4P and UFO-10GS-I3-01v9-L7P SApNPs, with T_m, $\Delta T_{1/2}$,
1548 and T_{on} measured by DSC. (**F**) Site-specific glycoform analysis of E2p-L4P and I3-01v9-L7P
1549 SApNPs before and after glycan trimming. The proportion of each glycoform on each site is
1550 represented as the mean of three analytical repeats ± SEM, with oligomannose-type glycans
1551 colored in green and complex-type glycans in pink. The proportion of PNGS lacking a glycan
1552 modification are colored in grey and glycans cleaved with endo H are in blue. (**G**) Reducing SDS-
1553 PAGE of BG505 UFO-E2p-L4P and UFO-10GS-I3-01v9-L7P SApNPs before and after endo H

1554 treatment under two different conditions: 25°C for 5 hours (condition 1) and protein denaturation
1555 at 100°C followed by treatment at 37°C for 1 hour (condition 2).

1556 **Fig. 4. Antigenicity of BG505 UFO Env immunogens with wildtype and modified glycans.**
1557 (**A**) Antigenic profiles of BG505 UFO trimer (top) and its three SApNPs based on FR, E2p-L4D,
1558 and I3-01v9-L7P (bottom) with different glycan treatments (wildtype, expressed in the presence
1559 of kifunensine, and endo H treatment). A total of 13 NAbs/bNAbs and eight non-NAbs were tested
1560 by BLI. Sensorgrams were obtained from an Octet RED96 using an antigen titration series of six
1561 concentrations (starting at 266.7 nM for the UFO trimer, 14.9 nM for the FR SApNP, 5.5 nM for
1562 the E2p and I3-01v9 SApNPs followed by two-fold dilution) and are shown in Fig. S4. The peak
1563 values at the highest concentration are summarized in the matrix, in which cells are colored in red
1564 and green for (b)NAbs and non-NAbs, respectively. Higher color intensity indicates greater
1565 binding signal measured by Octet. (**B**) Negative-stain EM analysis of the glycan-trimmed BG505
1566 UFO trimer in complex with bNAb PGT128. Examples of 2D class images (top) and comparison
1567 with a cryo-EM model of BG505 SOSIP/PGT128 complex (bottom, EMDB-3121, cornflower
1568 blue). (**C**) Negative-stain EM analysis of the glycan-trimmed BG505 UFO trimer in complex with
1569 bNAb VRC01. Examples of 2D class images (top) and superposition of the 3D reconstruction onto
1570 two previously reported BG505 SOSIP/VRC01 models derived from negative-stain EM (EMDB-
1571 6252, orange) and cryo-EM (PDB ID: 6V8X, cyan and green).

1572 **Fig. 5. Immunogenicity of HIV-1 UFO Env immunogens with wildtype glycans in mice and**
1573 **rabbits.** (**A**) Schematic representation of the mouse immunization regimen for two BG505 UFO
1574 trimer-presenting E2p and I3-01v9 SApNPs. (**B**) Neutralization of tier 2 clade A BG505.T332N
1575 and tier 1 clade B SF162 by purified mouse IgG from week 11. (**C**) Percent neutralization of week
1576 11 mouse IgG from four vaccine responders against BG505.T332N and its I396R mutant. Vaccine

1577 responders are those subjects with IC_{50} < 300 μg/ml in IgG neutralization against BG505.T332N.
1578 Color coding indicates the level of reduction in % neutralization relative to BG505.T332N. In both
1579 (B) and (C), the TZM-bl assay was performed in duplicate, starting at an IgG concentration of 300
1580 μg/ml (unless otherwise indicated by *) and a 3-fold dilution series. (**D**) Schematic representation
1581 of the rabbit immunization protocol. Seven groups of rabbits, 6 per group, were immunized to test
1582 the BG505 UFO trimer and its FR, E2p, and I3-01v9 SApNPs, with a cocktail group added for
1583 each SApNP by mixing equal amounts of three SApNPs that display BG505 UFO, CH505 UFO-
1584 BG, or H078.14 UFO-BG trimers (termed Env mix). (**E**) Longitudinal analysis of rabbit plasma
1585 neutralization between weeks 2 and 28. For each group, average ID_{50} values against BG505.T332N
1586 are shown with the SEM. Groups that were immunized with the same vaccine platform are plotted
1587 on the same graph: trimer (red), FR (dark/light purple), E2p (dark/light green) and I3-01v9
1588 (dark/light blue). Week 0 data are omitted due to nonspecific background signals. (**F**) Percentage
1589 neutralization of select week 26 rabbit plasma (≥ 35% neutralization against BG505.T332N at the
1590 first dilution) against BG505.T332N and four glycan hole mutants. For each mutant virus, rabbit
1591 plasma was tested in duplicate, starting at 100-fold dilution followed by a 3-fold dilution series.
1592 Results are shown for BG505.T332N from (E) and the mutant virus at the 100-fold dilution. Color
1593 coding indicates the level of reduction in % neutralization relative to BG505.T332N.

1594 **Fig 6. Immunogenicity of BG505 UFO Env immunogens with trimmed glycans in mice and**
1595 **rabbits.** (**A**) Schematic representation of mouse and rabbit immunization regimen 1, where
1596 glycan-trimmed immunogens were used throughout, and regimen 2, where glycan-trimmed and
1597 wildtype immunogens were used as prime (doses 1 and 2) and boost (doses 3 and 4), respectively.
1598 A three-week interval was used to facilitate the rapid evaluation of various vaccine formulations.
1599 The number of animals in each group is the same as in **Fig. 5**. (**B**) Frequency of vaccine responders

1600 (FVR) calculated for groups in which mice were immunized with the BG505 UFO trimer (left),
1601 E2p SApNP (middle), and I3-01v9 SApNP (right). Purified mouse IgGs from week 11 were tested
1602 against tier 2 clade A BG505.T332N. The TZM-bl neutralization assay was done in duplicate at a
1603 starting concentration of 300 μg/ml and followed by a 3-fold dilution series. A vaccine responder
1604 is defined as a subject with $IC_{50} \leq 300$ μg/ml. No IgG was available for one mouse in the UFO
1605 trimer/AP regimen 1 group and two mice in the I3-01v9/AP regimen 1 (1st repeat) group. In the
1606 comparator groups, no IgG was available for one mouse each in the wildtype E2p/AP and E2p/AV
1607 groups. **(C)** Percent neutralization values of week 11 mouse IgG from select mouse samples (≥
1608 30% autologous neutralization at the highest IgG concentration) against BG505.T332N and its
1609 I396R mutant. Color coding indicates the level of reduction in % neutralization relative to
1610 BG505.T332N. (**D**) Neutralization of tier 2 clade A BG505.T332N by purified rabbit IgG from
1611 week 11. (**E**) FVR of four rabbit groups based on the week 11 autologous neuralization data, with
1612 vaccine responder defined as in (B). (**F**) Percentage neutralization of select week 11 rabbit IgG
1613 samples (≥ 30% autologous neutralization at the highest IgG concentration) against BG505.T332N
1614 and its four glycan hole mutants. The TZM-bl assay was done in duplicate at a starting
1615 concentration of 300 ug/ml and followed by a 3-fold dilution series. Color coding from red to green
1616 indicates greater to lesser reduction in % neutralization relative to BG505.T332N.

1617 **Fig. 7. BG505 UFO Env-SApNP vaccines induce long-term retention in lymph node follicles.**
1618 (**A**) BG505 UFO trimer-presenting I3-01v9 SApNP distribution in a lymph node 12 hours after a
1619 single-dose injection (10 μg/injection, 40 μg/mouse). Anti-Env VRC01, PGT124 and PGDM1400
1620 bNAbs were used to stain the lymph node tissue sections. (**B**) Schematic illustration of I3-01v9
1621 SApNP accumulation in a lymph node. (**C**) Histological images of the distribution of the BG505
1622 UFO trimer and trimer-presenting E2p and I3-01v9 SApNP trafficking and retention in lymph

1623 node follicles 30 minutes to 8 weeks after a single-dose injection. Scale bar = 50 μm for each
1624 image. All immunogens had wildtype glycans except that a glycan-trimmed (GT) I3-01v9 SApNP
1625 was included for comparison. (**D**) Time-dependent curve and (**E**) Area under the curve (AUC) of
1626 the VRC01-stained area in histological images of the vaccine retention in lymph node follicles
1627 over 8 weeks. (**F**) Quantification of vaccine accumulation in lymph node follicles 48 hours after a
1628 single-dose injection. Data were collected from more than 10 lymph node follicles (n = 3-5
1629 mice/group). (**G**) BG505 UFO trimer and trimer-presenting SApNP vaccine interaction with FDC
1630 networks in lymph node follicles 48 hours after a single-dose injection. All BG505 Env-SApNP
1631 immunogens, regardless of the NP platform and glycan treatment, were colocalized with FDC
1632 networks. Immunofluorescent images are pseudo-color-coded ($CD21^+$, green; $CD169^+$, red;
1633 VRC01, white). Scale bars = 500 and 100 μm for complete lymph node and enlarged image of a
1634 follicle, respectively. The data points are expressed as mean ± SEM for (**D**) and SD for (**F**). The
1635 data were analyzed using one-way ANOVA followed by Tukey's multiple comparison post hoc
1636 test. ****$p < 0.0001$.

1637 **Fig. 8. Representative TEM images of BG505 UFO Env-SApNPs interacting with FDCs and**
1638 **phagocytic cells in lymph nodes.** (**A**) TEM images of BG505 UFO-E2p-L4P SApNPs (yellow
1639 arrows) and AddaVax adjuvant (green arrows) presented on the FDC dendrites in a lymph node
1640 12 hours after a single-dose injection (50 μg/injection). (**B**) and (**C**) TEM images of BG505 UFO-
1641 10GS-I3-01v9-L7P SApNPs (yellow arrows), wildtype and glycan-trimmed (GT), aligned on FDC
1642 dendrites without observable aluminum phosphate (AP) adjuvant 12 hours after a single-dose
1643 injection. (**D**) TEM images of BG505 UFO-E2p-L4P SApNPs (yellow arrows) and AddaVax
1644 adjuvant (green arrows) colocalized on the surface or inside of endolysosomes of a macrophage
1645 12 hours after injection. (**E**) and (**F**) TEM images of BG505 UFO-10GS-I3-01v9-L7P SApNPs

1646 (yellow arrows), wildtype and glycan-trimmed (GT), and aluminum phosphate adjuvant (green
1647 arrows) internalized inside endolysosomes of a macrophage, with only SApNPs (yellow arrows)
1648 on the macrophage surface (E) 48 hours, or (F) 12 hours after the injection.

1649 **Fig. 9.** H**IV-1 SApNP vaccines induce robust long-lived germinal centers in lymph nodes.** (A)
1650 Top: Representative immunohistological images of BG505 UFO-10GS-I3-01v9 SApNP vaccine
1651 induced germinal centers (GCs) at two weeks after a single-dose injection (10 μg/injection, 40
1652 μg/mouse). Bottom left: GC B cells (GL7+, red) adjacent to FDCs (CD21+, green) in lymph node
1653 follicles. Bottom Right: Tfh cells in the light zone (LZ) of GCs. Scale bars = 500 and 100 μm for
1654 complete lymph node and enlarged image of a follicle, respectively. (**B**) and (**C**) Quantification of
1655 GCs using immunofluorescent images at week 2, 5 and 8 after (B) a single-dose or (C) prime-
1656 boost injections (n = 5-10 mice/group). The GC/FDC ratio and GC size were determined and
1657 plotted here. (**D**) and (**E**) Representative immunohistological images of GCs included by the
1658 BG505 UFO trimer, E2p, I3-01v9, and GT I3-01v9 SApNP vaccines at week 8 after (D) a single-
1659 dose or (E) prime-boost injections. Scale bar = 50 μm for each image. (**F**) and (**G**) Quantification
1660 of GCs by flow cytometry after (F) a single-dose or (G) prime-boost injections. Percentage and
1661 number of GC B cells and T_{fh} cells were determined and plotted. The data points are shown as
1662 mean ± SD. The data were analyzed using one-way ANOVA followed by Tukey's multiple
1663 comparison post hoc test for each timepoint. *$p < 0.05$, **$p < 0.01$, ***$p < 0.001$, ****$p < 0.0001$.

1664 **SUPPLEMENTAL LEGENDS**

1665 **Table S1.** Cryo-EM data collection information.

1666 **Table S2.** Model building and refinement statistics for the BG505 UFO E2p-L4P NP core.

1667 **Figure S1**. Design and in vitro characterization of BG505 UFO trimer-presenting SApNPs.

1668 **Figure S2.** Cryo-EM analysis of BG505 UFO-E2p-L4P and UFO-10GS-I3-01v9-L7P SApNPs.

1669 **Figure S3.** Site-specific glycan analysis of BG505 UFO trimer and SApNPs.

1670 **Figure S4.** Antigenic characterization of BG505 UFO trimer and trimer-presenting SApNPs with

1671 wildtype and modified glycans.

1672 **Figure S5.** Neutralization data from the evaluation of Env immunogens with wildtype glycans.

1673 **Figure S6.** Neutralization data from the evaluation of Env immunogens with trimmed glycans.

1674 **Figure S7.** Immunohistological images of BG505 UFO trimer and SApNPs in lymph nodes.

1675 **Figure S8.** TEM images of BG505 UFO trimer and SApNPs interacting with FDCs and phagocytic

1676 cells in a lymph node.

1677 **Figure S9.** Immunohistological analysis of BG505 UFO and SApNP vaccine-induced GCs.

1678 **Figure S10.** Flow cytometry analysis of BG505 UFO trimer and SApNP vaccine-induced GCs.

Figure 1

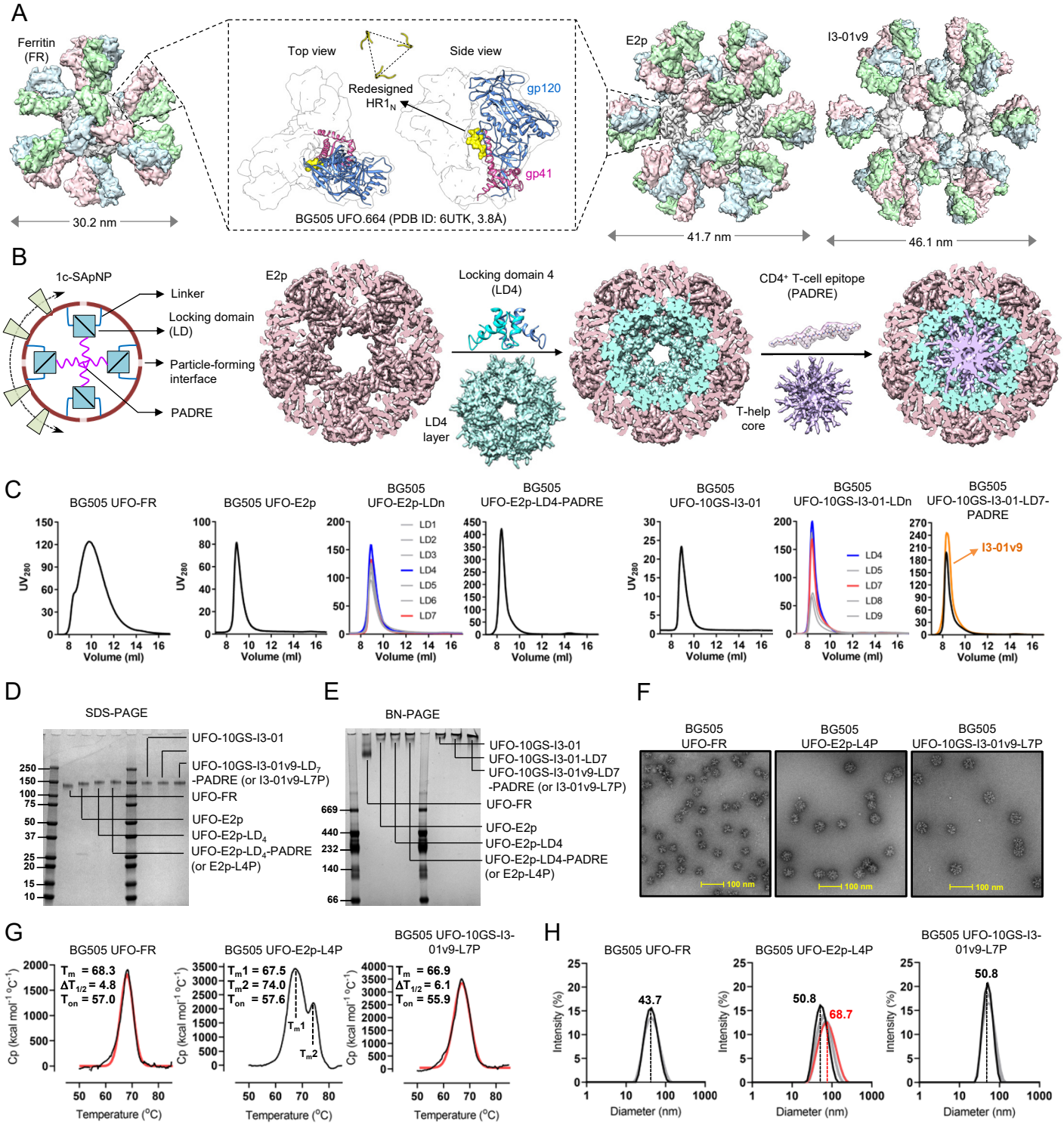
A
Ferritin (FR)
30.2 nm
Top view
Side view
Redesigned HR1N
gp120
gp41
BG505 UFO.664 (PDB ID: 6UTK, 3.8Å)
E2p
41.7 nm
I3-01v9
46.1 nm
B
1c-SApNP
Linker
Locking domain (LD)
Particle-forming interface
PADRE
E2p
Locking domain 4 (LD4)
LD4 layer
CD4+ T-cell epitope (PADRE)
T-help core
C
BG505 UFO-FR
BG505 UFO-E2p
BG505 UFO-E2p-LDn
BG505 UFO-E2p-LD4-PADRE
BG505 UFO-10GS-I3-01
BG505 UFO-10GS-I3-01-LDn
BG505 UFO-10GS-I3-01-LD7-PADRE
UV280
Volume (ml)
LD1
LD2
LD3
LD4
LD5
LD6
LD7
LD8
LD9
I3-01v9
D
SDS-PAGE
UFO-10GS-I3-01
UFO-10GS-I3-01v9-LD7 -PADRE (or I3-01v9-L7P)
UFO-FR
UFO-E2p
UFO-E2p-LD4
UFO-E2p-LD4-PADRE (or E2p-L4P)
E
BN-PAGE
UFO-10GS-I3-01
UFO-10GS-I3-01-LD7
UFO-10GS-I3-01v9-LD7 -PADRE (or I3-01v9-L7P)
UFO-FR
UFO-E2p
UFO-E2p-LD4
UFO-E2p-LD4-PADRE (or E2p-L4P)
F
BG505 UFO-FR
BG505 UFO-E2p-L4P
BG505 UFO-10GS-I3-01v9-L7P
100 nm
G
BG505 UFO-FR
Tm = 68.3
ΔT1/2 = 4.8
Ton = 57.0
BG505 UFO-E2p-L4P
Tm1 = 67.5
Tm2 = 74.0
Ton = 57.6
Tm1
Tm2
BG505 UFO-10GS-I3-01v9-L7P
Tm = 66.9
ΔT1/2 = 6.1
Ton = 55.9
Cp (kcal mol-1 °C-1)
Temperature (°C)
H
BG505 UFO-FR
43.7
BG505 UFO-E2p-L4P
50.8
68.7
BG505 UFO-10GS-I3-01v9-L7P
50.8
Intensity (%)
Diameter (nm)

Figure 2

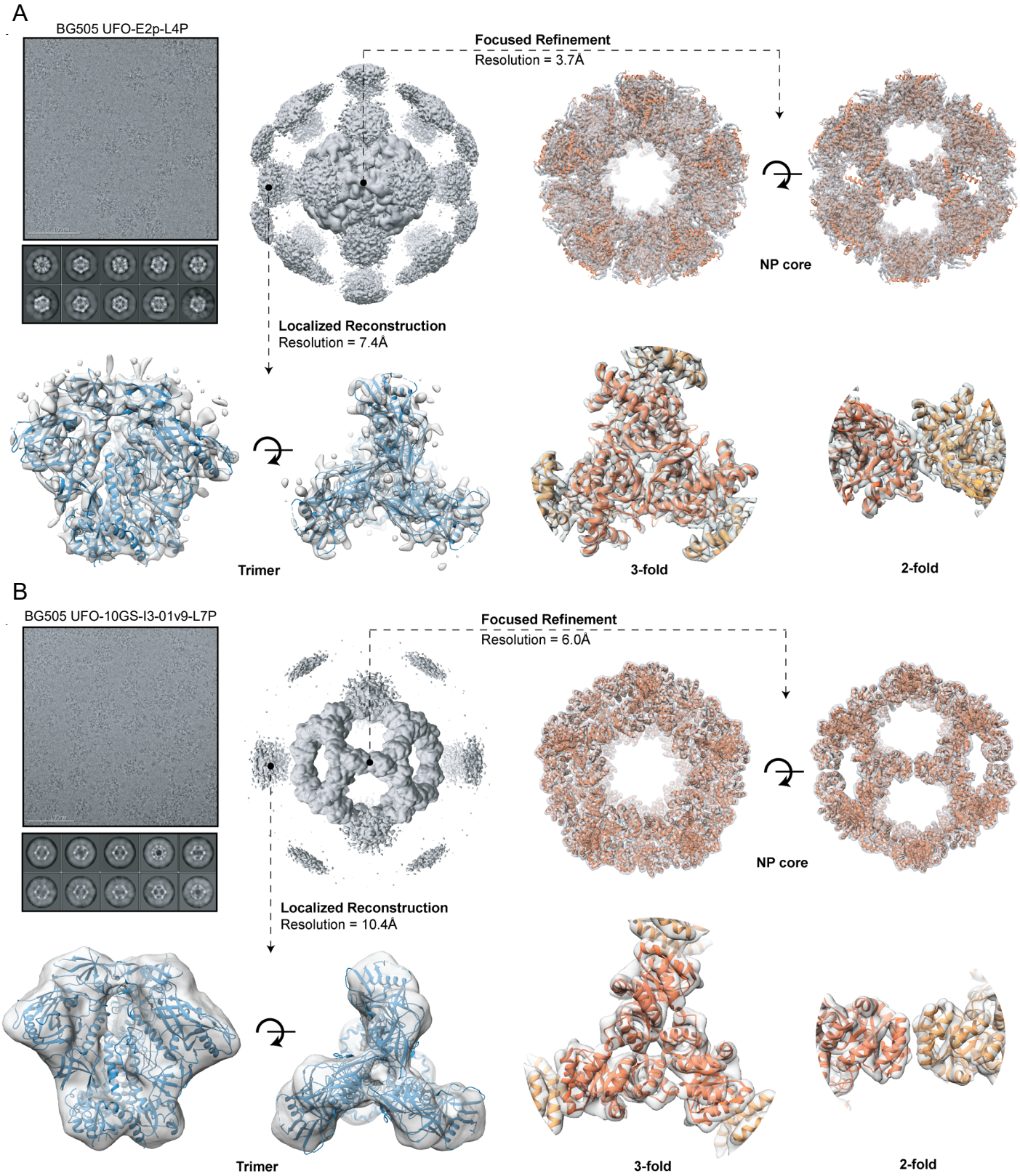
A
BG505 UFO-E2p-L4P
Focused Refinement
Resolution = 3.7Å
NP core
Localized Reconstruction
Resolution = 7.4Å
Trimer
3-fold
2-fold
B
BG505 UFO-10GS-I3-01v9-L7P
Focused Refinement
Resolution = 6.0Å
NP core
Localized Reconstruction
Resolution = 10.4Å
Trimer
3-fold
2-fold

Figure 3

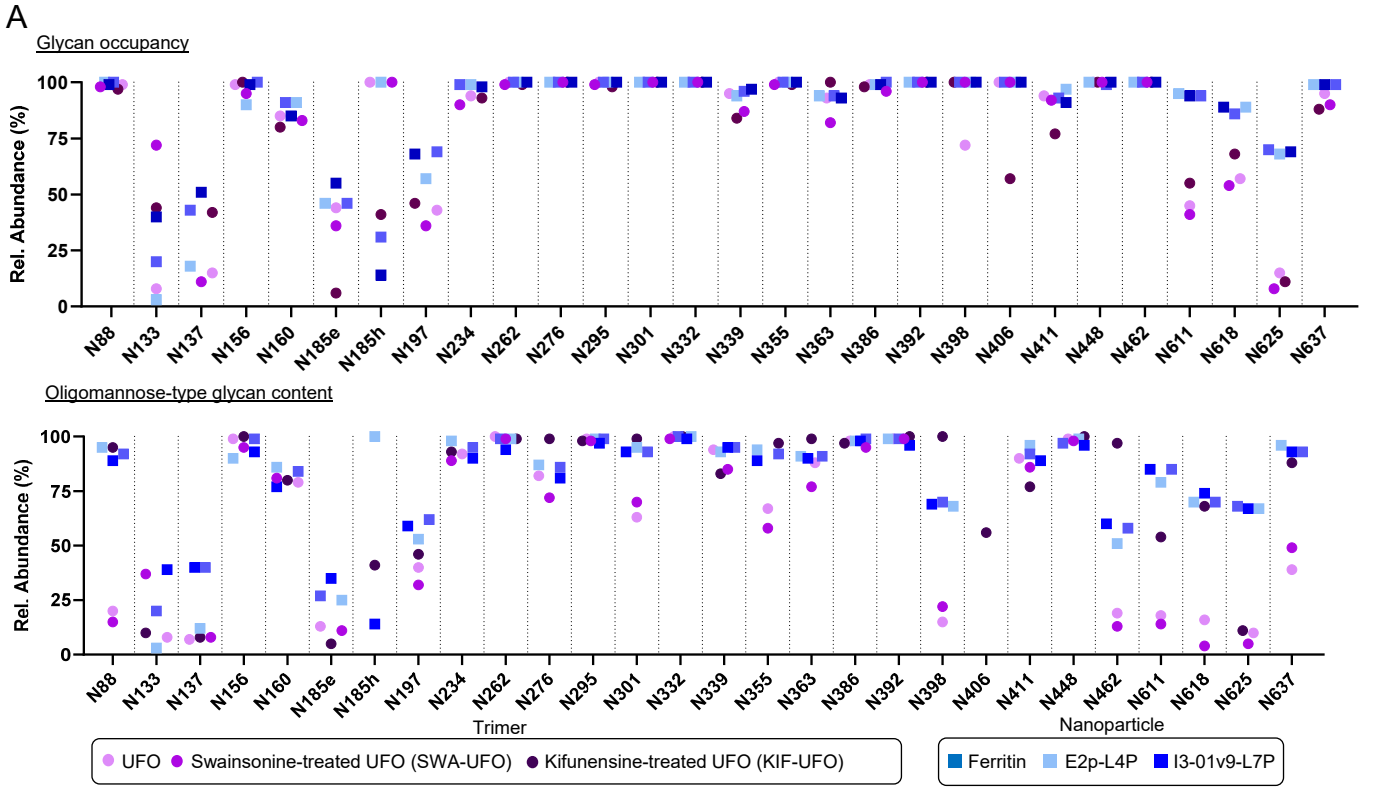
A
Glycan occupancy
Rel. Abundance (%)
Oligomannose-type glycan content
Trimer
Nanoparticle
UFO
Swainsonine-treated UFO (SWA-UFO)
Kifunensine-treated UFO (KIF-UFO)
Ferritin
E2p-L4P
I3-01v9-L7P

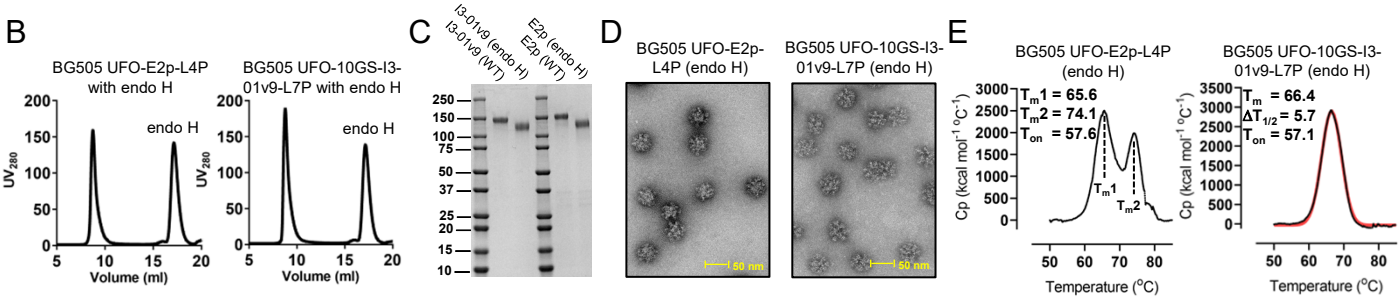
B
BG505 UFO-E2p-L4P with endo H
BG505 UFO-10GS-I3-01v9-L7P with endo H
endo H
Volume (ml)
C
I3-01v9 (endo H)
I3-01v9 (WT)
E2p (endo H)
E2p (WT)
D
BG505 UFO-E2p-L4P (endo H)
BG505 UFO-10GS-I3-01v9-L7P (endo H)
50 nm
E
BG505 UFO-E2p-L4P (endo H)
BG505 UFO-10GS-I3-01v9-L7P (endo H)
Cp (kcal mol⁻¹ °C⁻¹)
Temperature (°C)

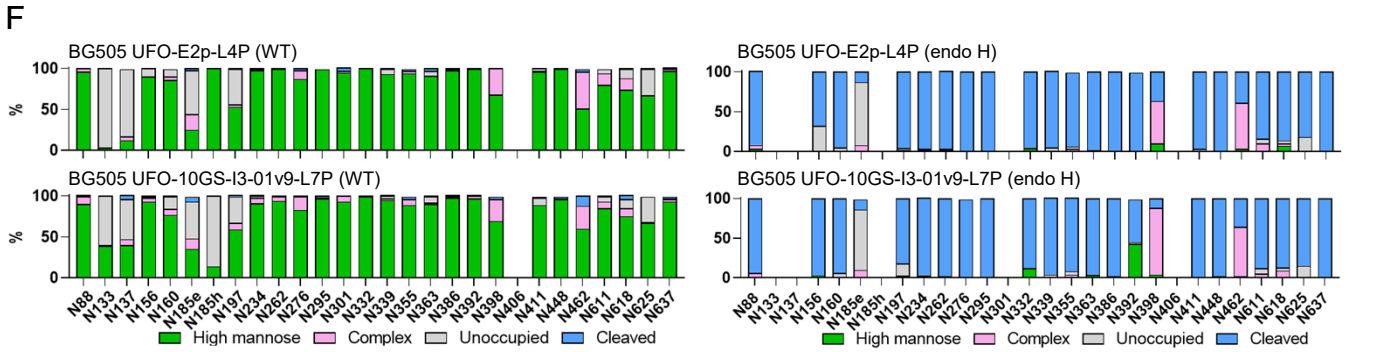
F
BG505 UFO-E2p-L4P (WT)
BG505 UFO-E2p-L4P (endo H)
BG505 UFO-10GS-I3-01v9-L7P (WT)
BG505 UFO-10GS-I3-01v9-L7P (endo H)
%
High mannose
Complex
Unoccupied
Cleaved

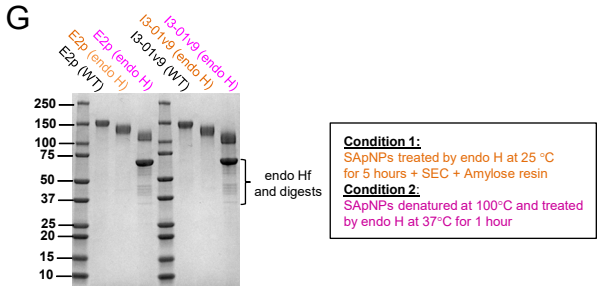
G
E2p (WT)
E2p (endo H)
I3-01v9 (WT)
I3-01v9 (endo H)
endo Hf and digests
Condition 1:
SApNPs treated by endo H at 25 °C for 5 hours + SEC + Amylose resin
Condition 2:
SApNPs denatured at 100°C and treated by endo H at 37°C for 1 hour

Figure 4

A

	PGDM1400	PGT145	PG16	PGT121	PGT128	PGT135	438-B11	2G12	VRC01	VRC34	PGT151	35O22	M4H2K1	F105	b6	19b	446-52D	F240	7B2	17b	A32
Trimer comparison																					
BG505 UFO trimer (WT)	1.0	0.5	0.5	0.7	0.8	0.4	0.7	0.6	0.9	0.8	0.6	0.6	0.7	0.1	0.3	0.7	0.5	0.0	0.0	0.0	0.1
BG505 UFO trimer (KIF)	0.2	0.2	0.1	0.3	0.6	0.2	0.4	0.4	0.5	0.5	0.0	0.5	0.4	0.1	0.2	0.4	0.2	0.0	0.0	0.1	0.0
BG505 UFO trimer (endo H)	0.2	0.2	0.1	0.3	0.4	0.4	0.3	0.4	0.8	0.4	0.1	0.3	0.4	0.1	0.3	0.3	0.2	0.1	0.0	0.1	0.1
Trimer-SApNP comparison																					
BG505 UFO trimer (WT)	1.1	0.6	0.5	0.7	0.7	0.4	0.8	0.6	0.8	0.9	0.6	0.6	0.6	0.2	0.3	0.7	0.5	0.0	0.0	0.0	0.1
BG505 UFO-FR (WT)	2.7	2.1	1.7	1.5	2.1	0.8	1.5	1.9	1.1	0.4	0.2	0.3	1.3	0.2	0.3	1.8	1.4	0.0	0.0	0.0	0.1
BG505 UFO-E2p-L4P (WT)	3.3	2.8	2.3	1.7	2.7	1.0	1.9	2.6	1.3	0.5	0.1	0.4	1.6	0.2	0.3	1.9	2.0	0.1	0.1	0.1	0.1
BG505 UFO-10GS-I3-01v9-L7P (WT)	2.9	2.5	2.0	1.5	2.3	1.0	1.7	2.3	1.3	0.5	0.4	0.4	1.5	0.2	0.3	1.8	1.7	0.1	0.0	0.0	0.1
BG505 UFO trimer (KIF)	0.4	0.5	0.2	0.6	0.7	0.3	0.7	0.6	0.8	0.8	0.0	0.7	0.6	0.2	0.4	0.7	0.4	0.0	0.0	0.1	0.1
BG505 UFO-FR (KIF)	2.3	2.2	1.6	1.2	2.0	0.7	1.7	1.7	1.0	0.2	0.0	0.2	1.2	0.2	0.3	1.5	1.3	0.0	0.0	0.0	0.1
BG505 UFO-E2p-L4P (KIF)	2.6	2.7	1.7	1.3	2.6	1.1	2.2	2.4	0.9	0.3	0.0	0.5	1.3	0.2	0.3	1.8	1.9	0.0	0.0	0.1	0.1
BG505 UFO-10GS-I3-01v9-L7P (KIF)	2.3	2.4	1.7	1.3	2.3	1.2	1.9	2.1	1.1	0.3	0.0	0.5	1.4	0.3	0.4	1.9	1.7	0.1	0.0	0.1	0.1
BG505 UFO trimer (endo H)	0.5	0.4	0.1	0.6	0.6	0.6	0.6	0.6	1.1	0.6	0.4	0.5	0.6	0.3	0.5	0.6	0.4	0.0	0.0	0.0	0.1
BG505 UFO-FR (endo H)	2.6	2.1	1.9	1.5	1.9	1.4	1.6	1.9	2.2	0.7	0.1	0.7	1.7	0.4	0.5	1.9	1.6	0.1	0.0	0.1	0.1
BG505 UFO-E2p-L4P (endo H)	2.8	2.2	2.5	1.7	2.4	1.7	1.7	2.2	2.5	0.7	0.1	0.7	2.1	0.2	0.3	1.9	1.8	0.1	0.0	0.1	0.1
BG505 UFO-10GS-I3-01v9-L7P (endo H)	2.3	2.2	2.1	1.6	2.2	1.6	1.6	2.2	2.4	0.7	0.0	0.8	2.0	0.3	0.5	1.8	1.8	0.0	0.0	0.0	0.1

B

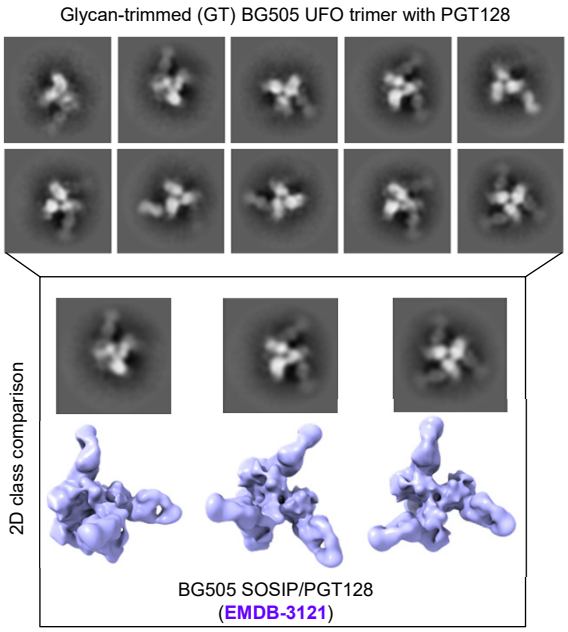

C

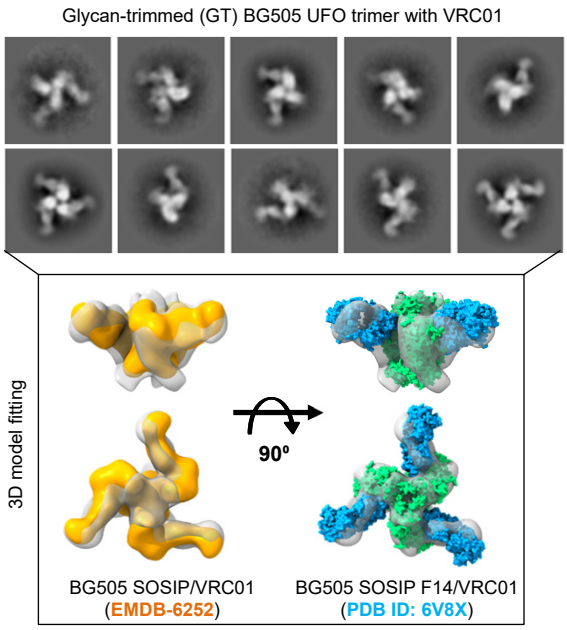

Figure 5

A

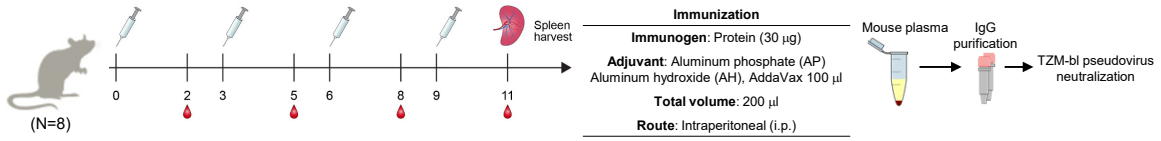

B

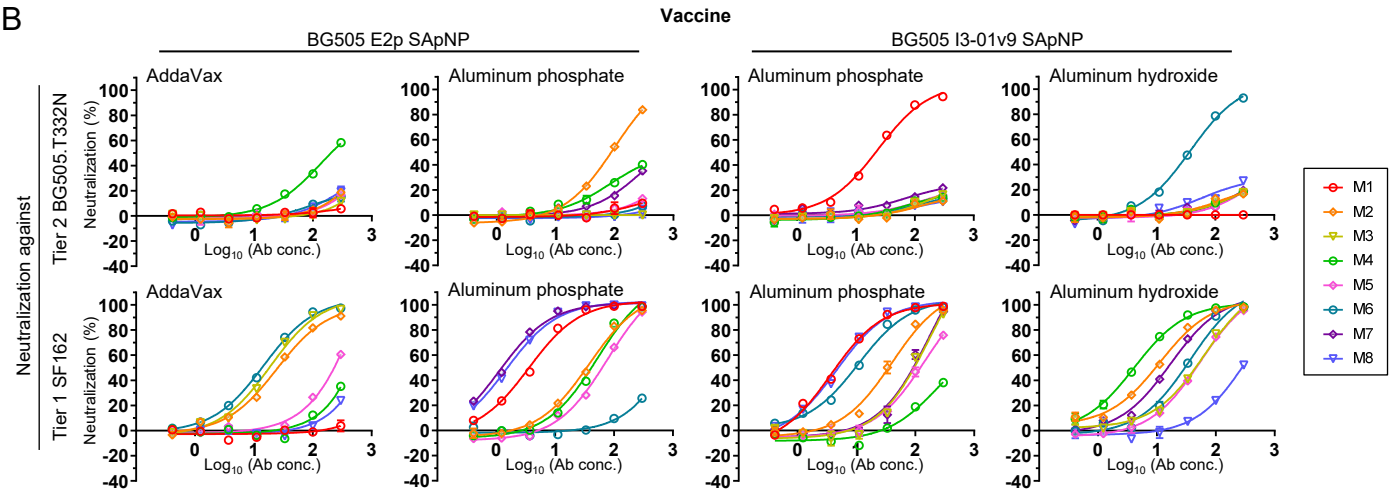

C

% neutralization of mouse IgG against BG505.T332N.I396R mutant [a.]				
Vaccine:	**BG505 E2p SApNP**		**BG505 I3-01v9 SApNP**	
Animal ID:	**G2-M4***	**G3-M2**	**G3-M1**	**G4-M6**
BG505.T332N	33	84	94	93
BG505.T332N.I396R	6	17	52	26

a. Color coding indicates percentage reduction with respect to the % neutralization value obtained for BG505.T332N, <25% green, 25-50% yellow, 50-75% orange, >75% red.
*results shown for this IgG are at ~100 μg/ml for both BG505.T332N & mutant viruses

D

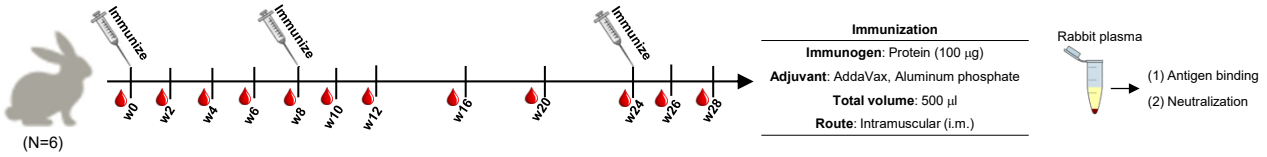

E

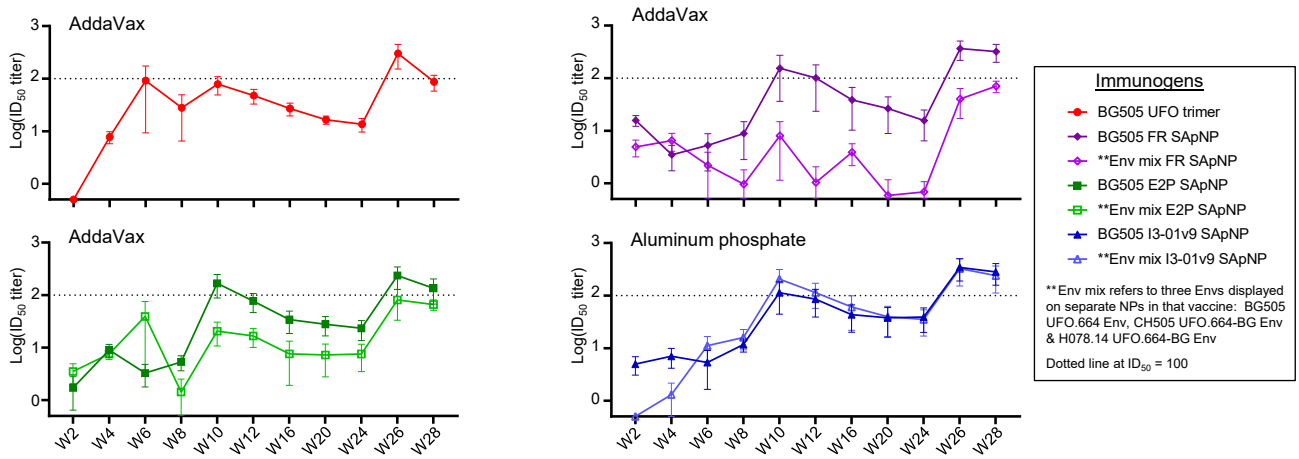

F

% neutralization of W26 rabbit sera against BG505.T332N glycan hole mutants [b.]																								
Vaccine	**BG505 UFO trimer**				**BG505 FR SApNP**				**Env Mix FR SApNP**		**BG505 E2p SApNP**					**Env Mix E2p SApNP**	**BG505 I3-01v9 SApNP**			**Env Mix I3-01v9 SApNP**				
Animal ID	121	122	123	124	126	127	128	130	132	143	137	156	158	159	160	141[c.]	143[c.]	146	147	149	150	151	152	154
BG505.T332N	72	83	64	82	95	95	49	95	37	73	93	45	47	55	96	78	94	84	98	88	86	99	67	42
BG505.T332N.**Q130N**	86	86	75	89	98	90	69	98	61	90	98	45	59	72	96	60	85	84	99	93	67	98	92	24
BG505.T332N.**S241N**	6	69	54	-19	82	85	63	51	37	72	86	48	56	12	88	73	87	74	82	83	77	82	69	51
BG505.T332N.**P291T**	-12	47	31	-14	92	80	27	94	24	63	73	43	37	25	91	68	94	67	97	83	65	96	31	17
BG505.T332N.**T465N**	79	85	42	79	50	43	23	67	24	38	83	24	23	64	36	33	72	52	54	33	62	38	58	21

b. Color coding indicates percentage reduction with respect to the % neutralization value obtained for BG505.T332N, <25% green, 25-50% yellow, 50-75% orange, >75% red.
c. Against BG505.T332N.Q130N: W28 plasma used for rabbits 141 and 143. The % neutralization change is <25% in comparison to BG505.T332N at either W28 (data not shown) or W26 (above) .

Figure 6

A

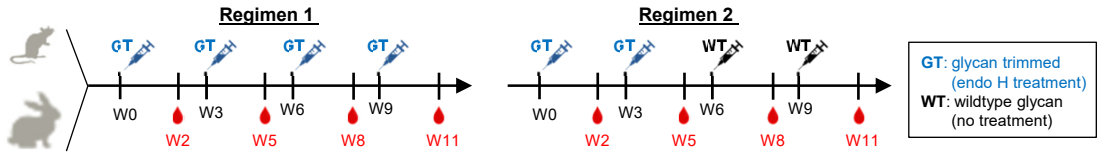

B **Neutralization against tier 2 BG505.T332N by purified mouse IgG**

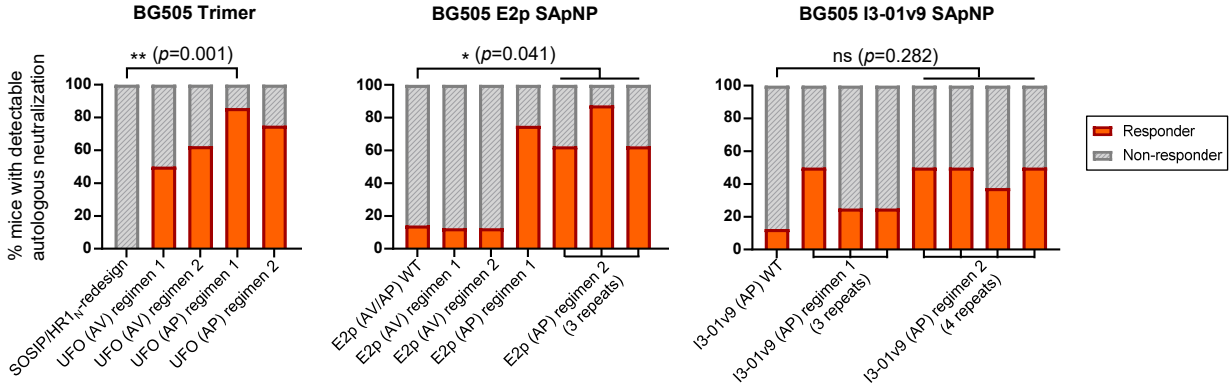

C

% neutralization of mouse IgG against BG505.T332N.I396R mutant [a.]																				
Vaccine	**BG505 UFO trimer (Aluminum phosphate)**																**BG505 E2p SApNP (AddaVax)**			
Glycan trimming regimen	**Regimen 1**							**Regimen 2**									**Regimen 1**			**Regimen 2**	
Animal ID	G3-M1	G3-M2	G3-M4	G3-M5	G3-M6	G3-M7	G3-M8	G4-M1	G4-M2	G4-M3	G4-M4	G4-M5	G4-M6	G4-M7	G4-M8	G1-M2	G1-M3	G1-M5	G2-M4	G2-M8
BG505.T332N	95	51	76	98	97	56	37	70	86	97	68	95	33	38	84	51	32	90	32	86
BG505.T332N. I396R	37	28	63	28	29	46	29	32	24	30	34	33	31	42	42	89	36	27	13	95

Vaccine	**BG505 E2p SApNP (Aluminum phosphate)**													**BG505 I3-01v9 SApNP (Aluminum phosphate)**						
Glycan trimming regimen	**Regimen 1**							**Regimen 2**						**Regimen 1**			**Regimen 2**			
Animal ID	G1-M1	G1-M2	G1-M3	G1-M4	G1-M5	G1-M6	G1-M7	G2-M2	G2-M3	G2-M4	G2-M6	G2-M7	G2-M8	G3-M1	G3-M3	G3-M8	G4-M2	G4-M3	G4-M4	G4-M5
BG505.T332N	49	71	73	71	93	39	89	92	98	60	88	91	38	70	49	91	93	82	91	87
BG505.T332N. I396R	40	71	87	80	86	39	30	89	58	62	92	41	37	66	43	43	98	94	96	46

a. Color coding indicates percentage reduction with respect to the % neutralization value obtained for BG505.T332N, <25% green, 25-50% yellow, 50-75% orange, >75% red.

D **Neutralization against tier 2 BG505.T332N by week 11 purified rabbit IgG**

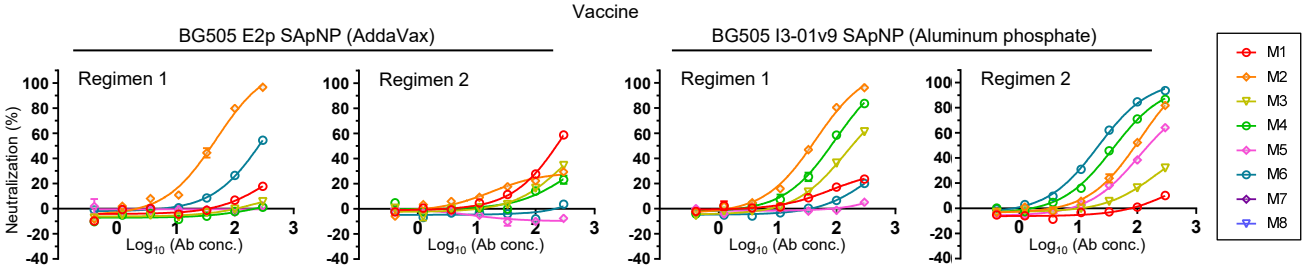

E

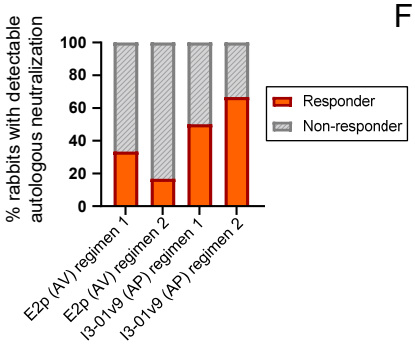

F

% neutralization of rabbit IgG against BG505.T332N glycan hole mutants [b.]												
Vaccine	**BG505 E2p SApNP**				**BG505 I3-01v9 SApNP**							
Glycan trimming regimen	**Regimen 1**		**Regimen 2**		**Regimen 1**			**Regimen 2**				
Animal ID	G1-2	G1-6	G2-1	G2-3	G3-2	G3-3	G3-4	G4-2	G4-3	G4-4	G4-5	G4-6
BG505.T332N	97	54	59	34	96	61	84	82	32	87	64	94
BG505.T332N.**Q130N**	97	53	69	38	97	58	90	87	5	91	77	96
BG505.T332N.**S241N**	99	2	89	26	100	32	96	90	71	91	62	98
BG505.T332N.**P291T**	96	2	74	7	97	11	88	86	53	88	59	95
BG505.T332N.**T465N**	16	59	16	39	36	59	26	65	54	39	49	95

b. Color coding indicates percentage reduction with respect to the % neutralization value obtained for BG505.T332N, <25% green, 25-50% yellow, 50-75% orange, >75% red.

Figure 7

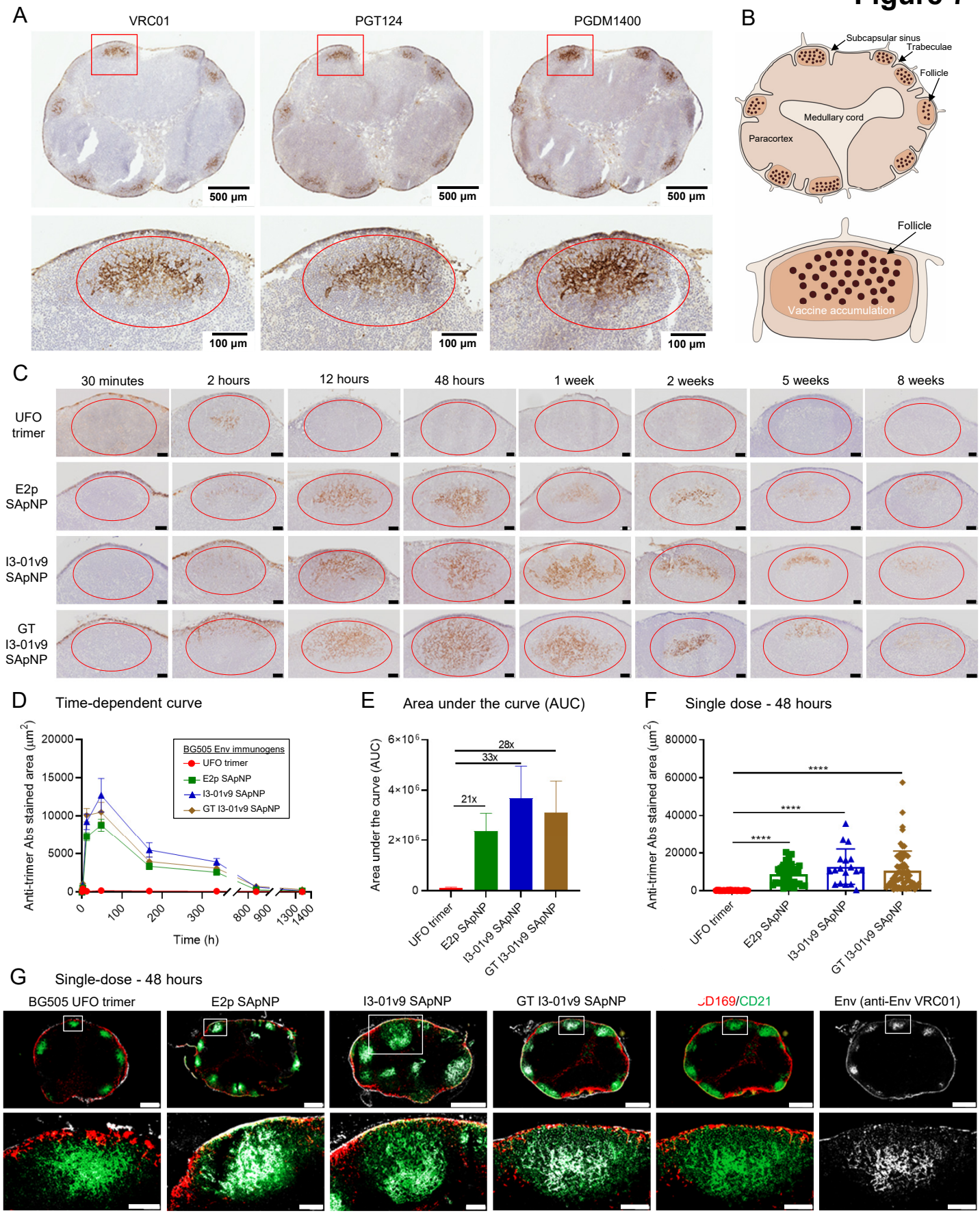
A
VRC01
PGT124
PGDM1400
500 µm
100 µm
B
Subcapsular sinus
Trabeculae
Follicle
Medullary cord
Paracortex
Follicle
Vaccine accumulation
C
30 minutes
2 hours
12 hours
48 hours
1 week
2 weeks
5 weeks
8 weeks
UFO trimer
E2p SApNP
I3-01v9 SApNP
GT I3-01v9 SApNP
D
Time-dependent curve
Anti-trimer Abs stained area (µm²)
Time (h)
BG505 Env immunogens
UFO trimer
E2p SApNP
I3-01v9 SApNP
GT I3-01v9 SApNP
E
Area under the curve (AUC)
Area under the curve (AUC)
21x
33x
28x
UFO trimer
E2p SApNP
I3-01v9 SApNP
GT I3-01v9 SApNP
F
Single dose - 48 hours
Anti-trimer Abs stained area (µm²)
****
UFO trimer
E2p SApNP
I3-01v9 SApNP
GT I3-01v9 SApNP
G
Single-dose - 48 hours
BG505 UFO trimer
E2p SApNP
I3-01v9 SApNP
GT I3-01v9 SApNP
CD169/CD21
Env (anti-Env VRC01)

Figure 8

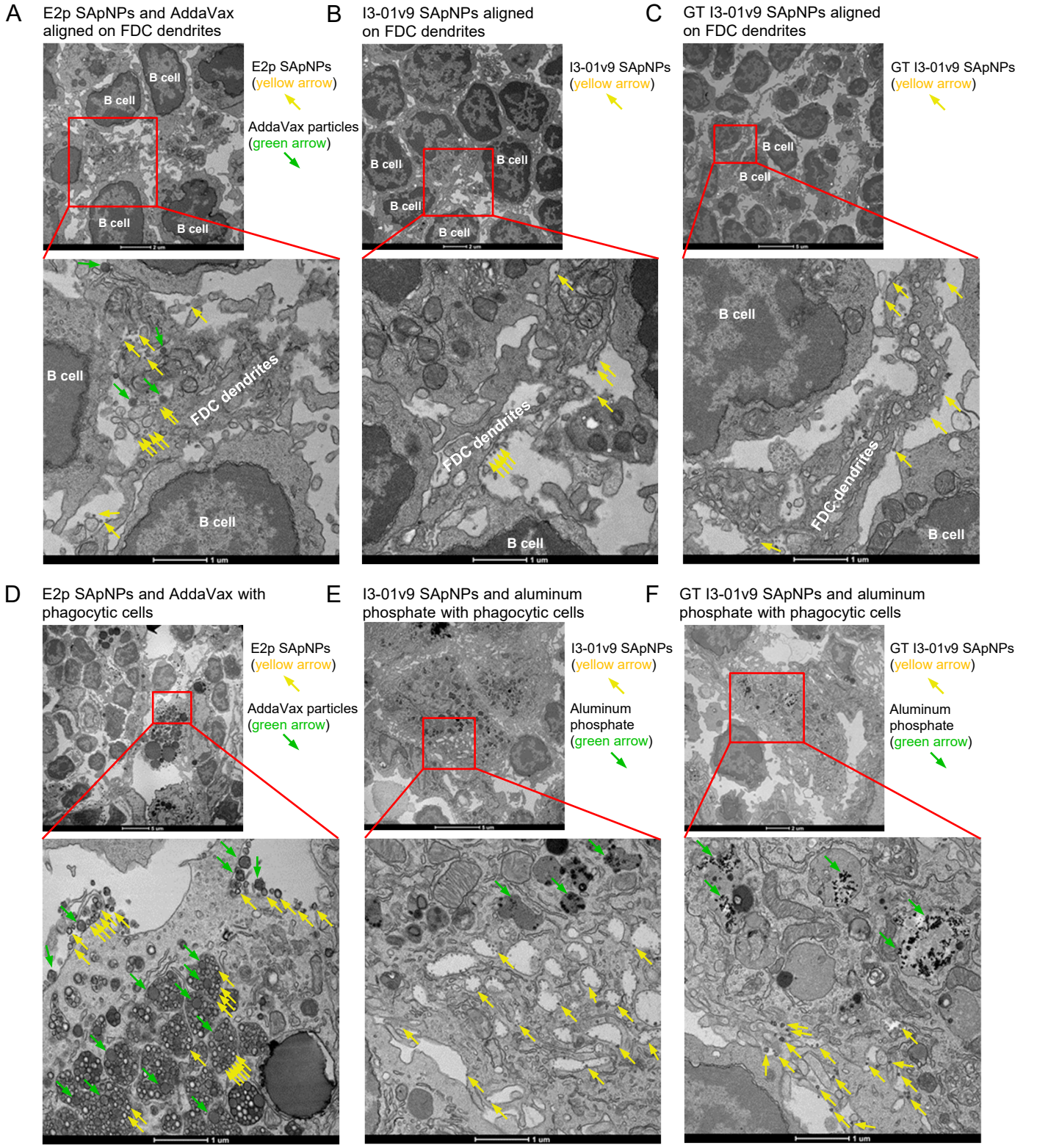
A
E2p SApNPs and AddaVax aligned on FDC dendrites
B
I3-01v9 SApNPs aligned on FDC dendrites
C
GT I3-01v9 SApNPs aligned on FDC dendrites
E2p SApNPs (yellow arrow)
AddaVax particles (green arrow)
I3-01v9 SApNPs (yellow arrow)
GT I3-01v9 SApNPs (yellow arrow)
B cell
FDC dendrites
D
E2p SApNPs and AddaVax with phagocytic cells
E
I3-01v9 SApNPs and aluminum phosphate with phagocytic cells
F
GT I3-01v9 SApNPs and aluminum phosphate with phagocytic cells
Aluminum phosphate (green arrow)
1 um

Figure 9

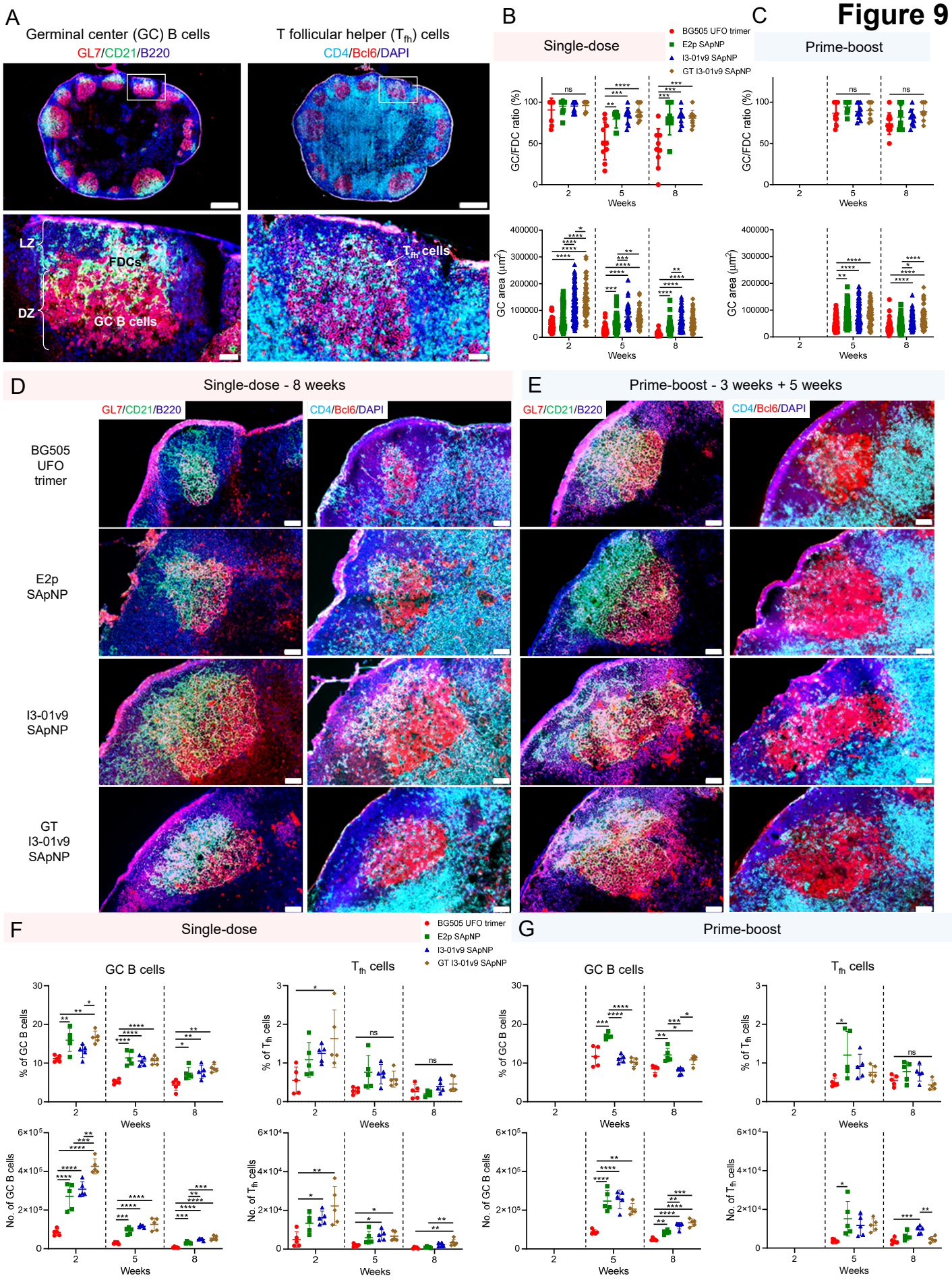
A
Germinal center (GC) B cells
GL7/CD21/B220
T follicular helper (T_{fh}) cells
CD4/Bcl6/DAPI
LZ
FDCs
DZ
GC B cells
T_{fh} cells
B
Single-dose
C
Prime-boost
BG505 UFO trimer
E2p SApNP
I3-01v9 SApNP
GT I3-01v9 SApNP
GC/FDC ratio (%)
GC area (μm²)
Weeks
D
Single-dose - 8 weeks
E
Prime-boost - 3 weeks + 5 weeks
BG505 UFO trimer
E2p SApNP
I3-01v9 SApNP
GT I3-01v9 SApNP
F
Single-dose
G
Prime-boost
GC B cells
T_{fh} cells
% of GC B cells
% of T_{fh} cells
No. of GC B cells
No. of T_{fh} cells

Table S1. Cryo-EM data collection information.

	BG505 UFO-10GS-I3-01v9-L7P	BG505 UFO-E2p-L4P
Microscope	Talos Arctica	Titan Krios
Voltage (kV)	200	300
Detector	Gatan K2 Summit	Gatan K2 Summit
Recording mode	Counting	Counting
Magnification	36,000 ×	29,000 ×
Movie micrograph pixel size	1.15	1.03
Dose rate (e−/Å2/s)	4.2	4.9
No. of frames per movie micrograph	48	41
Frame exposure time (ms)	250	250
Movie micrograph exposure time (s)	12	10.25
Total dose (e−/Å2)	50.4	50.2
Under focus range (μm)	0.6 – 2.0	0.7 – 1.5
Number of movie micrographs	1200	2300

Table S2. Model building and refinement statistics for the BG505 UFO E2p-L4P NP core.

	BG505 UFO-E2p-L4P core
Map Resolution	3.7
EMDB ID	-
PDB	-
Residues	13980
Amino-acids	13980
Carbohydrates	0
RMSD Bonds	0.019
RMSD Angles	1.605
Ramachandran	
Outliers (%)	0.0
Allowed (%)	1.3
Favored (%)	98.7
Rotamer outliers	0.00
Clash score	0.00
Molprobity score	0.50
EMRinger score	3.51

fig. S1

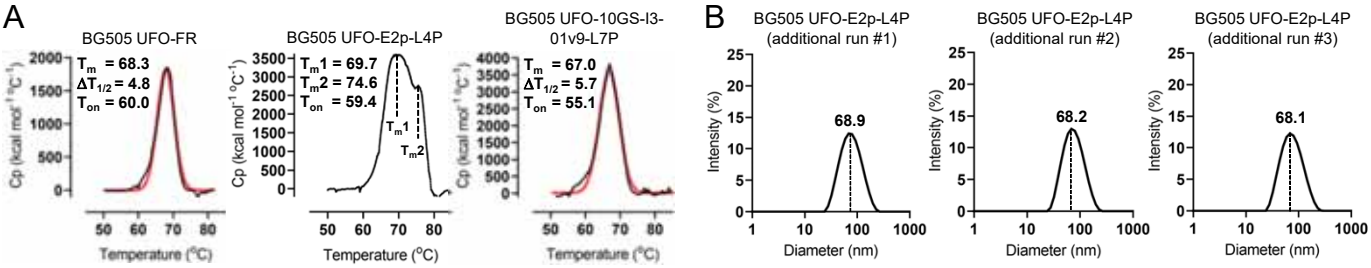

C

>BG505 UFO-FR

MDAMKRGLCCVLLLCGAVFVSPSQEIHARFRRGARSRAENLWVTVYYGVPVWKDAETTLFCASDAKAYDTEKHNVWATHACVPTDPNPQEIHLENVTEEFNM
WKNNMVEQMHTDIISLWDQSLKPCVKLTPLCVTLQCTNVTNNITDDMRGELKNCSFNMTTELRDKKQKVYSLFYRLDVVQINENQGNRSNNSNKEYRLINCN
TSAITQACPKVSFEPIPIHYCAPAGFAILKCKDKKFNGTGPCPSVSTVQCTHGIKPVVSTQLLLNGSLAEEEVMIRSENITNNAKNILVQFNTPVQINCTRP
NNNTRKSIRIGPGQAFYATGDIIGDIRQAHCNVSKATWNETLGKVVKQLRKHFGNNTIIRFANSSGGDLEVTTHSFNCGGEFFYCNTSGLFNSTWISNTSVQ
GSNSTGSNDSITLPCRIKQIINMWQRIGQAMYAPPIQGVIRCVSNITGLILTRDGGSTNSTTETFRPGGGDMRDNWRSELYKYKVVKIEPLGVAPTRCKRRV
VGGGGGSGGGGSAVGIGAVFLGFLGAAGSTMGAASMTLTVQARNLLSGNPDWLPDMTVWGIKQLQARVLAVERYLRDQQLLGIWGCSGKLICCTNVPWNSSW
SNRNLSEIWDNMTWLQWDKEISNYTQIIYGLLEESQNQQEKNEQDLLALDASGDIIKLLNEQVNKEMQSSNLYMSMSSWCYTHSLDGAGLFLFDHAAEEYEH
AKKLIIFLNENNVPVQLTSISAPEHKFEGLTQIFQKAYEHEQHISESINNIVDHAIKSKDHATFNFLQWYVAEQHEEEVLFKDILDKIELIGNENHGLYLAD
QYVKGIAKSRKS

>BG505 UFO-E2p-LD4-PADRE (or E2p-L4P)

MDAMKRGLCCVLLLCGAVFVSPSQEIHARFRRGARSRAENLWVTVYYGVPVWKDAETTLFCASDAKAYDTEKHNVWATHACVPTDPNPQEIHLENVTEEFNM
WKNNMVEQMHTDIISLWDQSLKPCVKLTPLCVTLQCTNVTNNITDDMRGELKNCSFNMTTELRDKKQKVYSLFYRLDVVQINENQGNRSNNSNKEYRLINCN
TSAITQACPKVSFEPIPIHYCAPAGFAILKCKDKKFNGTGPCPSVSTVQCTHGIKPVVSTQLLLNGSLAEEEVMIRSENITNNAKNILVQFNTPVQINCTRP
NNNTRKSIRIGPGQAFYATGDIIGDIRQAHCNVSKATWNETLGKVVKQLRKHFGNNTIIRFANSSGGDLEVTTHSFNCGGEFFYCNTSGLFNSTWISNTSVQ
GSNSTGSNDSITLPCRIKQIINMWQRIGQAMYAPPIQGVIRCVSNITGLILTRDGGSTNSTTETFRPGGGDMRDNWRSELYKYKVVKIEPLGVAPTRCKRRV
VGGGGGSGGGGSAVGIGAVFLGFLGAAGSTMGAASMTLTVQARNLLSGNPDWLPDMTVWGIKQLQARVLAVERYLRDQQLLGIWGCSGKLICCTNVPWNSSW
SNRNLSEIWDNMTWLQWDKEISNYTQIIYGLLEESQNQQEKNEQDLLALDASGAAAKPATTEGEFPETREKMSGIRRAIAKAMVHSKHTAPHVTLMDEADVT
KLVAHRKKFKAIAAEKGIKLTFLPYVVKALVSALREYPVLNTAIDDETEEIIQKHYYNIGIAADTDRGLLVPVIKHADRKPIFALAQEINELAEKARDGKLT
PGEMKGASCTITNIGSAGGQWFTPVINHPEVAILGIGRIAEKPIVRDGEIVAAPMLALSLSFDHRMIDGATAQKALNHIKRLLSDPELLLMGGGGSFSEEQK
KALDLAFYFDRRLTPEWRRYLSQRLGLNEEQIERWFRRKEQQIGWSHPQFEKGSAKFVAAWTLKAAA

>BG505 UFO-10GS-I3-01v9-LD7-PADRE (or I3-01v9-L7P)

MDAMKRGLCCVLLLCGAVFVSPSQEIHARFRRGARSRAENLWVTVYYGVPVWKDAETTLFCASDAKAYDTEKHNVWATHACVPTDPNPQEIHLENVTEEFNM
WKNNMVEQMHTDIISLWDQSLKPCVKLTPLCVTLQCTNVTNNITDDMRGELKNCSFNMTTELRDKKQKVYSLFYRLDVVQINENQGNRSNNSNKEYRLINCN
TSAITQACPKVSFEPIPIHYCAPAGFAILKCKDKKFNGTGPCPSVSTVQCTHGIKPVVSTQLLLNGSLAEEEVMIRSENITNNAKNILVQFNTPVQINCTRP
NNNTRKSIRIGPGQAFYATGDIIGDIRQAHCNVSKATWNETLGKVVKQLRKHFGNNTIIRFANSSGGDLEVTTHSFNCGGEFFYCNTSGLFNSTWISNTSVQ
GSNSTGSNDSITLPCRIKQIINMWQRIGQAMYAPPIQGVIRCVSNITGLILTRDGGSTNSTTETFRPGGGDMRDNWRSELYKYKVVKIEPLGVAPTRCKRRV
VGGGGGSGGGGSAVGIGAVFLGFLGAAGSTMGAASMTLTVQARNLLSGNPDWLPDMTVWGIKQLQARVLAVERYLRDQQLLGIWGCSGKLICCTNVPWNSSW
SNRNLSEIWDNMTWLQWDKEISNYTQIIYGLLEESQNQQEKNEQDLLALDASGGGGSGGGGSMKMEELFKKHKIVAVLRANSVEEAKMKALAVFVGGVHLIE
ITFTVPDADTVIKELSFLKELGAIIGAGTVTSVEQCRKAVESGAEFIVSPHLDEEISQFCKEKGVFYMPGVMTPTELVKAMKLGHTILKLFPGEVVGPQFVK
AMKGPFPNVKFVPTGGVNLDNVCEWFKAGVLAVGVGSALVKGTIAEVAAKAAAFVEKIRGCTEGGGGSSPAVDIGDRLDELEKALEALSAEDGHDDVGQRLE
SLLRRWNSRRADGSAKFVAAWTLKAAA

fig S1. Design and in vitro characterization of BG505 UFO trimer-presenting SApNPs. (**A**) Additional thermostability data for BG505 UFO trimer-presenting FR (left), E2p-L4P, and I3-01v9-L7P NPs, with T_m (T_{m1} and T_{m2} for E2p), ΔT1/2, and T_{on} measured by differential scanning calorimetry (DSC) and labeled on the plots. For FR and I3-01v9 NPs, the raw and Gaussian-fitted DSC data are shown in black and red lines, respectively. (**B**) Additional particle size data for BG505 UFO trimer-presenting E2p-L4P NP measured by dynamic light scattering using a Zetasizer. The average particle size is labeled on the plots. (**C**) Construct sequences of BG505 UFO trimer-presenting FR (left), E2p-L4P, and I3-01v9-L7P NPs, with the gene fragments of leader sequence, restriction site, BG505 UFO Env, flexible linker, NP-forming subunit, locking domain (LD), and PADRE highlighted in yellow, green, gray, light magenta, cyan, olive green, and red shades, respectively.

fig. S2

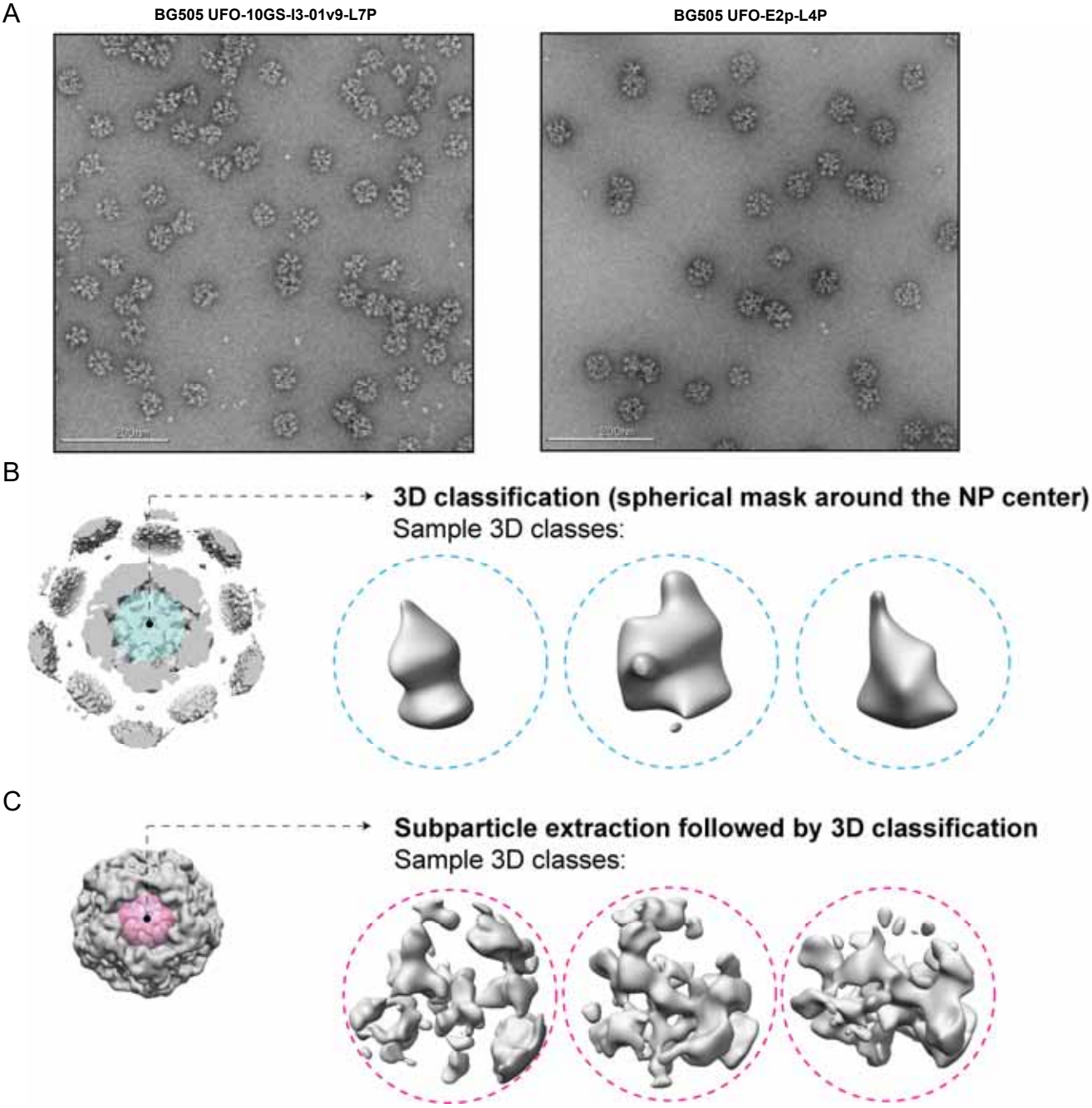

fig S2. Cryo-EM analysis of BG505 UFO-E2p-L4P and UFO-10GS-I3-01v9-L7PSApNPs. (**A**) Negative stain EM of the two multilayered SApNP immunogens to validate their structural integrity. For BG505 UFO-E2p-L4P SApNP, cryo-EM data are shown for (**B**) 3D classification (spherical mask around the NP center) and (**C**) Subparticle extraction followed by 3D classification.

fig. S3

A WT BG505 UFO trimer

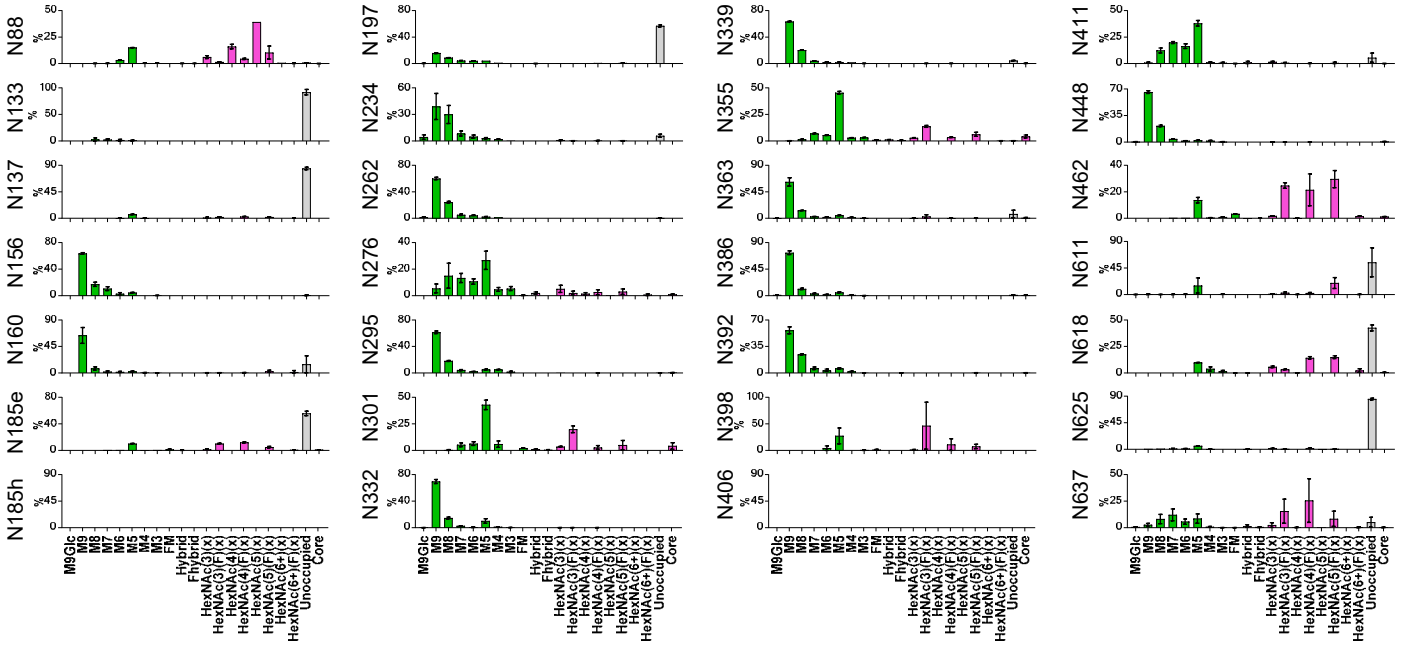

B BG505 UFO trimer expressed in the presence of Swainsonine

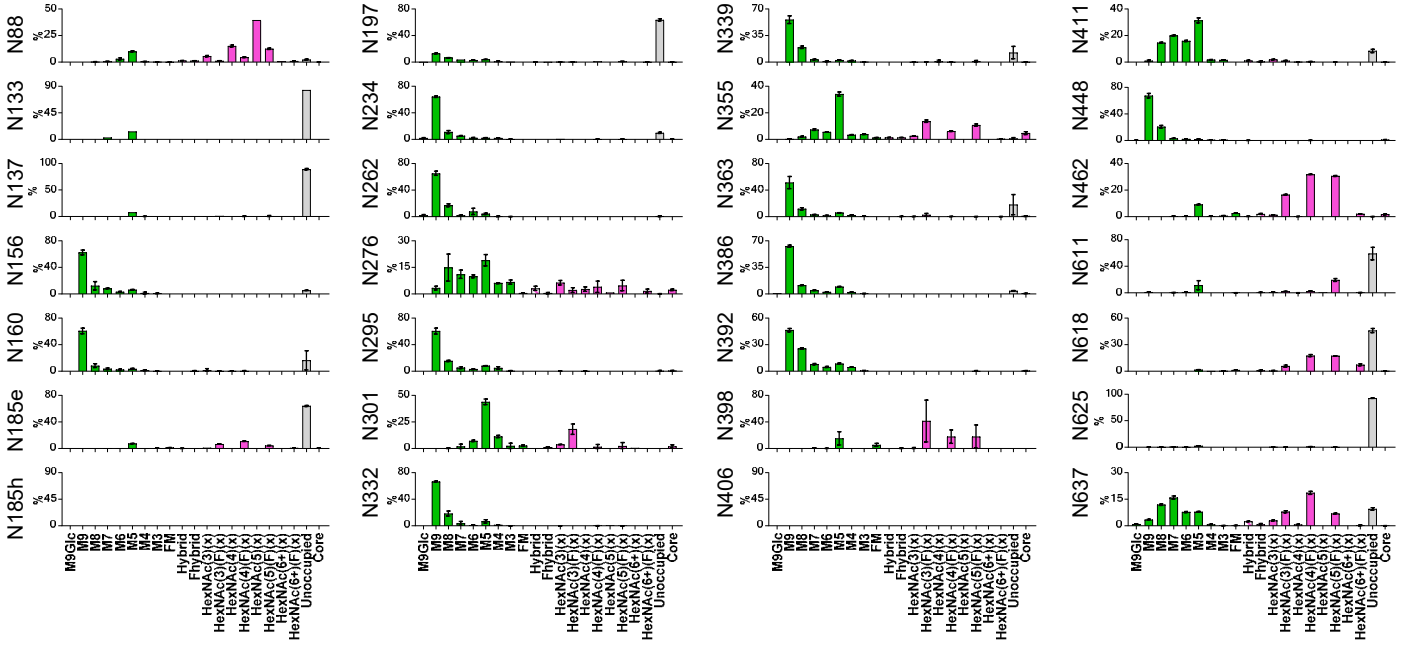

fig. S3 (continued)

C BG505 UFO trimer expressed in the presence of kifunensine

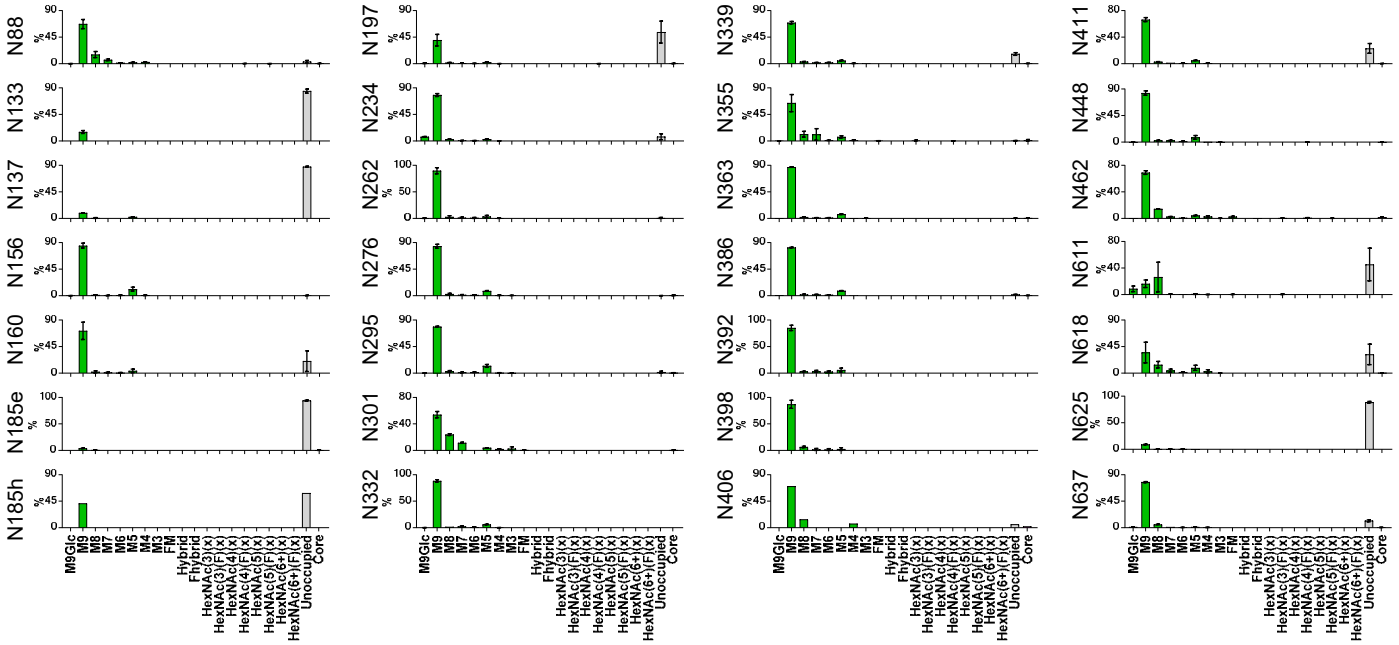

D WT BG505 UFO-FR SApNP

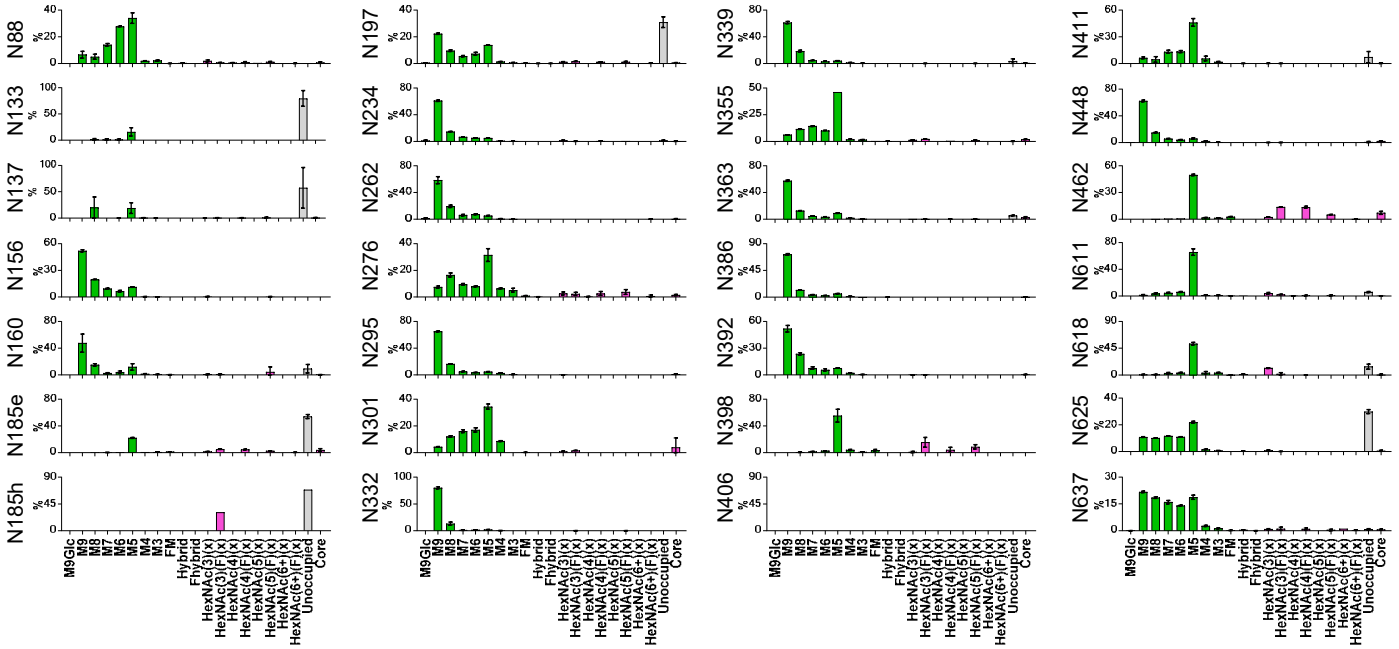

fig. S3 (continued)

E WT BG505 UFO-E2p-L4P SApNP

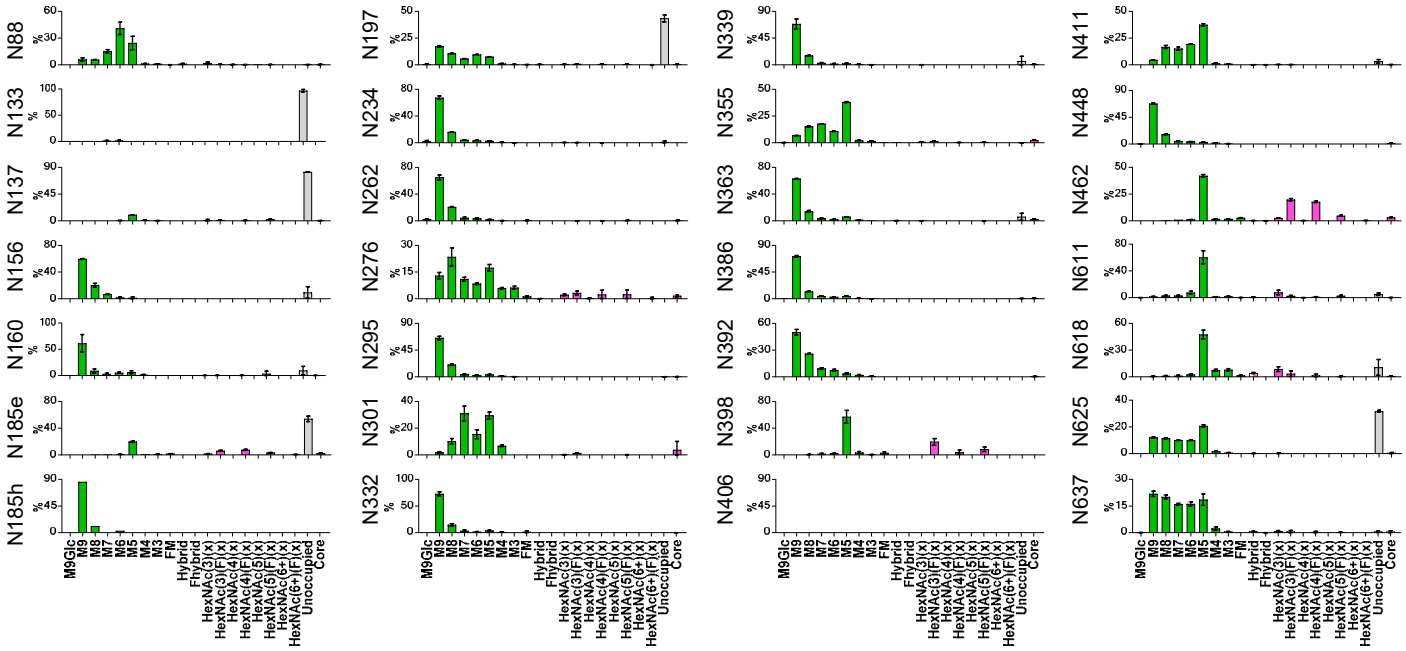

F WT BG505 UFO-10GS-I3-01v9-L7P SApNP

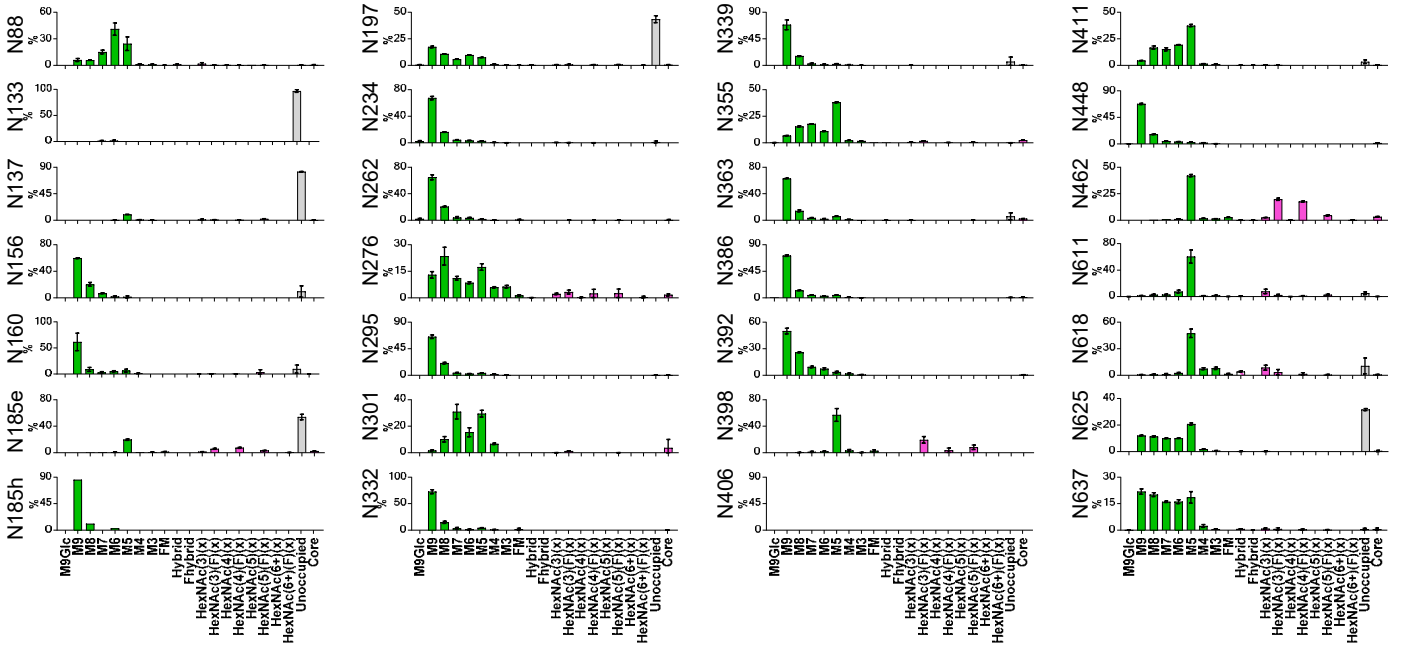

G Endo H-treated BG505 UFO-E2p-L4P SApNP

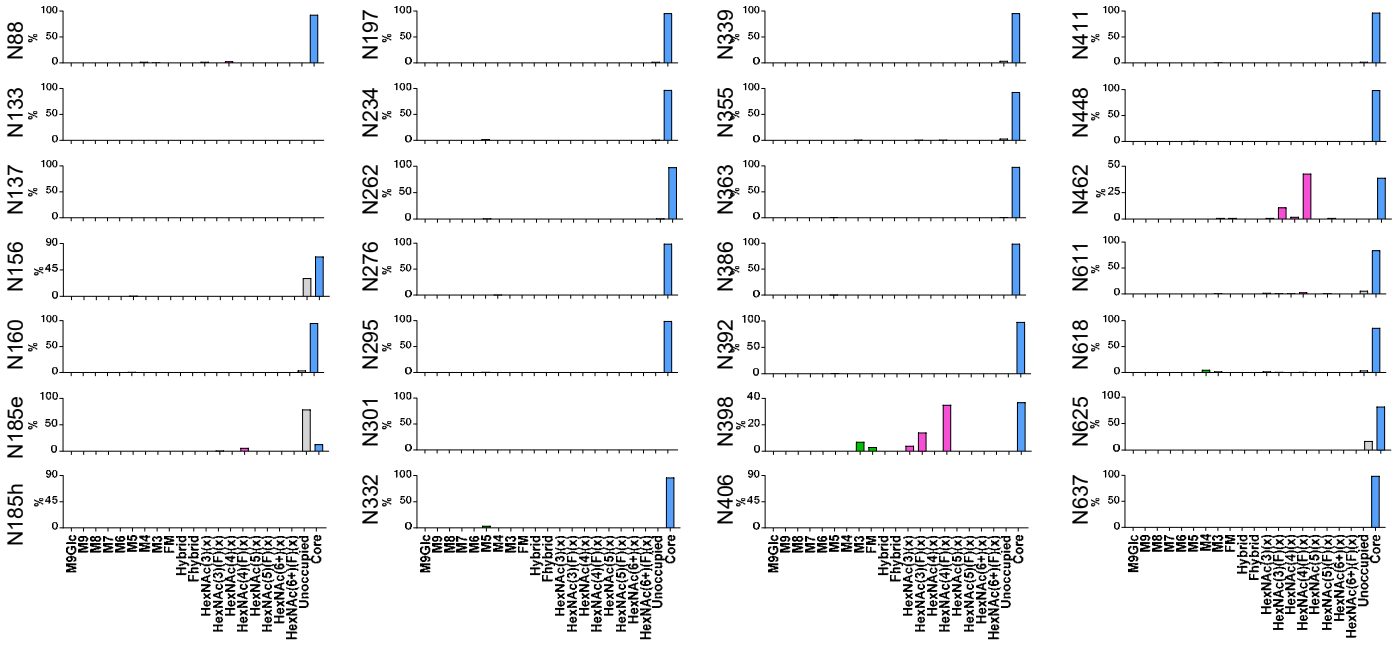

H Endo H-treated BG505 UFO-10GS-I3-01v9-L7P SApNP

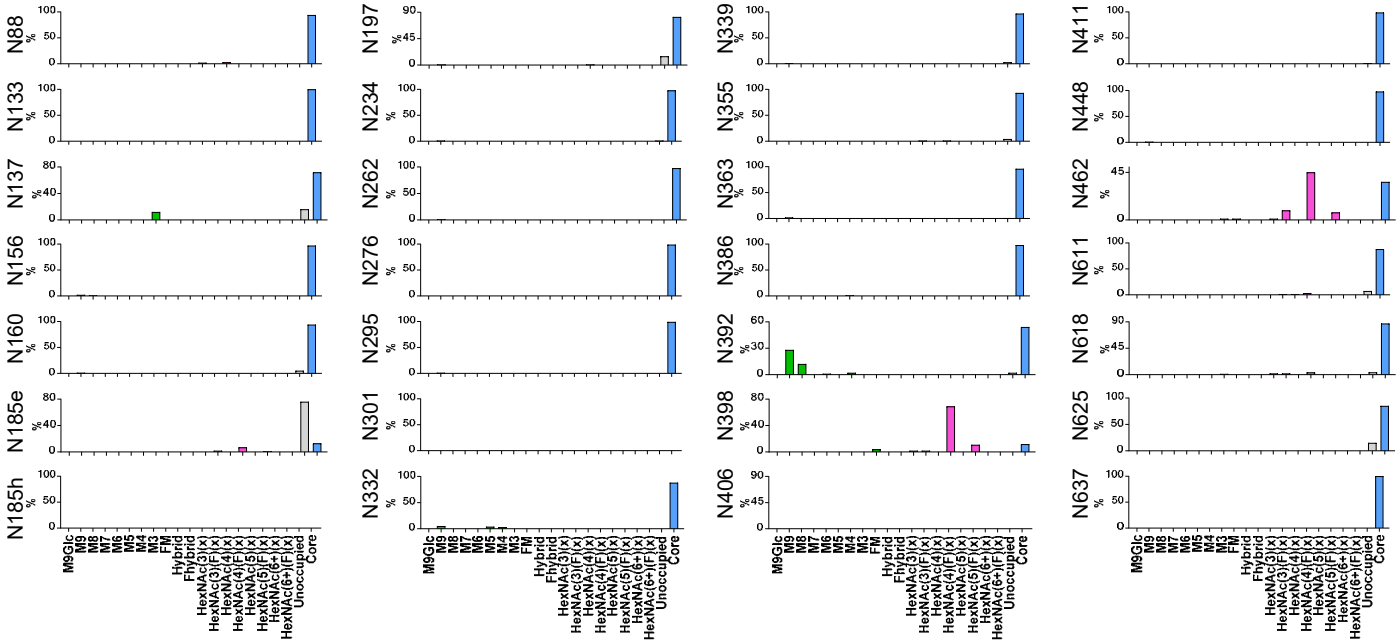

I

Summary of OD_{450} values in ELISA of glycan-trimmed I3-01v9 and E2p SApNPs binding to an anti-MBP antibody and bNAb VRC01[a].

A. BG505 UFO-10GS-I3-01v9-L7P SApNP

	μg/ml	No endo H treatment	Endo H-treated sample-1	Endo H-treated sample-2	Endo H-treated sample-3	Endo H-treated sample-4	Endo H-treated sample-5	Endo H-treated sample-6	Endo H-treated sample-7	Endo H-treated sample-8	Endo H-treated sample-9	Endo H-treated sample-10	Endo Hf
VRC01	1	2.61	2.77	2.66	2.72	2.72	2.75	2.81	2.79	2.70	2.74	2.62	0.09
	0.1	2.63	2.73	2.73	2.60	2.82	2.80	2.71	2.69	2.72	2.71	2.51	0.06
	0.01	1.87	2.18	2.12	2.08	2.22	2.16	2.08	2.16	2.07	2.15	2.16	0.05
	0.001	0.45	0.69	0.69	0.66	0.64	0.66	0.65	0.64	0.63	0.66	0.64	0.06

	dilution	No endo H treatment	Endo H-treated sample-1	Endo H-treated sample-2	Endo H-treated sample-3	Endo H-treated sample-4	Endo H-treated sample-5	Endo H-treated sample-6	Endo H-treated sample-7	Endo H-treated sample-8	Endo H-treated sample-9	Endo H-treated sample-10	Endo Hf
MBP mAb	×466	0.09	0.09	0.10	0.10	0.09	0.11	**0.15**	0.10	0.10	0.07	0.06	2.32
	×4660	0.05	0.08	0.10	0.10	0.08	0.10	0.13	0.09	0.09	0.06	0.06	2.10
	×46600	0.05	0.06	0.08	0.07	0.06	0.06	0.08	0.07	0.06	0.05	0.05	0.89
	×466000	0.05	0.06	0.06	0.06	0.05	0.06	0.06	0.06	0.05	0.05	0.05	0.25

B. BG505 UFO-E2p-L4P SApNP

	μg/ml	No endo H treatment	Endo H-treated sample-1	Endo H-treated sample-2	Endo H-treated sample-3	Endo H-treated sample-4	Endo H-treated sample-5	Endo H-treated sample-6	Endo H-treated sample-7	Endo H-treated sample-8	Endo H-treated sample-9	Endo H-treated sample-10	Endo Hf
VRC01	1	2.78	2.78	2.82	2.76	2.62	2.63	2.71	2.68	2.80	2.69	2.72	0.09
	0.1	2.60	2.76	2.53	2.63	2.61	2.65	2.48	2.61	2.72	2.67	2.69	0.06
	0.01	1.70	2.14	2.18	2.24	2.13	2.10	2.10	2.02	2.18	2.12	1.96	0.05
	0.001	0.38	0.62	0.65	0.68	0.62	0.66	0.59	0.62	0.63	0.61	0.47	0.06

	dilution	No endo H treatment	Endo H-treated sample-1	Endo H-treated sample-2	Endo H-treated sample-3	Endo H-treated sample-4	Endo H-treated sample-5	Endo H-treated sample-6	Endo H-treated sample-7	Endo H-treated sample-8	Endo H-treated sample-9	Endo H-treated sample-10	Endo Hf
MBP mAb	×466	0.06	0.18	0.24	0.22	0.20	0.19	0.15	**0.30**	0.20	0.18	0.17	2.32
	×4660	0.06	0.13	0.17	0.17	0.16	0.14	0.12	0.25	0.16	0.13	0.13	2.10
	×46600	0.07	0.08	0.10	0.10	0.09	0.08	0.07	0.13	0.09	0.08	0.07	0.89
	×466000	0.07	0.06	0.07	0.07	0.07	0.06	0.06	0.08	0.06	0.06	0.06	0.25

[a] Wildtype SApNP (without endo H treatment) and endo Hf (a fusion of endo H and MBP) were included in the ELISA binding analysis as controls, shown in the first and last columns respectively.

fig S3. Site-specific glycan analysis of BG505 UFO trimer and SApNPs. Site-specific glycan profiles are shown for the following immunogens: (**A**) WT BG505 UFO trimer. (**B**) BG505 UFO trimer expressed in the presence of Swainsonine, (**C**) BG505 UFO trimer expressed in the presence of kifunensine, (**D**) WT BG505 UFO-FR SApNP, (**E**) WT BG505 UFO-E2p-L4P SApNP, (**F**) WT BG505 UFO-10GS-I3-01v9-L7P SApNP, (**G**) Endo H-treated BG505 UFO-E2p-L4P SApNP, and (**H**) Endo H-treated BG505 UFO-10GS-I3-01v9-L7P SApNP. (**I**) The OD450 readout obtained from an ELISA binding test of endo H-treated SApNPs against an MBP-specific mouse antibody and bNAb VRC01. A total of 10 samples generated from different productions run were tested in this analysis. Four concentrations were tested for VRC01, while four dilutions were used in the ELISA test against an MBP-specific mouse antibody (The initial ×466 dilution was based on the manufacturer's recommendation). The OD450 values obtained from the highest antibody concentration in the MBP mAb binding assay are highlighted in grey shade, with the highest OD450 values colored in red.

fig. S4

A **WT BG505 UFO trimer (AHC)**

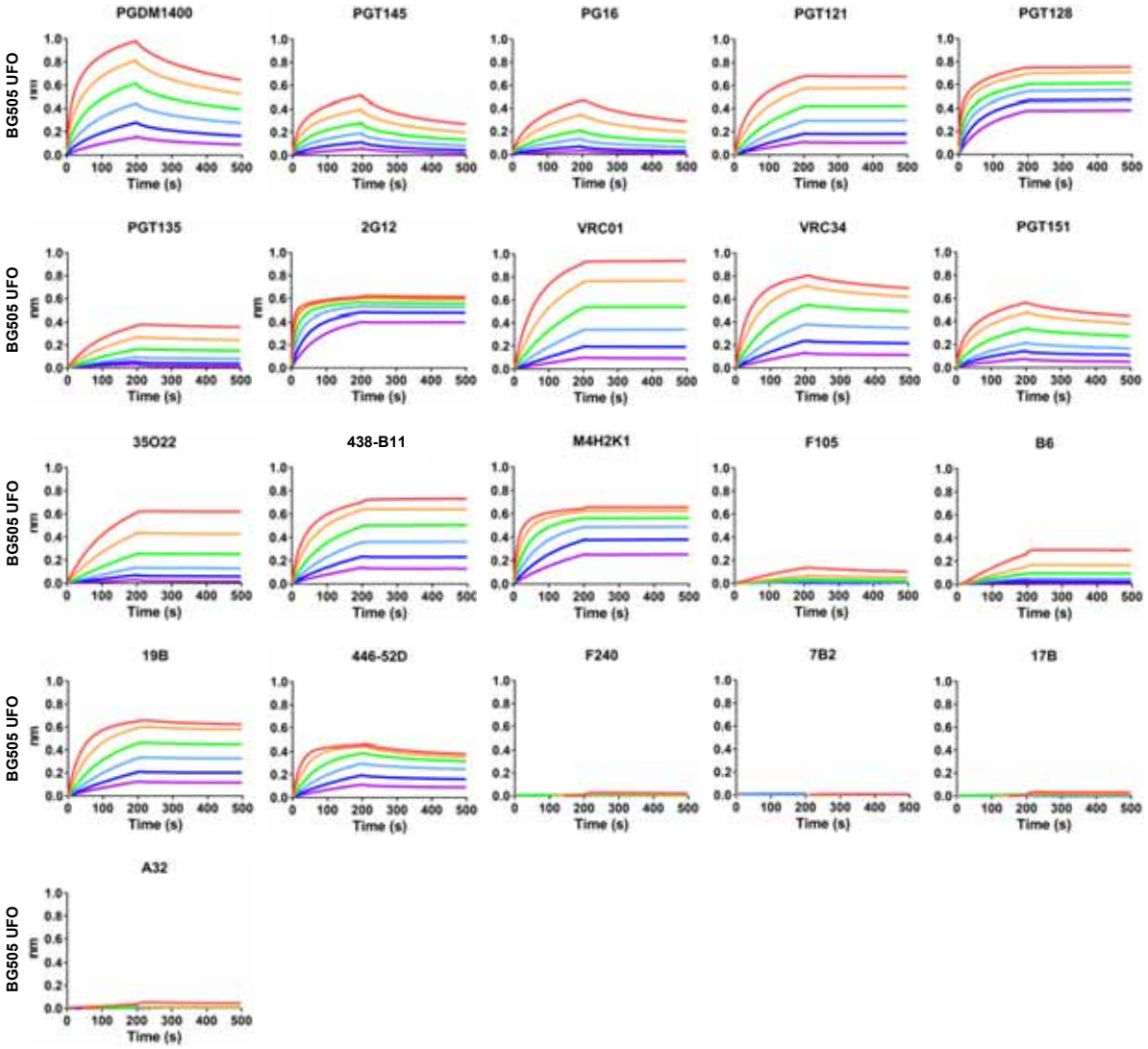

B **BG505 UFO trimer expressed in the presence of kifunensine (AHC)**

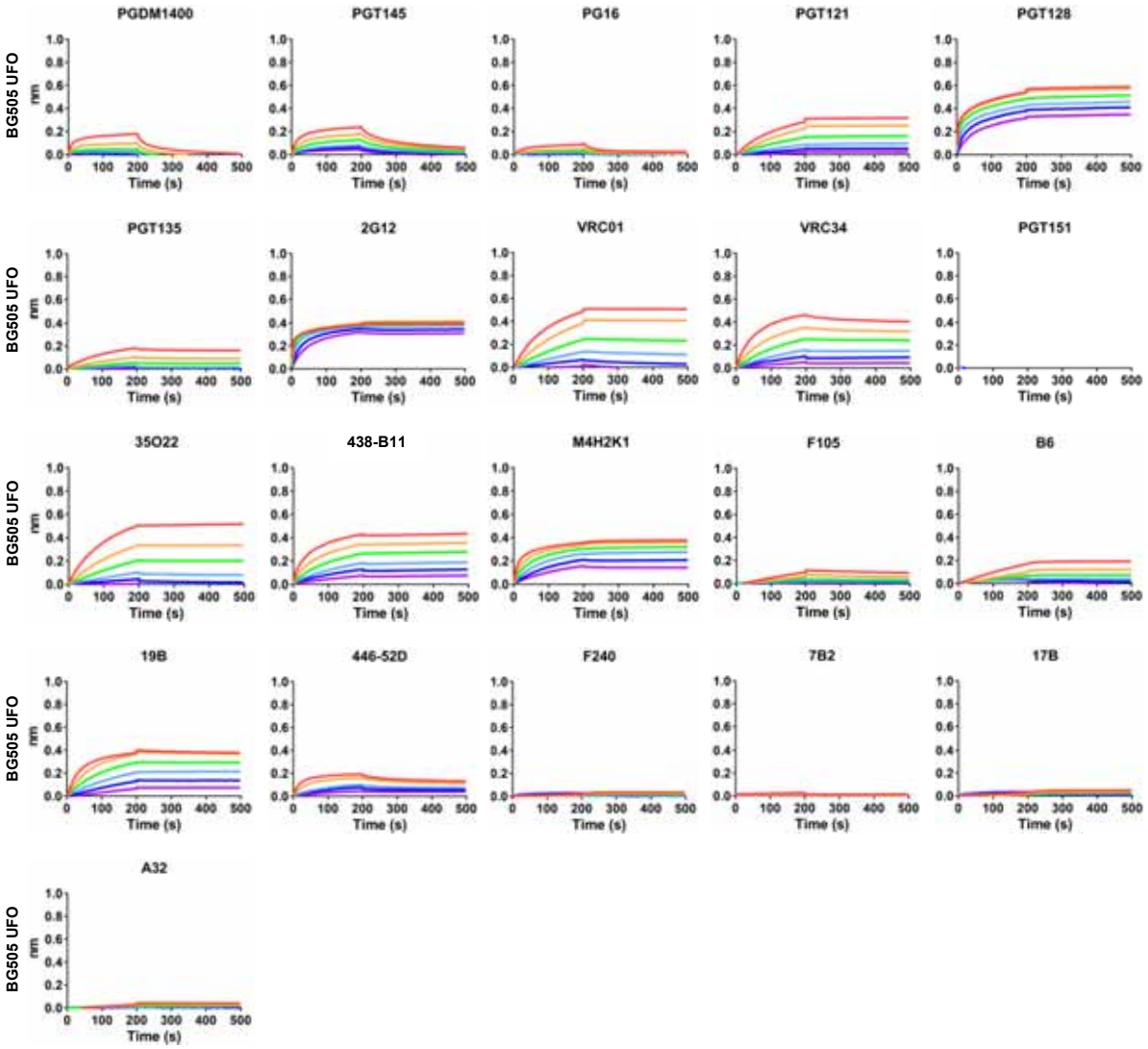

C BG505 UFO trimer treated by endo H (AHC)

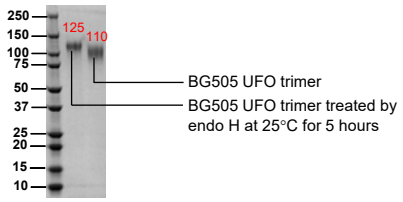

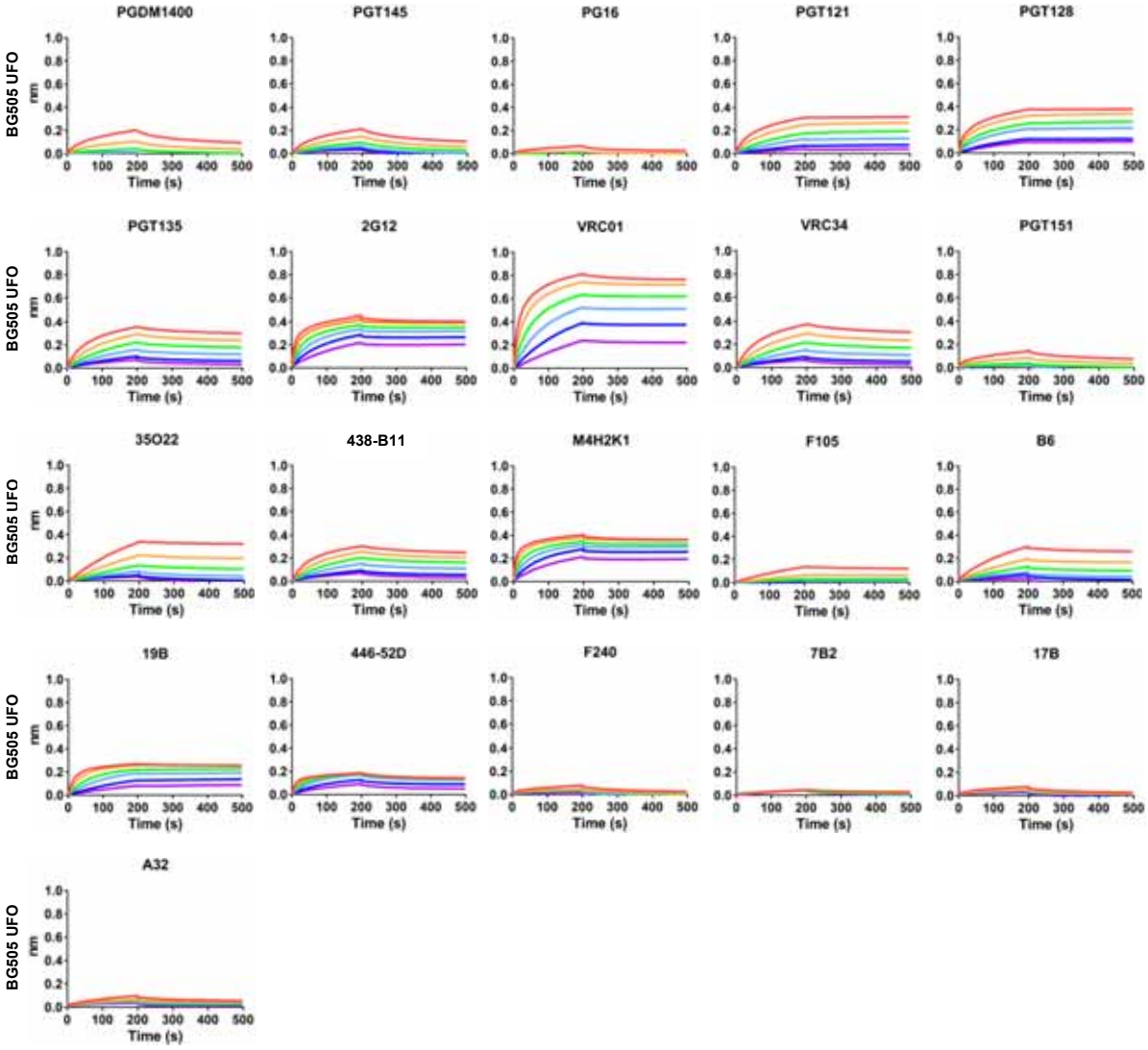

D **WT BG505 UFO trimer (AHQ)**

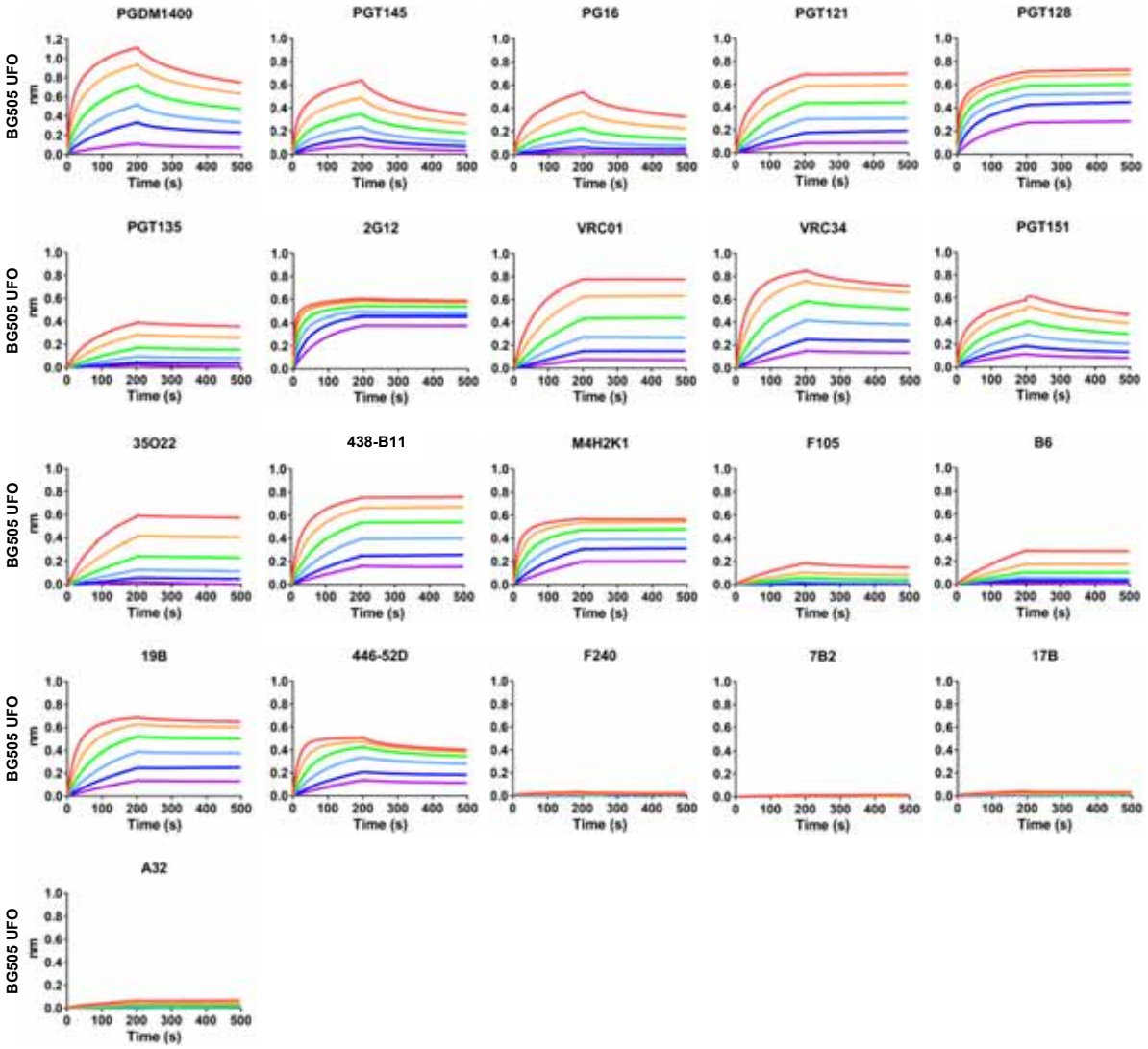

E **WT BG505 UFO trimer-presenting FR SApNP (AHQ)**

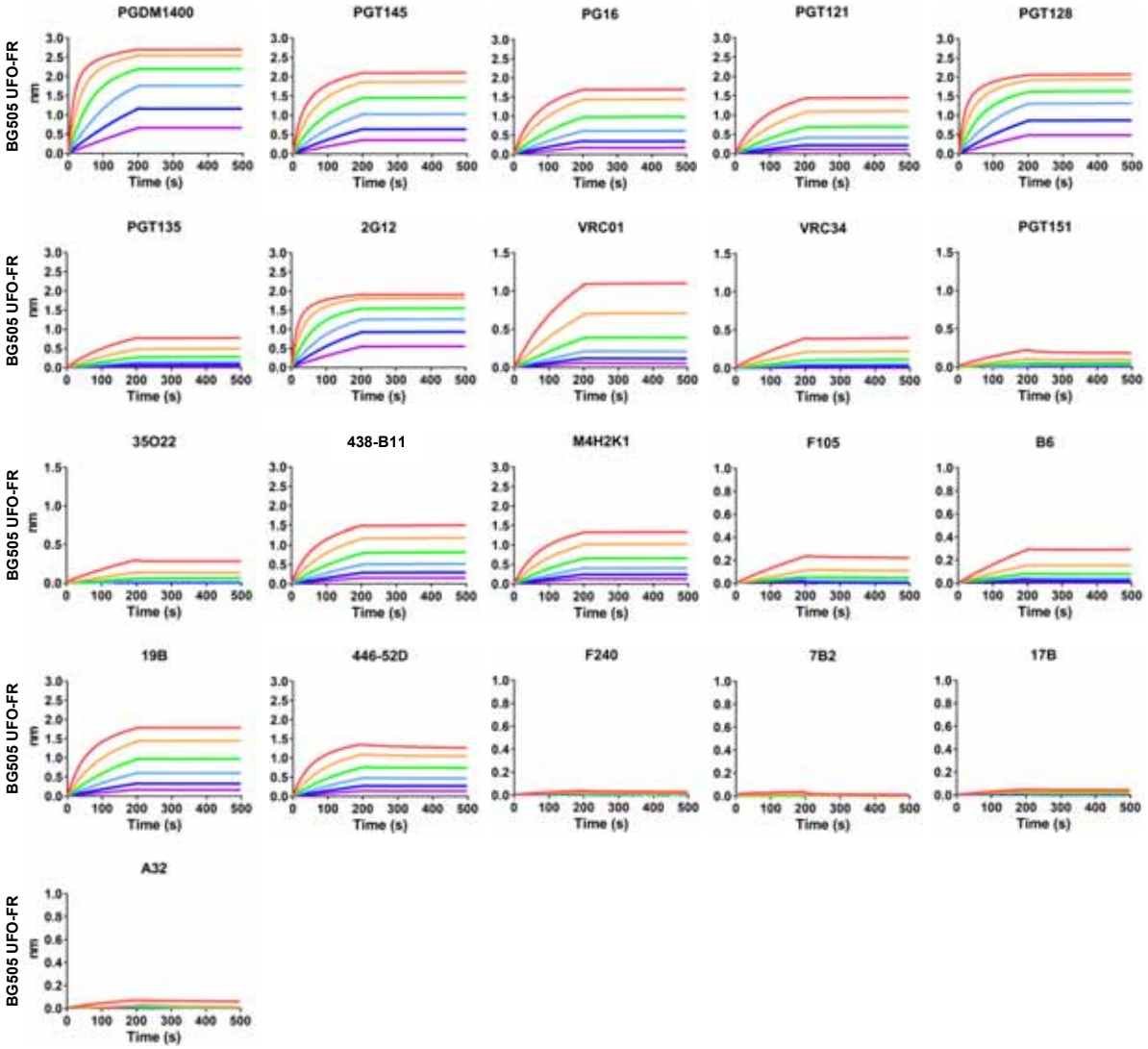

F **WT BG505 UFO trimer-presenting E2p-L4P SApNP (AHQ)**

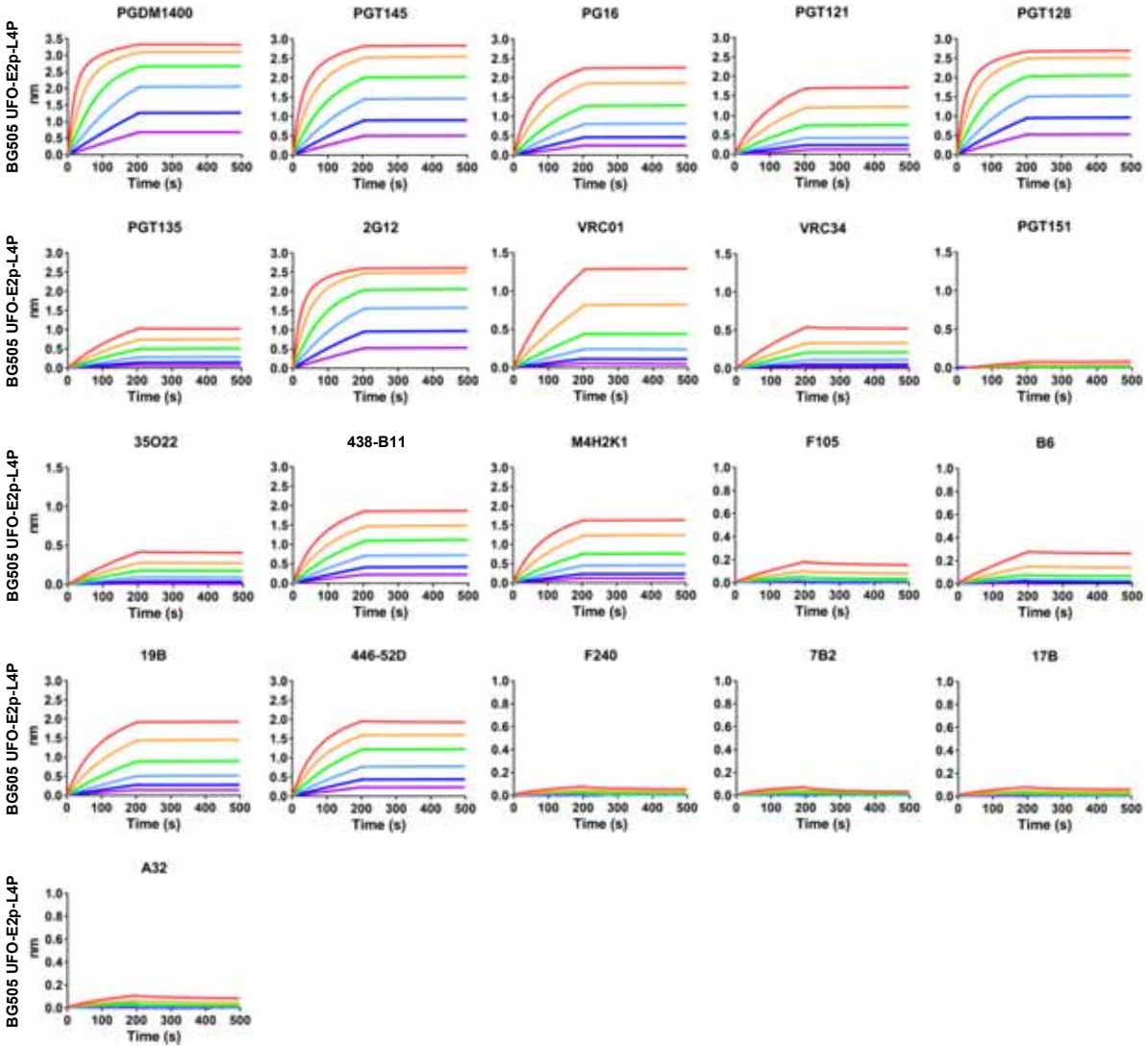

G WT BG505 UFO trimer-presenting I3-01v9 SApNP (AHQ)

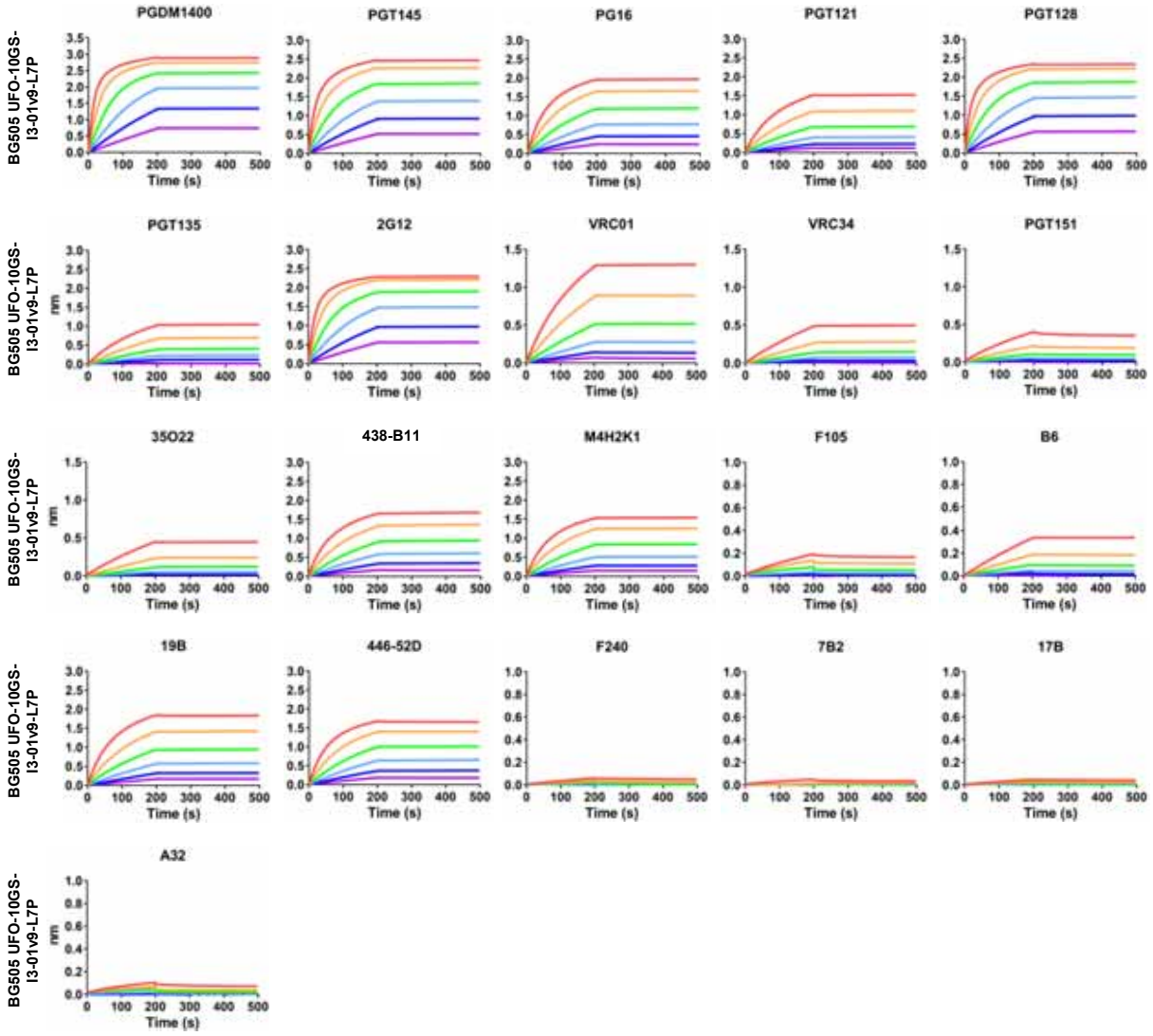

H BG505 UFO trimer expressed in the presence of kifunensine (AHQ)

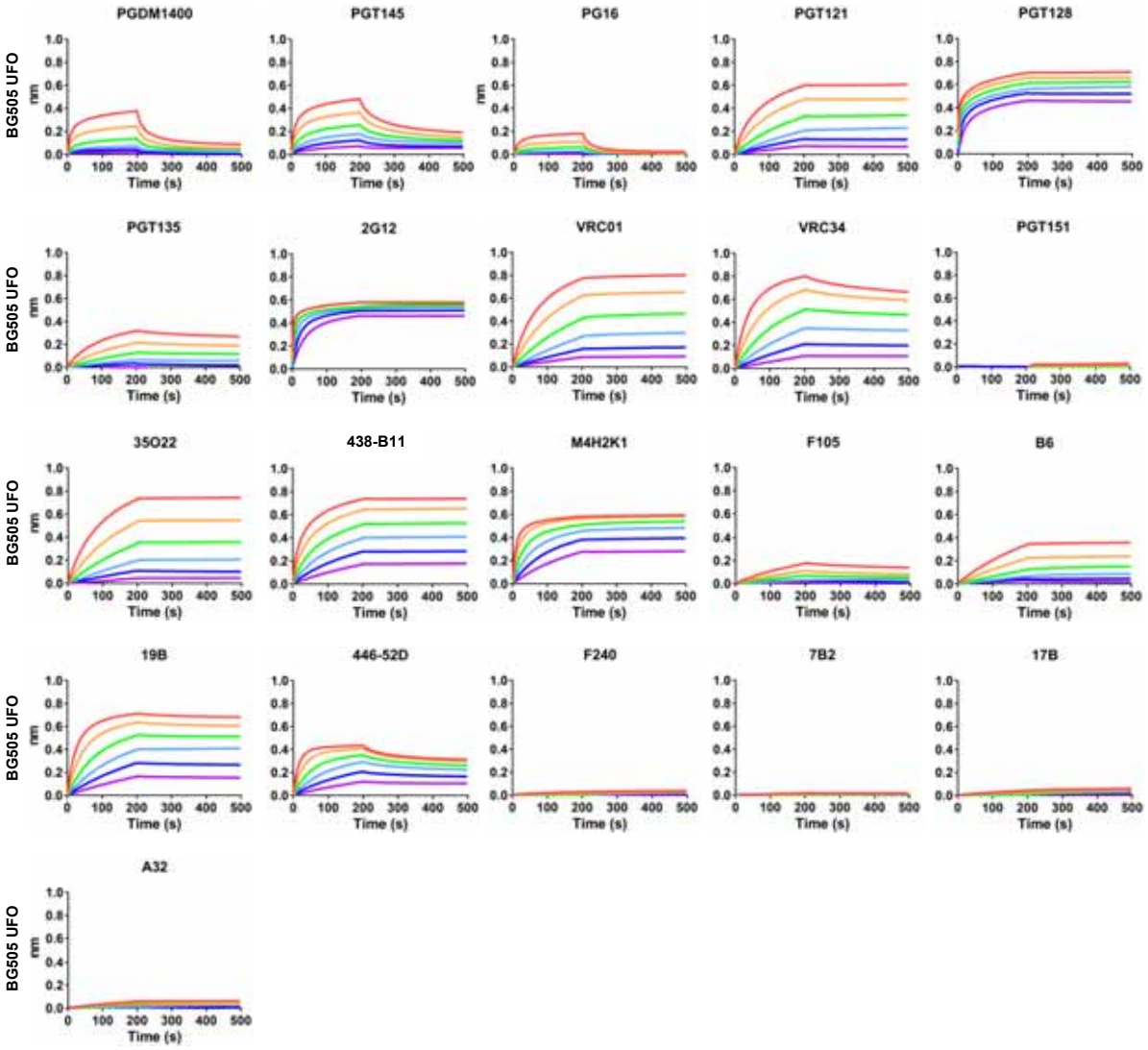

BG505 UFO trimer-presenting FR SApNP expressed in the presence of kifunensine (AHQ)

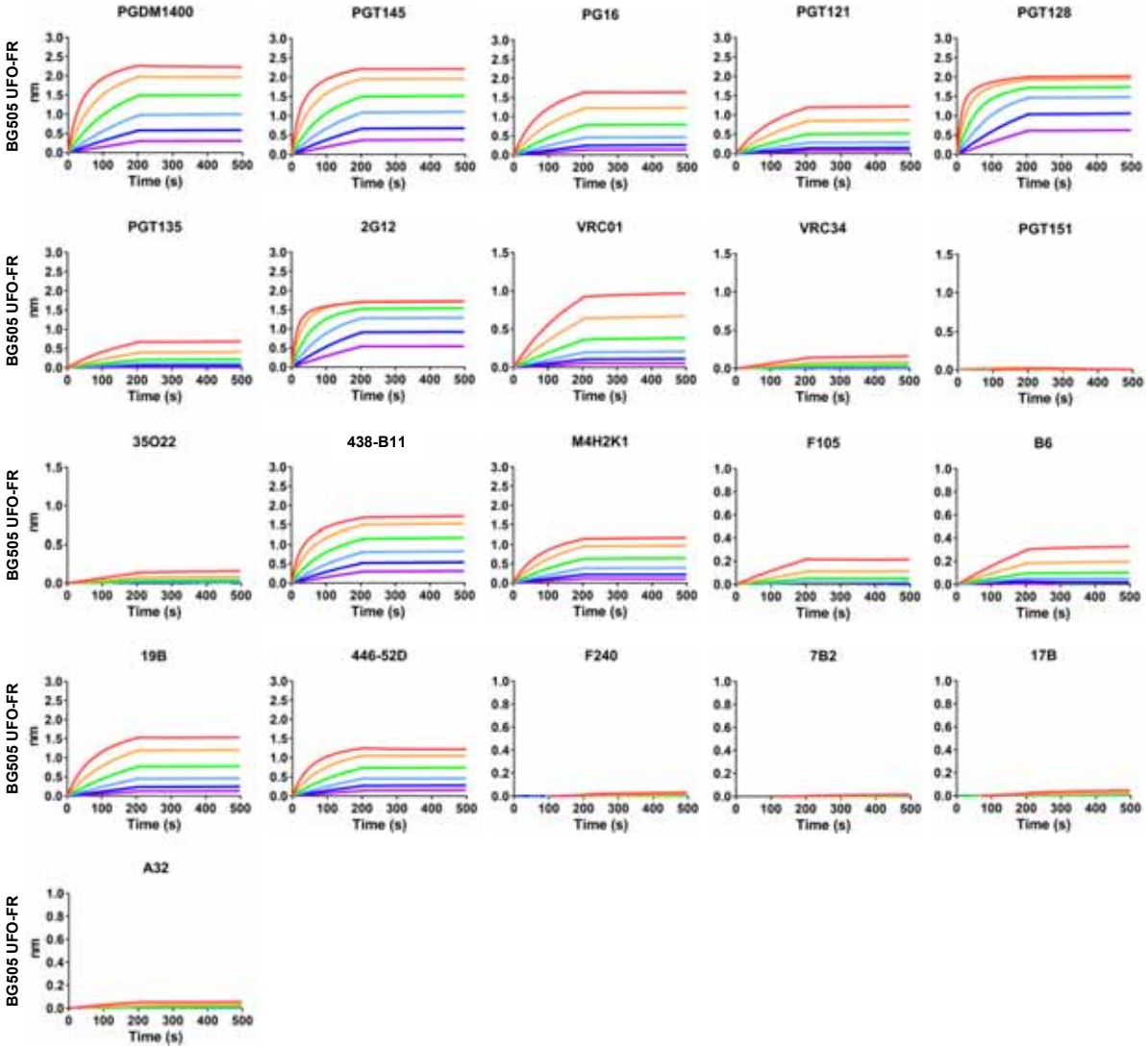

J **BG505 UFO trimer-presenting E2p-L4P SApNP expressed in the presence of kifunensine (AHQ)**

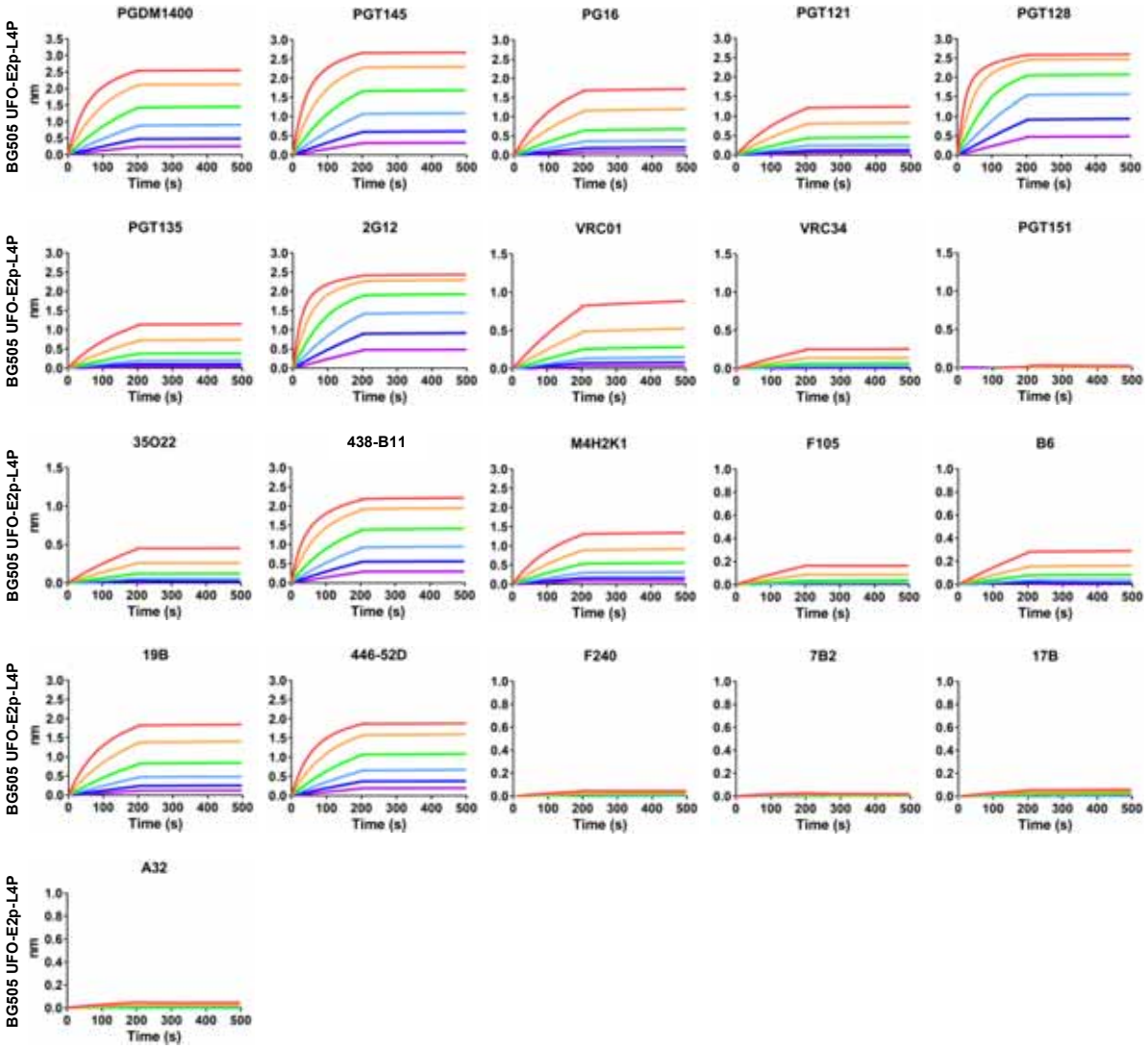

K BG505 UFO trimer-presenting I3-01v9 SApNP expressed in the presence of kifunensine (AHQ)

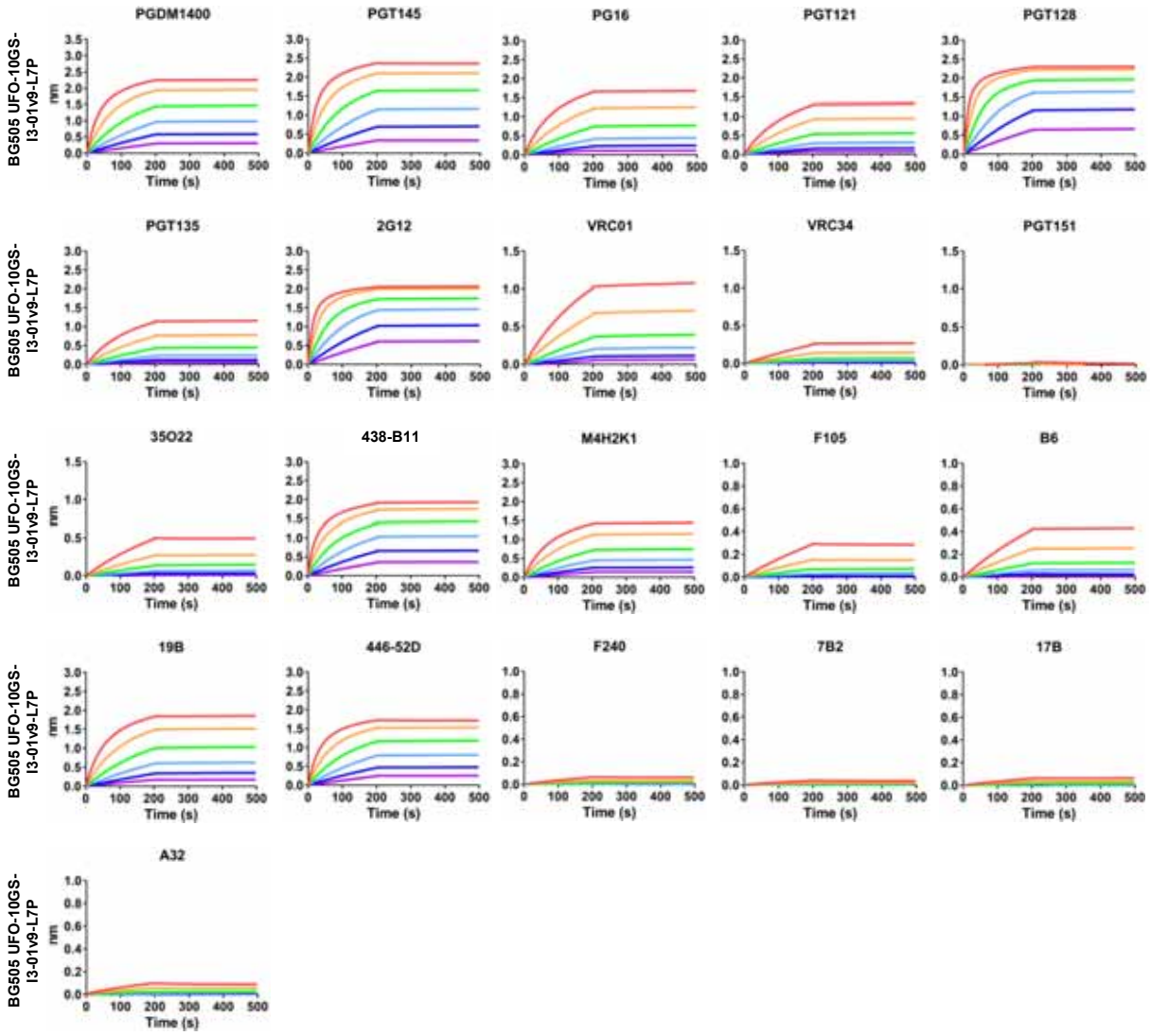

L **BG505 UFO trimer treated by endo H (AHQ)**

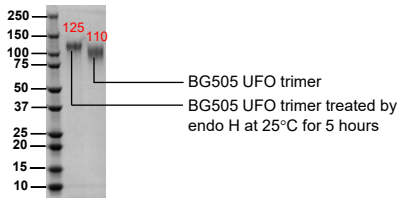

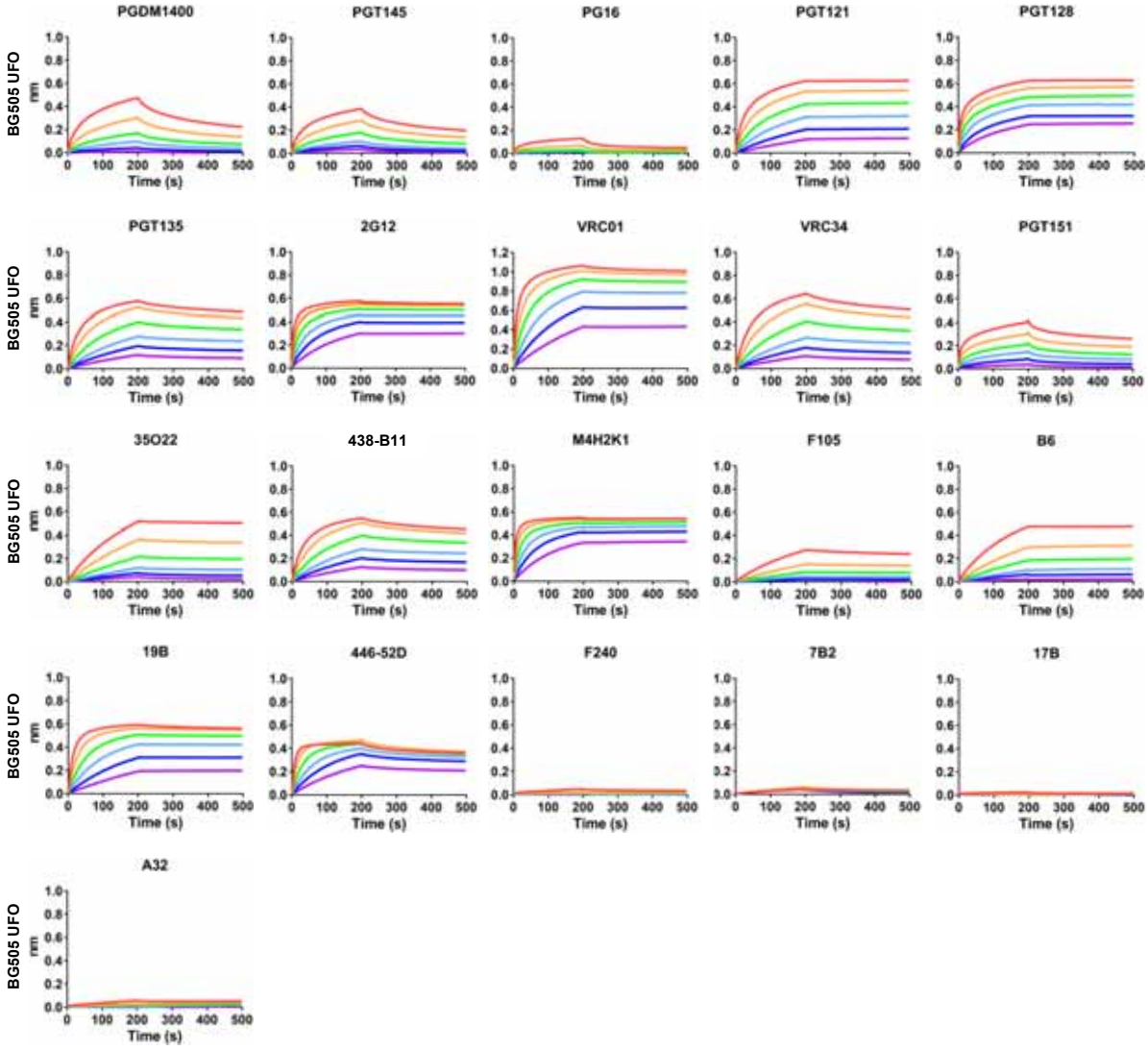

M **BG505 UFO trimer-presenting FR SApNP treated by endo H (AHQ)**

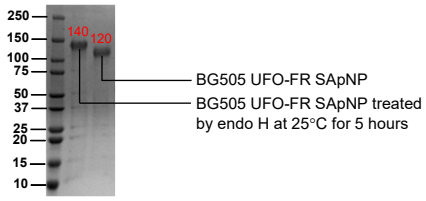

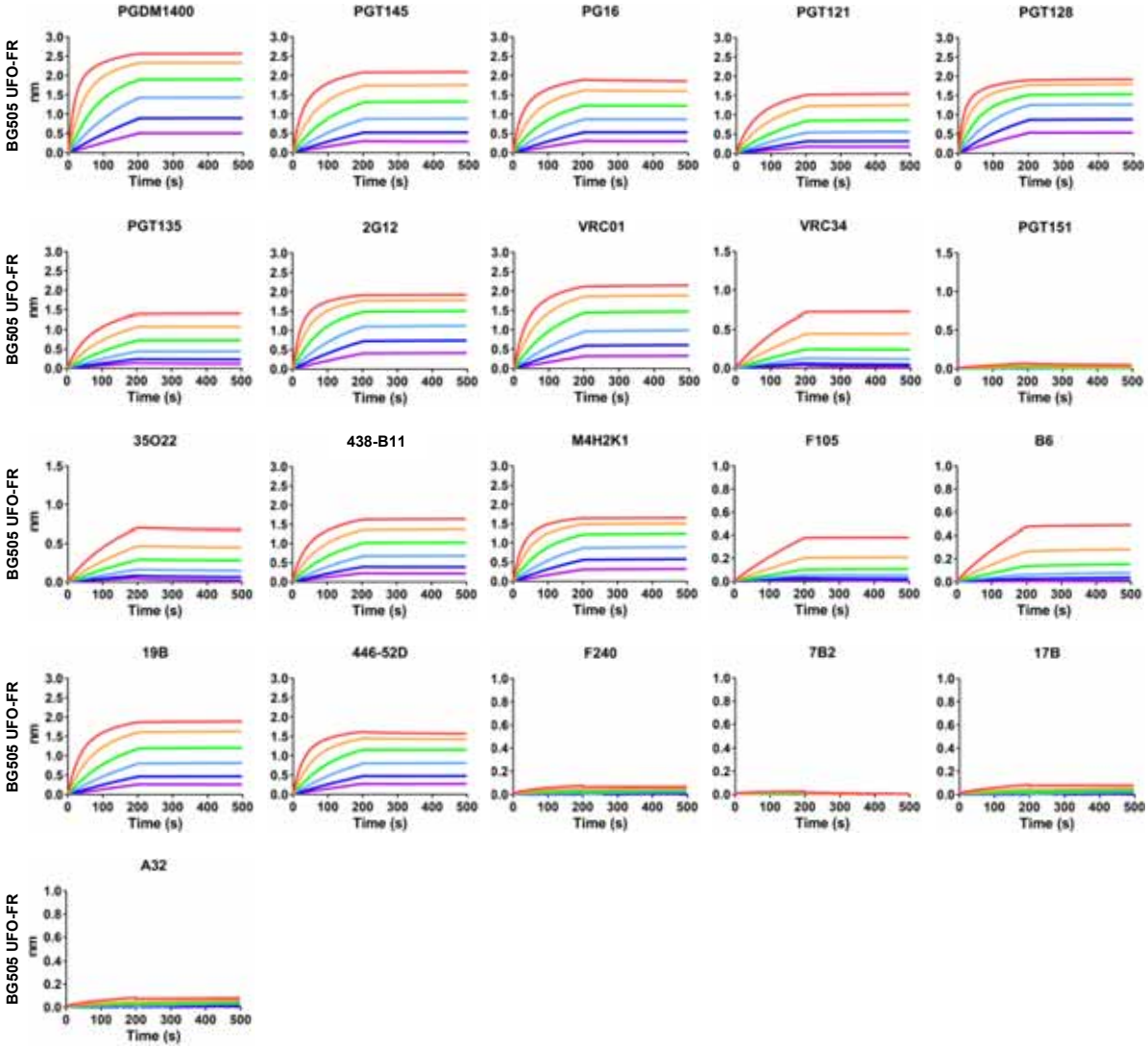

N **BG505 UFO trimer-presenting E2p-L4P SApNP treated by endo H (AHQ)**

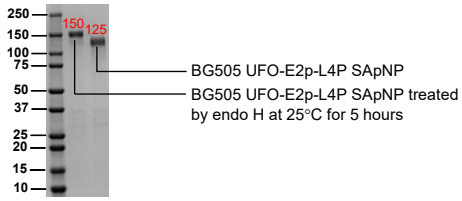

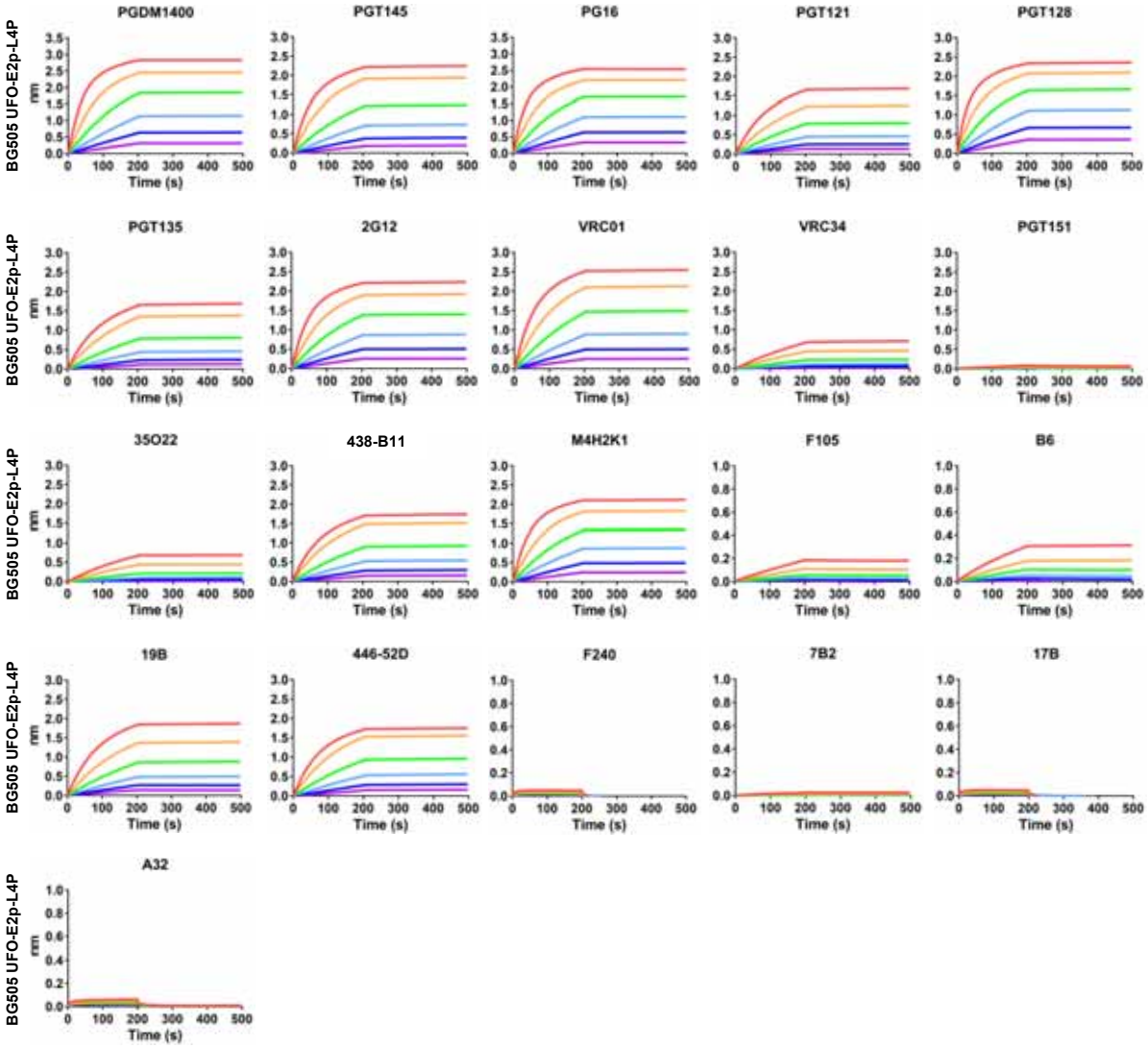

○ **BG505 UFO trimer-presenting I3-01v9-L7P SApNP treated by endo H (AHQ)**

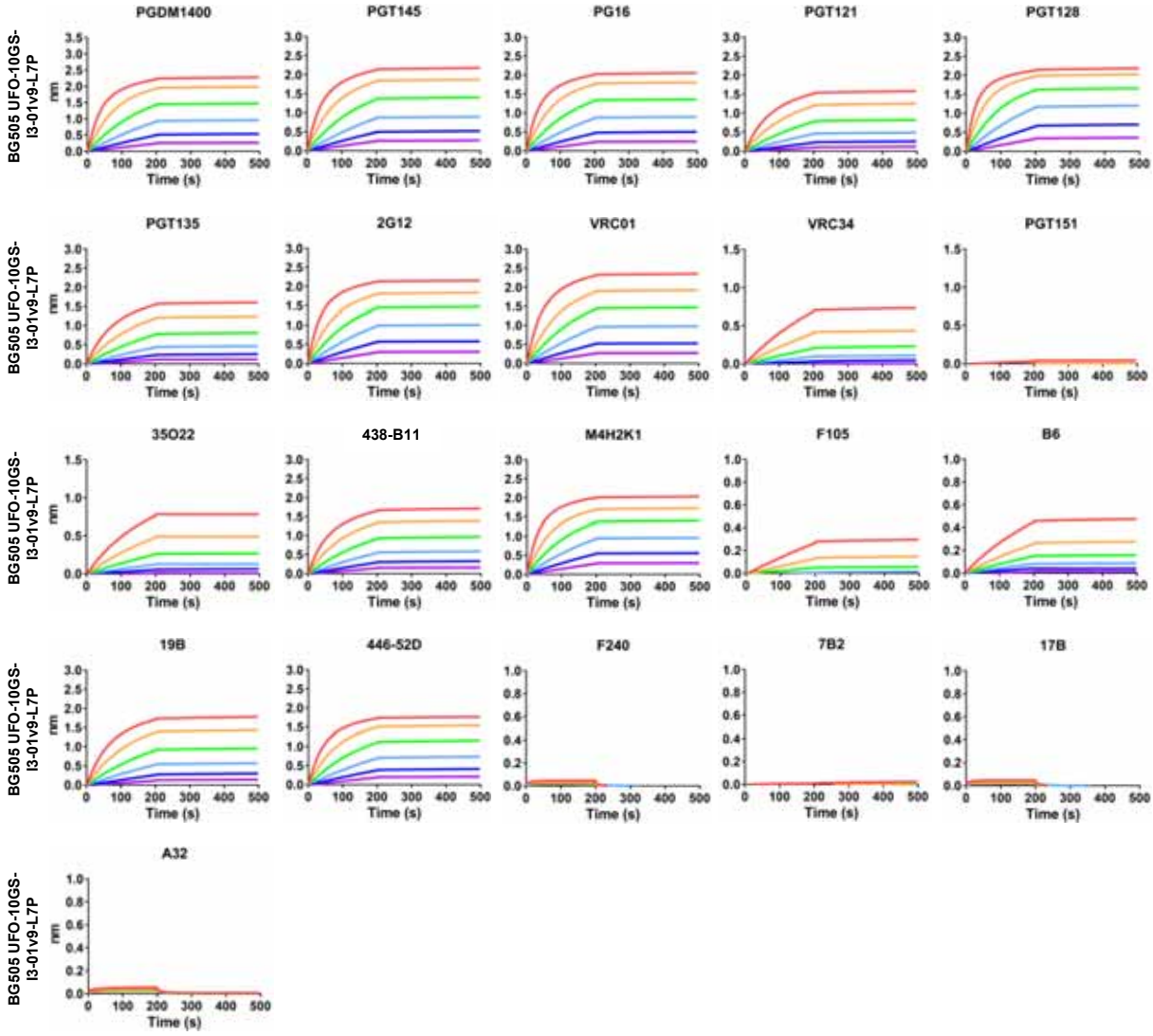

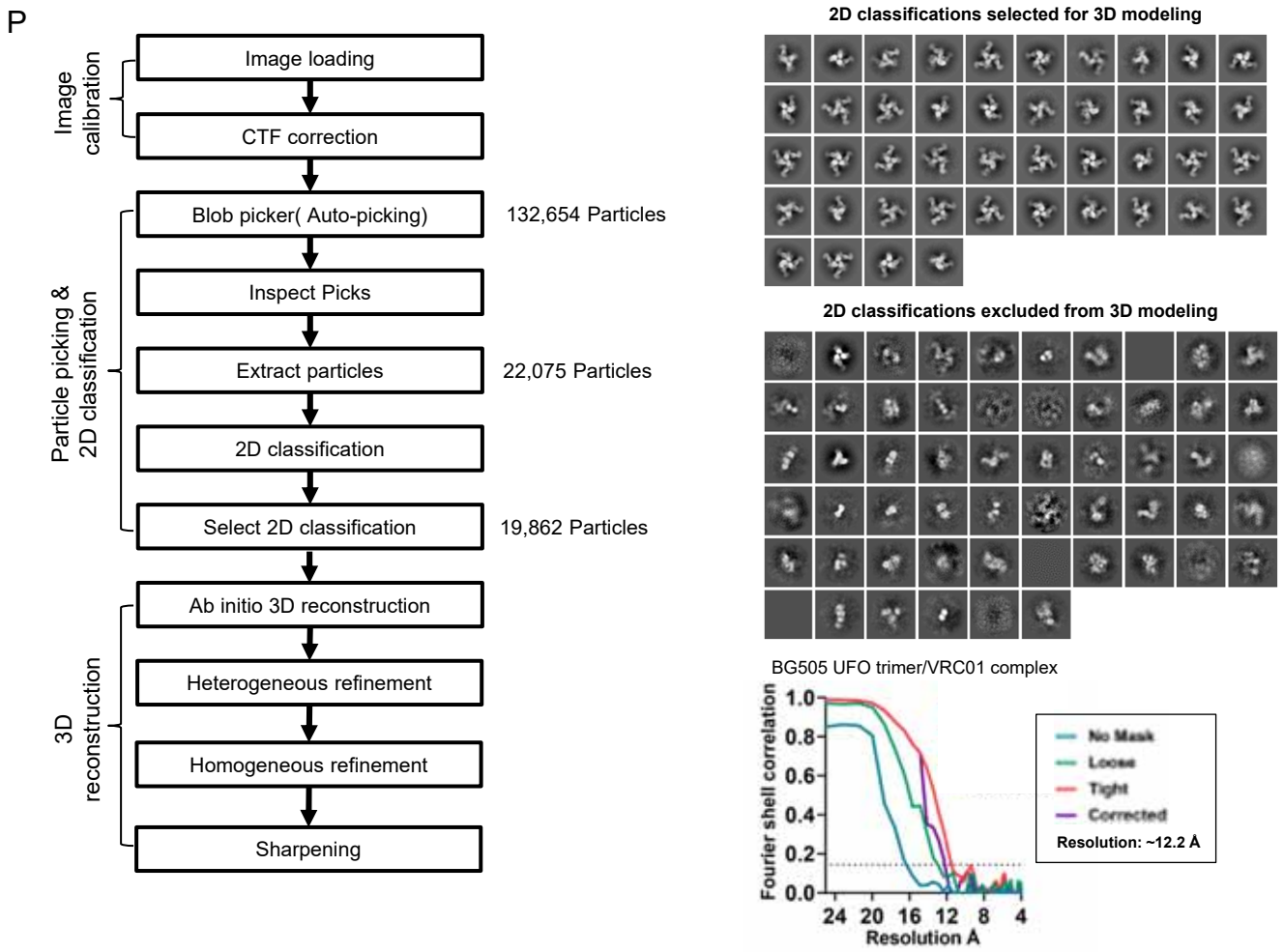

fig. S4. **Antigenic characterization of BG505 UFO trimer and trimer-presenting SApNPs with wildtype and modified glycans**. BG505 Env immunogens were tested against a panel of 21 HIV-1 antibodies including NAbs, bNAbs, and nNAbs by BLI. Sensorgrams were obtained from an Octet RED96 instrument using two types of biosensors, AHC and AHQ. The antigens tested here include (**A**) WT BG505 UFO trimer (AHC), (**B**) BG505 UFO trimer expressed in the presence of kifunensine (AHC), (**C**) BG505 UFO trimer treated by endo H (AHC), (**D**) WT BG505 UFO trimer (AHQ), (**E**) WT BG505 UFO trimer-presenting FR SApNP (AHQ), (**F**) WT BG505 UFO trimer-presenting E2p-L4P SApNP (AHQ), (**G**) WT BG505 UFO trimer-presenting I3-01v9-L7P SApNP (AHQ), (**H**) BG505 UFO trimer expressed in the presence of kifunensine (AHQ), (**I**) BG505 UFO trimer-presenting FR SApNP expressed in the presence of kifunensine (AHQ), (**J**) BG505 UFO trimer-presenting E2p-L4P SApNP expressed in the presence of kifunensine (AHQ), (**K**) BG505 UFO trimer-presenting I3-01v9-L7P SApNP expressed in the presence of kifunensine (AHQ), (**L**) BG505 UFO trimer treated by endo H (AHQ), (**M)** BG505 UFO trimer-presenting FR SApNP treated by endo H (AHQ), (**N**) BG505 UFO trimer-presenting E2p-L4P SApNP treated by endo H (AHQ), and (**O**) BG505 UFO trimer-presenting I3-01v9-L7P SApNP treated by endo H (AHQ). A two-fold concentration gradient of antigen, starting at 266.7 nM for the UFO trimer, 14.9 nM for the FR SApNP, and 5.5 nM for the E2p and I3-01v9 SApNPs, was used in a titration series of six. SDS-PAGE was run for (C), (L), (M), (N), and (O) to estimate molecular weight of glycan-trimmed vs. WT BG505 Env immunogens to ensure that molar concentration was comparable in their BLI assays. (**P**) Negative-stain EM analysis of the glycan-trimmed BG505 UFO trimer in complex with bNAb VRC01. Left: flowchart for image processing. Right top: 2D classes selected for 3D reconstruction and excluded from 3D reconstruction. Right bottom: Estimated resolution (12.2 Å) of the EM reconstruction for the BG505 UFO trimer/VRC01 complex was calculated from the Fourier shell correlation (FSC) using a cut-off of 0.143.

fig. S5

A **Week 11 mouse IgG neutralization against HIV-1 BG505.T332N**

Vaccine	Adjuvant	IC_{50} titers (µg/ml)							
		M1	M2	M3	M4	M5	M6	M7	M8
BG505 E2p SApNP	No adjuvant	>300	>300	>300	>300	No IgG	>300	>300	>300
	AddaVax	>300	>300	>300	200	>300	>300	No IgG	>300
	Aluminum phosphate	>300	90	No IgG	>300	>300	>300	>300	>300
	Aluminum hydroxide	>300	>300	>300	>300	>300	>300	>300	>300
	AddaVax/Aluminum phosphate	>300	>300	>300	>300	>300	>300	>300	>300
BG505 I3-01v9 SApNP	No adjuvant	>300	>300	>300	>300	>300	>300	>300	>300
	AddaVax	>300	>300	>300	>300	>300	>300	>300	>300
	Aluminum phosphate	21	>300	>300	>300	>300	>300	>300	>300
	Aluminum hydroxide	No IgG	>300	>300	>300	>300	36	>300	>300
	AddaVax/Aluminum phosphate	>300	>300	>300	>300	>300	>300	>300	>300

No IgG: indicates no IgG available to test.

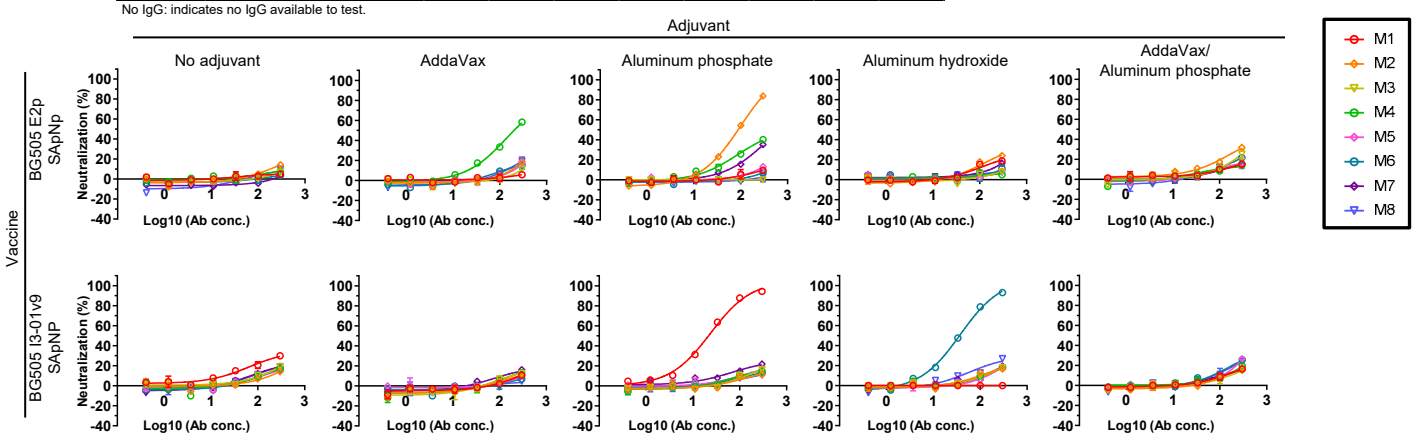

Week 11 mouse IgG neutralization against HIV SF162

Vaccine	Adjuvant	IC_{50} titers (µg/ml)							
		M1	M2	M3	M4	M5	M6	M7	M8
BG505 E2p SApNP	No adjuvant	>300	>300	>300	>300	-	>300	>300	>300
	AddaVax	>300	26	18	>300	250	13	No IgG	>300
	Aluminum phosphate	4	34	No IgG	39	62	>300	1	2
	Aluminum hydroxide	14	2	7	29	104	9	>300	14
	AddaVax/Aluminum phosphate	77	83	20	287	4	1	>300	35
BG505 I3-01v9 SApNP	No adjuvant	>300	>300	>300	16	>300	>300	>300	12
	AddaVax	146	>300	11	2	79	26	11	89
	Aluminum phosphate	5	34	91	>300	126	9	86	5
	Aluminum hydroxide	No IgG	9	41	4	45	28	15	>300
	AddaVax/Aluminum phosphate	1	88	13	285	>300	14	>300	102

No IgG: indicates no IgG available to test.

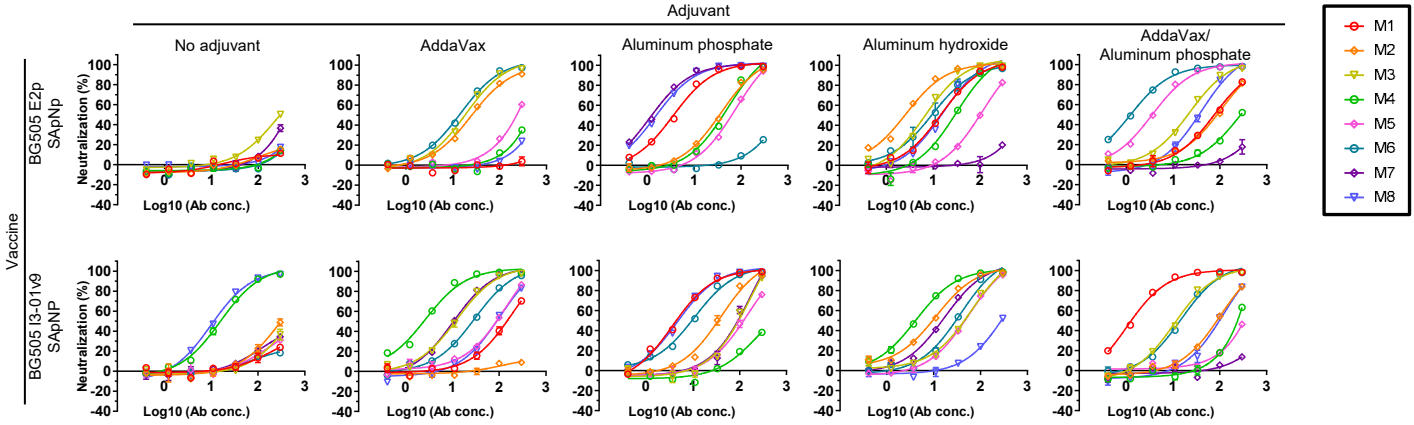

Week 11 mouse IgG neutralization against MLV (negative control)

Vaccine	Adjuvant	Animal ID	IC50 titers (µg/ml)
BG505 E2p SApNP	Aluminum phosphate	D-S19 G3-M2	>300
BG505 I3-01v9 SApNP	Aluminum phosphate	D-S20 G3-M1	>300
	Aluminum hydroxide	D-S20 G4-M6	>300

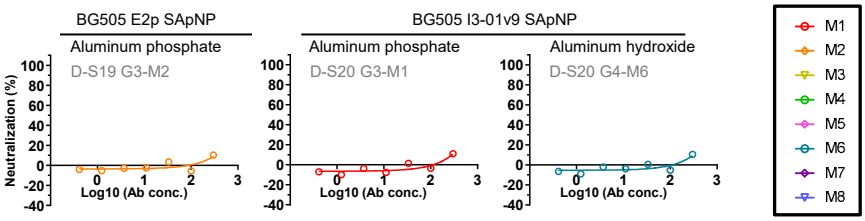

B **Week 11 mouse IgG neutralization IC_{50} titers against HIV-1 BG505.T332N and BG505.T332N.I396R mutant**

Vaccine	Adjuvant	Animal ID	IC_{50} titers (µg/ml)	
			BG505. T332N	BG505. T332N. I396R
BG505 E2p SApNP	AddaVax	D-S19 G2-M4*	200	>300
	Aluminum phosphate	D-S19 G3-M2	90	>300
BG505 I3-01v9 SApNP	Aluminum phosphate	D-S20 G3-M1	21	293
	Aluminum hydroxide	D-S20 G4-M6	36	>300

* starting concentration for this sample was at 95 µg/ml against the BG505.T332N I396R as inadequate sample left to start at 300 µg/ml

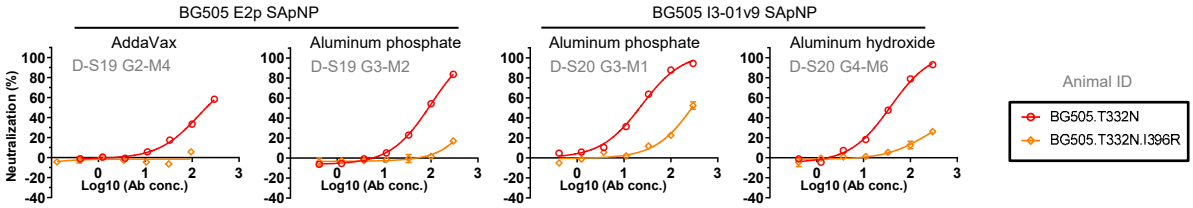

C **Week 11 mouse IgG neutralization IC_{50} and IC_{30} titers against HIV-1 12 virus panel, BG505.T332N, SF162 & MLV (control)**

Vaccine	Adjuvant	Animal ID	IC_{50} titers (µg/ml) for each virus (clade)														
			TRO11 (B)	25710 (C)	398F1 (A)	CNE8 (AE)	X2278 (B)	BJOX-2000 (BC)	X1632 (G)	CE1176 (C)	246F3 (AC)	CH119 (BC)	CE0217 (C)	CNE55 (AE)	BG505. T332N (A)	SF162 (B)	MLV (control)
BG505 E2p SApNP	Aluminum phosphate	D-S19 G3-M2	>300	>300	>300	>300	>300	>300	>300	>300	>300	>300	>300	>300	90	34	>300
BG505 I3-01v9 SApNP	Aluminum phosphate	D-S20 G3-M1	>300	>300	269	>300	>300	>300	>300	>300	>300	>300	>300	>300	21	5	>300
	Aluminum hydroxide	D-S20 G4-M6	>300	>300	>300	>300	>300	>300	>300	>300	>300	>300	>300	>300	36	28	>300

Vaccine	Adjuvant	Animal ID	IC_{30} titers (µg/ml) for each virus (clade)														
			TRO11 (B)	25710 (C)	398F1 (A)	CNE8 (AE)	X2278 (B)	BJOX-2000 (BC)	X1632 (G)	CE1176 (C)	246F3 (AC)	CH119 (BC)	CE0217 (C)	CNE55 (AE)	BG505. T332N (A)	SF162 (B)	MLV (control)
BG505 E2p SApNP	Aluminum phosphate	D-S19 G3-M2	>300	>300	254	>300	>300	>300	>300	>300	>300	>300	>300	>300	39	14	>300
BG505 I3-01v9 SApNP	Aluminum phosphate	D-S20 G3-M1	>300	>300	115	>300	>300	255	>300	>300	>300	>300	>300	>300	9	2	>300
	Aluminum hydroxide	D-S20 G4-M6	>300	>300	197	>300	>300	>300	>300	221	>300	>300	>300	>300	16	12	>300

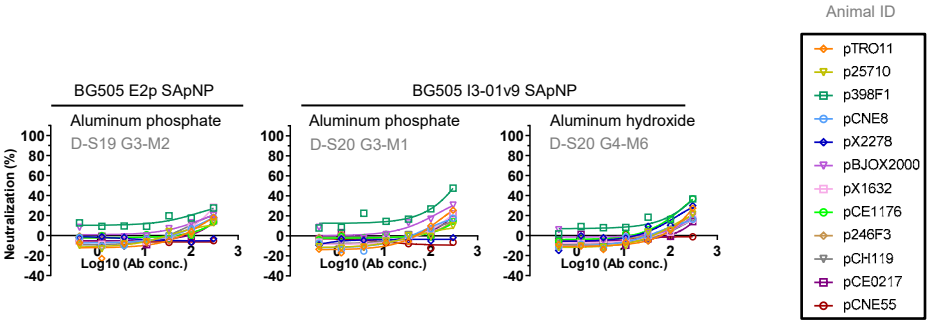

fig. S5

D **Weeks 0-28 rabbit plasma neutralization against HIV BG505.T332N, ID_{50} and ID_{30} titers**

Vaccine	Adjuvant	Animal ID	ID_{50} titers											
			w0	w2	w4	w6	w8	w10	w12	w16	w20	w24	w26	w28
BG505 UFO trimer	Addavax	119	<100	<100	<100	<100	<100	<100	<100	<100	<100	<100	<100	<100
		120	<100	<100	<100	<100	<100	<100	<100	<100	<100	<100	<100	<100
		121	<100	<100	<100	<100	<100	136	<100	<100	<100	<100	191	<100
		122	<100	<100	<100	<100	<100	116	<100	<100	<100	<100	381	139
		123	<100	<100	<100	<100	<100	<100	<100	<100	<100	<100	150	<100
		124	<100	<100	<100	501	134	178	<100	<100	<100	<100	996	194
BG505 FR SApNP	Addavax	125	<100	<100	<100	<100	<100	<100	<100	<100	<100	<100	<100	<100
		126	<100	<100	<100	<100	<100	737	485	179	113	<100	688	745
		127	<100	<100	<100	<100	<100	<100	<100	<100	<100	<100	601	511
		128	<100	<100	<100	<100	<100	<100	<100	<100	<100	<100	<100	<100
		129	<100	<100	<100	<100	<100	<100	<100	<100	<100	<100	<100	<100
		130	<100	<100	<100	<100	<100	105	<100	<100	<100	<100	760	454
Env Mix FR SApNP	Addavax	131	<100	<100	<100	<100	<100	<100	<100	<100	<100	<100	<100	<100
		132	<100	<100	<100	<100	<100	<100	<100	<100	<100	<100	<100	113
		133	<100	<100	<100	<100	<100	<100	<100	<100	<100	<100	<100	<100
		134	<100	<100	<100	<100	<100	<100	<100	<100	<100	<100	151	125
		135	<100	<100	<100	<100	<100	<100	<100	<100	<100	<100	<100	<100
		136	<100	<100	<100	<100	<100	<100	<100	<100	<100	<100	<100	<100
BG505 E2p SApNP	Addavax	155	<100	<100	<100	<100	<100	269	126	<100	<100	<100	563	331
		156	<100	<100	<100	<100	<100	<100	<100	<100	<100	<100	<100	<100
		157	<100	<100	<100	<100	<100	<100	<100	<100	<100	<100	<100	<100
		158	<100	<100	<100	<100	<100	<100	<100	<100	<100	<100	<100	<100
		159	<100	<100	<100	<100	<100	<100	<100	<100	<100	<100	<100	<100
		160	<100	<100	<100	<100	<100	521	208	<100	<100	<100	587	364
Env Mix E2p SApNP	Addavax	137	<100	<100	<100	<100	<100	<100	<100	<100	<100	<100	<100	<100
		138	<100	<100	<100	<100	<100	<100	<100	<100	<100	<100	<100	<100
		139	<100	<100	<100	<100	<100	<100	<100	<100	<100	<100	<100	<100
		140	<100	<100	<100	220	<100	<100	<100	<100	<100	<100	210	<100
		141	<100	<100	<100	<100	<100	<100	<100	<100	<100	<100	247	132
		142	<100	<100	<100	<100	<100	<100	<100	<100	<100	<100	<100	<100
BG505 I3-01v9 SApNP	Aluminum phosphate	143	<100	<100	<100	<100	<100	164	240	<100	<100	<100	659	492
		144	<100	<100	<100	<100	<100	<100	<100	<100	<100	<100	<100	153
		145	<100	<100	<100	<100	<100	<100	<100	<100	<100	<100	124	<100
		146	<100	<100	<100	<100	<100	<100	<100	<100	<100	<100	247	116
		147	<100	<100	<100	<100	<100	439	220	141	120	130	958	807
		148	<100	<100	<100	<100	<100	<100	<100	<100	<100	<100	<100	<100
Env Mix I3-01v9 SApNP	Aluminum phosphate	149	<100	<100	<100	<100	<100	402	252	<100	<100	<100	334	382
		150	<100	<100	<100	<100	<100	<100	<100	<100	<100	<100	271	155
		151	<100	<100	<100	<100	<100	656	330	241	142	111	1170	813
		152	<100	<100	<100	<100	<100	<100	<100	<100	<100	<100	128	<100
		153	<100	<100	<100	<100	<100	<100	<100	<100	<100	<100	<100	<100
		154	<100	<100	<100	<100	<100	<100	<100	<100	<100	<100	<100	<100

Vaccine	Adjuvant	Animal ID	ID_{30} titers											
			w0	w2	w4	w6	w8	w10	w12	w16	w20	w24	w26	w28
BG505 UFO trimer	Addavax	119	<100	<100	<100	<100	<100	<100	<100	<100	<100	<100	120	<100
		120	<100	<100	<100	<100	<100	<100	<100	<100	<100	<100	<100	<100
		121	<100	<100	<100	<100	<100	316	185	<100	<100	<100	446	179
		122	<100	<100	<100	<100	<100	270	164	<100	<100	<100	889	324
		123	<100	<100	<100	<100	<100	<100	<100	<100	<100	<100	351	197
		124	<100	<100	<100	1168	312	415	213	133	<100	<100	2324	454
BG505 FR SApNP	Addavax	125	<100	<100	<100	<100	<100	<100	<100	<100	<100	<100	<100	210
		126	<100	<100	<100	<100	<100	1720	1131	417	263	140	1605	1738
		127	<100	<100	<100	<100	<100	<100	<100	<100	<100	<100	1401	1193
		128	<100	<100	<100	<100	<100	109	<100	<100	<100	<100	186	140
		129	<100	<100	<100	<100	<100	<100	<100	<100	<100	<100	<100	124
		130	<100	<100	<100	<100	<100	245	<100	<100	<100	<100	1774	1060
Env Mix FR SApNP	Addavax	131	<100	<100	<100	<100	<100	<100	<100	<100	<100	<100	<100	115
		132	<100	<100	<100	<100	<100	<100	<100	<100	<100	<100	105	265
		133	<100	<100	<100	<100	<100	<100	<100	<100	<100	<100	<100	<100
		134	<100	<100	<100	<100	<100	<100	<100	<100	<100	<100	351	291
		135	<100	<100	<100	<100	<100	<100	<100	<100	<100	<100	<100	<100
		136	<100	<100	<100	<100	<100	<100	<100	<100	<100	<100	<100	190
BG505 E2p SApNP	Addavax	155	<100	<100	<100	<100	<100	627	293	212	147	115	1313	773
		156	<100	<100	<100	<100	<100	122	<100	<100	<100	<100	154	<100
		157	<100	<100	<100	<100	<100	175	<100	<100	133	<100	107	<100
		158	<100	<100	<100	<100	<100	170	<100	<100	<100	<100	149	<100
		159	<100	<100	<100	<100	<100	<100	<100	170	<100	<100	198	<100
		160	<100	<100	<100	<100	<100	1215	485	<100	<100	109	1369	849
Env Mix E2p SApNP	Addavax	137	<100	<100	<100	<100	<100	<100	<100	<100	<100	<100	<100	<100
		138	<100	<100	<100	<100	<100	117	<100	<100	<100	<100	<100	116
		139	<100	<100	<100	<100	<100	<100	<100	<100	<100	<100	<100	113
		140	<100	<100	<100	513	<100	<100	<100	<100	<100	<100	490	180
		141	<100	<100	<100	<100	<100	118	<100	<100	<100	<100	576	308
		142	<100	<100	<100	<100	<100	<100	<100	<100	<100	<100	<100	141
BG505 I3-01v9 SApNP	Aluminum phosphate	143	<100	<100	<100	<100	<100	382	561	198	208	114	1537	1148
		144	<100	<100	<100	<100	<100	<100	<100	<100	<100	<100	<100	357
		145	<100	<100	<100	<100	<100	<100	<100	<100	<100	<100	289	149
		146	<100	<100	<100	<100	<100	104	<100	<100	<100	<100	576	271
		147	<100	<100	<100	<100	<100	1025	514	328	280	302	2235	1883
		148	<100	<100	<100	<100	<100	<100	<100	<100	<100	<100	129	139
Env Mix I3-01v9 SApNP	Aluminum phosphate	149	<100	<100	<100	<100	106	939	589	218	161	157	780	892
		150	<100	<100	<100	<100	<100	123	<100	<100	<100	<100	631	363
		151	<100	<100	<100	<100	<100	1530	770	562	331	260	2731	1897
		152	<100	<100	<100	<100	<100	164	<100	<100	<100	<100	298	122
		153	<100	<100	<100	<100	<100	<100	<100	<100	<100	<100	<100	<100
		154	<100	<100	<100	<100	<100	114	<100	<100	<100	<100	145	<100

fig. S5

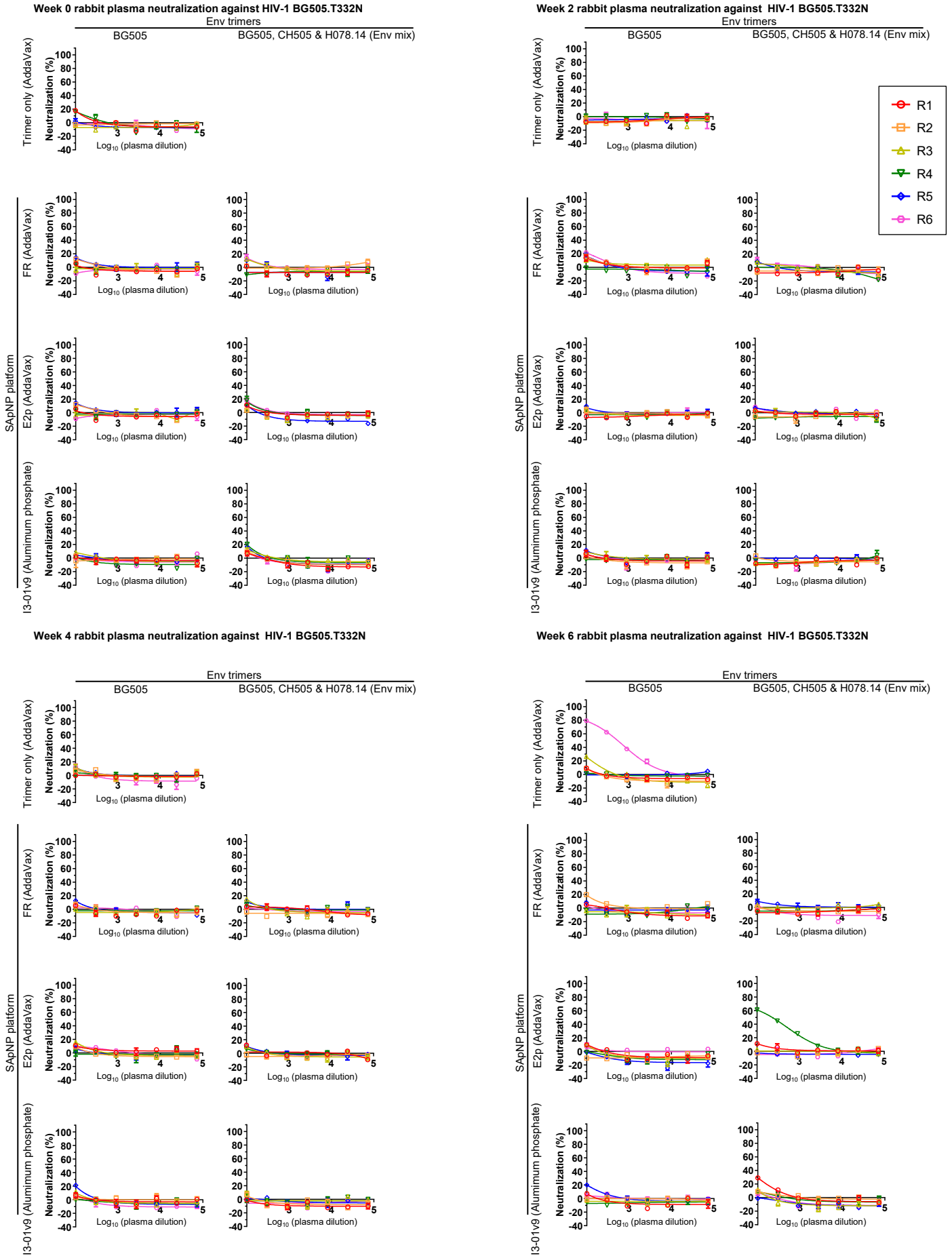
Week 0 rabbit plasma neutralization against HIV-1 BG505.T332N
Week 2 rabbit plasma neutralization against HIV-1 BG505.T332N
Week 4 rabbit plasma neutralization against HIV-1 BG505.T332N
Week 6 rabbit plasma neutralization against HIV-1 BG505.T332N
Env trimers
BG505
BG505, CH505 & H078.14 (Env mix)
Trimer only (AddaVax)
SApNP platform
FR (AddaVax)
E2p (AddaVax)
I3-01v9 (Alumimum phosphate)
Neutralization (%)
Log10 (plasma dilution)
R1
R2
R3
R4
R5
R6

fig. S5

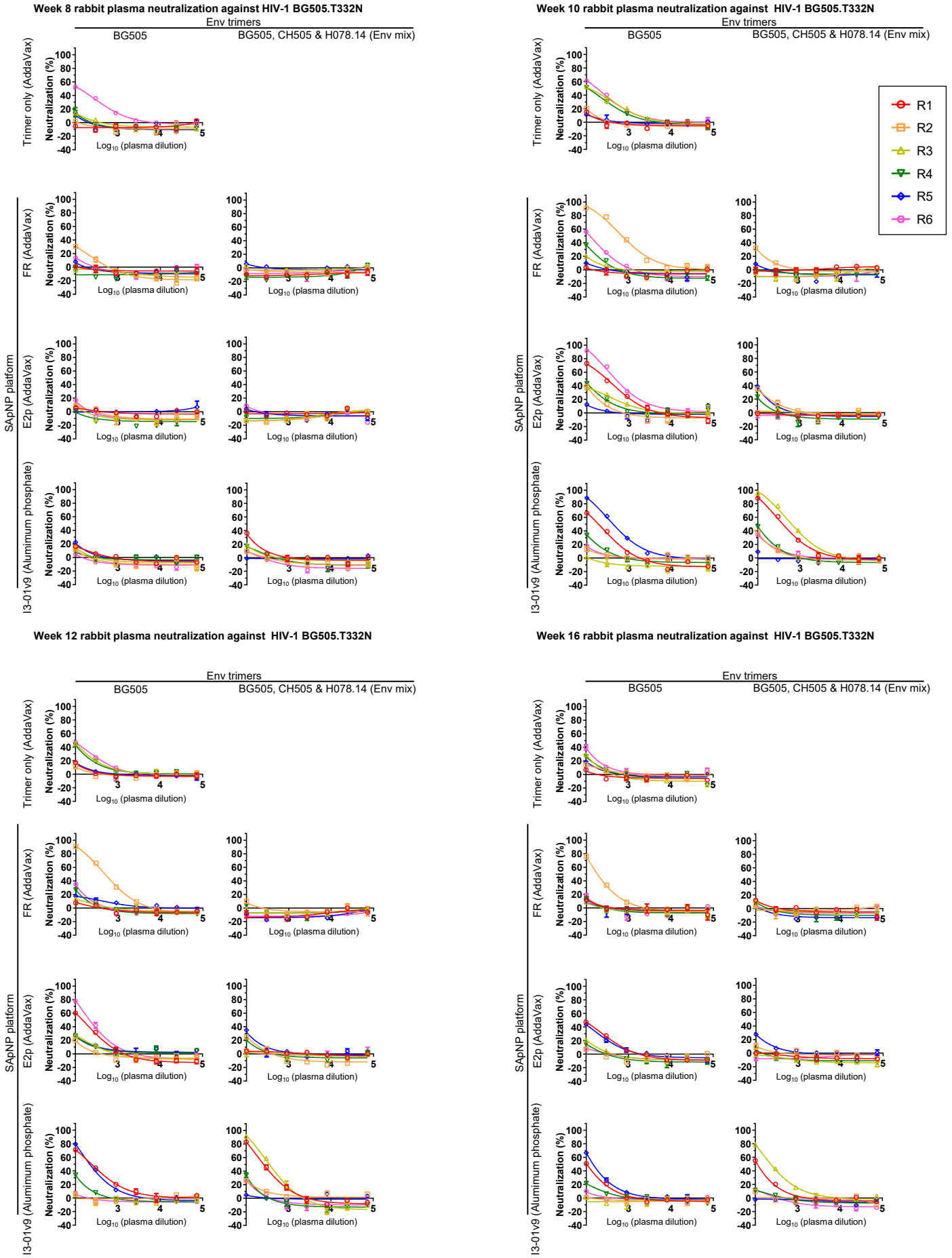
Week 8 rabbit plasma neutralization against HIV-1 BG505.T332N
Week 10 rabbit plasma neutralization against HIV-1 BG505.T332N
Week 12 rabbit plasma neutralization against HIV-1 BG505.T332N
Week 16 rabbit plasma neutralization against HIV-1 BG505.T332N
Env trimers
BG505
BG505, CH505 & H078.14 (Env mix)
Trimer only (AddaVax)
SApNP platform
FR (AddaVax)
E2p (AddaVax)
I3-01v9 (Alumimum phosphate)
Neutralization (%)
Log10 (plasma dilution)
R1
R2
R3
R4
R5
R6

fig. S5

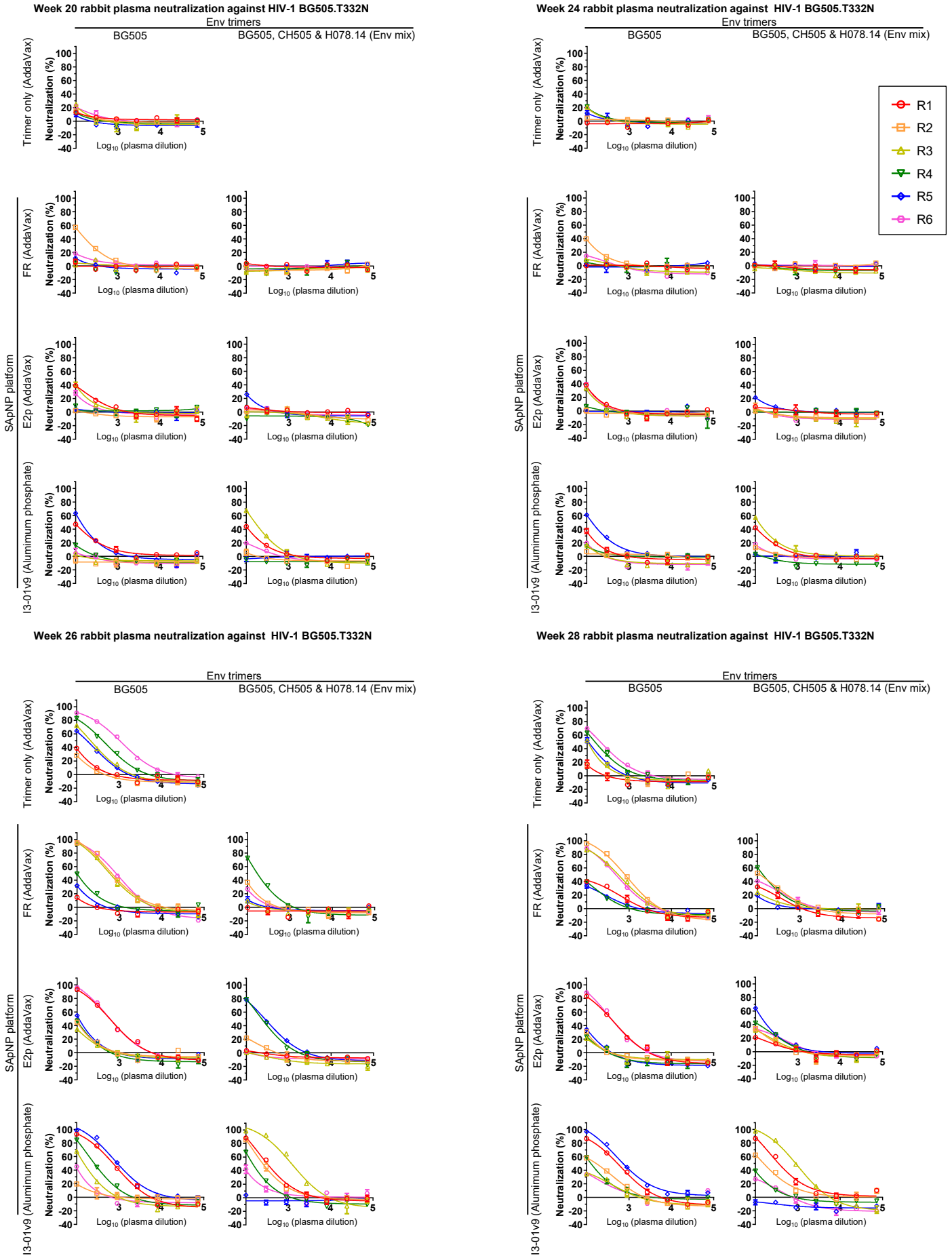
Week 20 rabbit plasma neutralization against HIV-1 BG505.T332N
Week 24 rabbit plasma neutralization against HIV-1 BG505.T332N
Week 26 rabbit plasma neutralization against HIV-1 BG505.T332N
Week 28 rabbit plasma neutralization against HIV-1 BG505.T332N
Env trimers
BG505
BG505, CH505 & H078.14 (Env mix)
Trimer only (AddaVax)
SApNP platform
FR (AddaVax)
E2p (AddaVax)
I3-01v9 (Alumimum phosphate)
Neutralization (%)
Log10 (plasma dilution)
R1
R2
R3
R4
R5
R6

fig. S5

E **Weeks 0-28 rabbit plasma neutralization against HIV SF162, ID_{50} titers**

Vaccine	Adjuvant	Animal ID	ID_{50} titers											
			w0	w2	w4	w6	w8	w10	w12	w16	w20	w24	w26	w28
BG505 UFO trimer	Addavax	119	<100	<100	<100	<100	<100	3429	920	375	<100	<100	1953	565
		120	<100	<100	<100	<100	<100	310	107	<100	<100	<100	1120	452
		121	<100	<100	<100	<100	<100	1926	821	362	108	101	1190	627
		122	<100	<100	<100	<100	<100	840	174	<100	<100	<100	938	280
		123	<100	<100	<100	<100	<100	661	135	<100	<100	<100	673	313
		124	<100	<100	<100	405	<100	641	153	<100	<100	<100	2015	689
BG505 FR SApNP	Addavax	125	<100	<100	<100	<100	<100	2056	894	423	<100	<100	3716	882
		126	<100	<100	102	219	164	2745	975	425	115	<100	1534	754
		127	<100	<100	<100	200	362	4060	1343	554	240	236	5866	1759
		128	<100	<100	<100	<100	113	4055	1069	265	129	103	4408	968
		129	<100	<100	<100	<100	<100	1553	521	228	<100	133	2736	829
		130	<100	<100	<100	<100	<100	927	256	106	<100	<100	2552	973
Env Mix FR SApNP	Addavax	131	<100	<100	<100	<100	359	1025	284	191	<100	<100	1541	562
		132	<100	<100	<100	103	111	1222	485	218	<100	<100	1534	210
		133	<100	<100	<100	<100	<100	566	180	104	<100	<100	1273	355
		134	<100	<100	<100	123	346	2494	1150	665	214	221	4272	641
		135	<100	<100	<100	129	215	2301	706	252	<100	122	3695	515
		136	<100	<100	<100	<100	<100	942	272	152	<100	<100	4795	225
BG505 E2p SApNP	Addavax	155	<100	<100	<100	<100	<100	474	162	<100	<100	<100	1424	606
		156	<100	<100	<100	<100	<100	1003	323	<100	<100	<100	1833	257
		157	<100	<100	<100	<100	<100	5656	1819	390	294	190	2726	820
		158	<100	<100	<100	<100	<100	1405	428	<100	<100	<100	866	317
		159	<100	<100	<100	<100	<100	2241	666	106	149	209	2712	1131
		160	<100	<100	<100	<100	<100	1063	311	183	<100	108	610	293
Env Mix E2p SApNP	Addavax	137	<100	<100	<100	<100	<100	912	329	167	<100	107	1061	275
		138	<100	<100	<100	<100	<100	1220	360	115	<100	<100	3029	660
		139	<100	<100	<100	202	309	1557	1018	643	395	334	7500	946
		140	<100	<100	<100	138	<100	2666	833	280	<100	<100	3422	517
		141	<100	<100	<100	<100	<100	1484	461	234	<100	<100	895	230
		142	<100	<100	<100	<100	<100	1949	836	467	230	244	3779	993
BG505 I3-01v9 SApNP	Aluminum phosphate	143	<100	<100	<100	<100	132	1101	342	173	<100	<100	2028	216
		144	<100	<100	<100	146	317	1641	833	464	297	359	5417	1031
		145	<100	<100	112	121	174	1084	415	223	114	139	5341	1272
		146	<100	<100	<100	102	262	1469	1250	693	233	245	2477	579
		147	<100	<100	287	1378	2413	3366	2188	1287	895	924	6167	1551
		148	<100	<100	<100	255	532	3835	1642	717	320	256	2790	514
Env Mix I3-01v9 SApNP	Aluminum phosphate	149	<100	<100	<100	291	449	996	418	124	<100	104	1396	363
		150	<100	<100	<100	210	370	2981	2027	275	147	158	5805	1113
		151	<100	<100	<100	<100	179	6838	1663	566	355	325	7193	3074
		152	<100	<100	<100	220	276	2487	726	230	110	114	5597	1552
		153	<100	<100	116	333	349	4624	1252	392	159	171	7687	3191
		154	<100	<100	<100	145	223	2588	737	250	163	215	3045	844

fig. S5

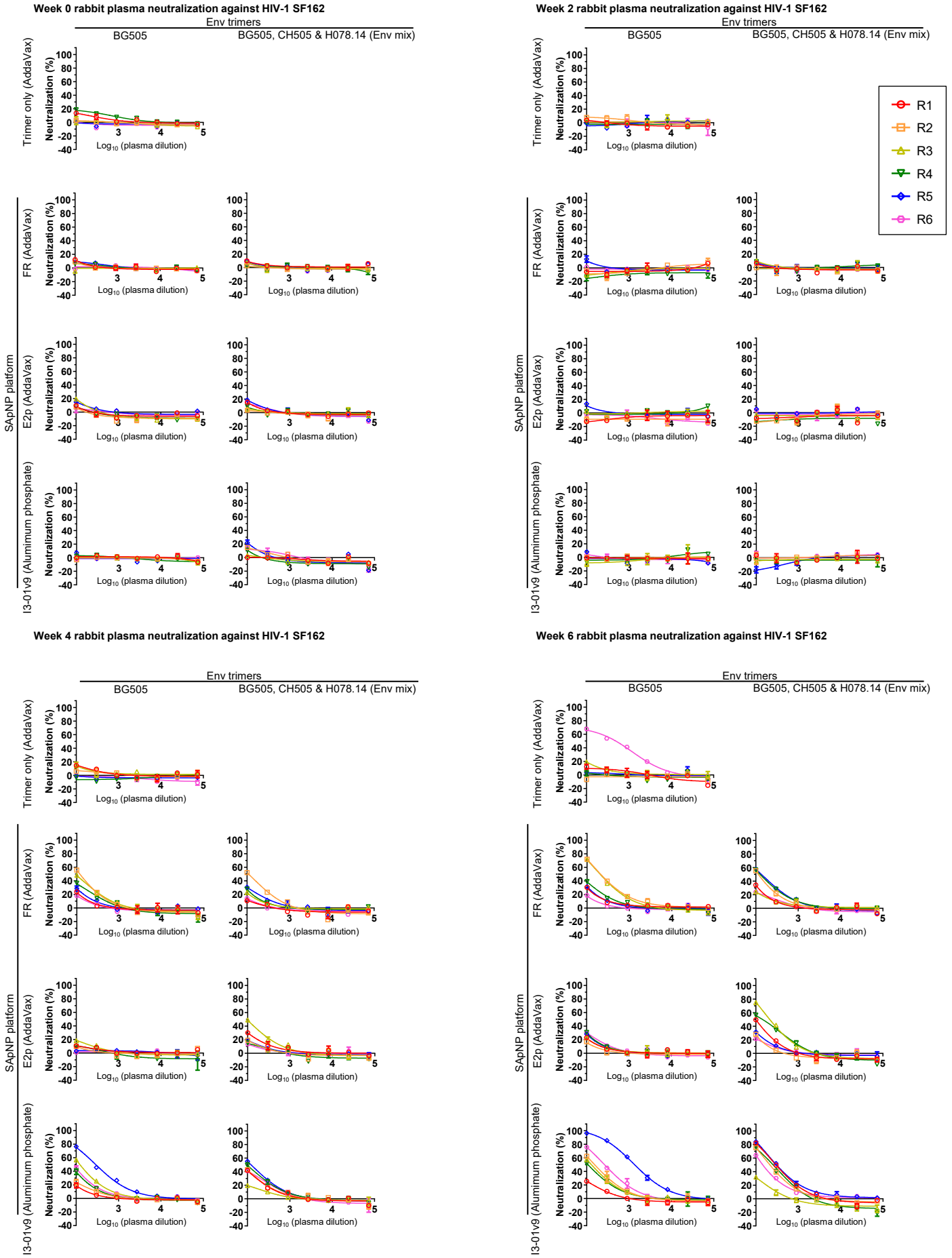
Week 0 rabbit plasma neutralization against HIV-1 SF162
Week 2 rabbit plasma neutralization against HIV-1 SF162
Week 4 rabbit plasma neutralization against HIV-1 SF162
Week 6 rabbit plasma neutralization against HIV-1 SF162
Env trimers
BG505
BG505, CH505 & H078.14 (Env mix)
Trimer only (AddaVax)
SApNP platform
FR (AddaVax)
E2p (AddaVax)
I3-01v9 (Alumimum phosphate)
Neutralization (%)
Log10 (plasma dilution)
R1
R2
R3
R4
R5
R6

fig. S5

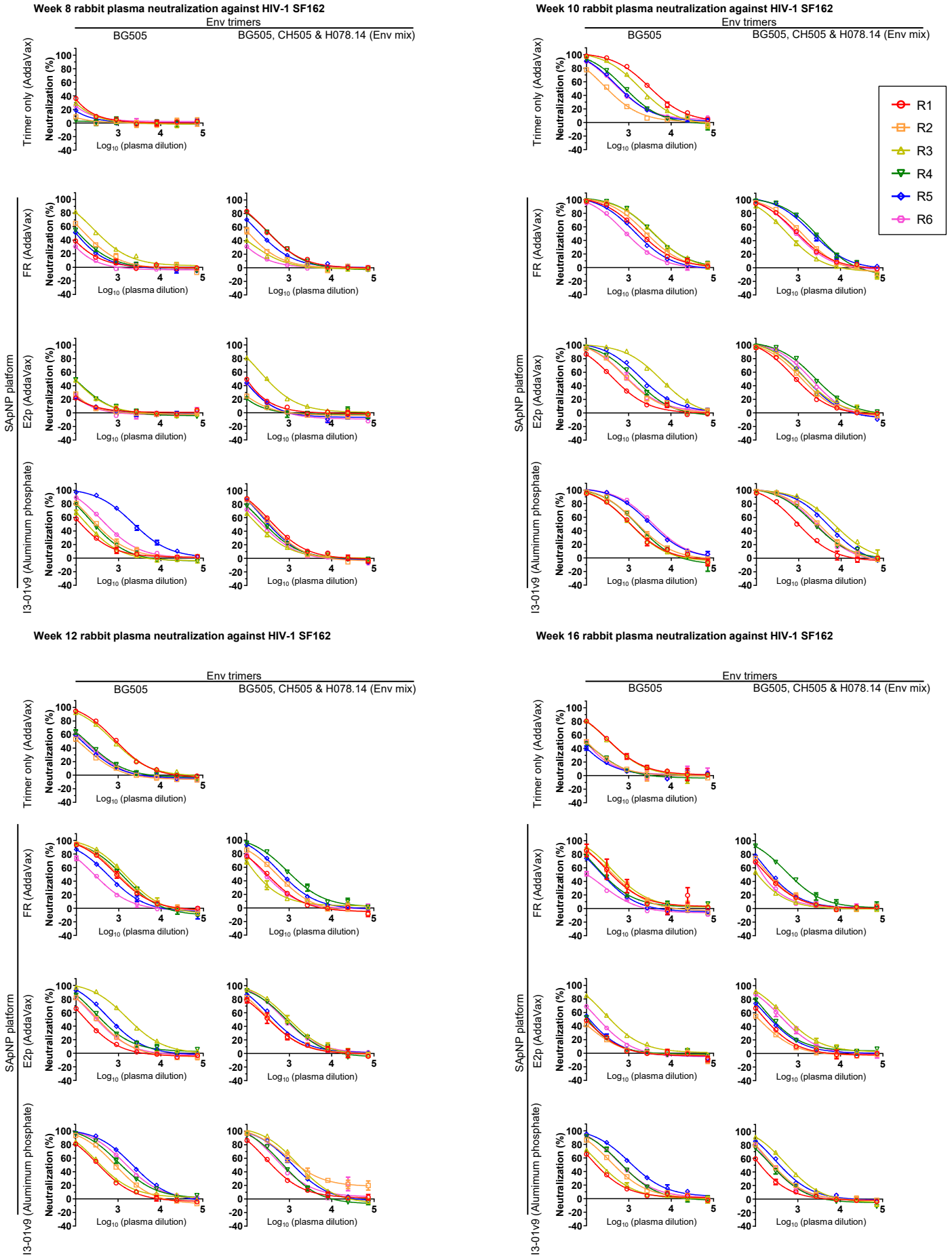
Week 8 rabbit plasma neutralization against HIV-1 SF162
Week 10 rabbit plasma neutralization against HIV-1 SF162
Week 12 rabbit plasma neutralization against HIV-1 SF162
Week 16 rabbit plasma neutralization against HIV-1 SF162
Env trimers
BG505
BG505, CH505 & H078.14 (Env mix)
Trimer only (AddaVax)
SApNP platform
FR (AddaVax)
E2p (AddaVax)
I3-01v9 (Alumimum phosphate)
Neutralization (%)
Log10 (plasma dilution)
R1
R2
R3
R4
R5
R6

fig. S5

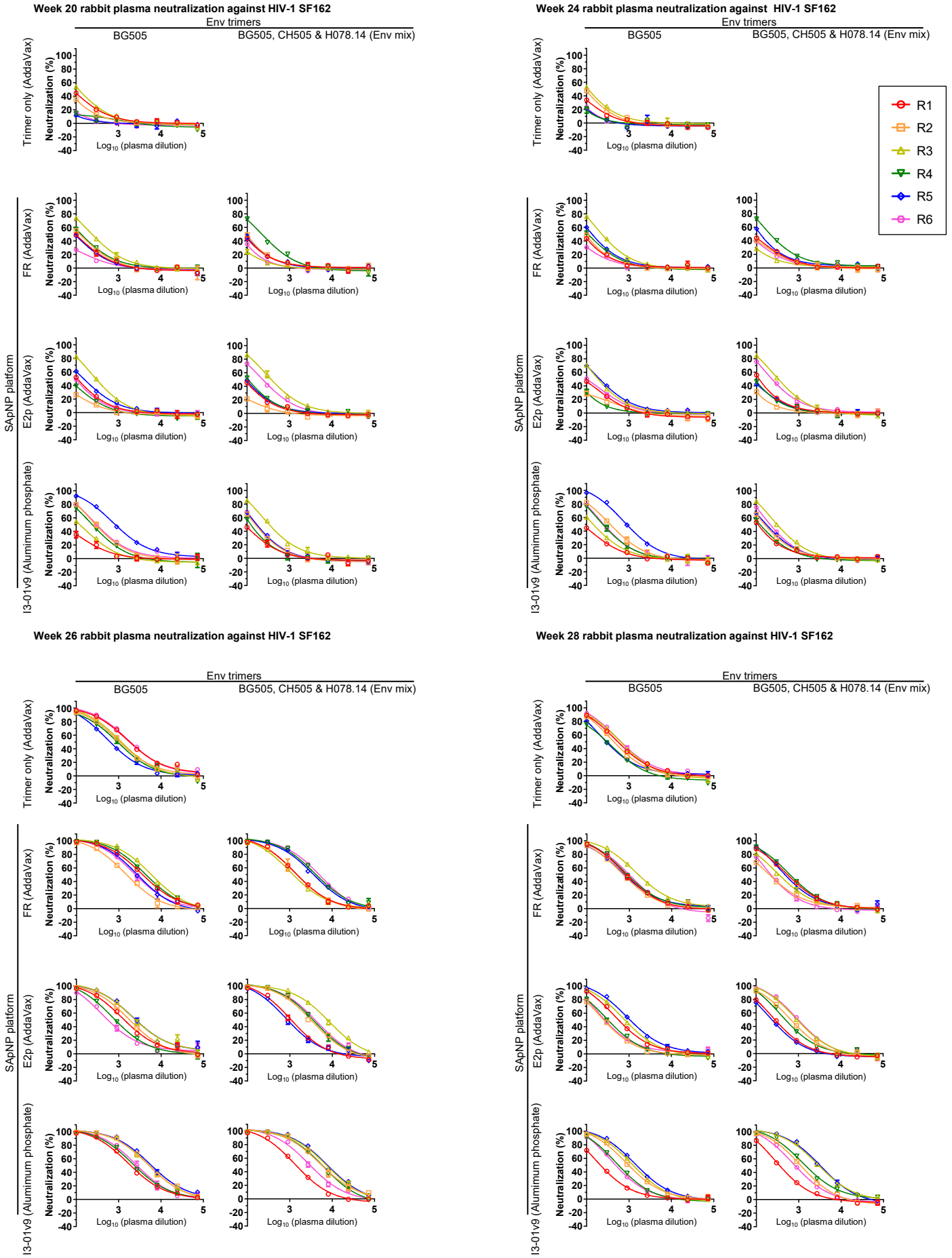
Week 20 rabbit plasma neutralization against HIV-1 SF162
Week 24 rabbit plasma neutralization against HIV-1 SF162
Week 26 rabbit plasma neutralization against HIV-1 SF162
Week 28 rabbit plasma neutralization against HIV-1 SF162
Env trimers
BG505
BG505, CH505 & H078.14 (Env mix)
SApNP platform
Trimer only (AddaVax)
FR (AddaVax)
E2p (AddaVax)
I3-01v9 (Alumimum phosphate)
Neutralization (%)
Log10 (plasma dilution)
R1
R2
R3
R4
R5
R6

fig. S5

F **Weeks 0, 2, 10 & 26 rabbit plasma neutralization against MLV, ID_{50} titers**

Vaccine	Adjuvant	Animal ID	ID_{50} titers			
			w0	w2	w10	w26
BG505 UFO trimer	Addavax	119	<100	<100	<100	<100
		120	<100	<100	<100	<100
		121	<100	<100	<100	<100
		122	<100	<100	<100	<100
		123	<100	<100	<100	<100
		124	<100	<100	<100	<100
BG505 FR SApNP	Addavax	125	<100	<100	<100	<100
		126	<100	<100	<100	<100
		127	<100	<100	<100	<100
		128	<100	<100	<100	<100
		129	<100	<100	<100	<100
		130	<100	<100	<100	<100
Env Mix FR SApNP	Addavax	131	<100	<100	<100	<100
		132	<100	<100	<100	<100
		133	<100	<100	<100	<100
		134	<100	<100	<100	<100
		135	<100	<100	<100	<100
		136	<100	<100	<100	<100
BG505 E2p SApNP	Addavax	155	<100	<100	<100	<100
		156	<100	<100	<100	<100
		157	<100	<100	<100	<100
		158	<100	<100	<100	<100
		159	<100	<100	<100	<100
		160	<100	<100	<100	<100
Env Mix E2p SApNP	Addavax	137	<100	<100	<100	<100
		138	<100	<100	<100	<100
		139	<100	<100	<100	<100
		140	<100	<100	<100	<100
		141	<100	<100	<100	<100
		142	<100	<100	<100	<100
BG505 I3-01v9 SApNP	Aluminum phosphate	143	<100	<100	<100	<100
		144	<100	<100	<100	<100
		145	<100	<100	<100	<100
		146	<100	<100	<100	<100
		147	<100	<100	<100	<100
		148	<100	<100	<100	<100
Env Mix I3-01v9 SApNP	Aluminum phosphate	149	<100	<100	<100	<100
		150	<100	<100	<100	<100
		151	<100	<100	<100	<100
		152	<100	<100	<100	<100
		153	<100	<100	<100	<100
		154	<100	<100	<100	<100

fig. S5

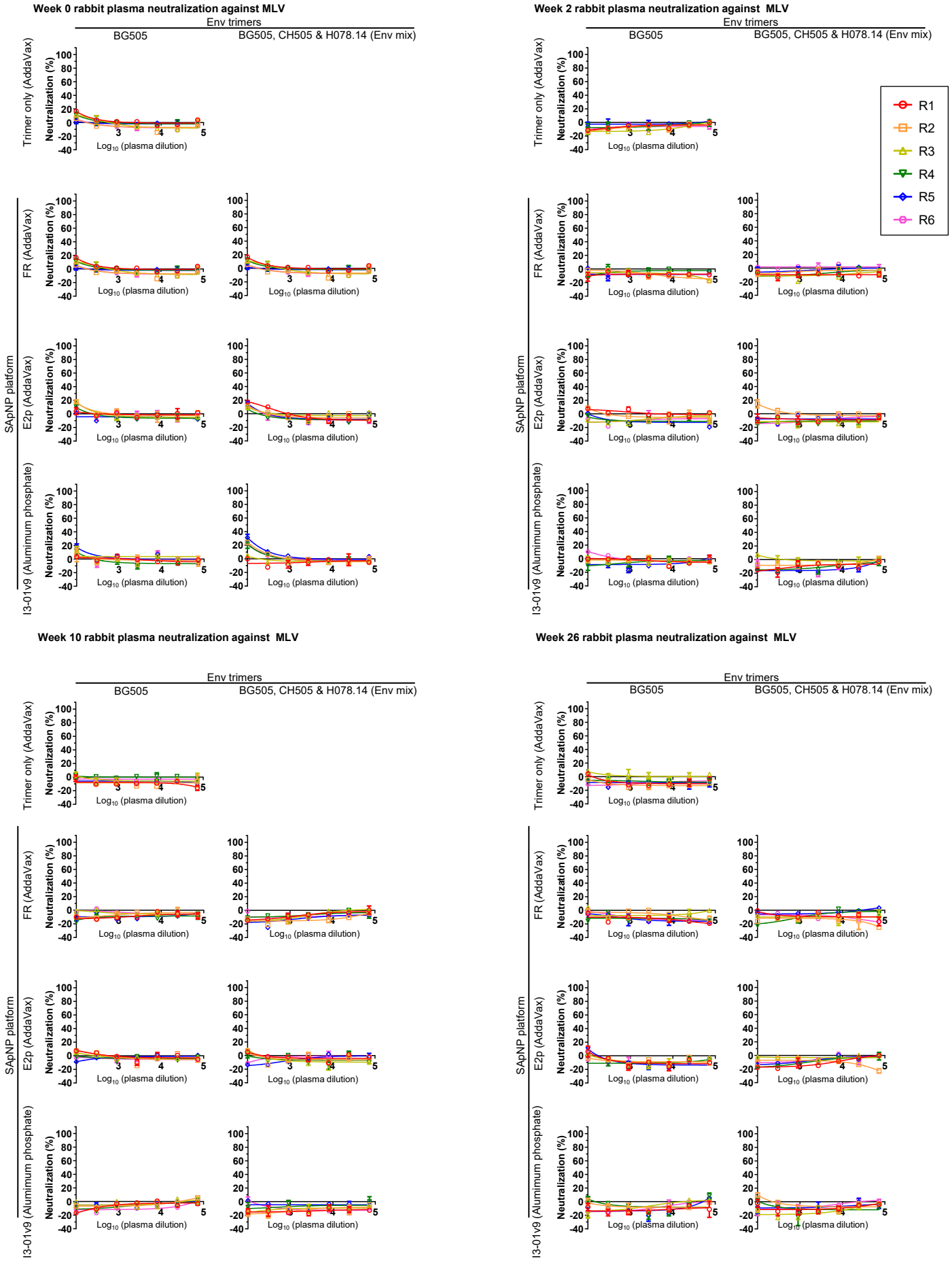
Week 0 rabbit plasma neutralization against MLV
Week 2 rabbit plasma neutralization against MLV
Week 10 rabbit plasma neutralization against MLV
Week 26 rabbit plasma neutralization against MLV
Env trimers
BG505
BG505, CH505 & H078.14 (Env mix)
Trimer only (AddaVax)
SApNP platform
FR (AddaVax)
E2p (AddaVax)
I3-01v9 (Alumimum phosphate)
Neutralization (%)
Log10 (plasma dilution)
R1
R2
R3
R4
R5
R6

fig. S5

G Week 26 rabbit plasma neutralization against the 12-virus global panel, ID_{50} and ID_{30} titers

Vaccine	Adjuvant	Rabbit ID	ID_{50} titers for each virus (clade)														
			TRO11 (B)	25710 (C)	398F1 (A)	CNE8 (AE)	X2278 (B)	BJOX-2000 (BC)	X1632 (G)	CE1176 (C)	246F3 (AC)	CH119 (BC)	CE0217 (C)	CNE55 (AE)	BG505.T332N (A)	SF162 (B)	MLV (control)
BG505 UFO trimer	Addavax	119	<40	<40	135	<40	<40	<40	<40	<40	<40	<40	<40	<40	<100	1953	<40
		120	<40	<40	80	<40	<40	<40	<40	<40	<40	<40	<40	<40	<100	1120	<40
		121	<40	<40	93	<40	<40	<40	<40	<40	<40	<40	<40	<40	191	1190	<40
		122	<40	<40	144	<40	<40	<40	<40	<40	<40	<40	<40	<40	381	938	<40
		123	57	54	258	48	<40	<40	<40	<40	43	<40	<40	<40	150	673	<40
		124	<40	<40	116	<40	<40	<40	<40	<40	<40	<40	<40	<40	510	2015	<40
BG505 FR SApNP	Addavax	125	<40	<40	221	<40	<40	<40	<40	<40	<40	<40	<40	<40	<100	3716	<40
		126	<40	<40	94	<40	<40	<40	<40	<40	<40	<40	<40	<40	688	1534	<40
		127	<40	<40	127	<40	<40	<40	<40	<40	<40	<40	<40	<40	601	5866	<40
		128	<40	<40	154	<40	<40	<40	<40	<40	<40	<40	<40	<40	<100	4408	<40
		129	<40	40	148	<40	<40	<40	<40	<40	<40	<40	<40	<40	<100	2736	<40
		130	<40	<40	100	<40	<40	<40	<40	<40	<40	<40	<40	<40	760	2552	<40
Env Mix FR SApNP	Addavax	131	<40	53	174	<40	<40	<40	<40	<40	<40	<40	<40	<40	<100	1541	<40
		132	<40	<40	106	<40	<40	<40	<40	<40	<40	<40	<40	<40	<100	1534	<40
		133	<40	71	179	48	<40	58	<40	47	41	<40	<40	<40	<100	1273	<40
		134	<40	<40	74	<40	<40	<40	<40	<40	<40	<40	<40	<40	151	4272	<40
		135	<40	<40	100	<40	<40	<40	<40	<40	<40	<40	<40	<40	<100	3695	<40
		136	<40	<40	106	<40	<40	<40	<40	<40	<40	<40	<40	<40	<100	4795	<40
BG505 E2p SApNP	Addavax	155	<40	<40	63	<40	<40	<40	<40	<40	<40	<40	<40	<40	563	1424	<40
		156	<40	<40	55	<40	<40	<40	<40	<40	<40	<40	<40	<40	<100	1833	<40
		157	<40	42	108	<40	<40	<40	<40	<40	<40	<40	<40	<40	<100	2726	<40
		158	<40	<40	103	<40	<40	<40	<40	<40	<40	<40	<40	<40	<100	866	<40
		159	54	<40	417	88	<40	<40	<40	59	76	44	<40	43	<100	2712	<40
		160	<40	<40	167	<40	<40	<40	<40	<40	<40	<40	<40	<40	587	610	<40
Env Mix E2p SApNP	Addavax	137	<40	<40	157	<40	<40	<40	<40	<40	<40	<40	<40	<40	<100	1061	<40
		138	<40	44	108	<40	<40	<40	<40	<40	<40	<40	<40	<40	<100	3029	<40
		139	<40	58	386	<40	<40	<40	<40	<40	<40	<40	<40	<40	<100	7500	<40
		140	<40	<40	171	<40	<40	<40	<40	<40	<40	<40	<40	<40	<100	3422	<40
		141	<40	44	202	<40	<40	<40	<40	<40	<40	<40	<40	<40	247	895	<40
		142	<40	51	228	<40	<40	<40	<40	<40	<40	<40	<40	<40	<100	3779	<40
BG505 I3-01v9 SApNP	Aluminum phosphate	143	<40	51	363	<40	<40	<40	<40	<40	<40	<40	<40	<40	973	2028	<40
		144	<40	<40	72	<40	<40	<40	<40	<40	<40	<40	<40	<40	<100	5417	<40
		145	<40	<40	174	<40	<40	<40	<40	<40	<40	<40	<40	<40	<100	5341	<40
		146	<40	<40	179	<40	<40	<40	<40	<40	<40	42	<40	<40	247	2477	<40
		147	<40	71	205	48	50	47	<40	<40	42	<40	<40	<40	958	6167	<40
		148	<40	80	172	<40	<40	<40	<40	<40	<40	<40	<40	43	<100	2790	<40
Env Mix I3-01v9 SApNP	Aluminum phosphate	149	<40	<40	257	<40	<40	<40	<40	<40	<40	<40	<40	<40	334	1396	<40
		150	<40	59	406	45	<40	<40	<40	<40	<40	<40	<40	<40	271	5805	<40
		151	<40	53	259	<40	<40	<40	<40	<40	<40	<40	<40	<40	1170	7193	<40
		152	<40	<40	178	<40	<40	<40	<40	<40	<40	<40	<40	<40	128	5597	<40
		153	<40	81	883	<40	<40	<40	<40	<40	<40	52	<40	<40	<100	7687	<40
		154	<40	61	225	<40	<40	42	<40	<40	<40	<40	<40	<40	<100	3045	<40

Vaccine	Adjuvant	Rabbit ID	ID_{30} titers for each virus (clade)														
			TRO11 (B)	25710 (C)	398F1 (A)	CNE8 (AE)	X2278 (B)	BJOX-2000 (BC)	X1632 (G)	CE1176 (C)	246F3 (AC)	CH119 (BC)	CE0217 (C)	CNE55 (AE)	BG505.T332N (A)	SF162 (B)	MLV (control)
BG505 UFO trimer	Addavax	119	62	90	309	59	49	45	<40	53	68	58	<40	<40	120	4558	<40
		120	<40	58	199	<40	<40	<40	<40	<40	<40	<40	<40	<40	<100	2614	<40
		121	<40	54	233	<40	<40	<40	<40	<40	<40	<40	<40	<40	446	2778	<40
		122	45	66	351	<40	<40	<40	<40	<40	<40	<40	<40	<40	889	2188	<40
		123	282	198	694	128	52	63	<40	61	126	103	<40	99	351	1571	<40
		124	<40	43	326	<40	<40	<40	<40	<40	<40	<40	<40	<40	1190	4701	<40
BG505 FR SApNP	Addavax	125	<40	94	758	59	<40	43	<40	52	43	<40	<40	<40	<100	8670	<40
		126	<40	77	250	43	<40	<40	<40	41	42	<40	<40	<40	1605	3579	<40
		127	<40	82	426	<40	<40	<40	<40	<40	<40	<40	<40	<40	1401	13687	<40
		128	<40	96	565	<40	<40	<40	<40	<40	<40	<40	<40	<40	186	10286	<40
		129	52	107	575	93	59	98	<40	52	59	42	<40	<40	<100	6385	<40
		130	<40	79	513	<40	<40	<40	<40	<40	<40	<40	<40	<40	1774	5955	<40
Env Mix FR SApNP	Addavax	131	<40	136	1093	72	<40	73	<40	<40	<40	<40	<40	<40	<100	3596	<40
		132	<40	82	450	47	<40	54	<40	<40	<40	<40	<40	<40	105	3580	<40
		133	88	278	680	119	67	137	57	116	100	80	56	100	<100	2971	<40
		134	<40	55	249	<40	<40	<40	<40	<40	<40	<40	<40	<40	351	9968	<40
		135	<40	69	296	<40	<40	51	<40	57	57	<40	<40	<40	<100	8622	<40
		136	<40	50	418	<40	<40	<40	<40	<40	<40	<40	<40	<40	<100	11188	<40
BG505 E2p SApNP	Addavax	155	41	73	171	62	<40	66	<40	43	55	59	<40	<40	1313	3323	<40
		156	<40	40	175	<40	<40	45	<40	<40	<40	<40	<40	<40	154	4276	<40
		157	<40	105	434	78	<40	88	<40	<40	<40	52	<40	<40	107	6360	<40
		158	<40	70	336	49	<40	53	<40	<40	<40	<40	<40	<40	149	2020	<40
		159	172	86	1808	271	<40	83	<40	167	262	97	47	99	198	6328	<40
		160	<40	<40	827	<40	<40	<40	<40	<40	94	<40	<40	<40	1369	1422	<40
Env Mix E2p SApNP	Addavax	137	<40	77	783	<40	<40	51	<40	<40	<40	<40	<40	<40	<100	2475	<40
		138	<40	121	592	<40	<40	<40	<40	<40	<40	<40	<40	<40	<100	7067	<40
		139	51	161	1509	51	65	<40	40	<40	<40	41	<40	<40	<100	17500	<40
		140	<40	63	457	<40	<40	<40	<40	<40	<40	<40	<40	<40	144	7986	<40
		141	<40	110	508	<40	<40	<40	<40	<40	<40	<40	<40	<40	576	2088	<40
		142	<40	144	587	44	<40	<40	<40	<40	<40	<40	<40	<40	<100	8818	<40
BG505 I3-01v9 SApNP	Aluminum phosphate	143	<40	192	1717	<40	<40	<40	<40	<40	<40	<40	<40	<40	2269	4732	<40
		144	<40	<40	197	<40	<40	44	<40	<40	<40	<40	<40	<40	<100	12639	<40
		145	<40	94	647	<40	<40	54	<40	<40	<40	<40	<40	<40	<100	12463	<40
		146	<40	95	507	<40	<40	47	<40	<40	45	106	<40	<40	576	5780	<40
		147	65	202	660	112	130	111	40	80	105	53	51	80	2235	14390	<40
		148	61	275	521	79	57	<40	<40	82	80	62	<40	156	108	6510	<40
Env Mix I3-01v9 SApNP	Aluminum phosphate	149	<40	80	1114	69	<40	<40	<40	<40	<40	<40	<40	<40	780	3257	<40
		150	53	154	1575	116	48	51	44	44	75	81	<40	54	631	13545	<40
		151	<40	139	1675	84	<40	<40	42	<40	58	<40	<40	<40	2731	16783	<40
		152	<40	68	747	78	<40	<40	<40	<40	41	<40	<40	<40	298	13060	<40
		153	<40	288	7874	45	<40	<40	<40	52	<40	417	<40	<40	<100	17936	<40
		154	51	158	981	69	52	113	<40	50	50	74	<40	<40	145	7105	<40

fig. S5. Neutralization data from the evaluation of Env immunogens with wildtype glycans. (**A**) Mouse IgG neutralization from ten groups of mice (8 per group) that were immunized with BG505 UFO trimer-presenting E2p and I3-01v9 SApNPs. In the first study, five groups of mice were immunized with BG505 UFO trimer-presenting E2p SApNP, each group with a different adjuvant condition: no adjuvant, AddaVax (AV), Aluminum phosphate (AP), Aluminum hydroxide or AVx2/APx2. In a second study, five groups were immunized with BG505 UFO trimer-presenting I3-01v9 SApNP, with the same five adjuvant conditions. Data are shown for neutralization of tier 2 clade A BG505.T332N, tier 1 clade B SF162, and MLV pseudoviruses (MLV-pps) by purified mouse IgG from the last time point, week 11. IC_{50} titers, and neutralization curves are shown. (**B**) Positive samples (>30% autologous neutralization) from (A) were tested against the BG505.T332N variant with the C3/V4 knockout mutation (I396R) and against **(C)** a 12-virus global panel of HIV-1 strains. For (A-C) an IgG concentration of 300 µg/ml was used as the starting point and subjected to a 3-times dilution series in the TZM-bl neutralization assay. Samples were tested in duplicate in the TZM-bl assay, except in the MLV, I396R mutant and the 12-virus global panel assays, where samples were tested in singlet due to a low quantity of remaining IgG. IgG samples no longer available at the time of an assay are marked '-' in the IC_{50}/IC_{30} titer tables. (**D**)-(**G**) Rabbit plasma neutralization from seven groups of rabbits that were immunized with BG505 or mixed Env vaccines. All antigens were mixed with AV except for I3-01v9 SApNPs, which were formulated with AP. BG505 UFO trimer and its three SApNPs (FR, E2p, and I3-01v9) were tested in groups 1, 2, 4, and 6, respectively, with a mixed Env group added for each SApNP platform and tested in groups 3, 5, and 7. The mixed Env vaccine is a cocktail containing equal amounts of SApNPs that present clade A BG505 UFO, clade B H078.14 UFO-BG, and clade C CH505 UFO-BG trimers. Data are shown for (**D**) Neutralization of tier 2 clade A BG505.T332N by rabbit plasma from all groups at every time point between week 0 (w0) and week 28 (w28). The heat-inactivated rabbit plasma was diluted 100 times as the starting point and subjected to a 3-times dilution series in the TZM-bl assay. Samples were tested in duplicate against all viruses. ID_{50} and ID_{30} titers and neutralization curves are graphed for each rabbit at each time point. (**E**) As (D), except neutralization is against tier 1 Clade B SF162. (**F**) As (D) and (E), except neutralization is against MLV-pps as a negative control, and only for key weeks 0, 2, 10 and 26. (**G**) ID_{50} and ID_{30} titers obtained from a large-scale TZM-bl neutralization assay against a 12-virus global panel with rabbit plasma diluted 40 times as the starting point for all 12 isolates. Of note, BG505.T332N, SF162, and MLV data from (D)-(F) were included in this table to facilitate comparison with the 12-virus panel.

fig. S6

A

E2p-expressing CHO-K1 cell clone #1 (~30 mg/l)

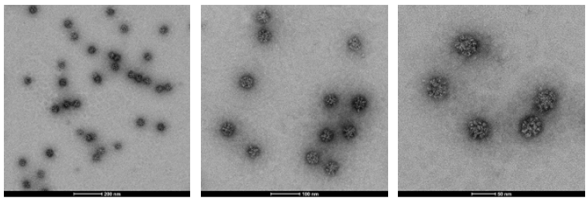

E2p-expressing CHO-K1 cell clone #2 (~100 mg/l)

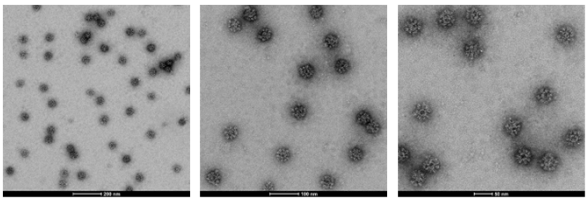

E2p-expressing CHO-K1 cell clone #3 (~40 mg/l)

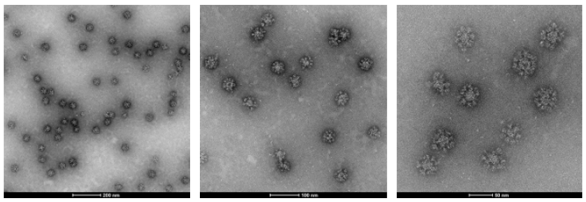

E2p-expressing CHO-K1 cell clone #4 (~50 mg/l)

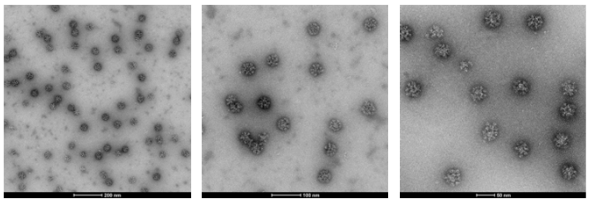

E2p-expressing CHO-K1 cell clone #5 (~130 mg/l)

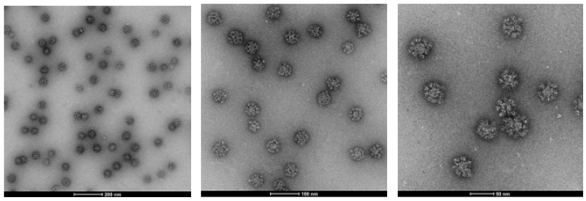

E2p-expressing CHO-K1 cell clone #6 (~60 mg/l)

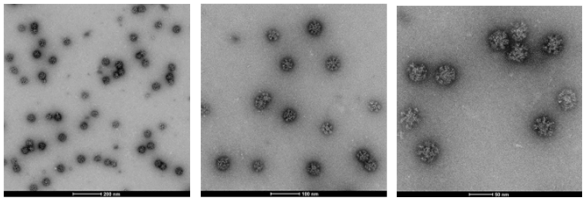

E2p-expressing CHO-K1 cell clone #7 (~25 mg/l)

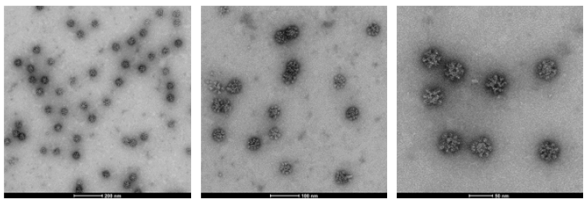

E2p-expressing CHO-K1 cell clone #8 (~19 mg/l)

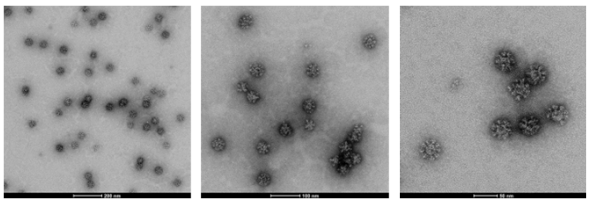

I3-01v9-expressing CHO-K1 cell clone #1 (~32 mg/l)

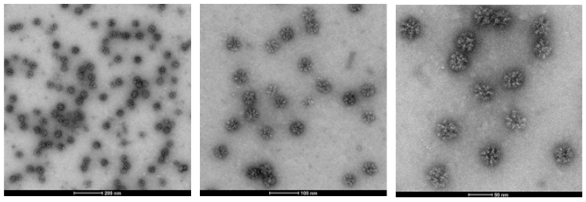

I3-01v9-expressing CHO-K1 cell clone #2 (~57 mg/l)

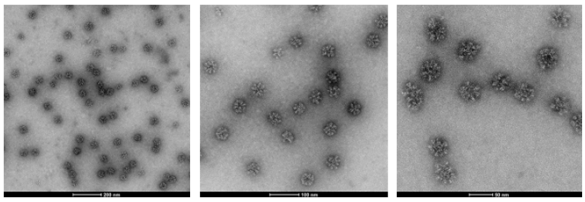

I3-01v9-expressing CHO-K1 cell clone #3 (~80 mg/l)

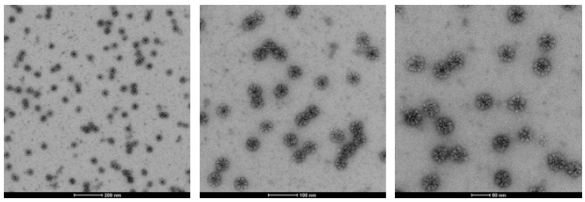

I3-01v9-expressing CHO-K1 cell clone #4 (~18 mg/l)

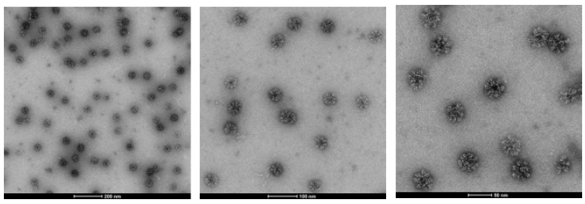

I3-01v9-expressing CHO-K1 cell clone #5 (~55 mg/l)

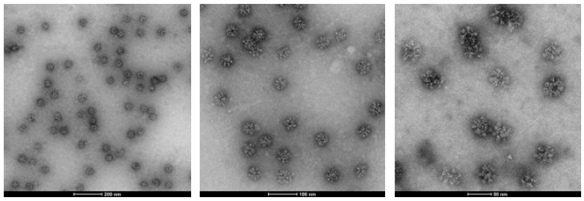

B **Week 11 mouse IgG neutralization against HIV-1 BG505.T332N. Immunization with glycan trimmed BG505 UFO trimers.**

Vaccine	Adjuvant	Glycan trimming regimen	IC_{50} titers (µg/ml)							
			M1	M2	M3	M4	M5	M6	M7	M8
BG505 UFO trimer	AddaVax	Regimen 1	>300	>300	68	20	>300	35	>300	22
		Regimen 2	1	254	>300	>300	17	>300	93	3
	Aluminum phosphate	Regimen 1	17	155	No IgG	44	2	8	158	>300 ★
		Regimen 2	118	13	5	48	10	>300	>300	66 ★

No IgG: indicates no IgG available to test ★ indicates samples from this group further tested against other HIV-1 viruses & MLV

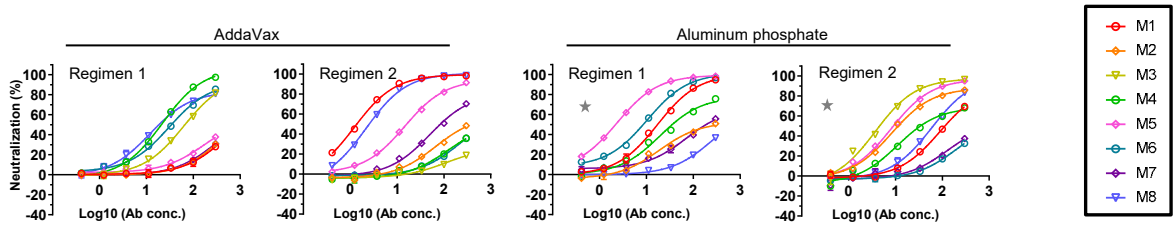

Week 11 mouse IgG neutralization against HIV SF162

Vaccine	Adjuvant	Glycan trimming regimen	IC_{50} titers (µg/ml)							
			M1	M2	M3	M4	M5	M6	M7	M8
BG505 UFO trimer	Aluminum phosphate	Regimen 1	53	15	No IgG	>300	19	6	5	1
		Regimen 2	11	34	62	7	15	11	14	1

No IgG: indicates no IgG available to test

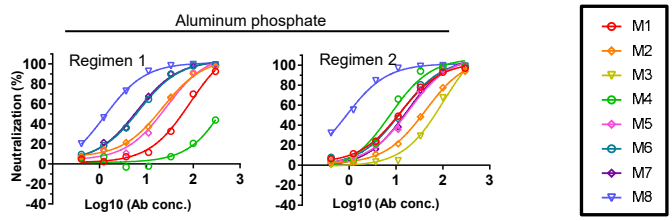

Week 11 mouse IgG neutralization against MLV (control)

Vaccine	Adjuvant	Glycan trimming regimen	IC_{50} titers (µg/ml)							
			M1	M2	M3	M4	M5	M6	M7	M8
BG505 UFO trimer	AddaVax	Regimen 1	>300	>300	>300	>300	>300	>300	>300	>300
		Regimen 2	>300	>300	>300	>300	>300	>300	>300	>300
	Aluminum phosphate	Regimen 1	>300	>300	No IgG	>300	>300	>300	>300	>300
		Regimen 2	>300	>300	>300	>300	>300	>300	>300	>300

No IgG: indicates no IgG available to test

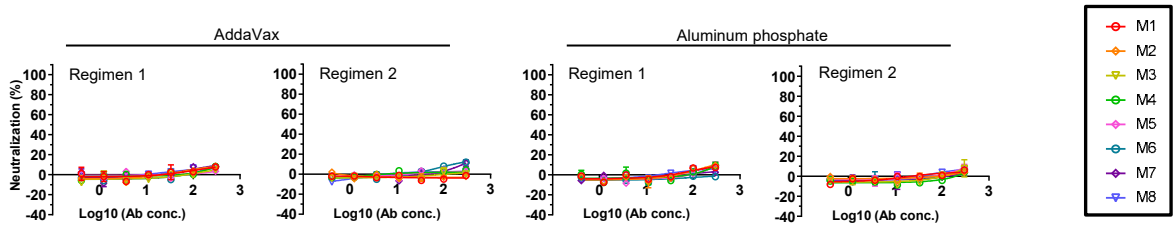

C **Week 11 mouse IgG neutralization against HIV-1 BG505.T332N. Immunization with glycan trimmed BG505 E2p SApNPs, with repeats.**

Vaccine	Adjuvant	Glycan trimming regimen	Repeat	IC_{50} titers (μg/ml)								
				M1	M2	M3	M4	M5	M6	M7	M8	
BG505 E2p SApNP	AddaVax	Regimen 1	1st	>300	>300	>300	>300	46	>300	>300	>300	★
		Regimen 2	1st	>300	>300	>300	>300	>300	>300	>300	70	★
	Aluminum phosphate	Regimen 1	1st	293	76	75	108	17	>300	16	>300	★
		Regimen 2	1st	28	194	11	>300	>300	27	>300	32	
			2nd	45	65	71	22	20	264	>300	220	
			3rd	>300	23	4	199	>300	42	8	>300	★

★ indicates samples from this group further tested against other HIV-1 viruses & MLV

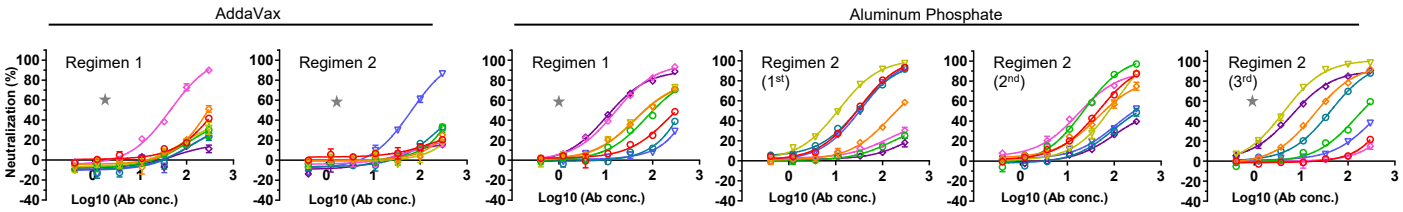

Week 11 mouse IgG neutralization against HIV-1 SF162. Immunization with glycan trimmed BG505 E2p SApNPs.

Vaccine	Adjuvant	Glycan trimming regimen	IC_{50} titers (μg/ml)							
			M1	M2	M3	M4	M5	M6	M7	M8
BG505 E2p SApNP	AddaVax	Regimen 1	5	3	6	6	22	35	121	3
		Regimen 2	37	9	65	13	46	3	6	3
	Aluminum phosphate	Regimen 1	7	25	14	12	6	24	39	12
		Regimen 2	8	1	4	29	6	8	18	3

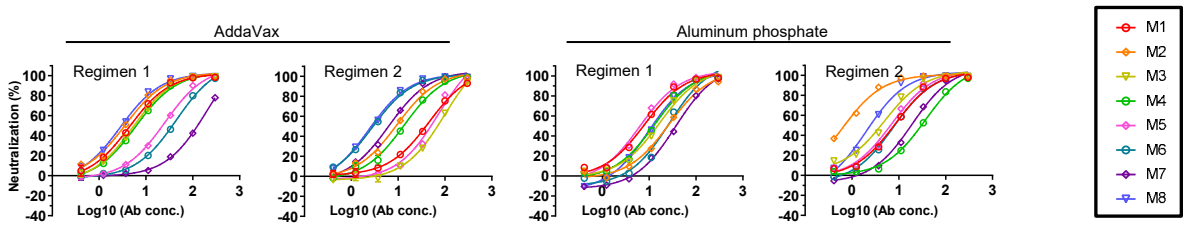

Week 11 mouse IgG neutralization against MLV (control). Immunization with glycan trimmed BG505 E2p SApNPs.

Vaccine	Adjuvant	Glycan trimming regimen	IC_{50} titers (μg/ml)							
			M1	M2	M3	M4	M5	M6	M7	M8
BG505 E2p SApNP	AddaVax	Regimen 1	>300	-	>300	>300	>300	>300	>300	>300
		Regimen 2	>300	>300	>300	>300	>300	>300	>300	>300
	Aluminum phosphate	Regimen 1	>300	>300	>300	>300	>300	>300	>300	>300
		Regimen 2	>300	>300	>300	>300	>300	>300	>300	>300

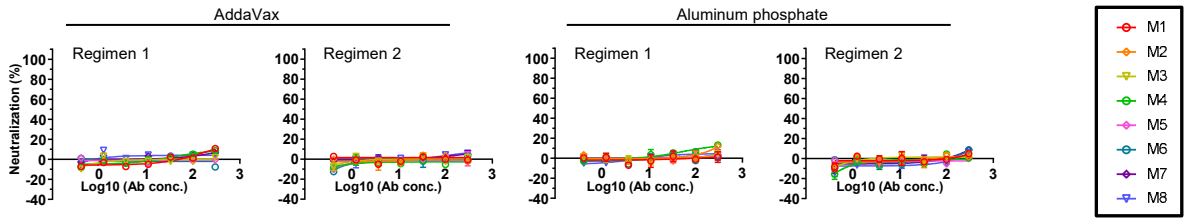

D **Week 11 mouse IgG neutralization against HIV-1 BG505.T332N. Immunization with glycan trimmed BG505 I3-01v9 SApNPs, with repeats.**

Vaccine	Adjuvant	Glycan trimming regimen	Repeat	IC_{50} titers (μg/ml)								
				M1	M2	M3	M4	M5	M6	M7	M8	
BG505 I3-01v9 SApNP	Aluminum phosphate	Regimen 1	1st	86	>300	275	>300	>300	No IgG	No IgG	48	★
			2nd	>300	>300	>300	>300	23	>300	>300	212	
			3rd	>300	>300	>300	>300	>300	26	>300	203	
		Regimen 2	1st	>300	17	85	37	39	>300	>300	>300	★
			2nd	59	>300	>300	>300	113	148	41	>300	
			3rd	109	>300	>300	>300	40	9	>300	>300	
			4th	>300	57	290	>300	16	>300	>300	14	

No IgG: indicates no IgG available to test ★ indicates samples from this group further tested against other HIV-1 viruses & MLV

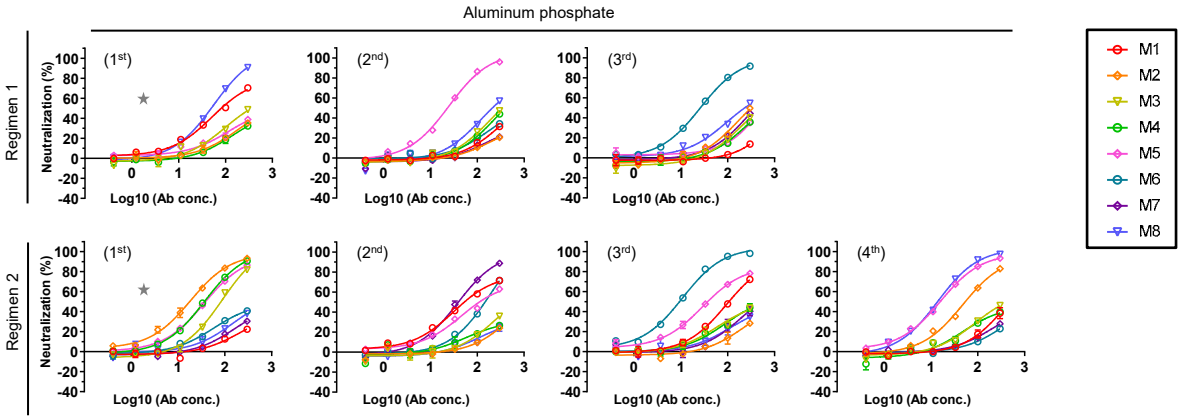

Week 11 mouse IgG neutralization against HIV-1 SF162. Immunization with glycan trimmed BG505 I3-01v9 SApNPs.

Vaccine	Adjuvant	Glycan trimming regimen	IC_{50} titers (μg/ml)							
			M1	M2	M3	M4	M5	M6	M7	M8
BG505 I3-01v9 SApNP	Aluminum phosphate	Regimen 1	11	15	5	125	7	No IgG	No IgG	8
		Regimen 2	2	16	3	12	8	12	11	11

No IgG: indicates no IgG available to test

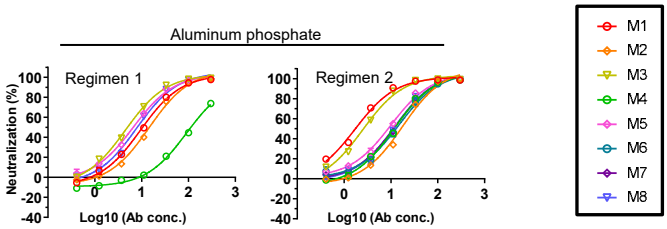

Week 11 mouse IgG neutralization against MLV (control). Immunization with glycan trimmed BG505 I3-01v9 SApNPs.

Vaccine	Adjuvant	Glycan trimming regimen	IC_{50} titers (μg/ml)							
			M1	M2	M3	M4	M5	M6	M7	M8
BG505 I3-01v9 SApNP	Aluminum phosphate	Regimen 1	>300	>300	>300	>300	>300	No IgG	No IgG	>300
		Regimen 2	>300	>300	>300	>300	>300	>300	>300	>300

No IgG: indicates no IgG available to test

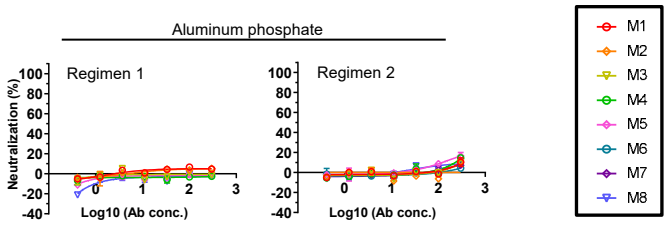

E **Week 11 mouse IgG neutralization IC_{50} titers against HIV-1 BG505.T332N and BG505.T332N.I396R mutant**

Vaccine	Adjuvant	Glycan trimming regimen	Animal ID	IC_{50} titers (μg/ml) BG505. T332N	IC_{50} titers (μg/ml) BG505. T332N. I396R
BG505 UFO trimer	Aluminum phosphate	Regimen 1	D-S24 G3-M1	17	>300
			D-S24 G3-M2	155	>300
			D-S24 G3-M4	44	172
			D-S24 G3-M5	2	>300
			D-S24 G3-M6	8	>300
			D-S24 G3-M7	158	>300
			D-S24 G3-M8	>300	>300
		Regimen 2	D-S24 G4-M1	118	>300
			D-S24 G4-M2	13	>300
			D-S24 G4-M3	5	>300
			D-S24 G4-M4	48	>300
			D-S24 G4-M5	10	>300
			D-S24 G4-M6	>300	>300
			D-S24 G4-M7	>300	>300
			D-S24 G4-M8	66	>300
BG505 E2p SApNP	AddaVax	Regimen 1	D-S21 G1-M2	>300	31
			D-S21 G1-M3	>300	>300
			D-S21 G1-M5	46	>300
		Regimen 2	D-S21 G2-M4	>300	>300
			D-S21 G2-M8	70	11

Vaccine	Adjuvant	Glycan trimming regimen	Animal ID	IC_{50} titers (μg/ml) BG505. T332N	IC_{50} titers (μg/ml) BG505. T332N. I396R
BG505 E2p SApNP	Aluminum phosphate	Regimen 1	D-S25 G1-M1	293	>300
			D-S25 G1-M2	76	87
			D-S25 G1-M3	75	22
			D-S25 G1-M4	108	89
			D-S25 G1-M5	17	46
			D-S25 G1-M6	>300	>300
			D-S25 G1-M7	16	>300
		Regimen 2	D-S25 G2-M2	23	31
			D-S25 G2-M3	4	202
			D-S25 G2-M4	199	180
			D-S25 G2-M6	42	27
			D-S25 G2-M7	8	>300
			D-S25 G2-M8	>300	>300
BG505 I3-01v9 SApNP	Aluminum phosphate	Regimen 1	D-S21 G3-M1	86	154
			D-S21 G3-M3	275	>300
			D-S21 G3-M8	48	>300
		Regimen 2	D-S21 G4-M2	17	6
			D-S21 G4-M3	85	23
			D-S21 G4-M4	37	17
			D-S21 G4-M5	39	277

Week 11 mouse IgG neutralization against HIV-1 BG505.T332N and BG505.T332N.I396R mutant

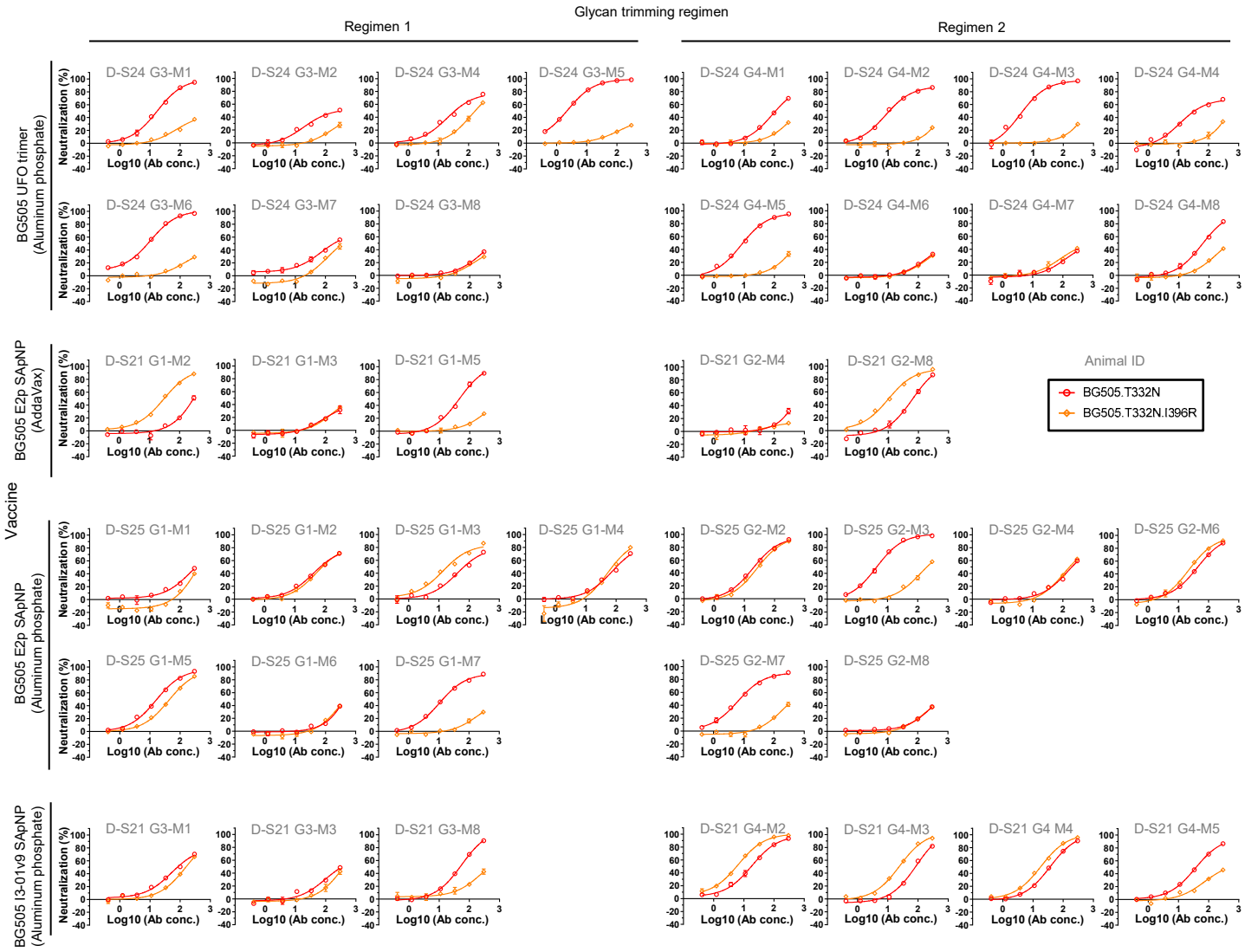

F **Week 11 mouse IgG neutralization IC_{50} and IC_{30} titers against HIV-1 12 virus global panel, BG505.T332N, SF162 & MLV (control)**

Vaccine	Adjuvant	Glycan trimming regimen	Animal ID	IC_{50} titers (µg/ml) for each virus (clade)														
				TRO11 (B)	25710 (C)	398F1 (A)	CNE8 (AE)	X2278 (B)	BJOX-2000 (BC)	X1632 (G)	CE1176 (C)	246F3 (AC)	CH119 (BC)	CE0217 (C)	CNE55 (AE)	BG505. T332N (A)	SF162 (B)	MLV (control)
BG505 E2p SApNP	AddaVax	Regimen 1	D-S21 G1-M2	-	>300	-	>300	-	>300	-	-	>300	>300	-	-	>300	3	-
			D-S21 G1-M3	>300	>300	275	151	263	>300	>300	217	>300	>300	>300	>300	>300	6	-
			D-S21 G1-M5	>300	300	225	195	-	>300	>300	>300	>300	>300	>300	-	46	22	>300
		Regimen 2	D-S21 G2-M4	>300	-	>300	-	>300	-	>300	>300	-	-	>300	>300	>300	13	>300
			D-S21 G2-M8	>300	>300	>300	>300	-	>300	>300	>300	>300	>300	>300	-	70	3	>300
BG505 I3-01v9 SApNP	Aluminum phosphate	Regimen 1	D-S21 G3-M1	>300	>300	298	>300	>300	>300	>300	>300	>300	>300	>300	>300	86	11	>300
			D-S21 G3-M3	>300	>300	>300	>300	>300	>300	>300	>300	>300	>300	>300	>300	275	5	>300
			D-S21 G3-M8	>300	>300	>300	224	>300	>300	>300	>300	>300	>300	>300	>300	48	8	>300
		Regimen 2	D-S21 G4-M2	>300	>300	291	>300	>300	>300	>300	>300	>300	>300	>300	>300	17	16	>300
			D-S21 G4-M3	>300	>300	236	236	>300	>300	>300	>300	>300	>300	>300	>300	85	3	>300
			D-S21 G4-M4	>300	>300	>300	>300	>300	>300	>300	>300	>300	>300	>300	-	37	12	>300
			D-S21 G4-M5	>300	267	284	>300	>300	>300	>300	>300	>300	>300	>300	>300	39	8	>300

Vaccine	Adjuvant	Glycan trimming regimen	Animal ID	IC_{30} titers (µg/ml) for each virus (clade)														
				TRO11 (B)	25710 (C)	398F1 (A)	CNE8 (AE)	X2278 (B)	BJOX-2000 (BC)	X1632 (G)	CE1176 (C)	246F3 (AC)	CH119 (BC)	CE0217 (C)	CNE55 (AE)	BG505. T332N (A)	SF162 (B)	MLV (control)
BG505 E2p SApNP	AddaVax	Regimen 1	D-S21 G1-M2	-	>300	-	138	-	240	-	-	>300	>300	-	-	143	1	-
			D-S21 G1-M3	225	149	118	65	113	>300	281	93	206	275	>300	>300	249	2	-
			D-S21 G1-M5	>300	129	97	84	-	166	208	168	277	277	>300	-	20	9	>300
		Regimen 2	D-S21 G2-M4	>300	-	173	-	>300	-	>300	>300	-	-	>300	>300	>300	5	>300
			D-S21 G2-M8	>300	>300	209	182	-	>300	225	>300	>300	>300	>300	-	30	1	>300
BG505 I3-01v9 SApNP	Aluminum phosphate	Regimen 1	D-S21 G3-M1	>300	192	128	>300	162	>300	>300	144	268	>300	>300	>300	37	5	>300
			D-S21 G3-M3	>300	153	190	129	>300	>300	204	178	256	>300	>300	>300	118	2	>300
			D-S21 G3-M8	266	137	160	96	>300	286	253	187	254	>300	>300	>300	21	3	>300
		Regimen 2	D-S21 G4-M2	292	176	125	>300	274	>300	>300	208	>300	>300	>300	>300	7	7	>300
			D-S21 G4-M3	256	130	101	101	284	175	145	164	188	208	>300	>300	37	1	>300
			D-S21 G4-M4	>300	143	151	153	>300	213	>300	215	281	>300	>300	-	16	5	>300
			D-S21 G4-M5	>300	267	284	>300	>300	>300	>300	>300	>300	>300	>300	>300	39	4	>300

Week 11 mouse IgG neutralization against HIV-1 12 virus global panel

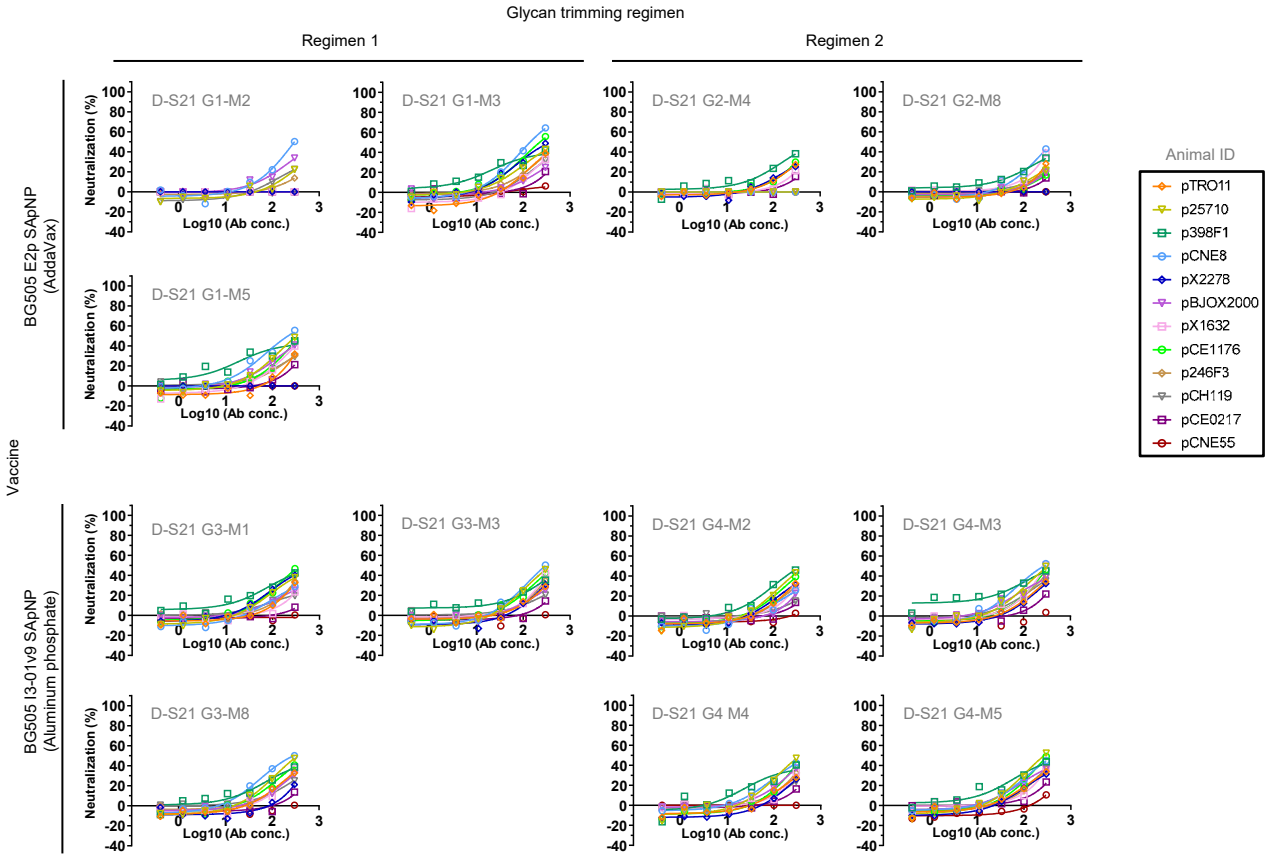

G **Week 0 rabbit IgG neutralization against HIV-1 BG505.T332N**

Vaccine	Adjuvant	Glycan trimming regimen	IC_{50} titers (µg/ml)					
			R1	R2	R3	R4	R5	R6
BG505 E2p SApNP	AddaVax	Regimen 1	>300	>300	>300	>300	>300	>300
		Regimen 2	>300	>300	>300	>300	>300	>300
BG505 I3-01v9 SApNP	Aluminum phosphate	Regimen 1	>300	>300	>300	>300	>300	>300
		Regimen 2	>300	>300	>300	>300	>300	>300

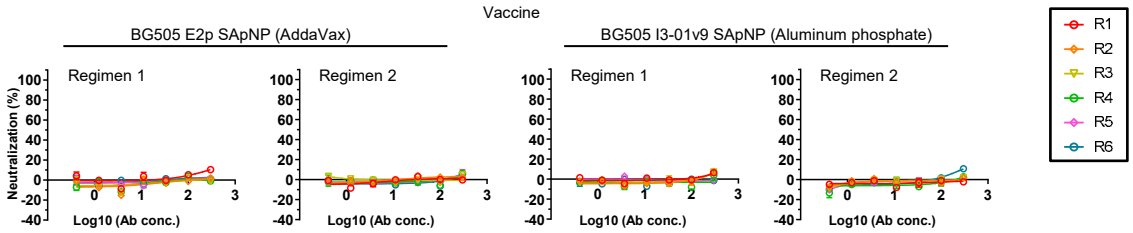

Week 0 rabbit IgG neutralization against HIV-1 SF162

Vaccine	Adjuvant	Glycan trimming regimen	IC_{50} titers (µg/ml)					
			R1	R2	R3	R4	R5	R6
BG505 E2p SApNP	AddaVax	Regimen 1	>300	>300	>300	>300	>300	>300
		Regimen 2	>300	>300	>300	>300	>300	>300
BG505 I3-01v9 SApNP	Aluminum phosphate	Regimen 1	>300	>300	>300	>300	>300	>300
		Regimen 2	>300	>300	>300	>300	>300	>300

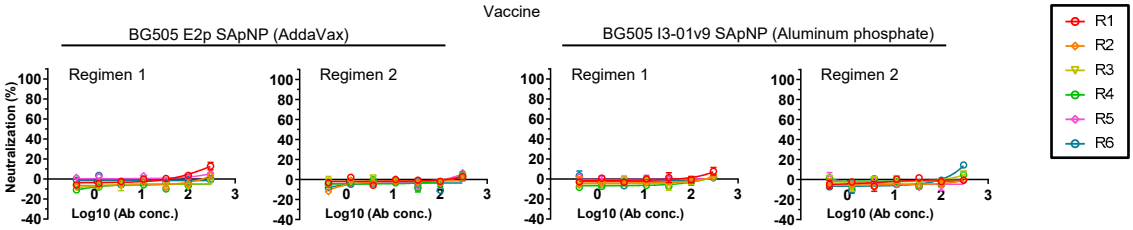

Week 0 rabbit IgG neutralization against MLV (control)

Vaccine	Adjuvant	Glycan trimming regimen	IC_{50} titers (µg/ml)					
			R1	R2	R3	R4	R5	R6
BG505 E2p SApNP	AddaVax	Regimen 1	>300	>300	>300	>300	>300	>300
		Regimen 2	>300	>300	>300	>300	>300	>300
BG505 I3-01v9 SApNP	Aluminum phosphate	Regimen 1	>300	>300	>300	>300	>300	>300
		Regimen 2	>300	>300	>300	>300	>300	>300

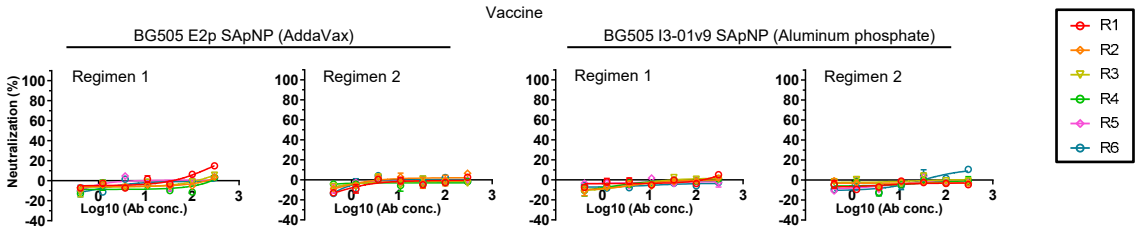

H **Week 11 rabbit IgG neutralization against HIV-1 BG505.T332N**

Vaccine	Adjuvant	Glycan trimming regimen	IC_{50} titers (µg/ml)					
			R1	R2	R3	R4	R5	R6
BG505 E2p SApNP	AddaVax	Regimen 1	>300	39	>300	>300	>300	272
		Regimen 2	233	>300	>300	>300	>300	>300
BG505 I3-01v9 SApNP	Aluminum phosphate	Regimen 1	>300	36	193	79	>300	>300
		Regimen 2	>300	93	>300	44	167	23

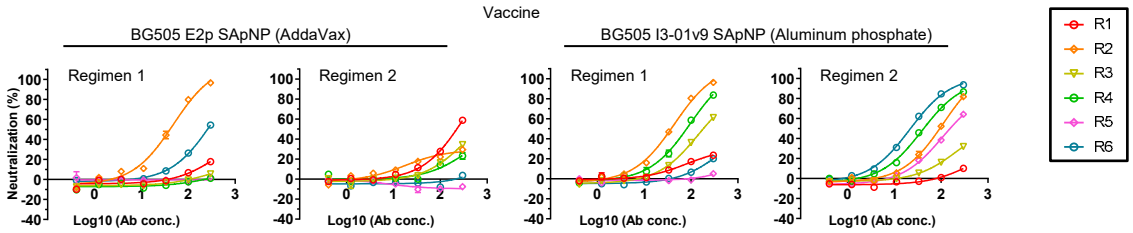

Week 11 rabbit IgG neutralization against HIV-1 SF162

Vaccine	Adjuvant	Glycan trimming regimen	IC_{50} titers (µg/ml)					
			R1	R2	R3	R4	R5	R6
BG505 E2p SApNP	AddaVax	Regimen 1	10	18	11	22	48	4
		Regimen 2	18	5	3	15	8	26
BG505 I3-01v9 SApNP	Aluminum phosphate	Regimen 1	3	4	4	22	41	9
		Regimen 2	2	6	6	4	2	11

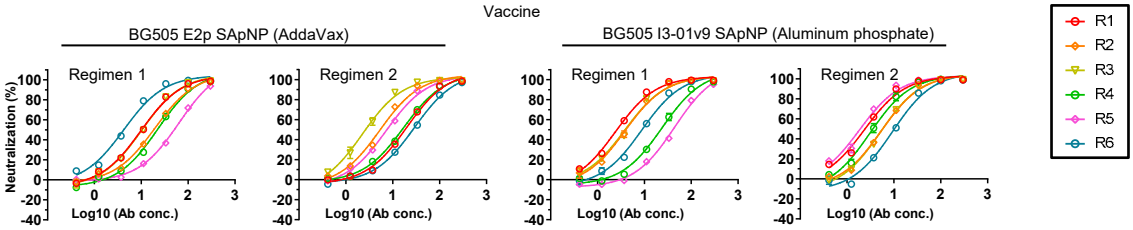

Week 11 rabbit IgG neutralization against MLV (control)

Vaccine	Adjuvant	Glycan trimming regimen	IC_{50} titers (µg/ml)					
			R1	R2	R3	R4	R5	R6
BG505 E2p SApNP	AddaVax	Regimen 1	>300	>300	>300	>300	>300	>300
		Regimen 2	>300	>300	>300	>300	>300	>300
BG505 I3-01v9 SApNP	Aluminum phosphate	Regimen 1	>300	>300	>300	>300	>300	>300
		Regimen 2	>300	>300	>300	>300	291	>300

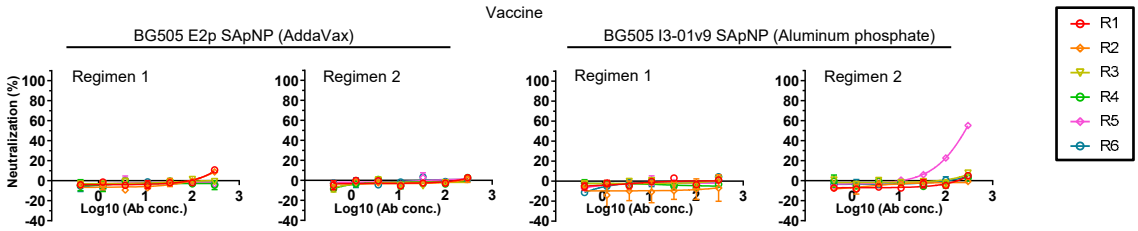

Week 11 rabbit IgG neutralization IC_{50} titers against BG505.T332N and glycan hole mutant viruses

Vaccine	Adjuvant	Glycan trimming regimen	Animal ID	IC_{50} values (µg/ml)				
				BG505.T332N	BG505.T332N.Q130N	BG505.T332N.S241N	BG505.T332N.P291T	BG505.T332N.T465N
BG505 E2p SApNP	AddaVax	Regimen 1	G1-2	39	31	15	29	>300
			G1-6	272	>300	>300	>300	231
		Regimen 2	G2-1	233	174	85	138	>300
			G2-3	>300	>300	>300	>300	>300
BG505 I3-01v9 SApNP	Aluminum phosphate	Regimen 1	G3-2	36	26	17	20	>300
			G3-3	193	227	>300	>300	186
			G3-4	79	60	31	52	>300
		Regimen 2	G4-2	93	73	25	59	169
			G4-3	>300	>300	74	214	211
			G4-4	44	29	12	33	>300
			G4-5	167	112	119	157	>300
			G4-6	23	14	8	12	18

Week 11 rabbit IgG neutralization against BG505.T332N and glycan hole mutant viruses

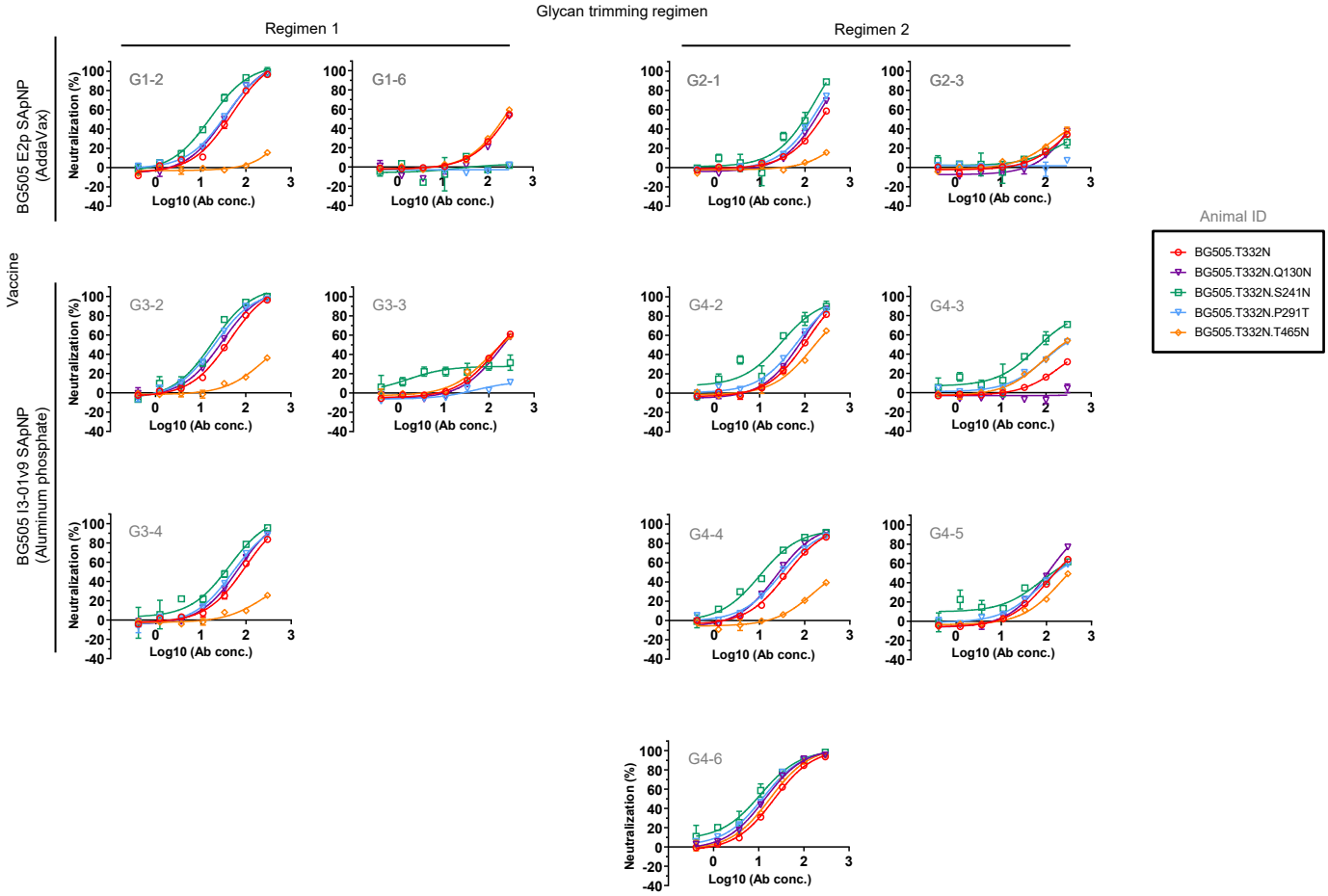

J **Week 11 rabbit IgG neutralization IC_{50} and IC_{30} titers against HIV-1 12 virus panel, BG505.T332N, SF162 & MLV pSG3**

Vaccine	Adjuvant	Glycan trimming regimen	Animal ID	IC_{50} titers (µg/ml) for each virus (clade)														
				TRO11 (B)	25710 (C)	398F1 (A)	CNE8 (AE)	X2278 (B)	BJOX-2000 (BC)	X1632 (G)	CE1176 (C)	246F3 (AC)	CH119 (BC)	CE0217 (C)	CNE55 (AE)	BG505.T332N (A)	SF162 (B)	MLV (control)
BG505 E2p SApNP	AddaVax	Regimen 1	G1-2	>300	>300	>300	>300	>300	>300	>300	>300	>300	>300	>300	>300	39	18	>300
			G1-6	>300	>300	>300	>300	>300	>300	>300	>300	>300	>300	>300	>300	272	4	>300
		Regimen 2	G2-1	>300	>300	>300	>300	>300	>300	>300	>300	>300	>300	>300	>300	233	18	>300
			G2-3	>300	279	>300	240	>300	>300	>300	>300	>300	>300	>300	>300	>300	3	>300
BG505 I3-01v9 SApNP	Aluminum phosphate	Regimen 1	G3-2	>300	>300	>300	>300	>300	>300	>300	>300	>300	>300	>300	>300	36	4	>300
			G3-3	>300	>300	>300	277	>300	>300	>300	>300	>300	>300	>300	>300	193	4	>300
			G3-4	>300	>300	>300	>300	>300	>300	>300	>300	>300	>300	>300	>300	79	22	>300
		Regimen 2	G4-2	>300	>300	>300	>300	>300	>300	>300	>300	>300	>300	>300	>300	93	6	>300
			G4-3	>300	>300	>300	>300	>300	>300	>300	>300	>300	>300	>300	>300	>300	6	>300
			G4-4	>300	>300	>300	>300	>300	>300	>300	>300	>300	>300	>300	>300	44	4	>300
			G4-5	>300	201	198	134	>300	156	210	177	239	218	>300	>300	167	2	291
			G4-6	>300	>300	>300	>300	>300	>300	>300	>300	>300	>300	>300	>300	23	11	>300

Vaccine	Adjuvant	Glycan trimming regimen	Animal ID	IC_{30} titers (µg/ml) for each virus (clade)														
				TRO11 (B)	25710 (C)	398F1 (A)	CNE8 (AE)	X2278 (B)	BJOX-2000 (BC)	X1632 (G)	CE1176 (C)	246F3 (AC)	CH119 (BC)	CE0217 (C)	CNE55 (AE)	BG505.T332N (A)	SF162 (B)	MLV (control)
BG505 E2p SApNP	AddaVax	Regimen 1	G1-2	>300	>300	>300	>300	>300	>300	>300	>300	>300	>300	>300	>300	17	8	>300
			G1-6	>300	272	>300	>300	>300	>300	>300	>300	>300	>300	>300	>300	116	2	>300
		Regimen 2	G2-1	>300	>300	>300	>300	>300	>300	>300	>300	>300	>300	>300	>300	100	8	>300
			G2-3	>300	120	278	103	>300	260	>300	>300	>300	>300	>300	>300	243	1	>300
BG505 I3-01v9 SApNP	Aluminum phosphate	Regimen 1	G3-2	>300	263	>300	251	>300	>300	>300	>300	>300	>300	>300	>300	16	2	>300
			G3-3	>300	132	253	119	>300	>300	>300	>300	>300	>300	>300	>300	83	2	>300
			G3-4	>300	183	233	196	>300	>300	>300	>300	>300	>300	>300	>300	34	9	>300
		Regimen 2	G4-2	>300	220	>300	203	>300	>300	>300	>300	>300	>300	>300	>300	40	3	>300
			G4-3	>300	162	195	166	>300	>300	>300	>300	>300	>300	>300	>300	262	3	>300
			G4-4	>300	166	144	134	>300	257	>300	>300	>300	>300	>300	>300	19	2	>300
			G4-5	148	86	85	58	192	67	90	76	103	94	158	182	71	1	125
			G4-6	>300	160	198	174	>300	>300	>300	>300	>300	>300	>300	>300	10	5	>300

Week 11 rabbit IgG neutralization against HIV-1 12 virus panel, BG505.T332N, SF162 & MLV pSG3

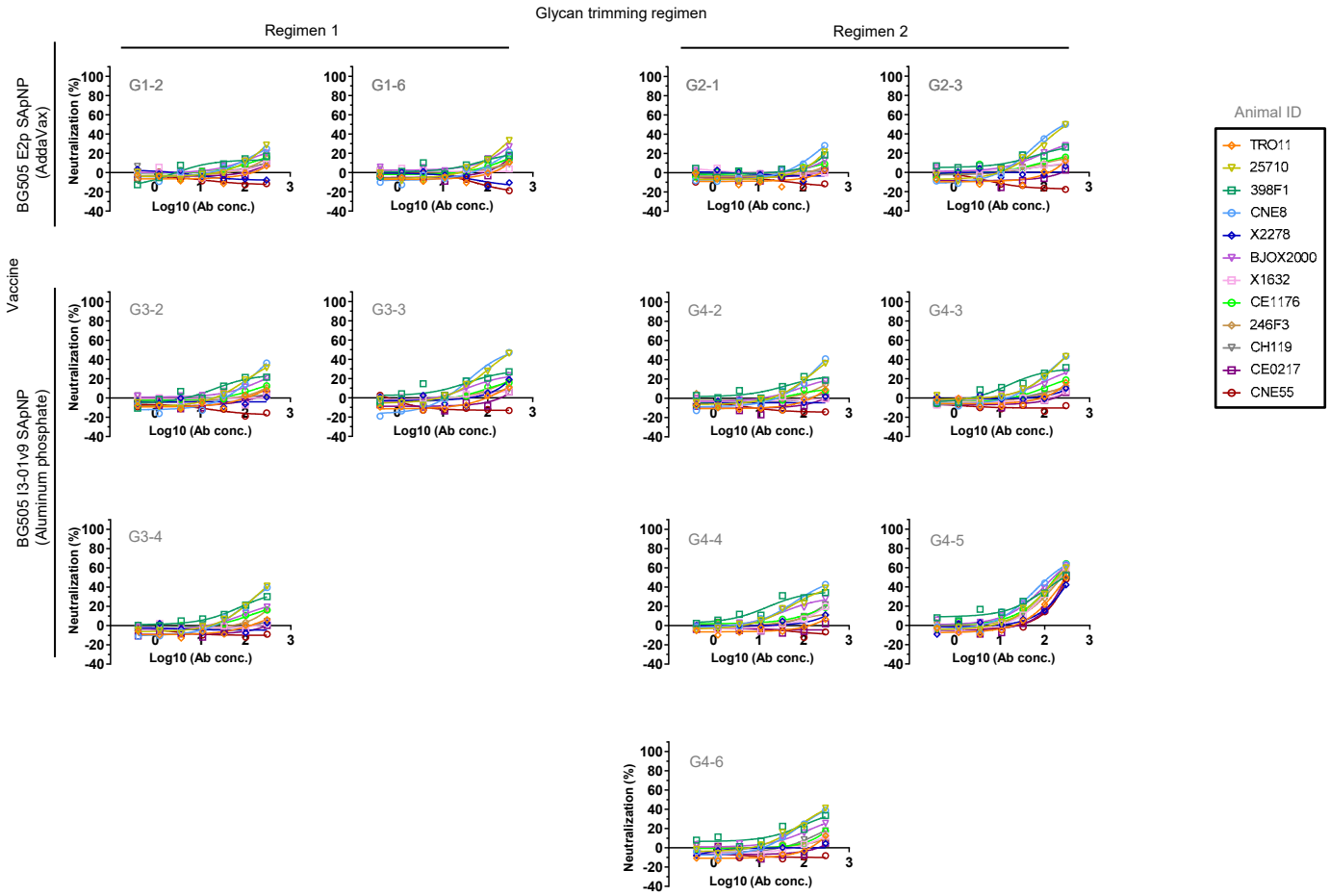

fig. S6. Neutralization data from the evaluation of Env immunogens with trimmed glycans. (**A**) Negative stain EM analysis to assess the structural integrity of SApNPs produced from 8 and 5 CHO-K1 cell clones that stably express E2p and I3-01v9 SApNPs, respectively. (**B**)-(**F**) Neutralization of purified IgG at week 11 from the mouse study. Groups of eight mice were immunized with BG505 Env immunogens mixed with AddaVax or aluminum phosphate adjuvants at weeks 0, 3, 6 and 9. Two glycan trimming regimens were tested: regimen 1 administers four doses of glycan-trimmed immunogens, whereas regimen 2 administers two doses of glycan-trimmed immunogens as prime and two doses of wildtype immunogens as boost. Immunization was repeated for some formulation/regimen groups to confirm the findings and are labeled in the summary. (**B**)-(**D**) Neutralization of week 11 IgG from mice immunized with (**B**) the BG505 UFO trimer and (**C**) UFO trimer-presenting SApNPs E2p and (**D**) I3-01v9 against autologous tier 2 clade A BG505.T332N, tier 1 clade B SF162, and MLV as a negative control. No IgG was available for one mouse in the UFO trimer/AP regimen 1 group and for two mice in the I3-01v9/AP regimen 1 (1st repeat) group, as the mice died during the immunization study. Of note, IgG samples from the two groups that tested trimer/AP and four groups that tested E2p/AV and I3-01v9/AP in regimens 1 and 2 were selected for further analyses in (E) or (E-F) respectively, which are shown below. (**E**) Neutralization of week 11 IgG from select mice (more than 30% autologous neutralization) in the abovementioned six mouse groups against a BG505.T332N variant with the C3/V4 knockout mutation (I396R). IC_{50} titers and neutralization curves are shown, with BG505.T332N data from (B-D) included for comparison. (**F**) Neutralization of week 11 IgG from the four abovementioned SApNP groups against a 12-virus global panel. IC_{50} and IC_{30} titers were calculated and are listed in two tables. For all the TZM-bl neutralization assays performed in (B)-(F), a starting IgG concentration of 300 µg/ml and a 3-times dilution series were used. Each IgG sample was run in duplicate in (B)-(D) except for some mice in the MLV assays and all mice in the 12-virus assays in (F). Of note, mice for which IgG samples were no longer available at the time of the MLV or 12-virus assays are marked '-' in the IC_{50}/IC_{30} titer tables. (**G**)-(**J**) Neutralization of purified IgG from the rabbit study. Four groups of rabbits (6 per group) were immunized to test the E2p/AV and I3-01v9/AP formulations for glycan trimming regimens 1 and 2, using a similar protocol to the mouse study. (**G**) Neutralization of week 0 rabbit IgG against BG505.T332N, SF162, and MLV. (**H**) Neutralization of week 11 rabbit IgG against BG505.T332N, SF162, and MLV. It should be noted that R5 IgG from the I3-01v9/AP regimen 2 group showed MLV neutralization and might contain non-specific antibodies. (**I**) Neutralization of select week 11 rabbit IgG (more than 30% autologous neutralization) against four BG505.T332N glycan hole mutant viruses. (**J**) Neutralization of select week 11 rabbit IgG (more than 30% autologous neutralization) against a 12-virus global panel. IC_{50} and IC_{30} titers were calculated and are listed in two tables with neutralization curves shown for each IgG sample against all 12 viruses. For all the TZM-bl neutralization assays performed in (G)-(J), a starting IgG concentration of 300 µg/ml and a 3-times dilution series were used. Each IgG sample was run in duplicate in (G-I) but in singlet in (J) due to the limited sample availability.

fig. S7

A **Naïve mouse**

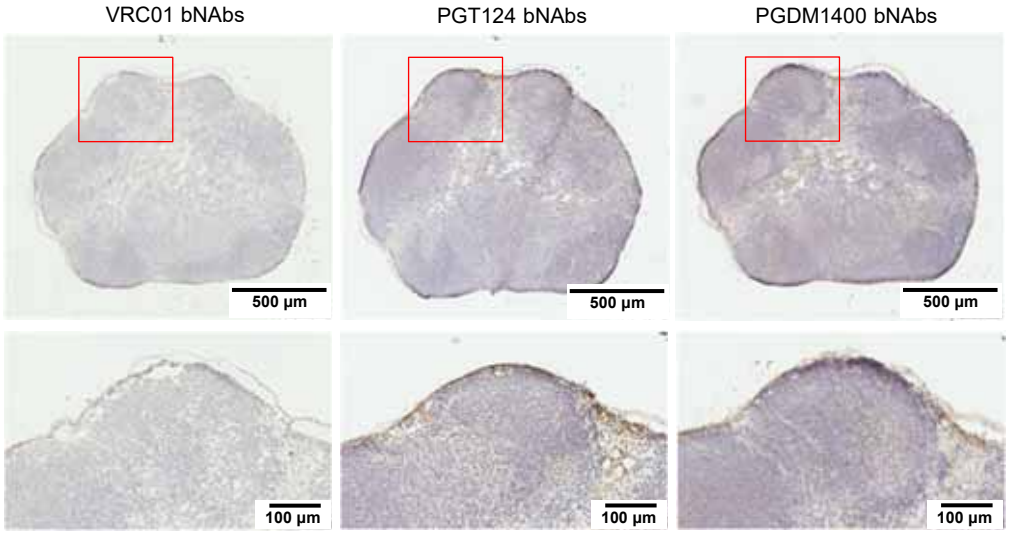

B

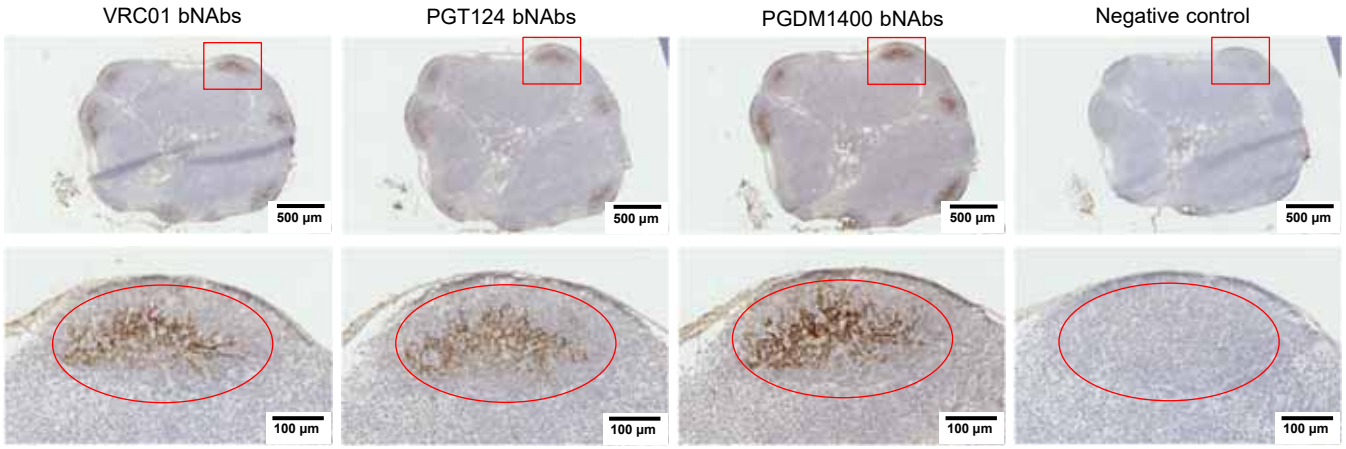

C **Single-dose - 30 minutes**

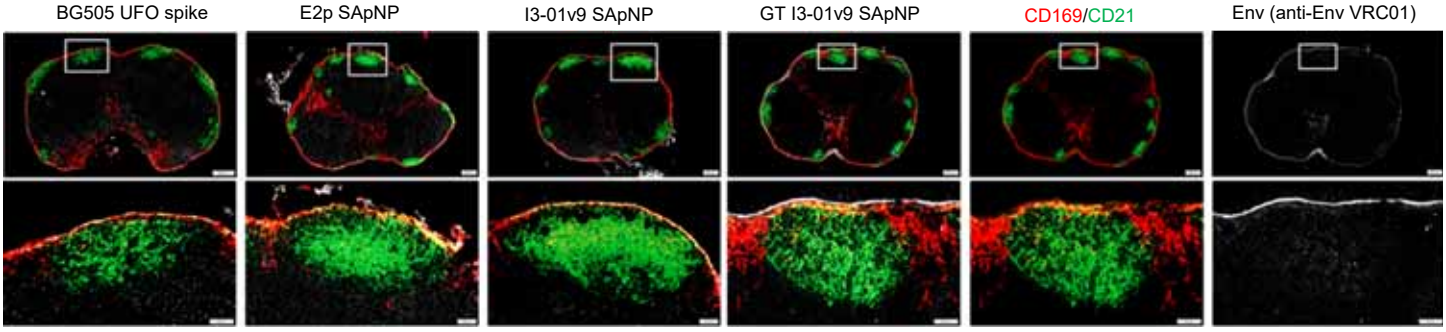

D **Single-dose - 2 hours**

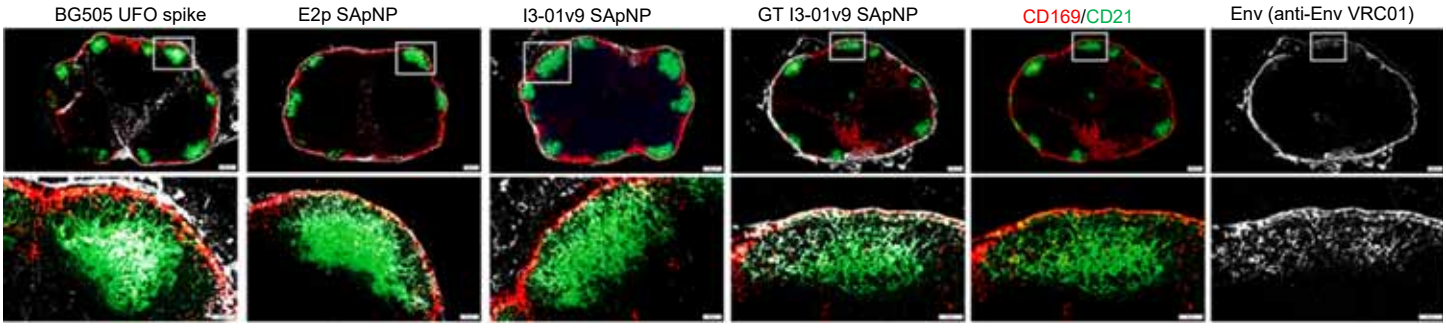

fig. S7

E **Single-dose - 12 hours**

BG505 UFO spike | E2p SApNP | I3-01v9 SApNP | GT I3-01v9 SApNP | CD169/CD21 | Env (anti-Env VRC01)

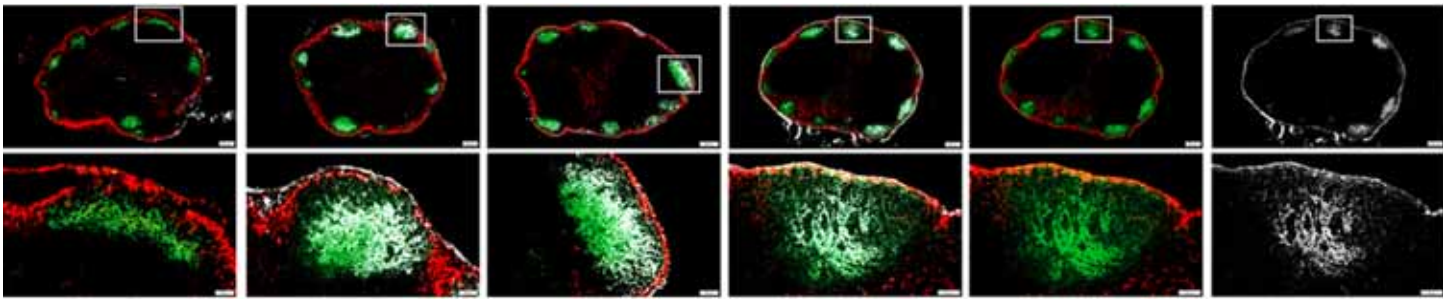

F **Single-dose - 1 week**

BG505 UFO spike | E2p SApNP | I3-01v9 SApNP | GT I3-01v9 SApNP | CD169/CD21 | Env (anti-Env VRC01)

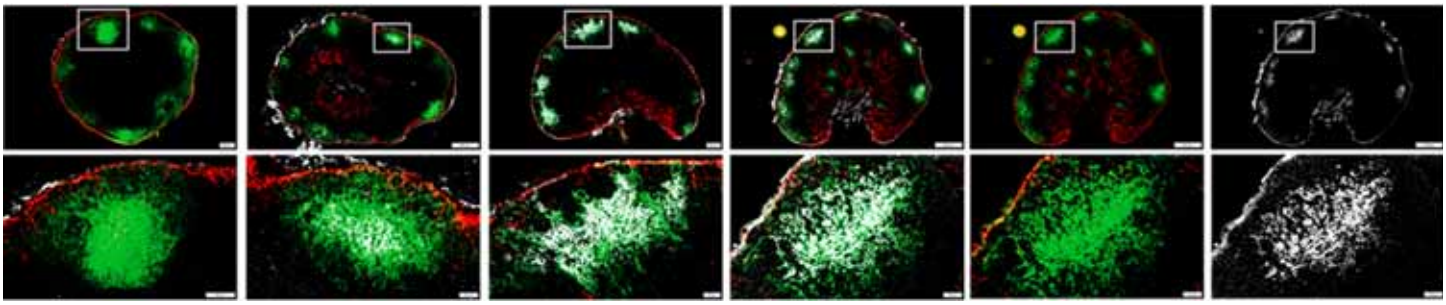

G **Single-dose - 2 weeks**

BG505 UFO spike | E2p SApNP | I3-01v9 SApNP | GT I3-01v9 SApNP | CD169/CD21 | Env (anti-Env VRC01)

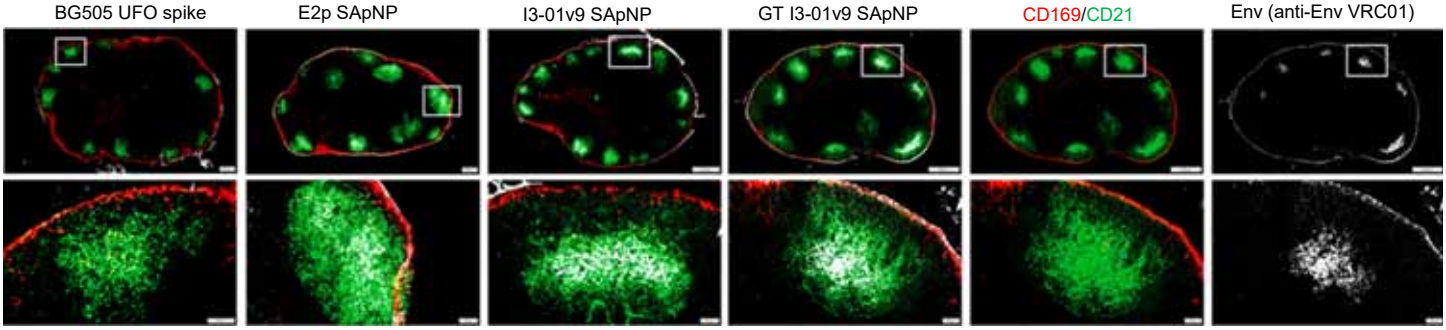

H **Single-dose - 5 weeks**

BG505 UFO spike | E2p SApNP | I3-01v9 SApNP | GT I3-01v9 SApNP | CD169/CD21 | Env (anti-Env VRC01)

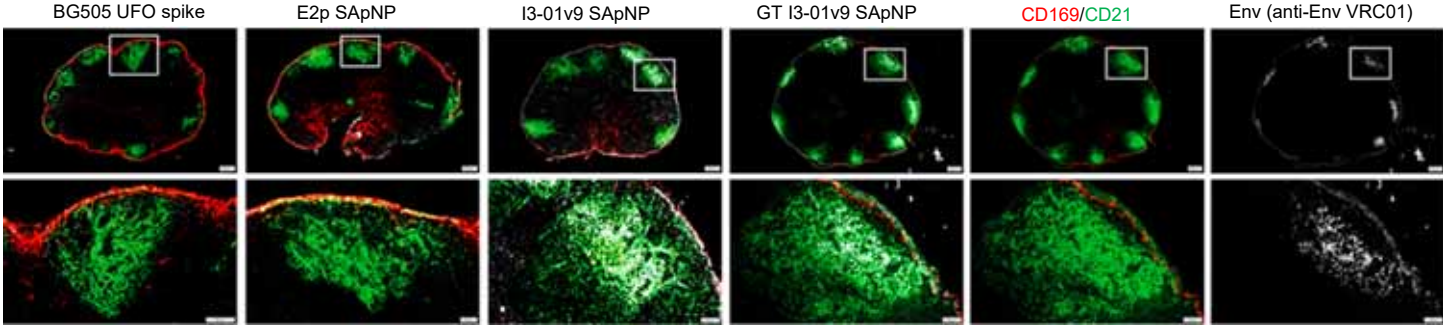

I **Single-dose - 8 weeks**

BG505 UFO spike | E2p SApNP | I3-01v9 SApNP | GT I3-01v9 SApNP | CD169/CD21 | Env (anti-Env VRC01)

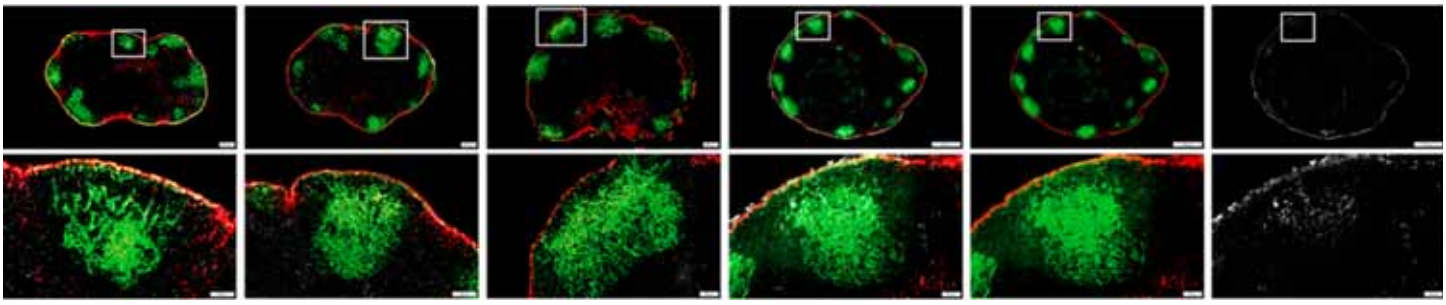

fig. S7. Immunohistological images of BG505 UFO trimer and SApNPs in lymph nodes. Immunostaining images of lymph node tissues from (**A**) naïve and (**B**) BG505 UFO-presenting SApNP injected mice stained with three anti-trimer antibody VRC01, PGT124 and PGDM1400. HIV-1 vaccine constructs of BG505 UFO trimer and BG505 UFO trimer-presenting E2p, I3-01v9, and GT I3-01v9 SApNPs interaction with FDC networks in lymph node follicles (**C**) 30 minutes, (**D**) 2 hours, (**E**) 12 hours, (**F**) 1 week, (**G**) 2 weeks, (**H**) 5 weeks, and (**I**) 8 weeks after a single-dose injection (10 μg per injection, totaling 40 μg per mouse). Immunofluorescent images are pseudo color coded (CD21+, green; CD169+, red; anti-Env VRC01, White), with a complete lymph node and an enlarged image of a follicle.

fig. S8

A E2p SApNPs (yellow arrow) and AddaVax (green arrow) are aligned on FDC dendrites after 2 hours of injection

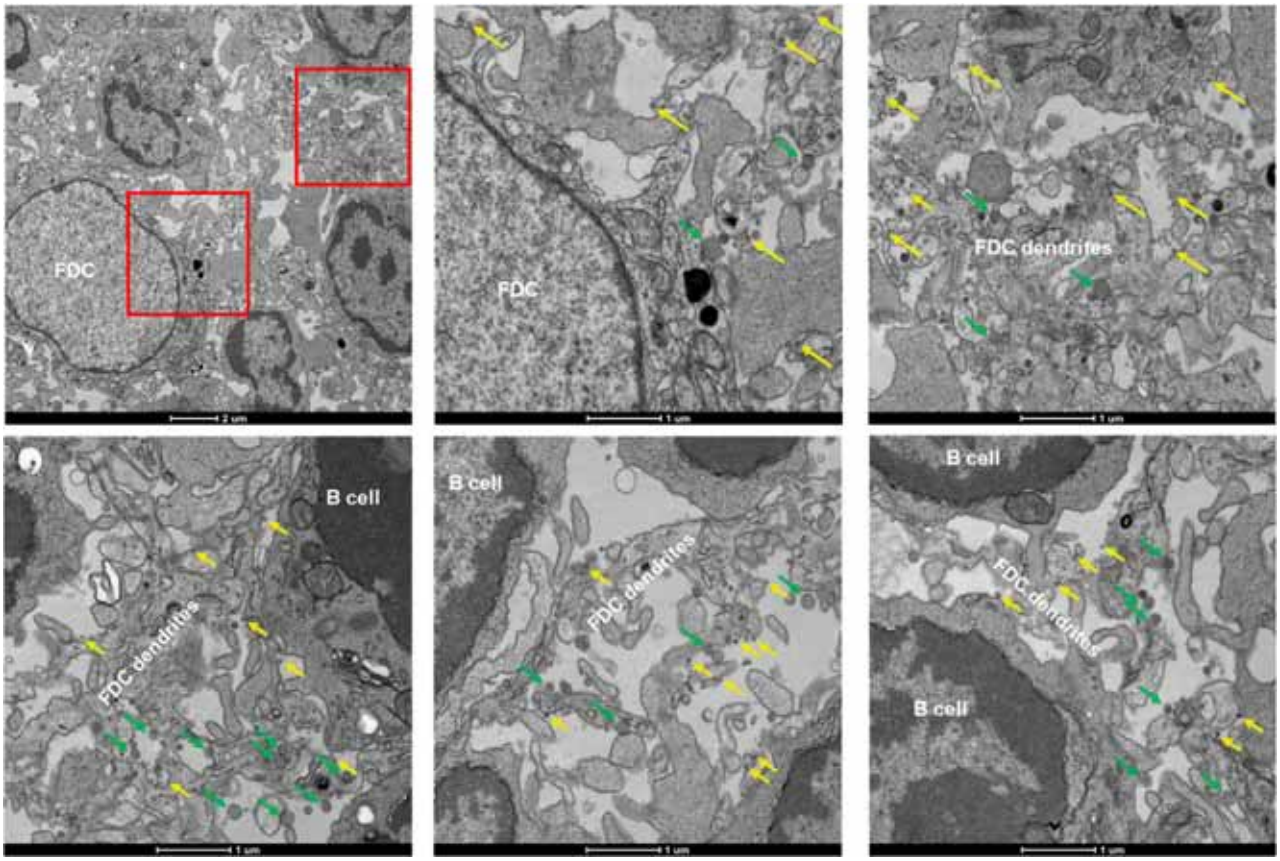

B E2p SApNPs (yellow arrow) and AddaVax (green arrow) are aligned on FDC dendrites after 12 hours of injection

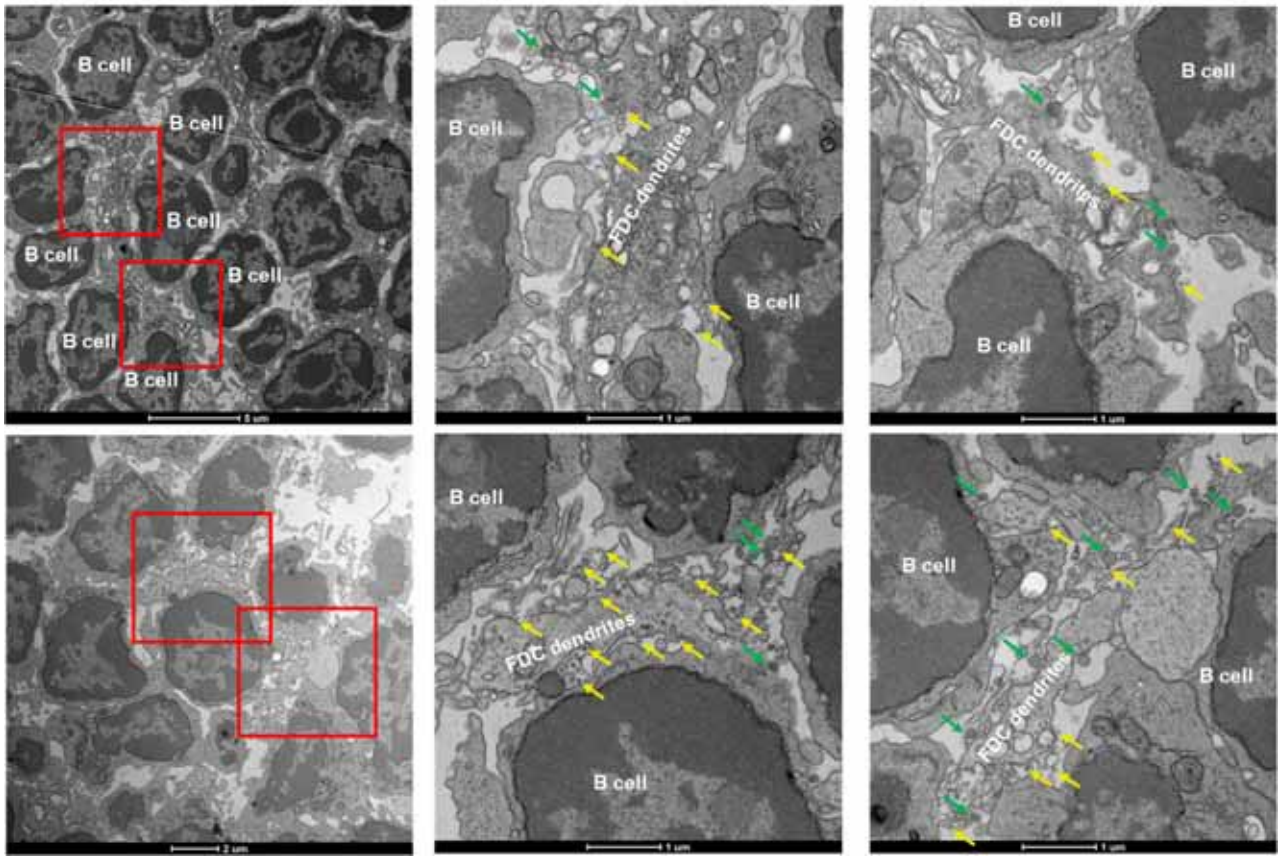

fig. S8

C E2p SApNPs (yellow arrow) are aligned on FDC dendrites or taken up by B cells after 48 hours of injection

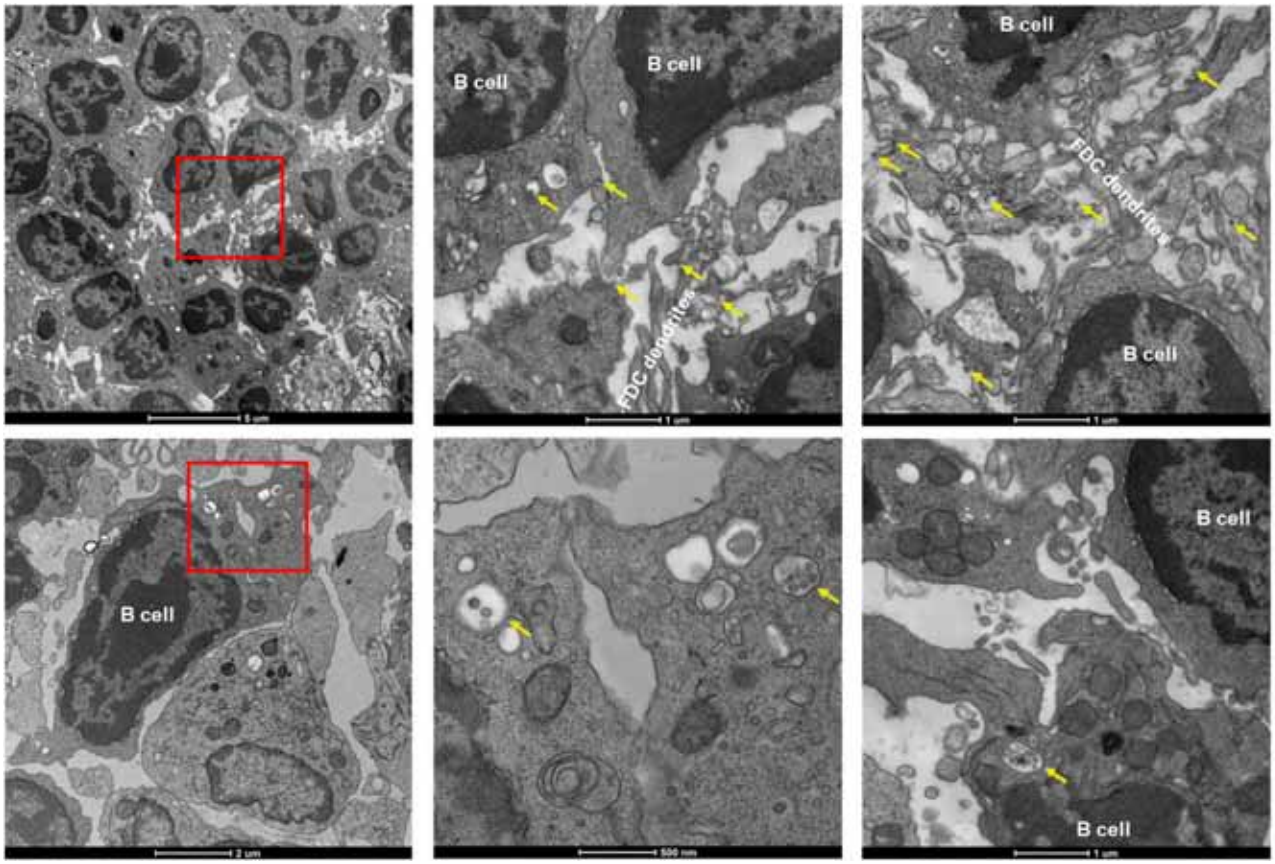

D I3-01v9 SApNPs (yellow arrow) are aligned on FDC dendrites after 2 hours of injection

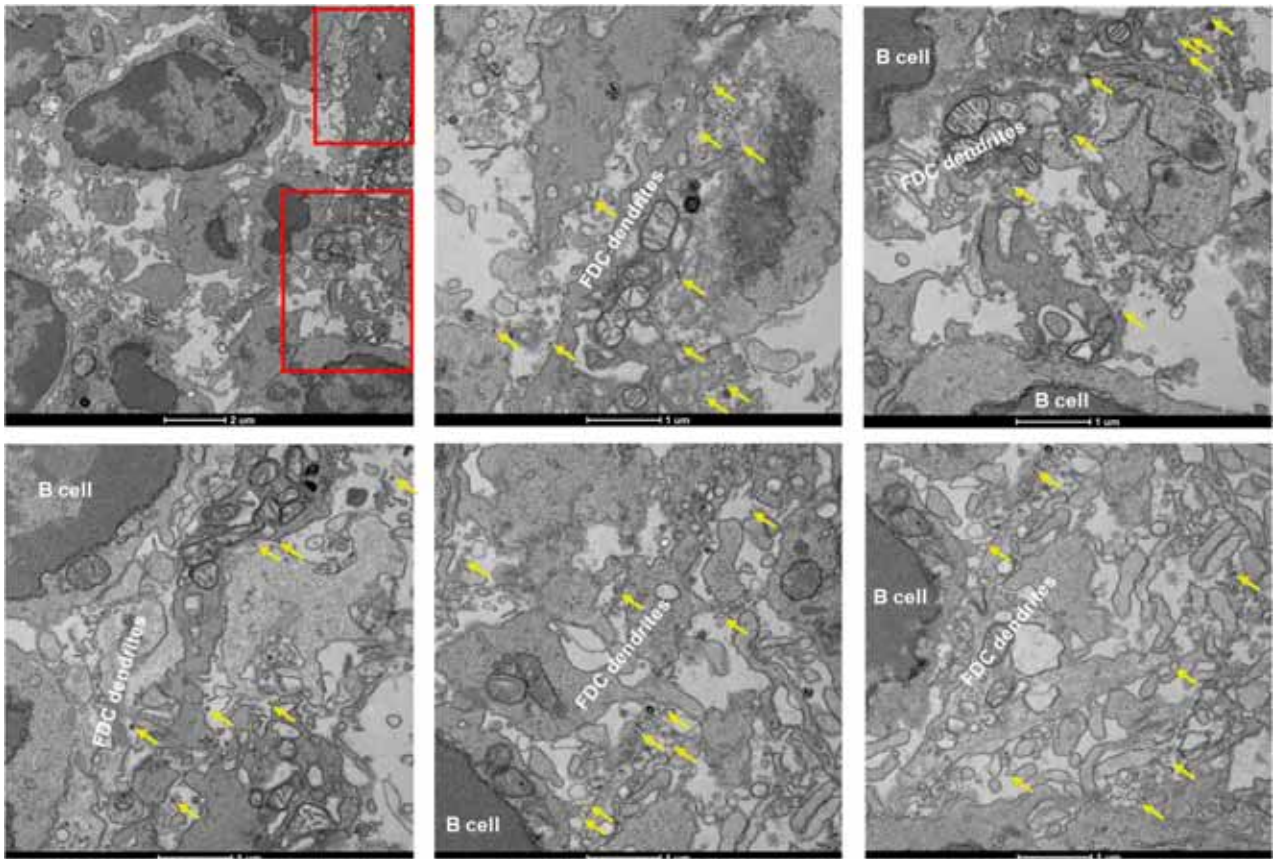

fig. S8

E I3-01v9 SApNPs (yellow arrow) are aligned on FDC dendrites after 12 hours of injection

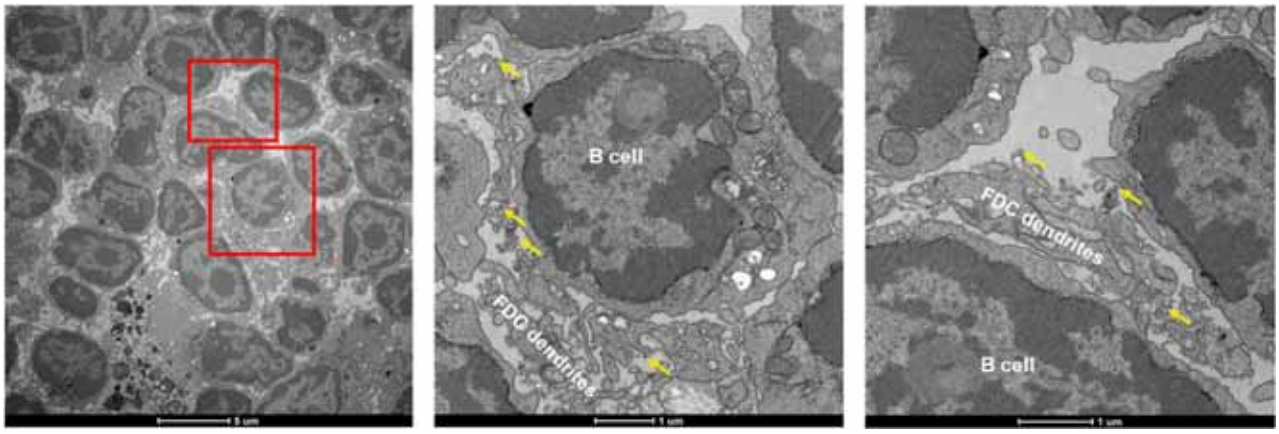

F I3-01v9 SApNPs (yellow arrow) are aligned on FDC dendrites after 48 hours of injection

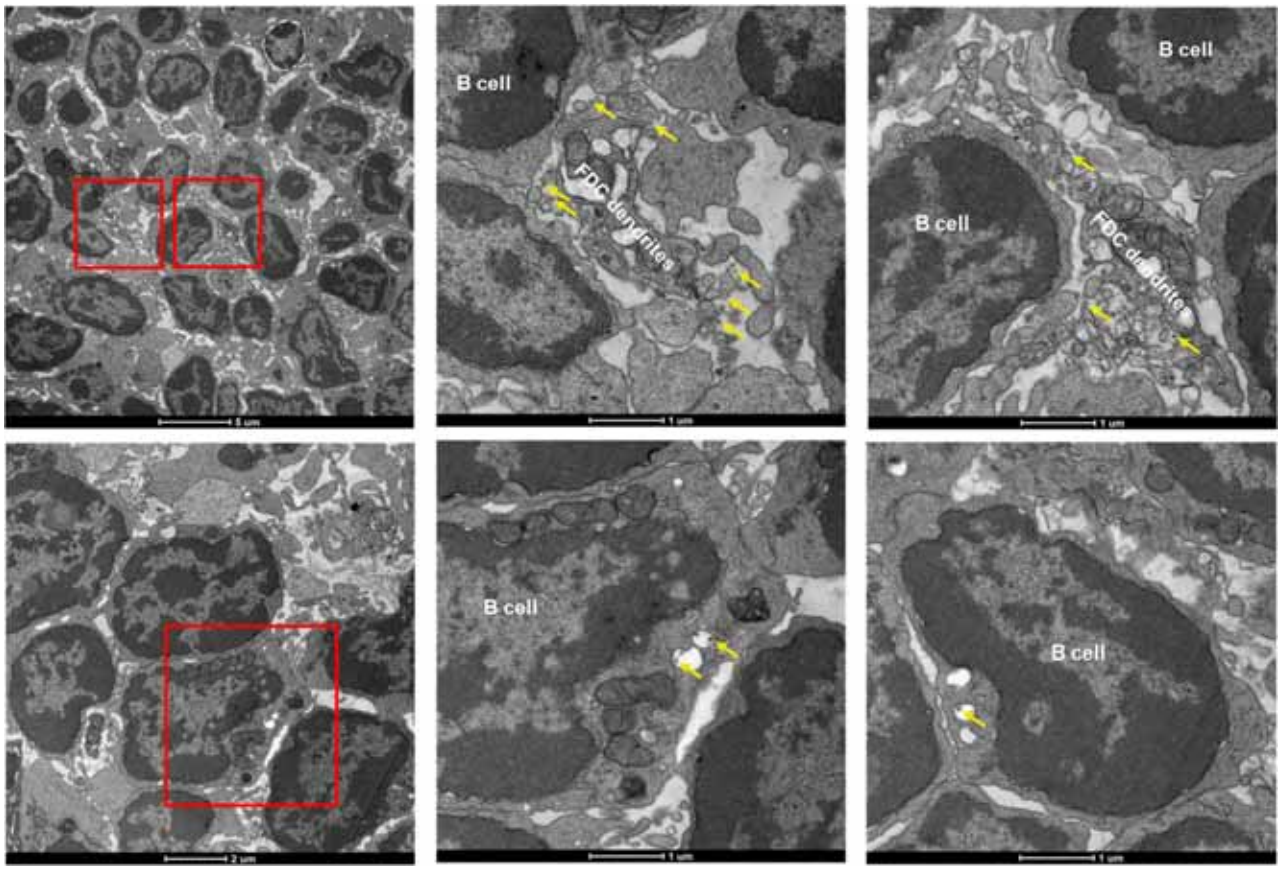

fig. S8

G GT I3-01v9 SApNPs (yellow arrow) are aligned on FDC dendrites after 2 hours of injection

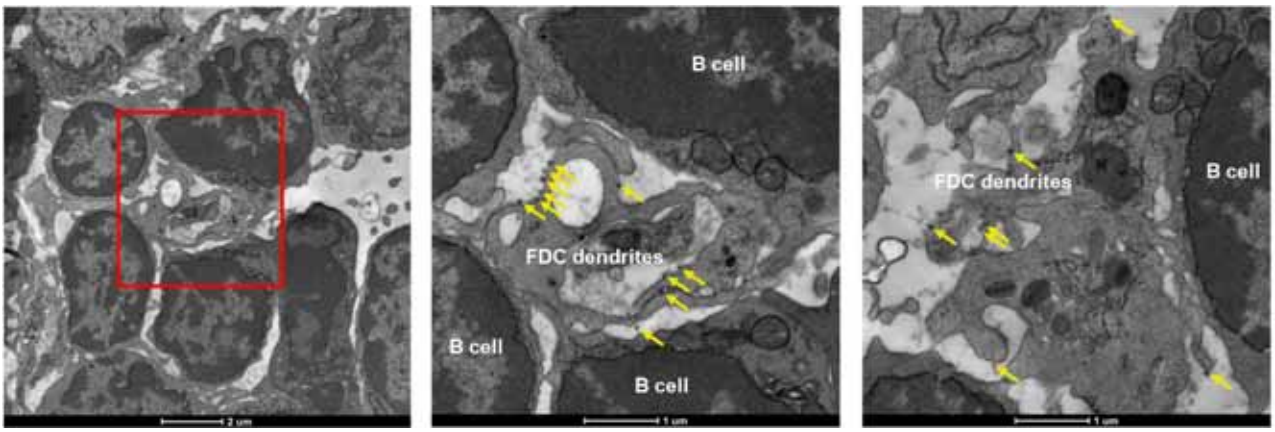

H GT I3-01v9 SApNPs (yellow arrow) are aligned on FDC dendrites after 12 hours of injection

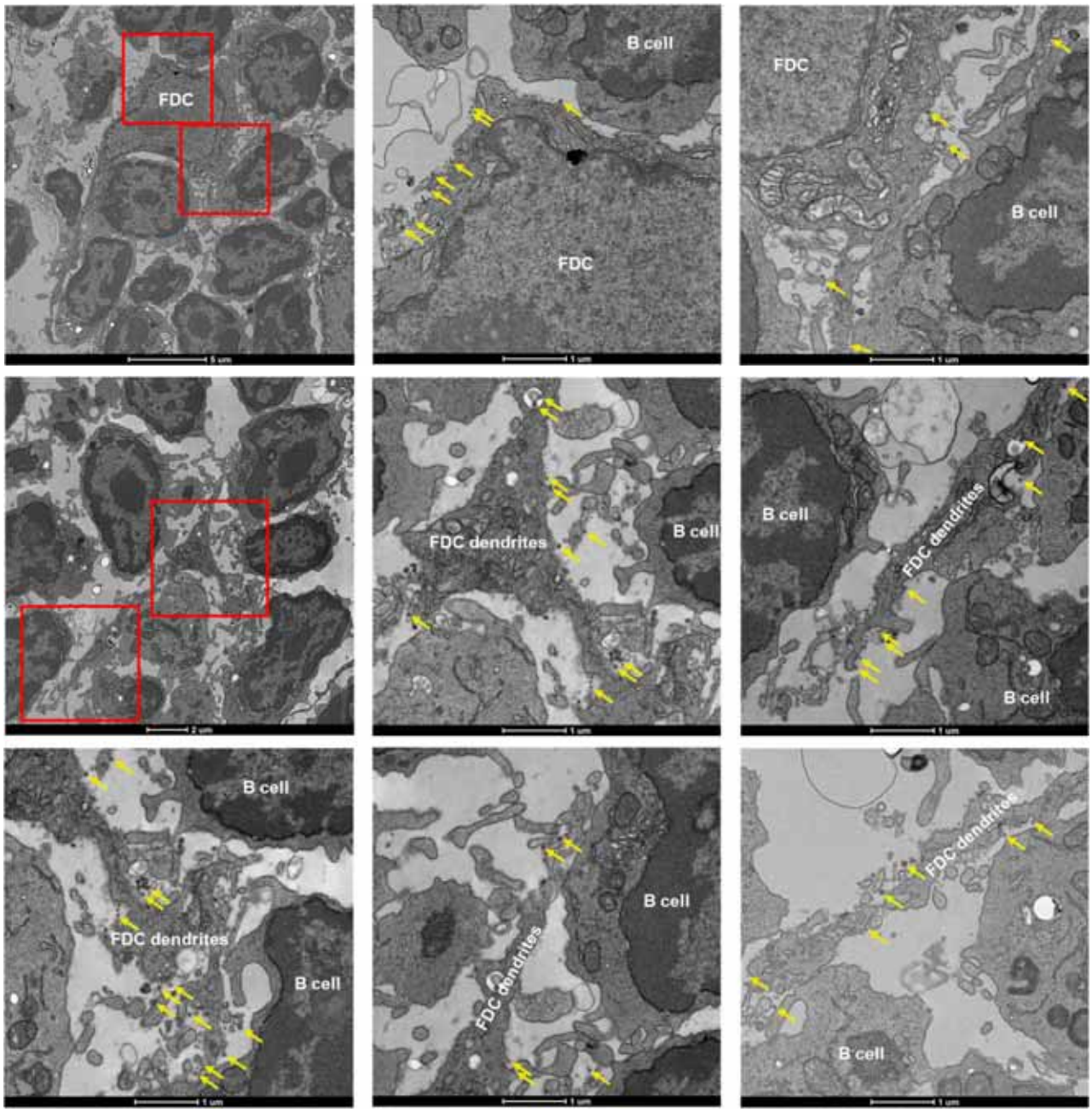

fig. S8

I GT I3-01v9 SApNPs (yellow arrow) are aligned on FDC dendrites after 48 hours of injection

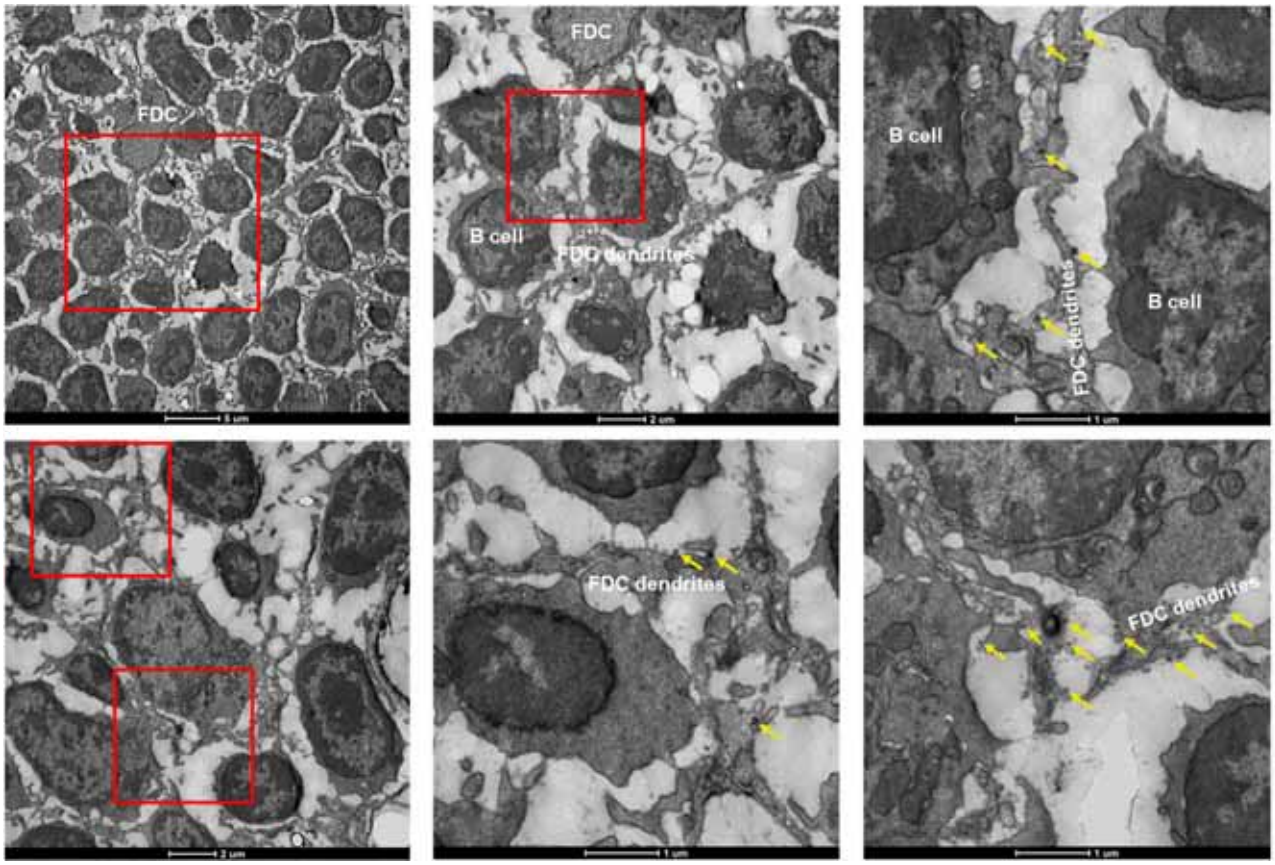

J E2p SApNPs (yellow arrow) alone are aligned on FDC dendrites after 12 hours of injection

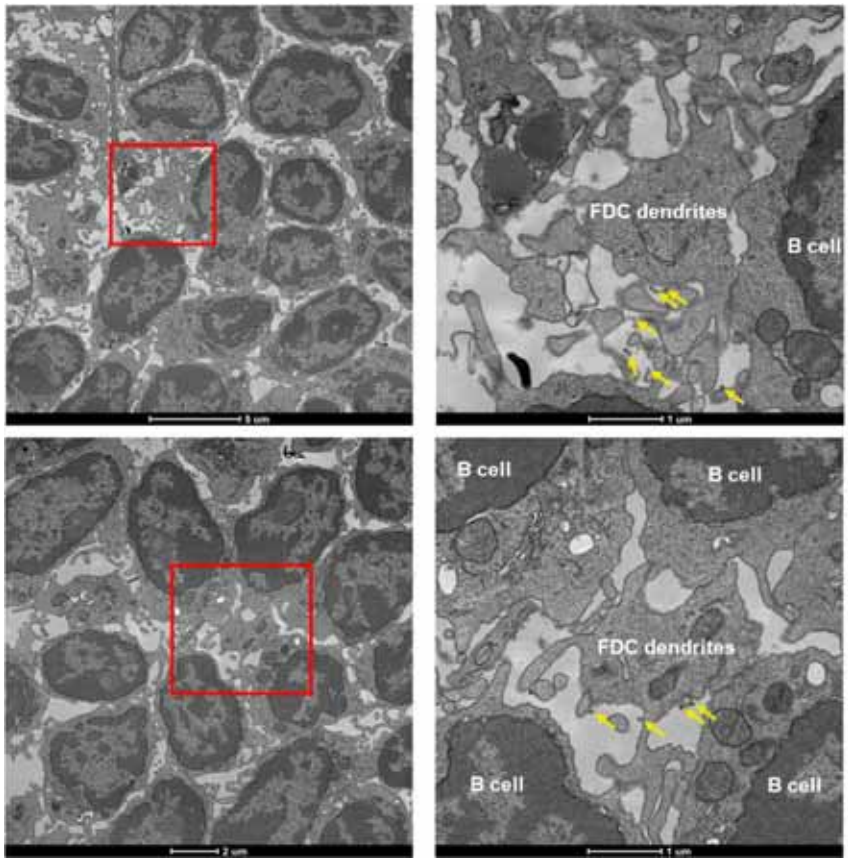

fig. S8

K I3-01v9 SApNPs alone (yellow arrow) are aligned on FDC dendrites after 12 hours of injection

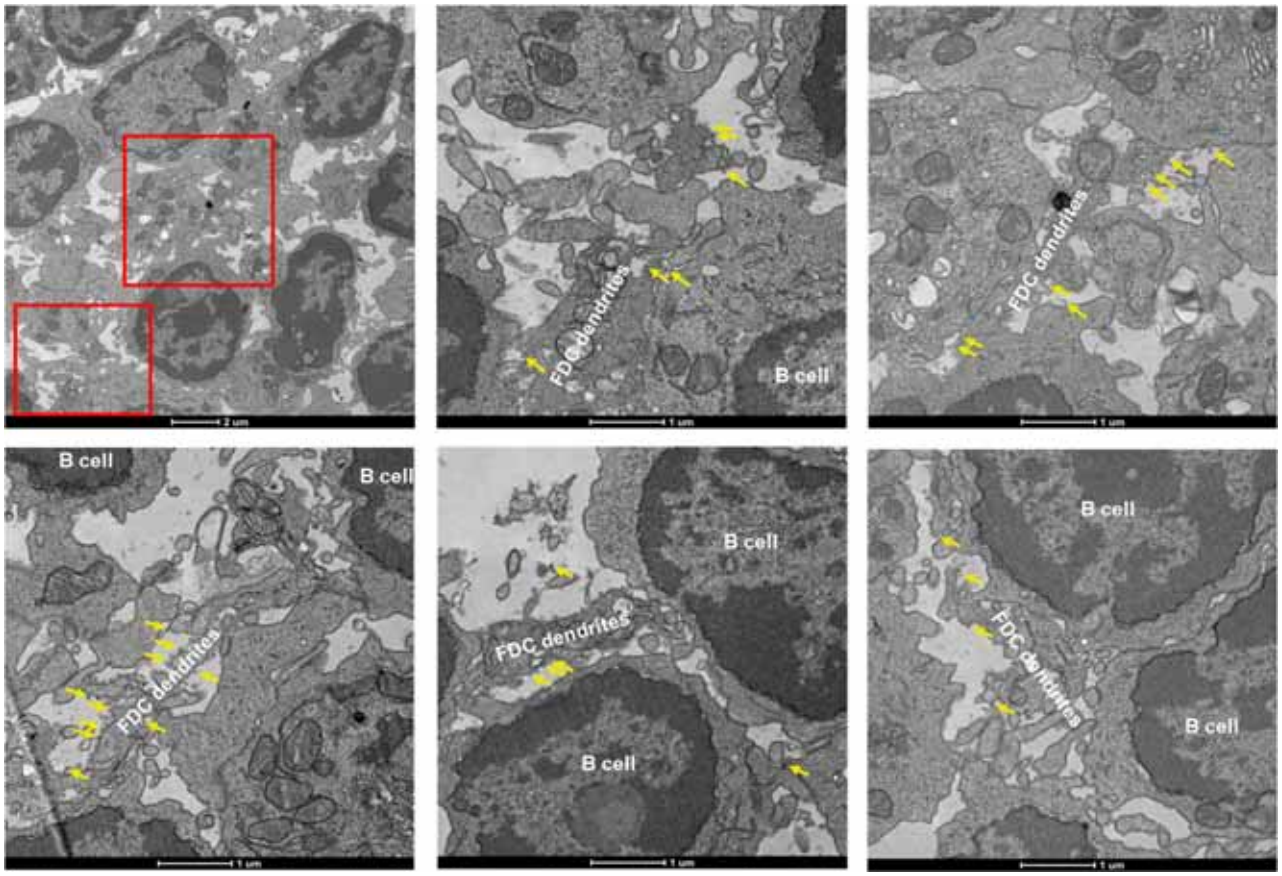

L AddaVax (green arrow) alone are aligned on FDC dendrites after 12 hours of injection

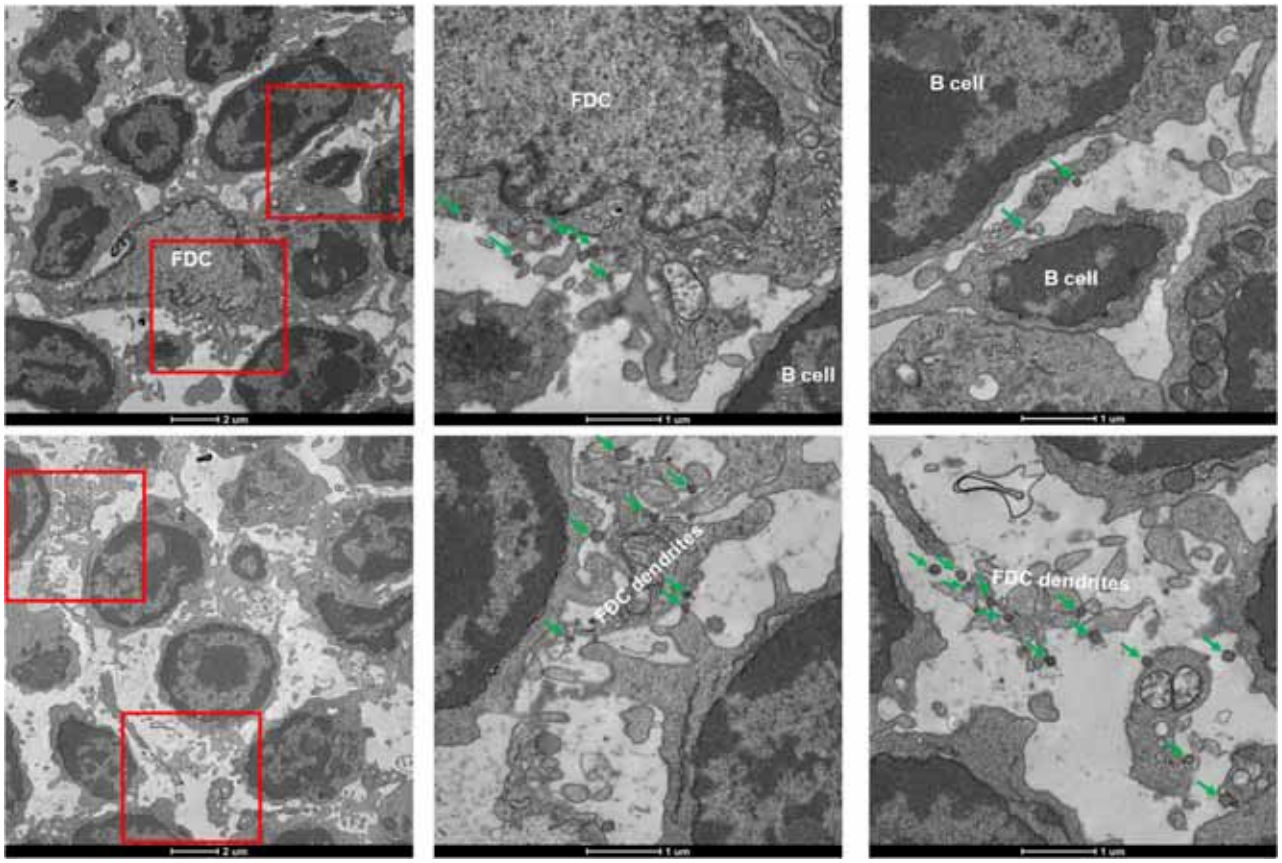

fig. S8

M FDC dendrites in Lymph nodes from naïve mouse

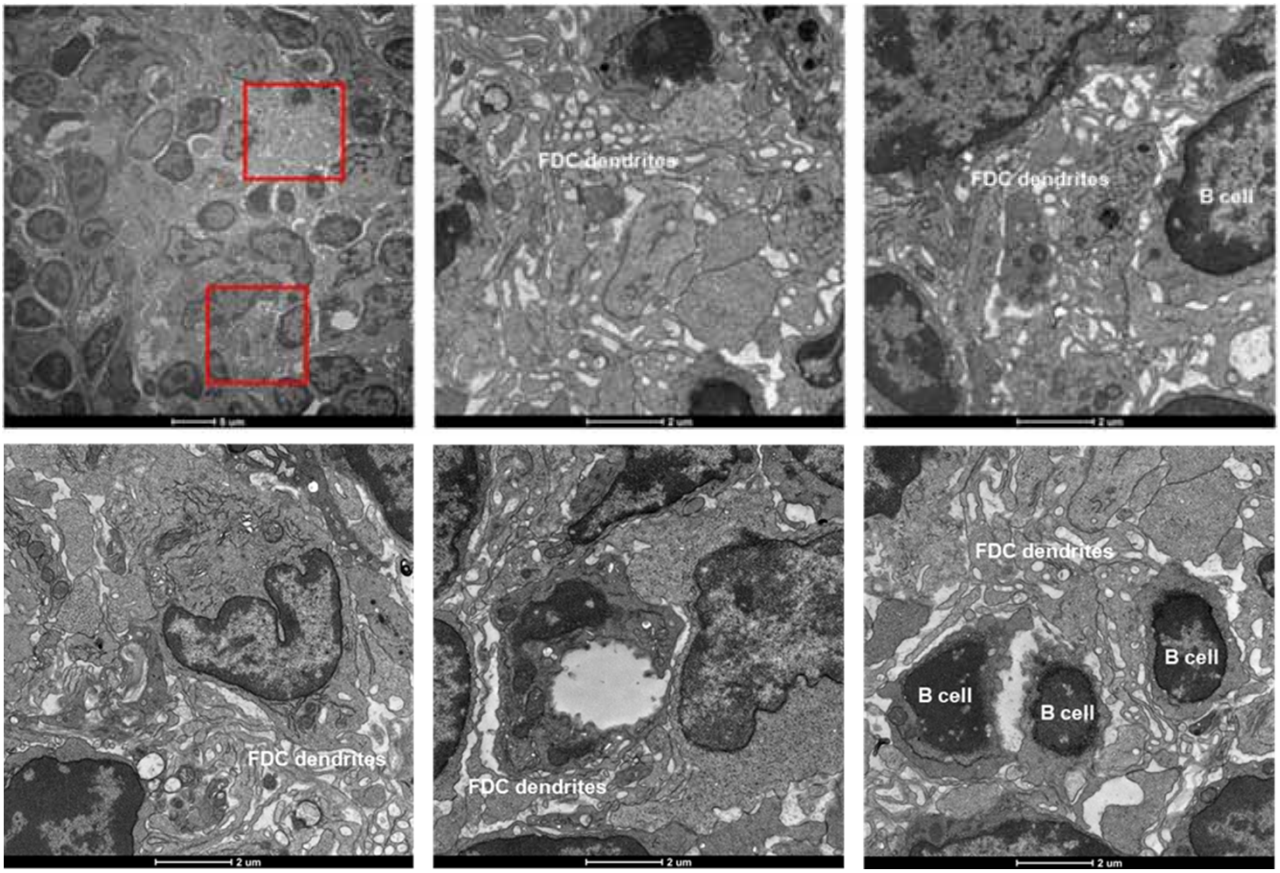

N E2p SApNPs (yellow arrow) and AddaVax (green arrow) are on the surface or inside the endolysosomes of phagocytic cells after 2 hours of injection

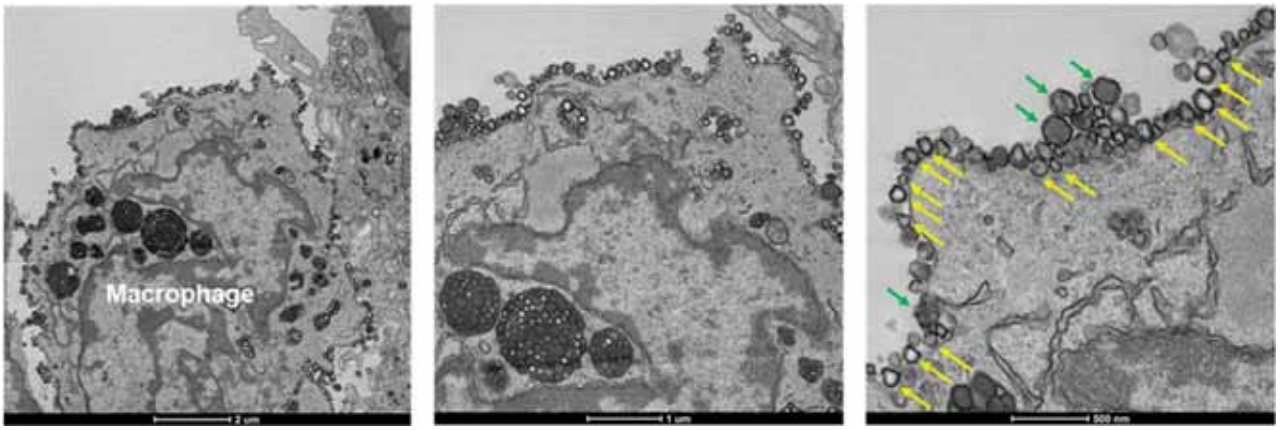

fig. S8

O I3-01v9 SApNPs (yellow arrow) are associated with phagocytic cells after 2 hours of injection

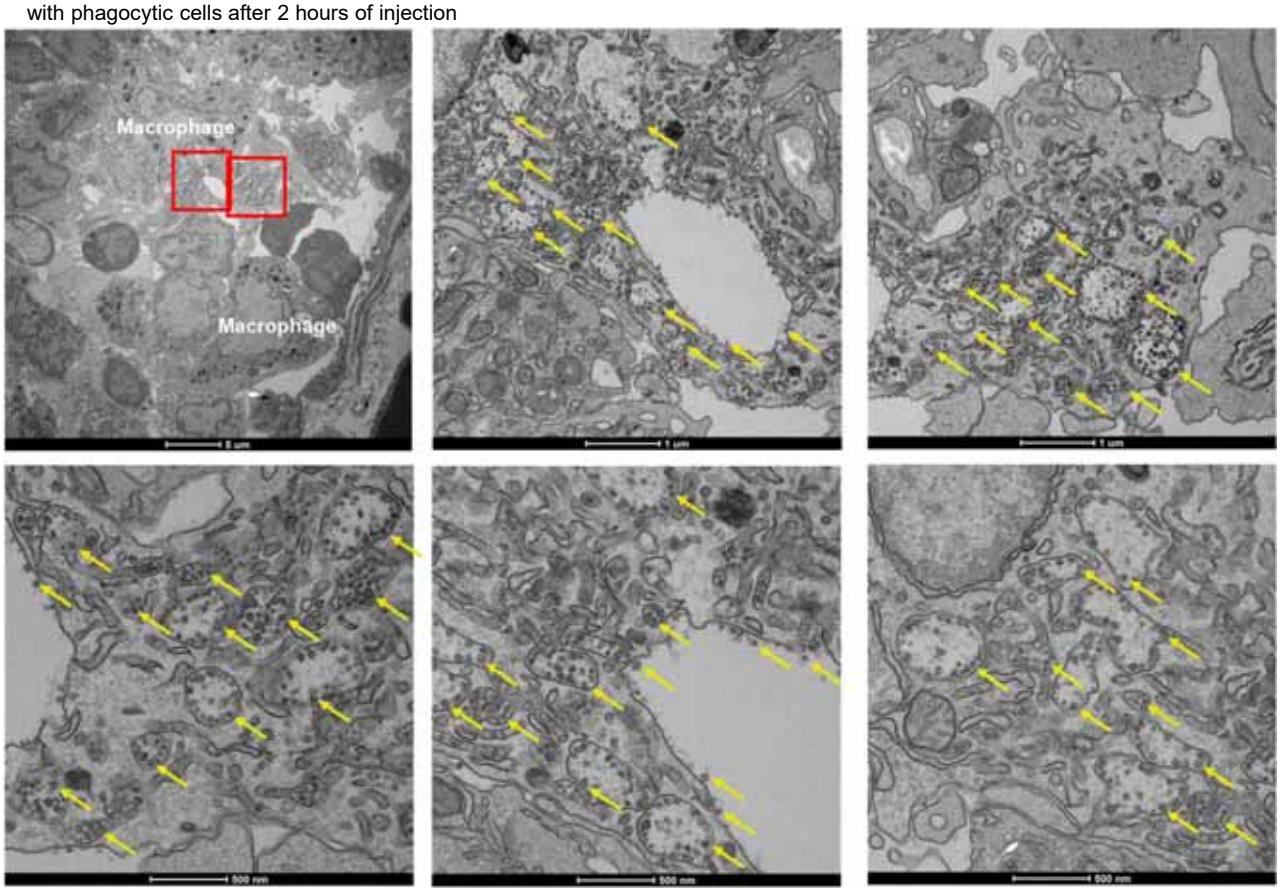

P I3-01v9 SApNPs (yellow arrow) are associated with phagocytic cells after 12 hours of injection

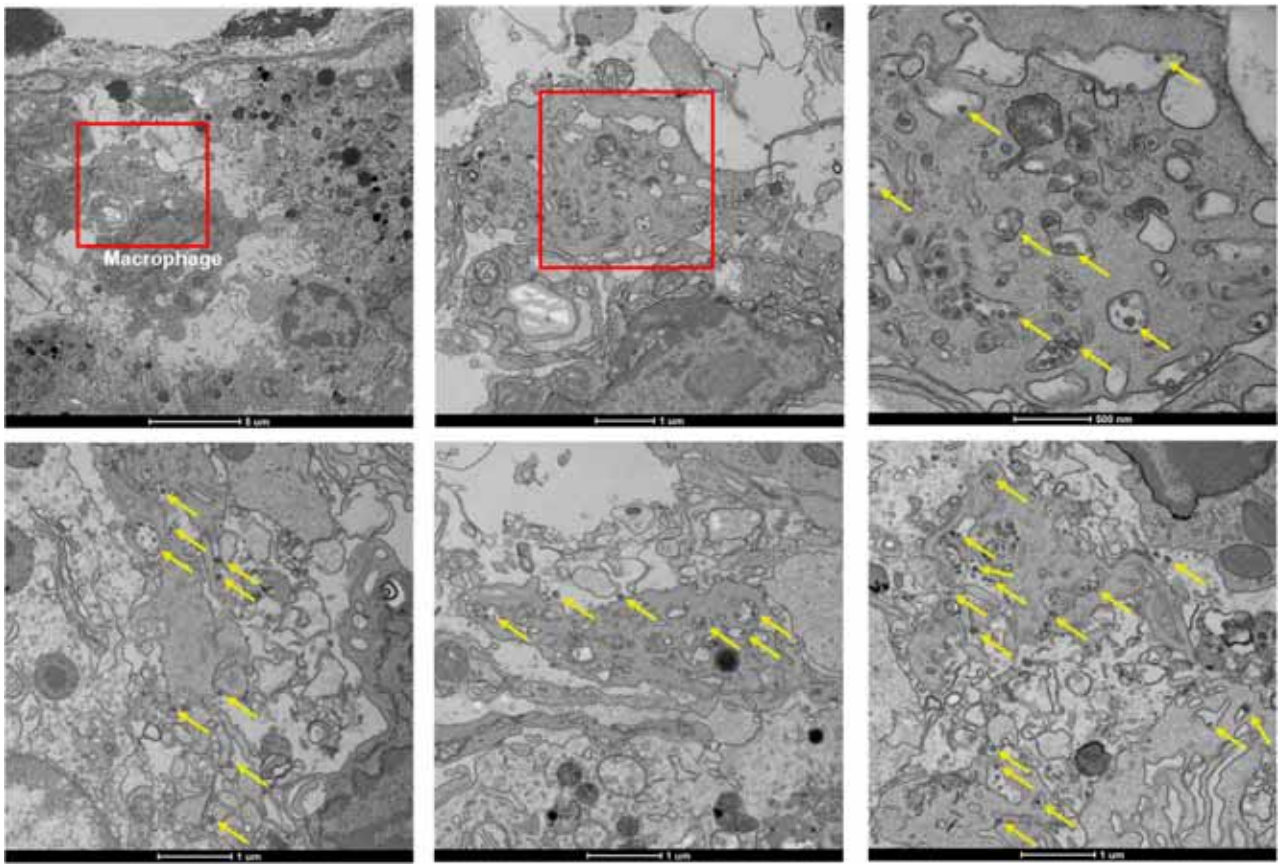

fig. S8

Q I3-01v9 SApNPs (yellow arrow) are associated with phagocytic cells after 48 hours of injection

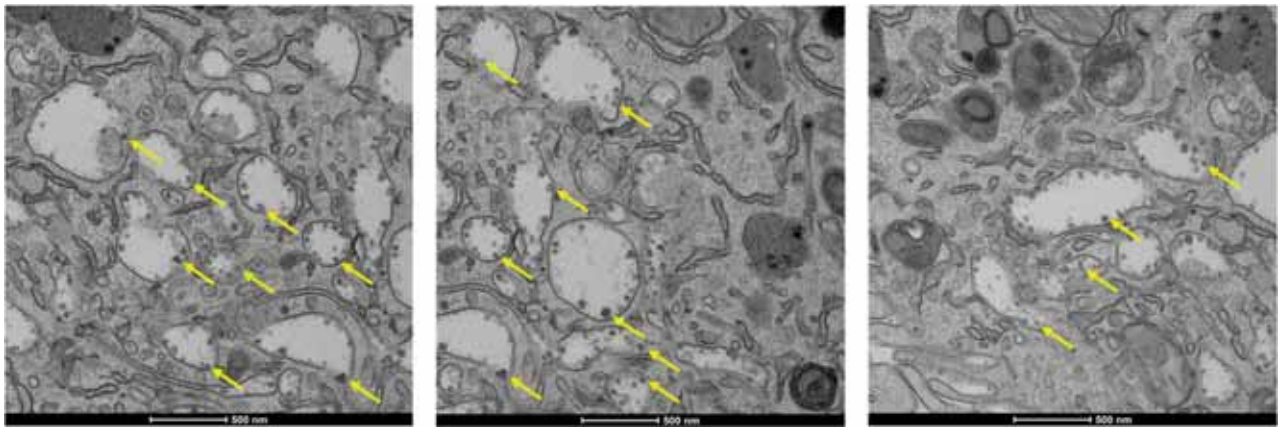

R GT I3-01v9 SApNPs (yellow arrow) are associated with phagocytic cells after 2 hours of injection

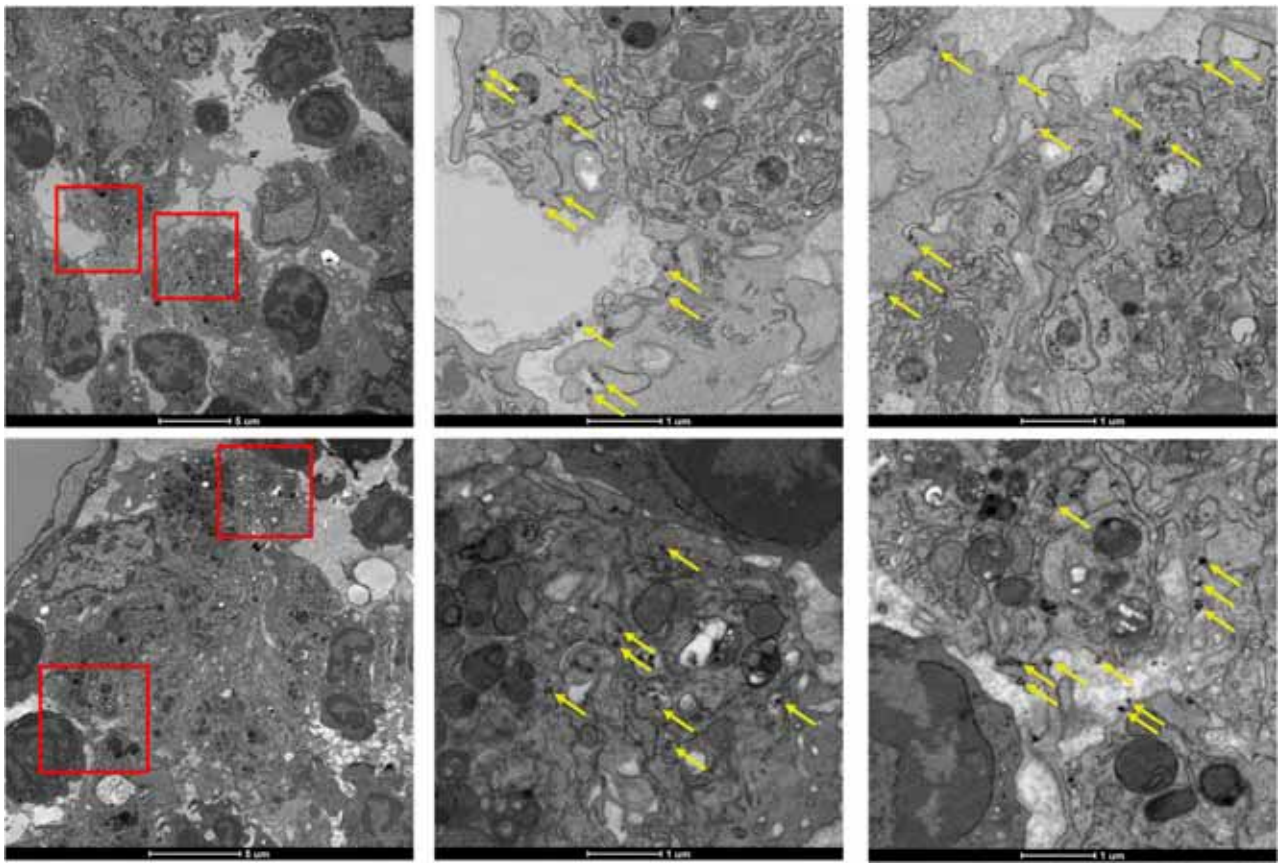

fig. S8

S GT I3-01v9 SApNPs (yellow arrow) and aluminum phosphate (green arrow) are associated with phagocytic cells after 12 hours of injection

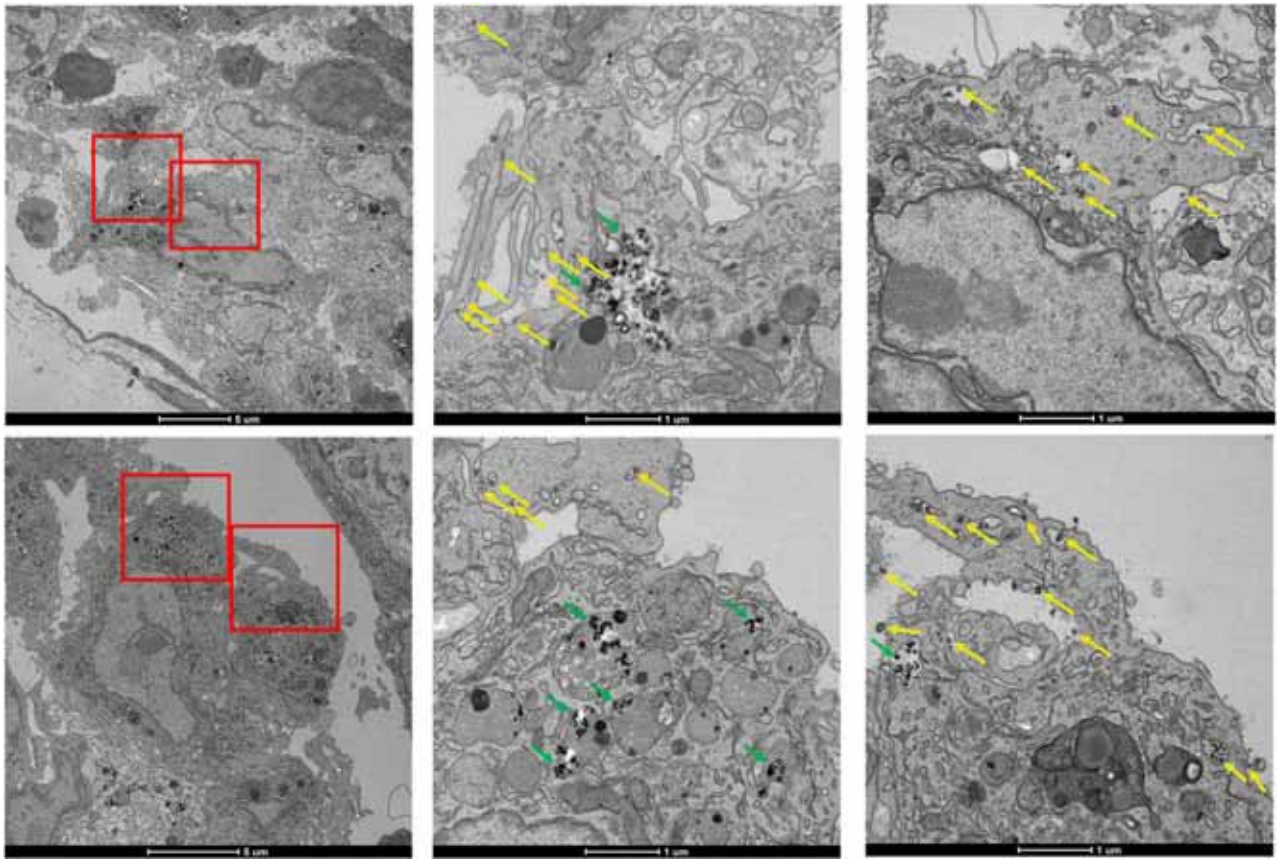

T GT I3-01v9 SApNPs (yellow arrow) are associated with phagocytic cells after 48 hours of injection

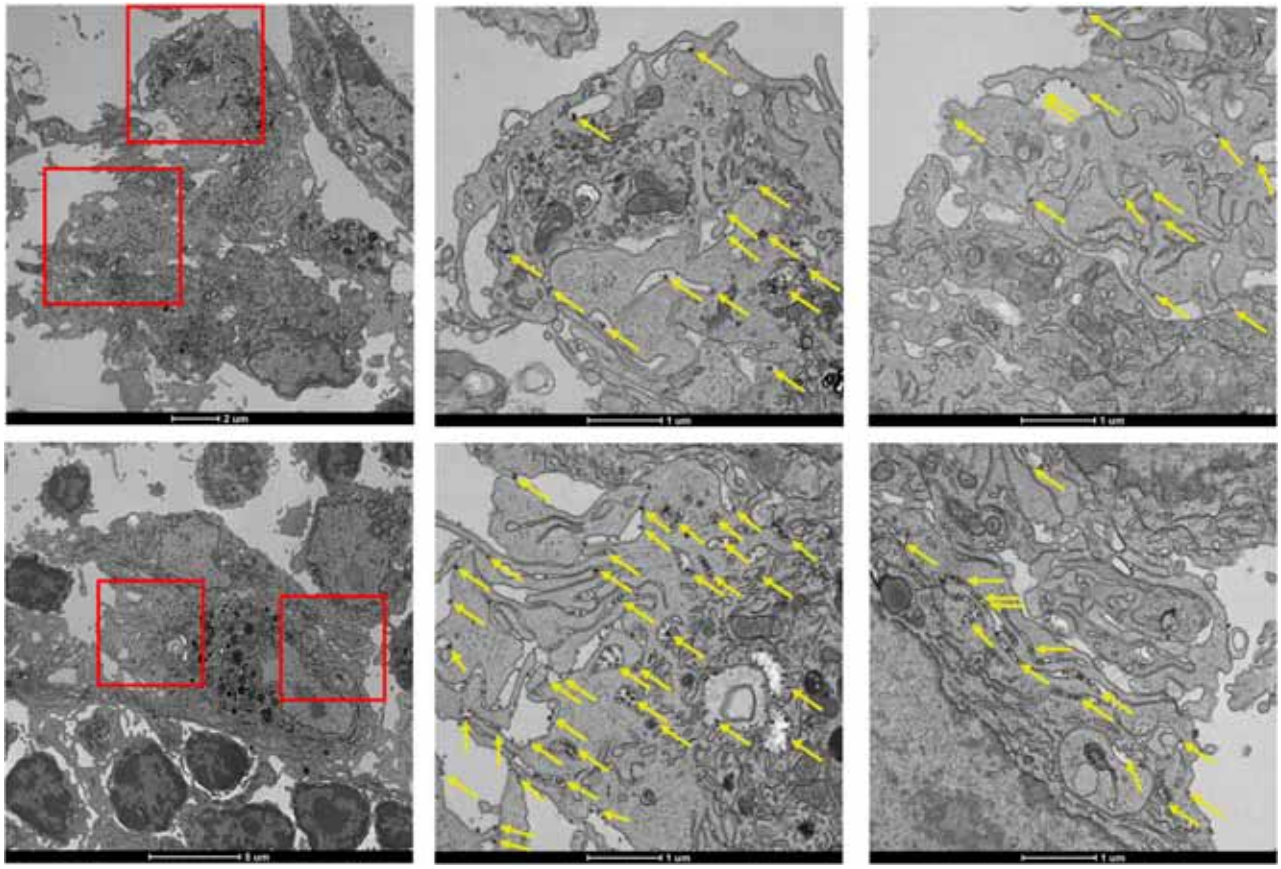

fig. S8

U Aluminum phosphate (green arrow) alone tends to aggregate and are observed inside the phagocytic cells, or in the ECM

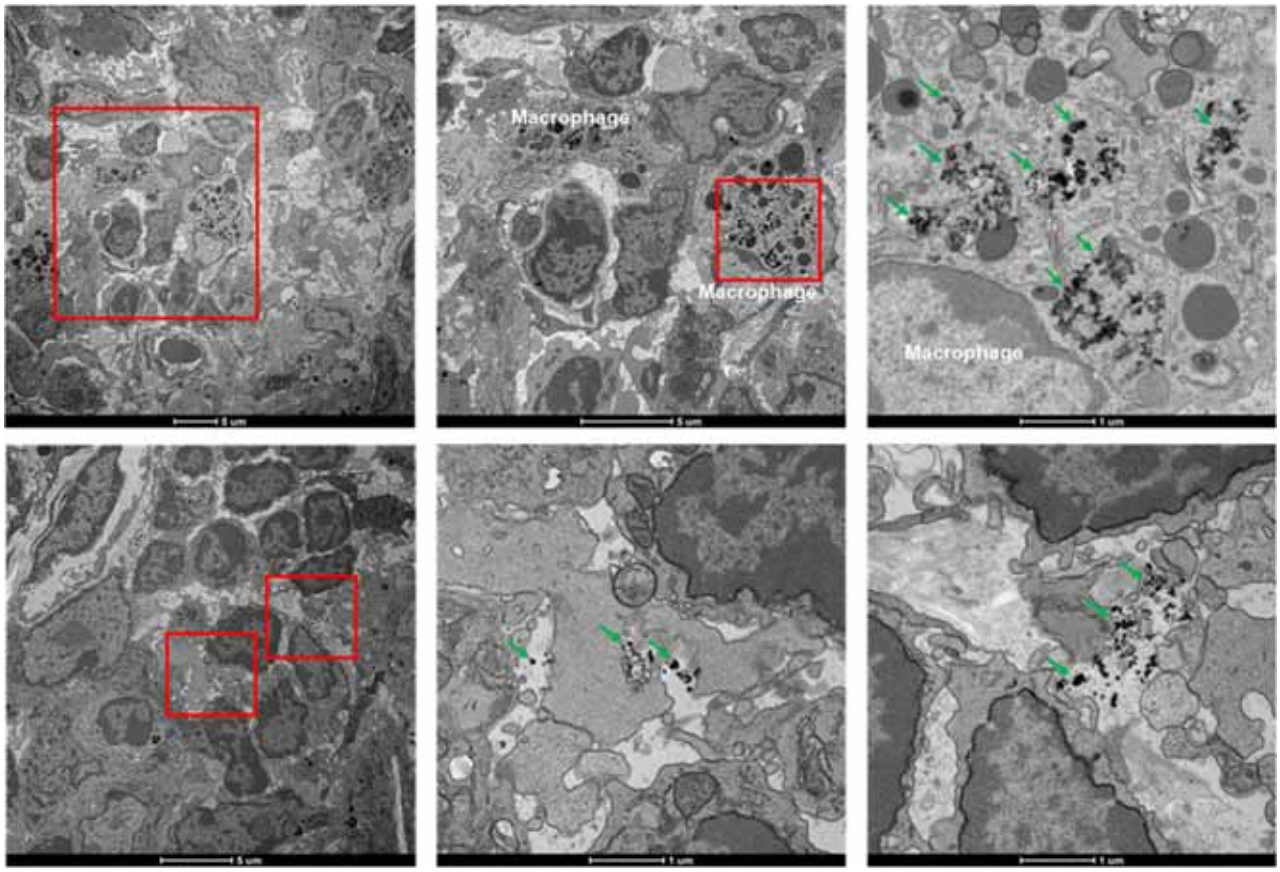

V Phagocytic cells in Lymph nodes from naïve mouse

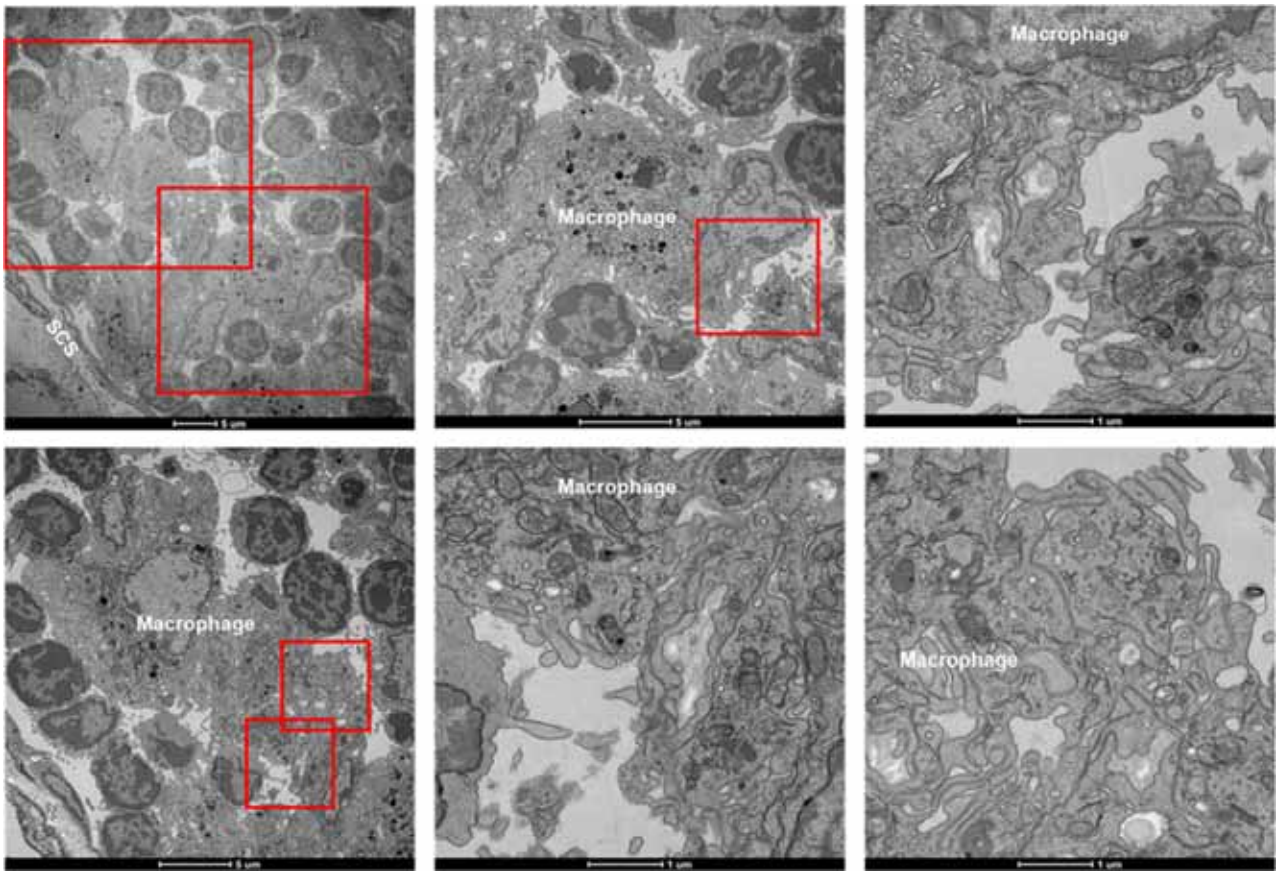

fig. S6. TEM images of HIV-1 trimer/trimer-presenting SApNP interaction with FDCs and phagocytic cells in a lymph node. BG505 UFO trimer-presenting E2p SApNPs formulated with AddaVax adjuvant are aligned on FDC dendrites (**A**) 2 hours, (**B**) 12 hours, and (**C**) 48 hours after a single-dose injection (50 µg). Adjuvanted BG505 UFO trimer-presenting (**D-F**) I3-01v9 and (**G-I**) GT I3-01v9 SApNPs are aligned on FDC dendrites 2, 12, and 48 hours after a single-dose injection (50 µg), whereas aluminum phosphate adjuvants were not associated with SApNPs on FDC dendrites. (**J**) BG505 UFO trimer-presenting E2p, (**K**) I3-01v9 SApNPs, or (**L**) AddaVax adjuvant alone can be presented on FDC dendrites 12 hours after injection. SApNPs are pointed by yellow arrows and adjuvants are pointed by green arrows. (**M**) FDC dendrites in Lymph nodes from naïve mouse. (**N**) BG505 UFO trimer-presenting E2p SApNPs formulated with AddaVax adjuvant are aligned on the surface or inside the endolysosomes of medullary sinus macrophages 2 hours after injection. Adjuvanted BG505 UFO trimer-presenting (**O-Q**) I3-01v9 and (**R-T**) GT I3-01v9 SApNPs are on macrophage surface or internalized by macrophages 2, 12, and 48 hours after injection. (**U**) Aluminum phosphate adjuvants are inside the phagocytic cells, or in the ECM. (**V**) Phagocytic cells in Lymph nodes from naïve mouse.

fig. S9

A

Single-dose - 2 w

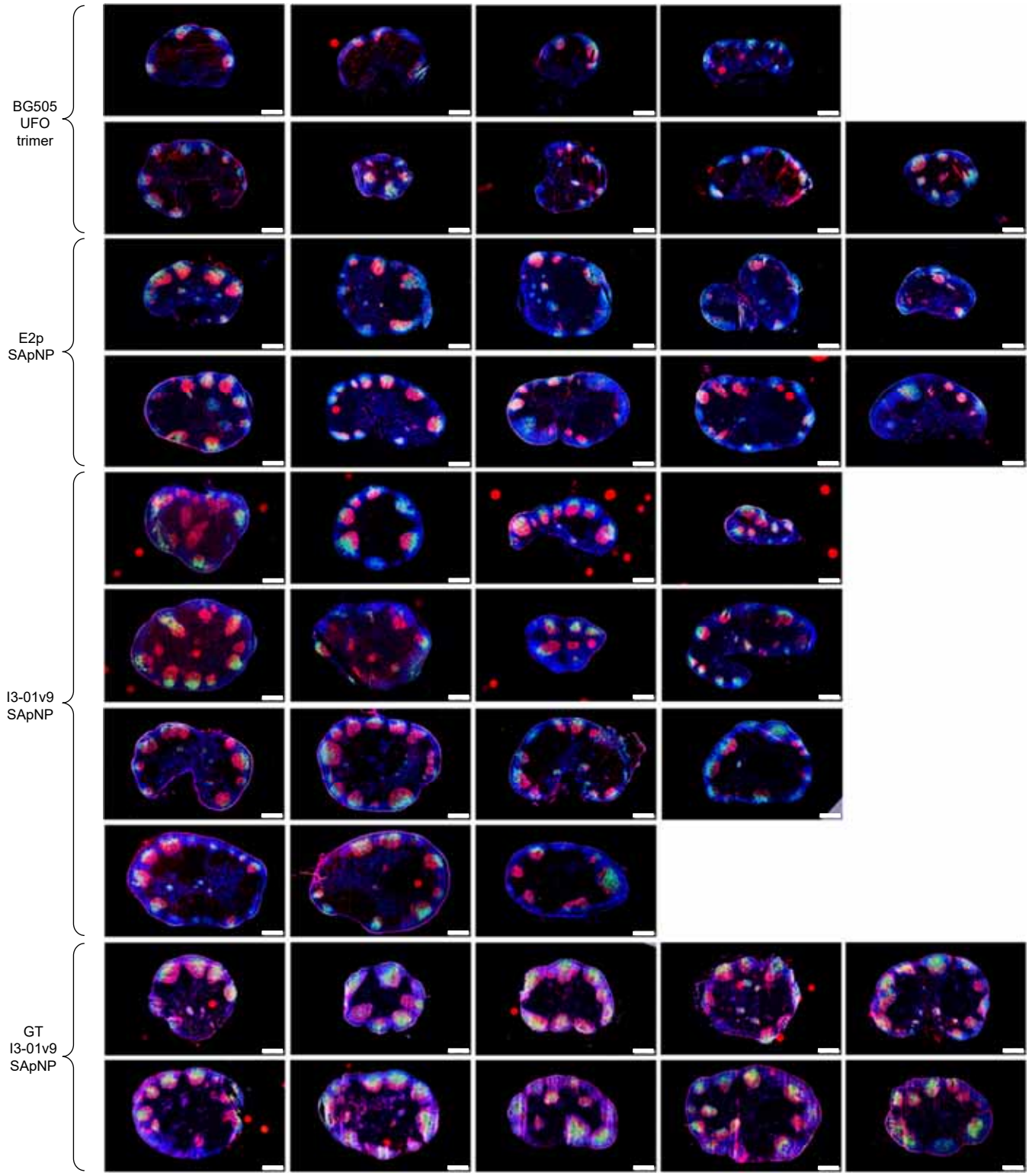

fig. S9

B **Single-dose - 5 w**

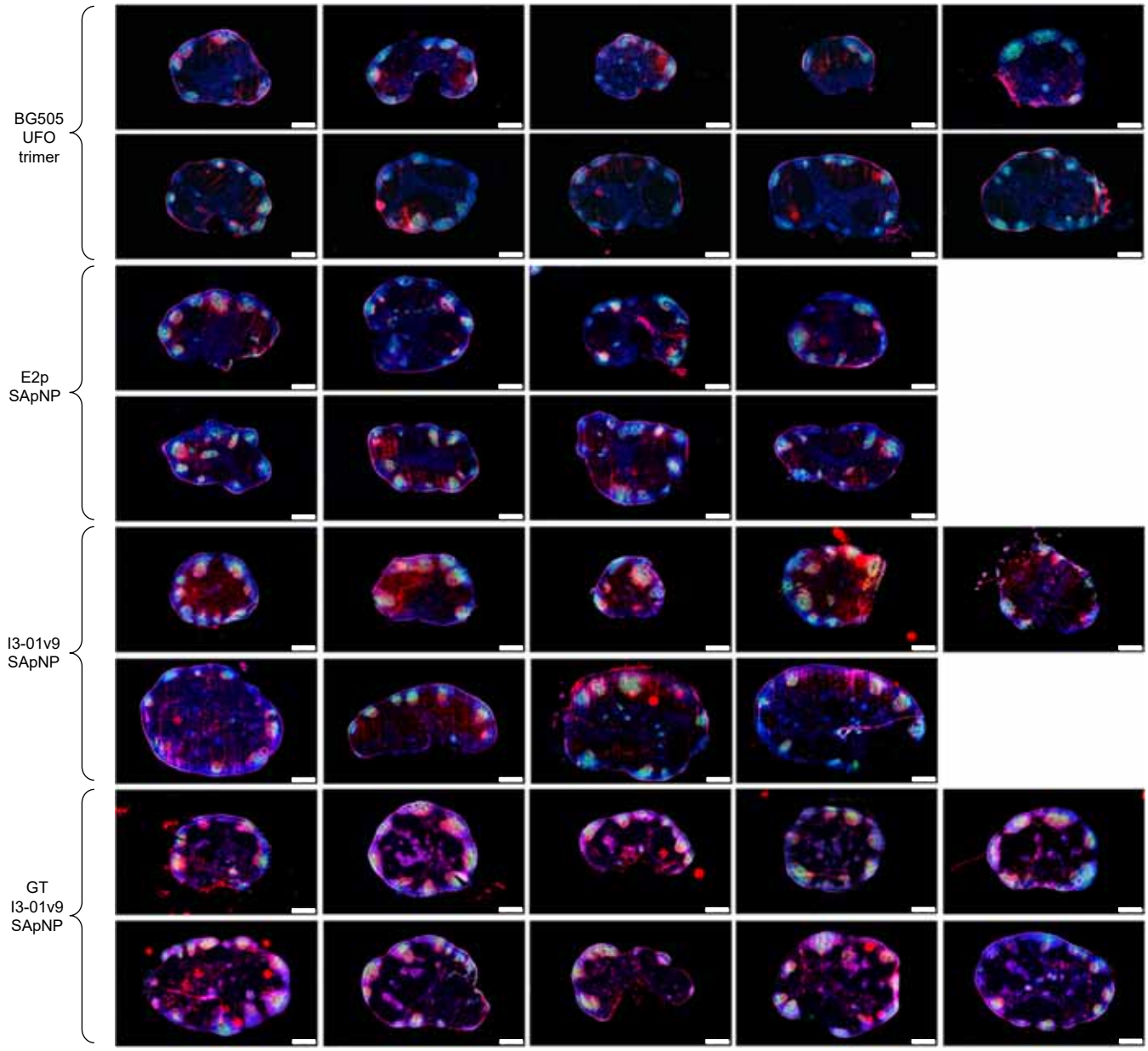

fig. S9

C

Single-dose - 8 w

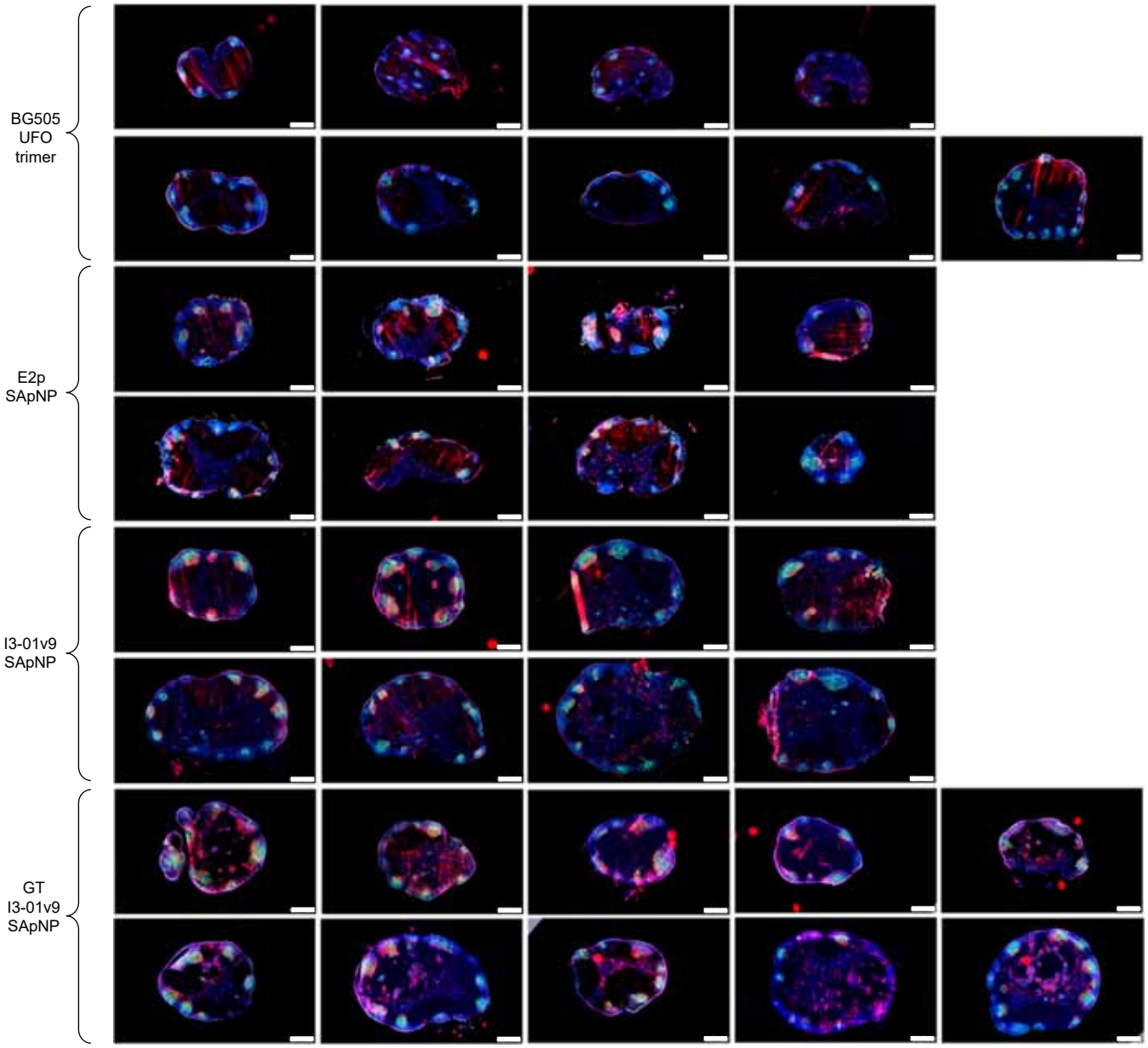

fig. S9

D

Prime-boost - 3 w + 2 w

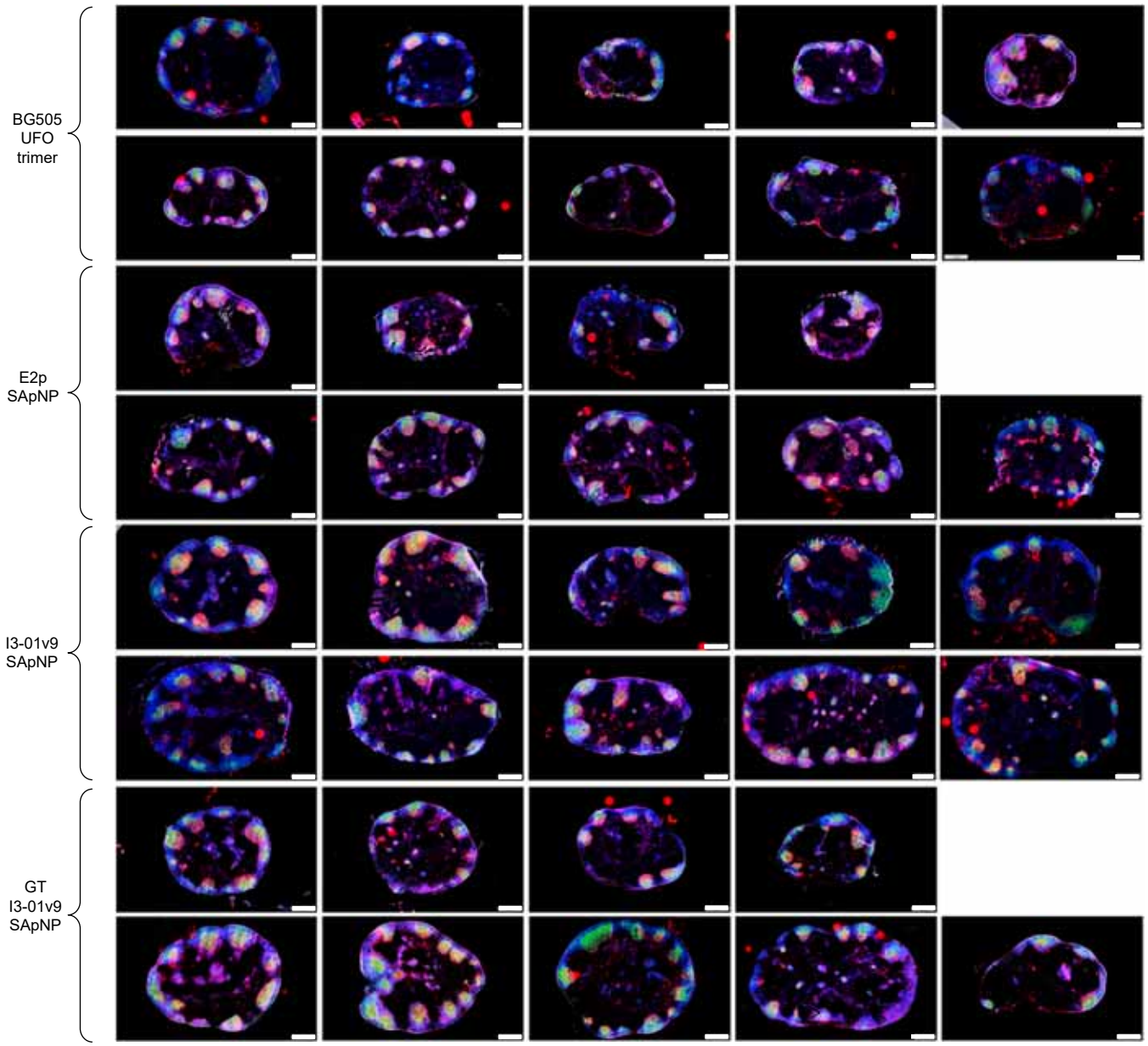

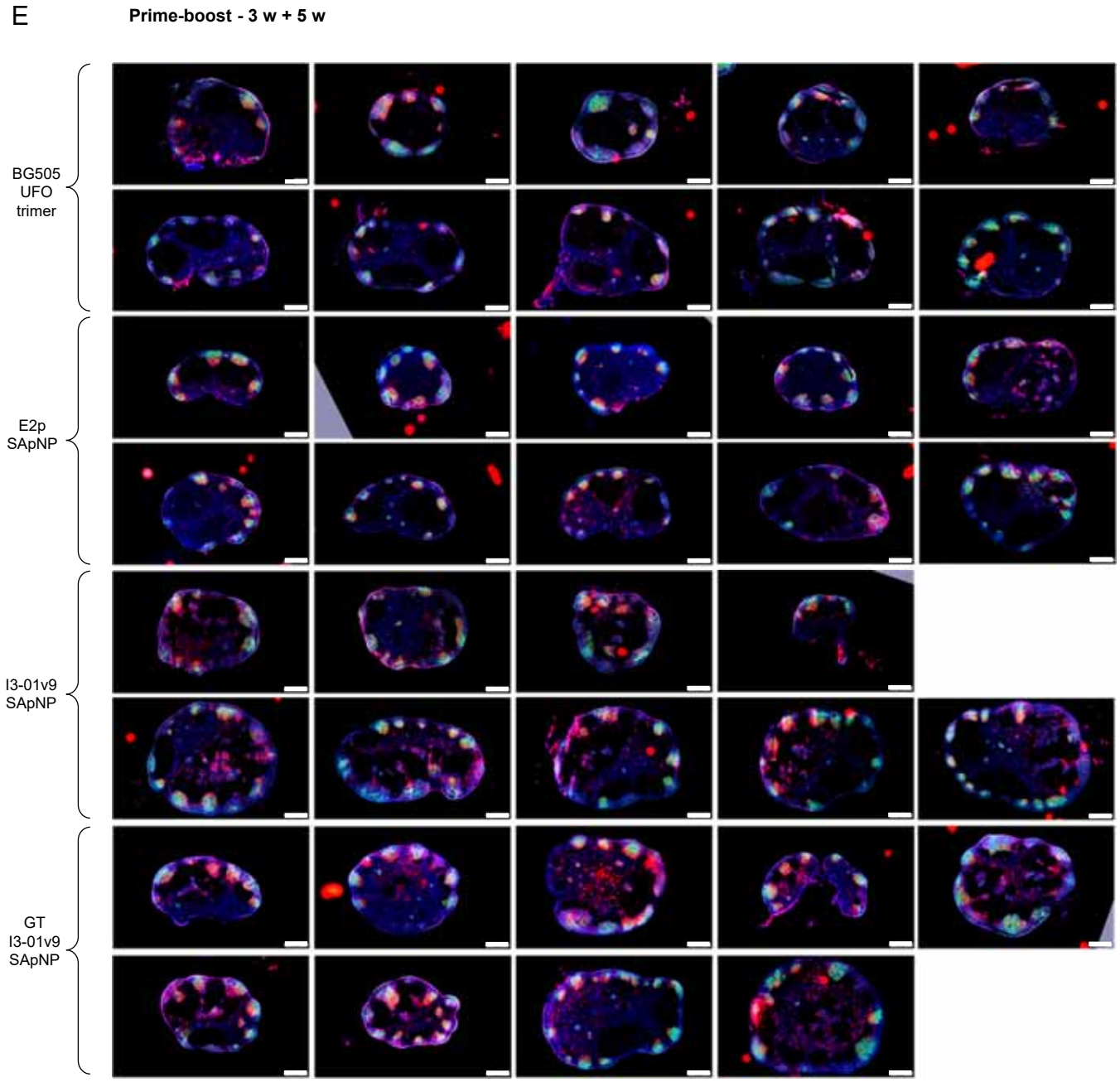

fig. S9. Immunohistological analysis of BG505 UFO and SApNP vaccine-induced GCs. Immunohistological images of GCs at (**A**) week 2, (**B**) week 5, and (**C**) week 8 after a single-dose injection of BG505 UFO trimer and BG505 UFO trimer-presenting E2p, I3-01v9, and GT I3-01v9 SApNP vaccines (10 μg per injection, totaling 40 μg per mouse), with a scale bar of 500 μm for each image. Images of GCs at (**D**) week 2 and (**E**) week 5 after prime-boost injections.

fig. S10

A

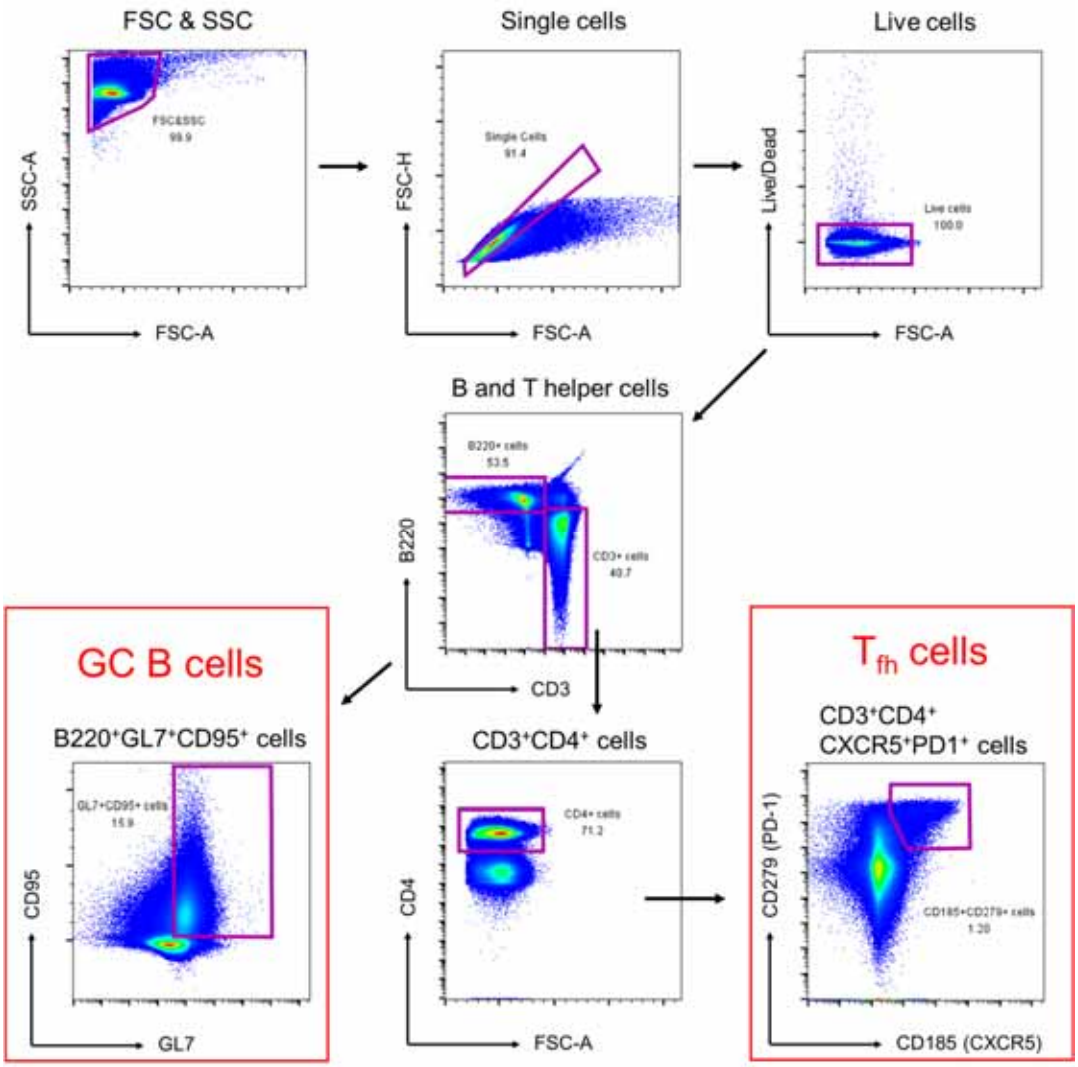
FSC & SSC
SSC-A
FSC-A
Single cells
FSC-H
FSC-A
Live cells
Live/Dead
FSC-A
B and T helper cells
B220
CD3
GC B cells
B220⁺GL7⁺CD95⁺ cells
CD95
GL7
CD3⁺CD4⁺ cells
CD4
FSC-A
Tfh cells
CD3⁺CD4⁺
CXCR5⁺PD1⁺ cells
CD279 (PD-1)
CD185 (CXCR5)

B **2 weeks after single-dose**

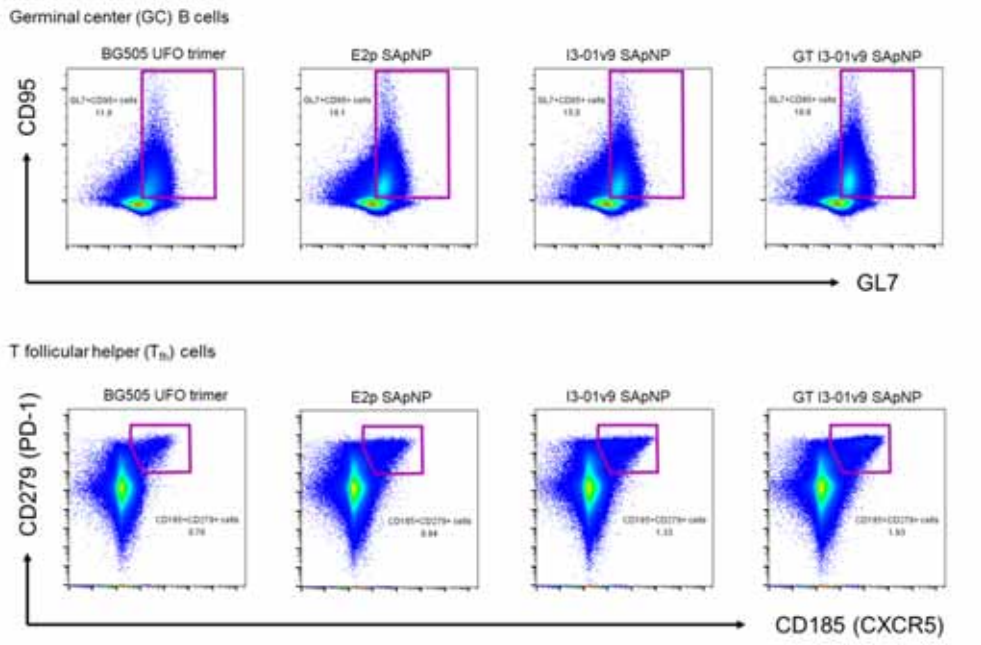

C **2 weeks after prime&boost**

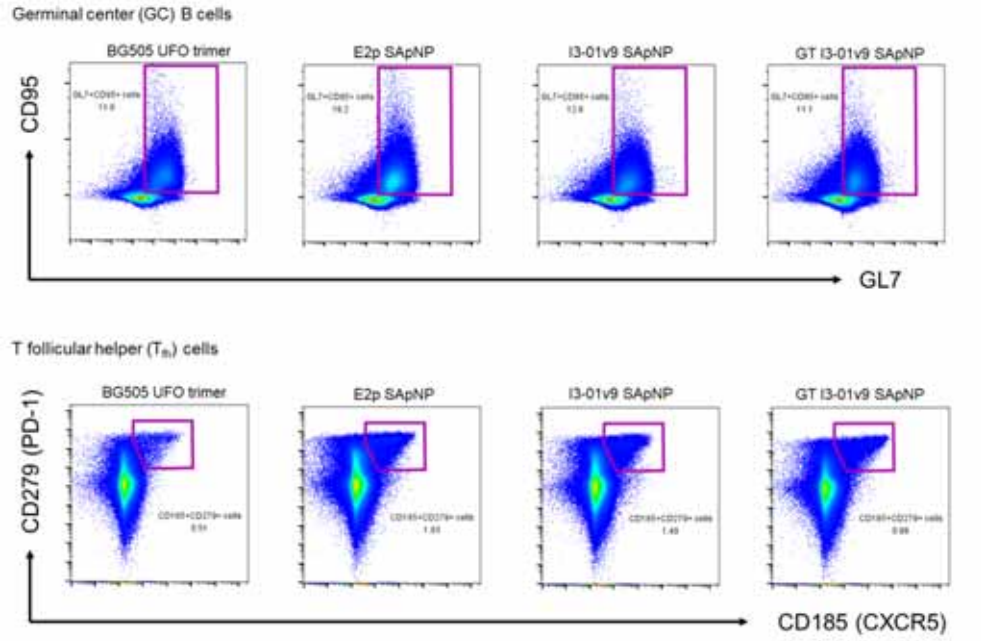

fig. S10. Flow cytometry analysis of BG505 UFO trimer and SApNP vaccine-induced GCs. (**A**) Gating strategy for analyzing GCs using flow cytometry. Flow plots of GC reactions (GC B cells and T follicular helper cells) at week 2 after (**B**) a single-dose (**C**) prime-boost injections of BG505 UFO trimer and BG505 UFO trimer-presenting E2p, I3-01v9, and GT I3-01v9 SApNP vaccines (10 μg per injection, totaling 40 μg per mouse).